

**RATIONAL DEVELOPMENT OF ANTI-INFECTIVES WITH  
NOVEL TARGET-SITES AND NEW MECHANISMS OF  
ACTION TO OVERCOME BACTERIAL RESISTANCES**

**DISSERTATION**

zur Erlangung des Grades  
des Doktors der Naturwissenschaften  
der Naturwissenschaftlich-Technischen Fakultät III  
Chemie, Pharmazie, Bio- und Werkstoffwissenschaften  
der Universität des Saarlandes

von

**Dipl. Pharmazeut Jan Henning Sahner**

Saarbrücken

2014

Tag des Kolloquiums:	06.03.2015
Dekan:	Prof. Dr. Dirk Bähre
Vorsitz:	Prof. Dr. Alexandra Kiemer
Berichterstatter:	Prof. Dr. Rolf Hartmann Prof. Dr. Rolf Müller Prof. Dr. Ulrike Holzgrabe
Akad. Mitarbeiter:	Dr. Jessica Hoppstädter

Die vorliegende Arbeit wurde von Januar 2012 bis November 2014 unter Anleitung von Herrn Prof. Dr. Rolf W. Hartmann am Helmholtz-Institut für Pharmazeutische Forschung Saarland (HIPS) angefertigt.

**„So eine Arbeit wird eigentlich nie fertig, man muß sie für fertig erklären, wenn man nach Zeit und Umständen das Mögliche getan hat.“**

**Johann Wolfgang von Goethe**

## ABSTRACT

Bacterial resistances are on the rise which necessitates the development of novel anti-infectives to stay forearmed against bacterial infections. In this work, two different strategies were pursued to accomplish this goal.

The “switch region” of bacterial RNA polymerase (RNAP) was chosen as a novel binding site, which was recently found to be targeted by the natural  $\alpha$ -pyrone antibiotic myxopyronin. It is of particular interest as the  $\alpha$ -pyrone antibiotics show no cross-resistance to the clinically used rifampicin. Based on a hit compound obtained during a pharmacophore-based virtual screening, a series of small molecule inhibitors was synthesized and their *in vitro* potency was evaluated. The resulting compounds display good antibacterial activity against Gram positive bacteria and Gram negative *Escherichia Coli* TolC, coming along with a reduced resistance frequency compared to rifampicin.

Furthermore, mutasynthesis was investigated as an approach to generate myxopyronin derivatives. Thereby, the substrate specificity of the involved biosynthetic enzymes was determined and the production of several myxopyronin analogs was analytically proven.

A second attempt aimed for a reduction of *P. aeruginosa* virulence by jamming its quorum sensing enzyme PqsD. The application of molecular docking complemented by biophysical methods enabled the rational design of potent PqsD inhibitors. Moreover the structural features of two distinct inhibitor classes could be successfully combined.

## ZUSAMMENFASSUNG

Bakterielle Resistenzen sind auf dem Vormarsch. Um weiterhin gegen bakterielle Infektionen gewappnet zu sein, ist die Entwicklung neuer Antiinfektiva erforderlich. In dieser Arbeit wurden zwei Strategien verfolgt um dieses Ziel zu erreichen.

Die „Switch Region“ der bakteriellen RNA Polymerase (RNAP), kürzlich als Angriffspunkt des natürlichen  $\alpha$ -Pyrone Antibiotikums Myxopyronin entdeckt, wurde als neue Bindestelle ausgewählt. Da die  $\alpha$ -Pyrone Antibiotika keine Kreuzresistenz mit Rifampicin aufweisen ist sie von besonderem Interesse. Basierend auf einer Hit-Verbindung aus einem Pharmakophor basierten virtuellen Screening, wurde eine Reihe von Inhibitoren synthetisiert und auf ihre *in vitro* Potenz untersucht. Die resultierenden Verbindungen weisen gute antibakterielle Effekte und eine verringerte Resistenz-Frequenz im Vergleich zu Rifampicin auf.

Daneben wurde die Mutasyntese als alternative Herstellungsmethode neuer Myxopyronin-Derivate untersucht. Hierbei konnte die Substratspezifität der beteiligten Biosynthese-Enzyme bestimmt und die Produktion verschiedener Myxopyronin Analoga analytisch nachgewiesen werden.

Ein zweiter Versuch hatte eine Reduktion der Virulenz von *P. aeruginosa* durch Hemmung seines quorum sensing Enzyms PqsD zum Ziel. Der Einsatz von Docking, ergänzt durch biophysikalische Methoden ermöglichte das rationale Design potenter PqsD Inhibitoren. Außerdem konnten die strukturellen Eigenschaften zweier unterschiedlicher Inhibitor-Klassen erfolgreich kombiniert werden.

## PAPERS INCLUDED IN THIS THESIS

This thesis is divided into five publications, which are referred to in the text by their letter A–E.

**A Novel small molecule inhibitors targeting the “switch region” of bacterial RNAP: Structure-based optimization of a virtual screening hit**

J. Henning Sahner, Matthias Groh, Matthias Negri, Jörg Hauptenthal, and Rolf W. Hartmann

*Eur. J. Med. Chem.* **2013**, *65*, 223-231.

**B Binding mode characterization of novel RNA polymerase inhibitors using a combined biochemical and NMR approach**

Martina Fruth, Alberto Plaza, Stefan Hinsberger, J. Henning Sahner, Jörg Hauptenthal, Markus Bischoff, Rolf Jansen, Rolf Müller, Rolf W. Hartmann.

*ACS Chem. Biol.* **2014**, *9*, 2656-2663.

**C Advanced mutasynthesis studies on natural  $\alpha$ -pyrone-antibiotics from *Myxococcus fulvus***

J. Henning Sahner, Hilda Sucipto, Silke C. Wenzel, Matthias Groh, Rolf W. Hartmann, and Rolf Müller

*ChemBioChem* **2015**, DOI: 10.1002/cbic.201402666.

**D Combining *in silico* and biophysical methods for the development of *Pseudomonas aeruginosa* quorum sensing inhibitors: an alternative approach for structure-based drug design**

J. Henning Sahner, Christian Brengel, Michael. P. Storz, Matthias Groh, Alberto Plaza, Rolf Müller, and Rolf W. Hartmann

*J. Med. Chem.* **2013**, *56*, 8656-8664.

**E Exploring the chemical space of ureidothiophene-2-carboxylic acids as inhibitors of the quorum sensing enzyme PqsD from *Pseudomonas aeruginosa***

J. Henning Sahner, Martin Empting, Ahmed Kamal, Elisabeth Weidel, Matthias Groh, Carsten Börger, and Rolf W. Hartmann

*Eur. J. Med Chem.* **2015**, submitted.

## CONTRIBUTION REPORT

The author wishes to clarify his contributions to the Publications **A–E** in the thesis.

- A** The author designed, synthesized and characterized most of the new inhibitors. Furthermore he performed the Hansch analysis and interpreted the biological results. He conceived and wrote the manuscript.
  
- B** The author synthesized and characterized the investigated compounds from the ureidothiophene class. Furthermore, he contributed to the interpretation of the results.
  
- C** The author synthesized and characterized most of the precursor compounds and contributed to the design and interpretation of the mutasynthesis experiments. He conceived and wrote the manuscript.
  
- D** The author designed, synthesized and characterized all compounds. Besides, he performed the underlying molecular docking studies and contributed to the design of the SPR competition experiment. He conceived and wrote the manuscript.
  
- E** The author designed, synthesized and characterized all new PqsD inhibitors and interpreted the biological results. Moreover he performed the *in silico* studies. He conceived and wrote the manuscript.

## **FURTHER PAPER OF THE AUTHOR THAT IS NOT PART OF THIS DISSERTATION**

**F *In vitro* reconstitution of the  $\alpha$ -pyrone ring formation in myxopyronin biosynthesis**

Hilda Sucipto, J. Henning Sahner, Jesko Koehnke, Evgeny Prusov, Silke Wenzel, Rolf W. Hartmann and Rolf Müller.

*Manuscript in preparation*

## ABBREVIATIONS

2-AA	2-Aminoacetophenon
2-ABA	2-Aminobenzoylacetate
3D	Three dimensional
3-oxo-C12-HSL	<i>N</i> -(3-oxo-dodecanoyl)- <i>L</i> -homoserine lactone
AA	Anthranilic acid
ACoA	Anthraniloyl coenzyme A
ACP	Acyl carrier protein
AHL	<i>N</i> -Acyl homoserine lactone
AQ	2-Alkyl-4-quinolone
C4-HSL	<i>N</i> -Butanoyl- <i>L</i> -homoserine lactone
CoA	Coenzyme A
CoMFA	Comparative molecular field analysis
cor	Corallopyronin
CP	Carrier protein
DCM	Dichloromethane
DHQ	2,4-Dihydroxyquinoline
DMF	Dimethylformamide
DMSO	Dimethyl sulfoxide
DNA	Deoxyribonucleic acid
EDG	Electron donating group
eq	Equivalents
EWG	Electron withdrawing group
FDA	Food and Drug Administration
HCN	Hydrogen cyanide
HHQ	2-Heptyl-4-quinolone
HPLC	High-performance liquid chromatography
HQNO	4-Hydroxy-2-heptylquinoline- <i>N</i> -oxide
IC <sub>50</sub>	Concentration of a drug that is required for 50% inhibition <i>in vitro</i>
INPHARMA	Interligand NOE for pharmacophore mapping
ITC	Isothermal titration calorimetry
K <sub>d</sub>	Dissociation constant
LE	Ligand efficiency

logP	Octanol-water partition coefficient
MALDI	Matrix-assisted laser desorption/ionization
MDR	Multidrug resistant
MIC	Minimal inhibitory concentration
MRSA	Methicillin resistant <i>Staphylococcus aureus</i>
MS	Mass spectrometry
MW	Molecular weight
myx	Myxopyronin
NAC	<i>N</i> -acetylcysteamine
NADH	Nicotinamide adenine dinucleotide
NMR	Nuclear magnetic resonance
NOE	Nuclear Overhauser effect
NRPS	Nonribosomal peptide synthetase
OD <sub>600</sub>	Optical density at 600 nm
PDS	Precursor-directed biosynthesis
PKS	Polyketide synthase
PQS	<i>Pseudomonas</i> quinolone signal; 2-Heptyl-3-hydroxy-4-quinolone
QS	Quorum sensing
QSAR	Quantitative structure activity relationships
RNA	Ribonucleic acid
RNAP	RNA polymerase
SAR	Structure activity relationships
SPR	Surface plasmon resonance
STD	Saturation transfer difference
TB	Tuberculosis
TOF	Time-of-flight
US	United States
WHO	World Health Organization
XDR	Extensively drug resistant

# TABLE OF CONTENTS

<b>1</b>	<b>Introduction</b> .....	<b>1</b>
1.1	Rational Drug Design .....	2
1.2	Bacterial RNA polymerase as a target for antibiotics .....	8
1.3	The “switch region” of bacterial RNAP; target site for $\alpha$ -pyrone antibiotics ..	10
1.4	Mutasynthesis .....	12
1.5	<i>Pseudomonas aeruginosa</i> .....	14
1.6	Quorum Sensing in <i>P. aeruginosa</i> .....	16
1.7	Inhibition of <i>P. aeruginosa</i> QS as an anti-virulence strategy .....	18
1.8	AQ Biosynthesis in <i>P. aeruginosa</i> .....	20
1.9	PqsD as a drug target .....	22
<b>2</b>	<b>Aim of the Thesis</b> .....	<b>24</b>
<b>3</b>	<b>Results</b> .....	<b>26</b>
3.1	Novel small molecule inhibitors targeting the “switch region” of bacterial RNAP: Structure-based optimization of a virtual screening hit .....	26
3.2	Binding mode characterization of novel RNA polymerase inhibitors using a combined chemical and NMR approach .....	48
3.3	Advanced Mutasynthesis Studies on Natural $\alpha$ -Pyrone Antibiotics from <i>Myxococcus fulvus</i> .....	66
3.4	Combining <i>in Silico</i> and Biophysical Methods for the Development of <i>Pseudomonas aeruginosa</i> Quorum Sensing Inhibitors: An Alternative Approach for Structure-Based Drug Design .....	86
3.5	Exploring the chemical space of ureidothiophene-2-carboxylic acids as inhibitors of the quorum sensing enzyme PqsD from <i>Pseudomonas aeruginosa</i> .....	108
<b>4</b>	<b>Final Discussion</b> .....	<b>127</b>
4.1	Structure activity relationships (SAR) .....	127
4.2	Binding mode validation .....	132
4.3	Intracellular activity .....	133

4.4	Overcoming existing resistances .....	134
4.5	Total/semi-synthesis vs. mutasynthesis.....	135
4.6	Ureidothiophene-2-carboxylic acids.....	136
4.7	Summary and outlook.....	137
<b>5</b>	<b>References .....</b>	<b>140</b>
<b>6</b>	<b>Supporting Information .....</b>	<b>148</b>
6.1	Supporting Information for Publication A .....	148
6.2	Supporting Information for Publication B .....	164
6.3	Supporting Information for Publication C .....	170
6.4	Supporting Information for Publication D .....	193
6.5	Supporting Information for Publication E .....	205
<b>7</b>	<b>Appendix .....</b>	<b>218</b>
7.1	Curriculum Vitae .....	218
7.2	Publications .....	219
7.3	Conference Contributions .....	220
<b>8</b>	<b>Acknowledgements .....</b>	<b>221</b>



# 1 Introduction

For thousands of years, bacterial infections were a main cause of death threatening mankind. The discovery of microorganisms as the trigger of these infections established the basis for a targeted treatment and prevention measures. Besides improvements in sanitation and hygiene as well as the introduction of vaccinations, the discovery of antibiotics in the late 19<sup>th</sup> century was a milestone in fighting infectious diseases [Davies and Davies 2010]. After the approval of sulfonamides and penicillins in the 1930s and 1940s, the rate of mortality dropped dramatically and the suffering of patients was alleviated [von Nussbaum et al. 2006]. Furthermore, antimicrobials enabled the prophylaxis and the treatment of surgery-related infections leading to advances in surgical techniques [Chopra. 2007]. This story of success continued for about 25 years. During that period more and more new classes of antibiotics like the aminoglycosides, macrolides and fluoroquinolones were developed and approved (Fig. 1). William Stewart, the US Surgeon General, was quoted in 1967 saying “the time has come to close the book on infectious diseases”, illustrating the growing optimism [Upshur 2008 WHO]. The premature celebration of the victory in the combat against bacterial pathogens resulted in declining interest and research efforts in the field of antibiotics. Blinded by the sudden and unexpected supremacy, no new classes of antibiotics were introduced in the years from 1962 to 2000 [Walsh and Wencewicz 2013].

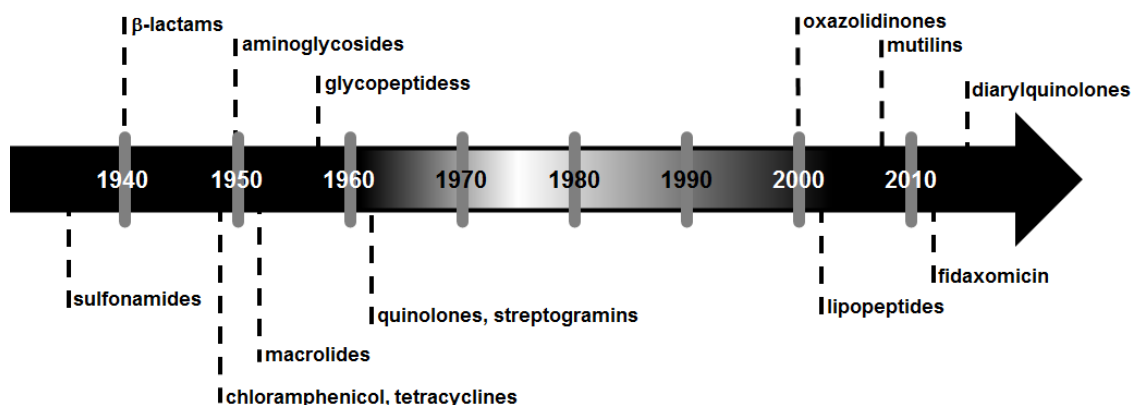


**Figure 1.** Approval of antibiotics in the time from 1935–2013 [Walsh and Wencewicz 2013].

Nowadays infectious diseases are gaining ground again and are high in number among the leading causes of death, especially in low income countries [WHO, World

Health Statistics 2014]. Stewart's statement was clearly falsified in the meantime by the development of bacterial resistances, which cause the emergence of microbes that are insensitive towards a particular antibiotic treatment. Resistances rise at an alarming rate and are about to turn back the clock to the pre-antibiotic era [von Nussbaum et al. 2006]. Especially hospitals, where antibiotics are heavily used, are a rich source for the development of new resistances [Leeb 2004]. The responsible genes are often located on plasmids, small circular DNAs, which can be independently replicated and swapped within the bacterial population [Walsh 2000]. Mechanisms of bacterial resistances are diverse. They comprise efflux pumps, target modifications, inactivating enzymes or bypasses of the affected pathways. Multidrug resistant (MDR) germs synergistically use these mechanisms and are therefore completely, or almost completely resistant to currently used antibiotics, drastically hampering the therapy options. *Mycobacterium tuberculosis* represents a prominent example as about 1.5 million patients die each year from tuberculosis (TB) infections [WHO 2014]. The emergence of MDR *M. tuberculosis* strains (MDR-TB), which are at least resistant to the first line TB drugs rifampicin and isoniazid or even extensively drug resistant strains (XDR-TB) that are additionally resistant towards at least one of the second line TB drugs, rises and is a major health threat [Dalton et al. 2012, Zignol et al. 2012, Haebich and von Nussbaum 2009]. Other examples are MDR resistant *Staphylococcus aureus* and *Pseudomonas aeruginosa* that are leading causes of nosocomial infections that are decreasingly under control and very difficult to treat [Baquero 1997, Aloush et al. 2006, Grundmann et al. 2006].

In the past, mainly two strategies were pursued to overcome existing resistances. One is the combined administration of several antibiotics, to lower the likelihood of resistance development. Another method aims for the resistance mechanisms themselves exemplified for the  $\beta$ -lactams, which can be applied together with the  $\beta$ -lactamase inhibitor clavulanic acid. Both strategies are ineligible to treat MDR pathogens, stressing the urgent need for antibacterials with novel target-sites or mechanisms of action.

## 1.1 Rational Drug Design

Prior to the 1960s, drug discovery was exclusively a trial and error process. Thousands of compounds with natural or synthetical origin were screened for a desired effect. Upon finding of a promising lead compound, medicinal chemists

generated libraries comprising hundreds of derivatives. Thereby, development of a safe and effective drug mainly depended on serendipity [Kaul 1998, Rester 2008]. A major drawback of screening is that it does not reveal the mode of action of the obtained hits and thus does not give any hints how to optimize the molecules [Reddy and Parrill 1999]. Rising costs and a focus on resource saving methods rendered the screening approach less attractive and triggered the development of rational drug discovery. Advancements in this field were mainly enabled by tremendous progress in computational techniques, statistics, structural biology and biophysical methods [Mavromoustakos et al. 2011].

### **1.1.1 Early statistical approaches**

Studies from Hansch and Topliss in 1960-1980 [Hansch et al. 1962, Hansch 1969; Topliss 1972, 1977] decisively changed the drug optimization process [Reddy and Parrill 1999]. Hansch developed a statistical method (Hansch analysis) that established the basis for quantitative structure activity relationships (QSAR). For the first time, biological activities were correlated with structural properties like the Hammett substituent and partition coefficients [Hansch et al. 1962]. Topliss applied the Hansch approach in drug design and developed systematic schemes, which should maximize the chances to obtain the most potent analogues of a compound series as early as possible [Topliss 1972, 1977].

### **1.1.2 Ligand-based approaches**

The next steps were taken through the introduction of ligand-based approaches, starting in the late 1970s [Marshall et al. 1979]. They can especially be utilized if no 3D target-structure is available [Yang 2010]. These methods make use of structural information about molecules that cause the same biological response [Reddy and Parrill 1999] and can be mainly separated into pharmacophore modeling and 3D-QSAR.

Pharmacophore modeling is a computational technique that generally encompasses two steps. Firstly a set of compounds binding to the same target (training set) is subjected to a flexible alignment. Herein the molecules are superimposed in a three dimensional space according to their structural features. In a second step, the common functionalities, necessary to ensure optimal biological activity, can be

determined. The ensemble of these features represents the so called pharmacophore model (Fig. 2) that can subsequently be used to guide *de novo* synthesis, or a targeted pharmacophore-based virtual screening of 3D databases, to develop new drugs with effects on the investigated target [Wermuth et al. 1998, Yang 2010, Vuorinen et al. 2014].

Comparative molecular field analysis (CoMFA) [Cramer et al. 1988] is an alternative ligand-based technique and has become a prototype of 3D QSAR [Podlogar and Ferguson 2000]. It considers the extent of molecular fields that surround ligands rather than their direct structural features. Like in the above mentioned process of pharmacophore determination, the ligands are first aligned in a 3D space and subsequently placed into a virtual 3D grid box. Afterwards, different chemical probes are used to determine the strength of interactions (hydrophobic, polar, hydrogen bonds etc.) at each grid point. The results of these measurements deliver a structure of interactions on the molecular surface. Thus, using CoMFA, the quantitative influence of specific molecular features on the biological activity can be identified [Verma et al. 2010].

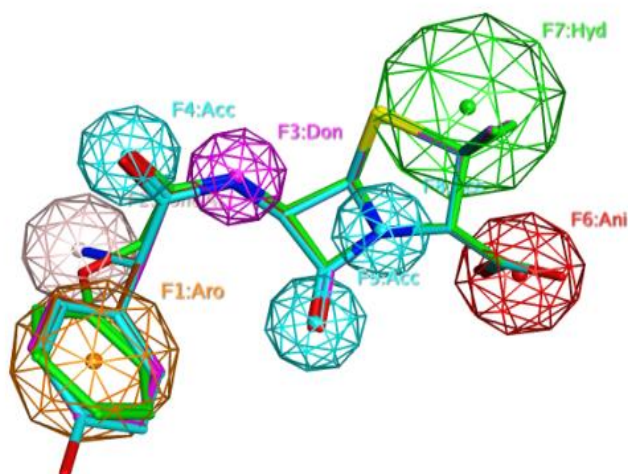


**Figure 2.** Pharmacophore model based on the flexible alignment of penicillin derivatives.

### 1.1.3 Structure-based approaches

Major breakthroughs in x-ray crystallography and nuclear magnetic resonance (NMR) investigations on proteins, caused the latest revolution in rational drug design. For the first time, 3D structural information of the protein could be utilized to search for, or

to synthesize molecules, exhibiting an appropriate conformation while carrying suitable functional groups to form favorable interactions with the target protein.

A pharmacophore, representing the prerequisite features for potent molecules, can also be determined as a negative fingerprint of a putative binding site. In contrast to the ligand based approach, such a pharmacophore can also include features that are not covered by known ligands and can also be used for virtual screening of chemical libraries or synthesis of matching compounds [Yang 2010].

The gold standard of modern structure based design is given by co-crystal structures that visualize how a ligand binds to its contact site. Important interactions as well as the appropriate conformation can be derived from such data. Thus, making use of complex-structures enables a targeted optimization of the ligands for example by rigidification or introduction of additional functional groups to generate new interactions. In some cases co-crystal structures of promising ligands cannot be obtained due to various reasons. Molecular docking, a computational technique, can be a solution of such problems. Based on complex algorithms it is able to predict the probability of different conformations and interactions of a ligand with a particular binding site. These results have to be treated with caution and need to be frequently evaluated by experimental results.

In conclusion, rational drug design provides several tools that allow a targeted optimization of hit and lead compounds enabling a straightforward drug development.

#### **1.1.4 Biophysical methods in rational drug design**

Modern biophysical techniques are currently involved in drug design in two ways: (1) qualitative detection of small molecules binding to a particular target and (2) quantitative determination of physical parameters associated to binding [Renaud and Delsuc 2009]. The latter enables detailed investigations of receptor ligand interactions contributing to a rational drug design strategy. Some of the available biophysical methods, utilized in this thesis, should be briefly introduced in the following.

#### 1.1.4.1 Isothermal titration calorimetry (ITC)

ITC is a technique to rapidly characterize the thermodynamics of interactions like for example binding of a ligand to a receptor. Thereby it enables the determination of enthalpic ( $\Delta H$  [kcal mol<sup>-1</sup>]) as well as entropic changes ( $\Delta S$  [kcal mol<sup>-1</sup>]) of the reaction that result in the free binding energy ( $\Delta G$  [kcal mol<sup>-1</sup>]) according to equation 1 ( $T$  = temperature [K];  $R$  = gas constant: 8.314 J (mol K)<sup>-1</sup>;  $K_A$  = association constant [mol L<sup>-1</sup>];  $K_D$  = dissociation constant [mol L<sup>-1</sup>]).

$$\text{Equation 1: } \Delta G = \Delta H - T\Delta S = RT\ln K_A = -RT\ln K_D$$

$\Delta G$  reports on the binding affinity in total. Whereas  $\Delta H$  is associated with forming and breaking of non-covalent bonds upon formation of the receptor-ligand complex, the change in entropy ( $\Delta S$ ) is due to the overall changes in the degrees of freedom of a system [Ladbury 2010]. These shifts can for example be caused by liberation of highly ordered water molecules in the binding site, or losses of ligand flexibility.

Being equipped with detailed knowledge on the thermodynamics of a molecular interaction, this information can help to better understand the biological system, and to optimize molecules in a rational design process.

Furthermore, ITC provides the opportunity of assessing the stoichiometry of a ligand-receptor interaction and thus enables to distinguish real hits and artifacts resulting from a screening.

#### 1.1.4.2 Surface plasmon resonance (SPR)

Application of SPR in drug discovery can be used to analyze the interaction between ligands and a particular receptor. In a typical SPR experiment, the receptor is immobilized on the surface of a biosensorchip while the ligand is injected in solution (Fig. 3). Binding of ligand molecules leads to an alteration of the refractive index near the medium of the surface. This change can be monitored in real time to measure accurately the amount of bound ligand, its affinity for the receptor and the association and dissociation kinetics of the interaction [Cooper 2002].

Availability of ligands with known binding sites allows for SPR competition experiments. In such experiments it can be investigated to which extent the binding

affinity of a compound of interest, is influenced by the presence of a known ligand. The results can be used to determine or narrow down the binding site of the investigated compounds.

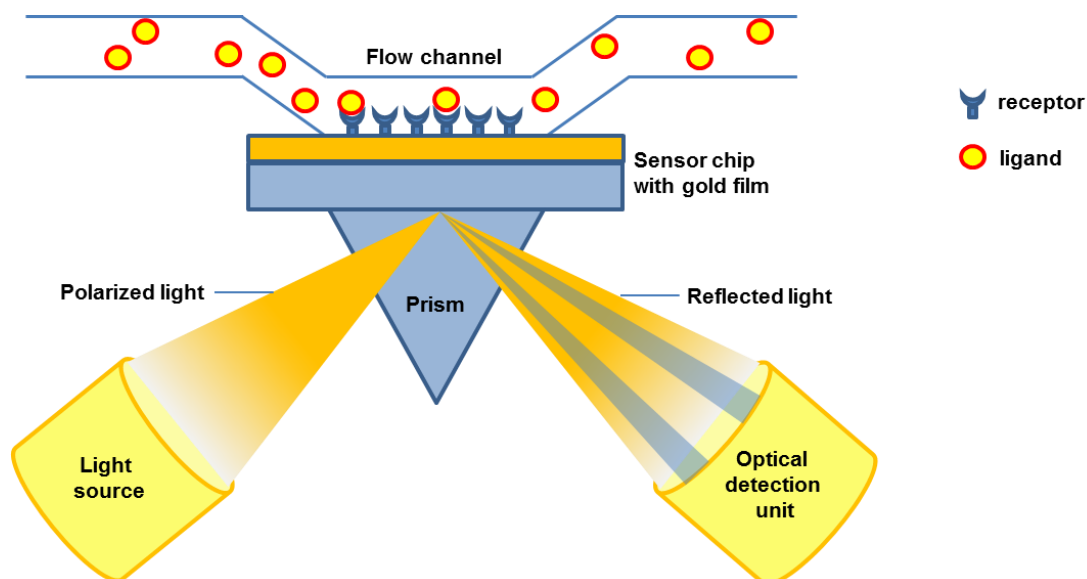


**Figure 3.** Schematic illustration of the set-up of a typical SPR experiment, adapted from [Cooper 2002]. A ligand solution is pipelined over a biosensorchip, loaded with immobilized receptor molecules. Binding of ligand molecules causes a change of the refractive index which can be determined by the optical detection unit.

#### 1.1.4.3 Nuclear magnetic resonance (NMR)

Ligand-based NMR experiments like saturation transfer difference (STD) NMR and interligand NOE for pharmacophore mapping (INPHARMA) that involve both, receptor and ligand, are valuable techniques to deeply study receptor-ligand interactions.

STD-NMR [Mayer and Meyer 1999] can be used to provide information on binding epitopes distinguishing the functional groups of a ligand that are involved in interactions to the receptor and such that are not. These results can facilitate the decision at which position a molecule should be modified in order to improve its binding affinity.

INPHARMA NMR is a powerful technique enabling determination of the relative orientation of two competitive ligands A and B. Therefore the receptor is incubated with a mixture of A and B, and a NOESY spectrum is recorded. In simplified terms, A binds to the receptor and one of its protons ( $H_A$ ) transfers its magnetization to proton

$H_R$  of the receptor. After dissociation of A, B can bind and the aforementioned magnetization can now be transferred to proton  $H_B$  of ligand B, causing a NOE signal meaning that  $H_A$  and  $H_B$  are in close proximity to  $H_R$  in the respective ligand-receptor complexes (Fig. 4). Observation of a number of such interligand NOE signals visualizes the relative orientation of the two ligands [Sanchez-Pedregal 2005]. In such cases where a crystal structure of the receptor with ligand A is available, this method enables a rational structure-based optimization of ligand B.

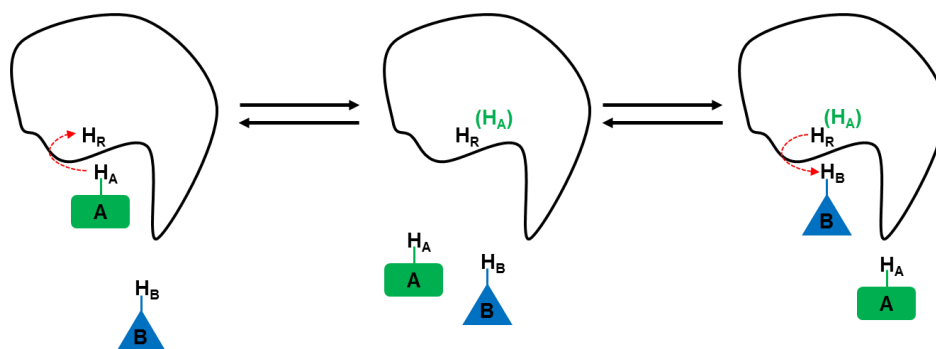


**Figure 4.** Schematic illustration of the proceedings during the INPHARMA NMR measurement, adapted from [Sánchez-Pedregal et al. 2005]. From left to right: When ligand A binds, proton  $H_A$  transfers its magnetization to the receptor proton  $H_R$ . After dissociation of the receptor-ligand A complex, B binds and the magnetization is then transferred to its proton  $H_B$ , resulting in an interligand NOE signal.

## 1.2 Bacterial RNA polymerase as a target for antibiotics

The bacterial RNA polymerase (RNAP) is a validated target for antibacterial substances which follows from three facts [Darst 2004, Chopra 2007, Mukhopadhyay et al. 2008]. It is a key enzyme in protein biosynthesis catalyzing the pivotal transcription process and therefore guarantees the efficacy of RNAP inhibitors. The enzyme is highly conserved among a wide range of bacteria, enabling the development of broad spectrum antibiotics. Finally, the protein sequences of bacterial and eukaryotic RNAP bear significant differences permitting therapeutic selectivity. The macromolecule is composed of a catalytic core comprising the subunits  $\alpha$ ,  $\beta$ ,  $\beta'$ ,  $\omega$ , and a dissociable  $\sigma$ -factor (Fig. 5). The latter is important for promoter recognition and therefore fine-tunes gene expression [Tupin et al. 2009]. Around the turn of the millennium, several x-ray structures of the bacterial RNAP have been elucidated revealing a “crab-claw” shaped structure [Zhang et al. 1999, Ebright 2000]. The pincers are formed by the two biggest subunits  $\beta$  and  $\beta'$  that

encase a 27 Å wide channel ending in a  $Mg^{2+}$  containing active center cleft. Opening of the claw allows a double-stranded DNA template to enter the enzyme and bind to the catalytic center. Subsequent clamp closure around the bound DNA enables transcription initiation [Brueckner and Cramer 2008, Haebich and von Nussbaum 2009].

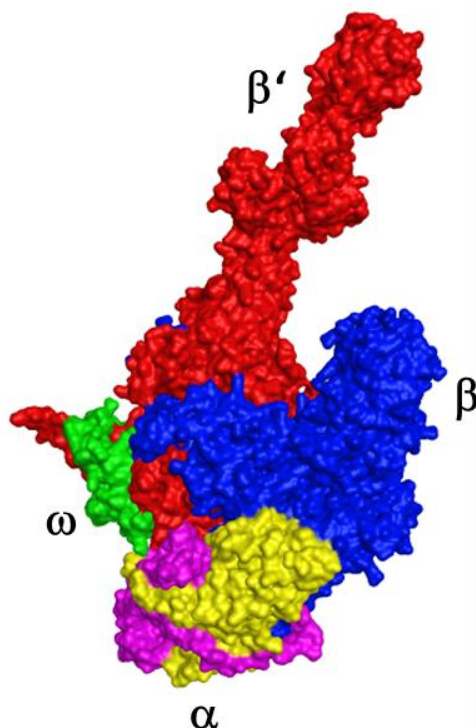


**Figure 5.** Schematic illustration of the bacterial RNA polymerase revealing the shape of a crab claw.

Although being a validated drug target, the rifamycins and the lately approved fidaxomicin are the only RNAP inhibitors in clinical use. Rifamycins are the most prominent RNAP inhibitors being used since the 1960s. Based on their outstanding antimycobacterial effects, rifamycins are first line drugs in the treatment of tuberculosis infections. They bind close to the active site of the RNAP, inhibiting the extension of small RNA transcripts and thus the transcription [Campbell et al. 2001, Chopra 2007]. Rifamycins are prone to resistance development as their contact site on the  $\beta$ -subunit is located in a relatively dispensable region [Campbell et al. 2001, Artsimovitch et al. 2005, 2012]. Thus, point mutations in this area drastically decrease their antibacterial activity. Moreover, the fitness costs associated with these mutations can be compensated by additional mutations in RNAP genes, supporting the evolution and competitiveness of resistant strains [Comas et al. 2011].

The second clinically used RNAP inhibitor fidaxomicin was approved by the US Food and Drug Administration (FDA) in 2011, as a narrow spectrum antibiotic for the treatment of *Clostridium difficile* infections [Artsimovitch et al. 2012]. Molecular biological experiments showed that fidaxomicin inhibits the separation of DNA strands which is necessary for transcription. Thus it only blocks the RNA synthesis if added before formation of the open promoter complex. In further experiments, spontaneous mutants were generated and sequenced. The results suggest, that fidaxomicin targets the “switch region” and thus binds distant from the rifamycins. Not surprisingly rifamycin-resistant bacteria possess no cross-resistance to fidaxomicin, which renders the “switch region” an interesting target site for the development of new RNAP inhibitors in order to overcome rifamycin resistances [Kurabachew et al. 2008, Venugopol and Johnson 2012].

### 1.3 The “switch region” of bacterial RNAP; target site for $\alpha$ -pyrone antibiotics

The “switch region” of bacterial RNAP is located at the conjunction of  $\beta$  and  $\beta'$  subunit at the lower end of the “crab claw”. It is often described as a hinge that mediates opening and closing of the active center cleft [Mukhopadhyay et al. 2008, Haebich and von Nussbaum 2009]. As it is conserved among various bacterial strains, the “switch region” bears the potential to be a target for broad spectrum antibacterials [Mukhopadhyay et al. 2008]. In 2008, the “switch region” was found to be the binding site for the closely related  $\alpha$ -pyrone antibiotics myxopyronin (**myx**) and corallopyronin (**cor**). **Myx** and **cor** were isolated for the first time in the mid 1980s by Irschik and co-workers [Irschik et al. 1983, 1985, Kohl et al. 1983] from the soil bacterium *Myxococcus fulvus* Mx f50. Both are composed of an  $\alpha$ -pyrone core decorated with a carbamate containing side-chain (eastern chain), and a hydrophobic side-chain (western chain) at the opposite site of the core (Chart 1). Besides low toxicity, **myx** and **cor** feature good *in vitro* inhibitory potency of bacterial RNAP coming along with strong antibacterial effects against Gram-positive strains. As already described for fidaxomicin, “switch region” inhibitors possess no cross-resistance to rifamycins which makes their further development worthwhile. In the meantime, the biosynthetic pathways of **myx** and **cor** have been elucidated [Erol et al. 2010, Sucipto et al. 2013]. In both cases the two chains are produced independently by multimodular

enzymatic machineries and combined in a final enzymatic step to give rise to the characteristic  $\alpha$ -pyrone ring (Fig. 6).

The crystal structure of *Thermus thermophilus* RNAP in complex with **myx** (PDB-ID 3DXJ) [Mukhopadhyay et al. 2008] reveals its binding contacts. The eastern sidechain reaches into a narrow channel. Its polar carbamate function forms several water mediated hydrogen bonds with the protein and is therefore decisive for binding. The carbonyl oxygen of the ester function in the  $\alpha$ -pyrone core interacts with a  $\beta$ -Ser1084 at the entrance of the “switch region”. The western chain of **myx** is lipophilic bearing two conjugated double bonds and consequently occupies a mainly hydrophobic area of the “switch region”.

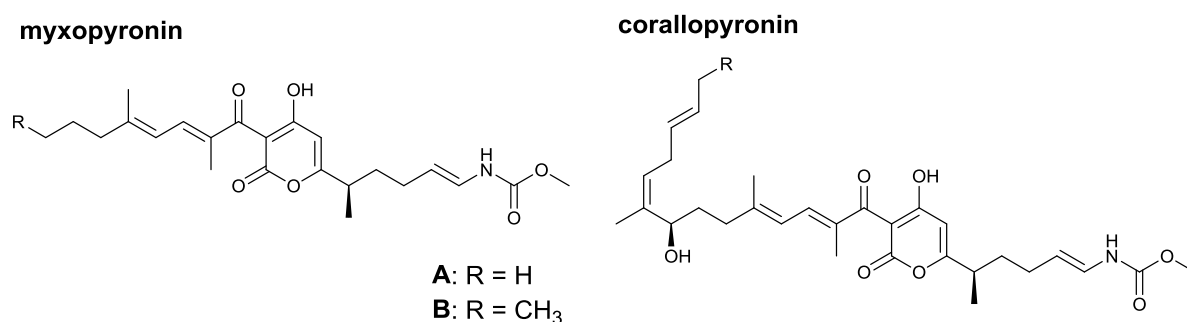


**Chart 1.** Natural  $\alpha$ -pyrone antibiotics **myx** A/B and **cor** A/B.

Despite structural similarity **myx** and **cor** display interesting differences in their inhibitory mechanisms. Whereas **myx** is not able to completely block the RNA synthesis even at very high concentrations, **cor** entirely prevents RNA formation, which has to be associated with the additional alkyl chain of **cor** [Irschik et al. 1985]. Nevertheless, **myx** shows better minimal inhibitory concentration (MIC) values against several pathogens including *M. tuberculosis*, *S. aureus* and *Enterococcus faecalis* [Srivastava et al. 2011]. The discovery of the RNAP “switch region” as a binding site for antibiotics triggered the development of synthetic inhibitors following medicinal chemistry approaches. Although the compounds displayed good activity in cell-free enzyme assays, significant antibacterial effects could not be achieved [McPhillie et al. 2011, Buurmann et al. 2012].

In conclusion, natural or synthetic RNAP inhibitors, binding to the “switch region”, are attractive for further development due to their activity against rifamycin resistant

strains. Furthermore, a wide conservation of the RNAP “switch region” enables the design of broad spectrum antibiotics.

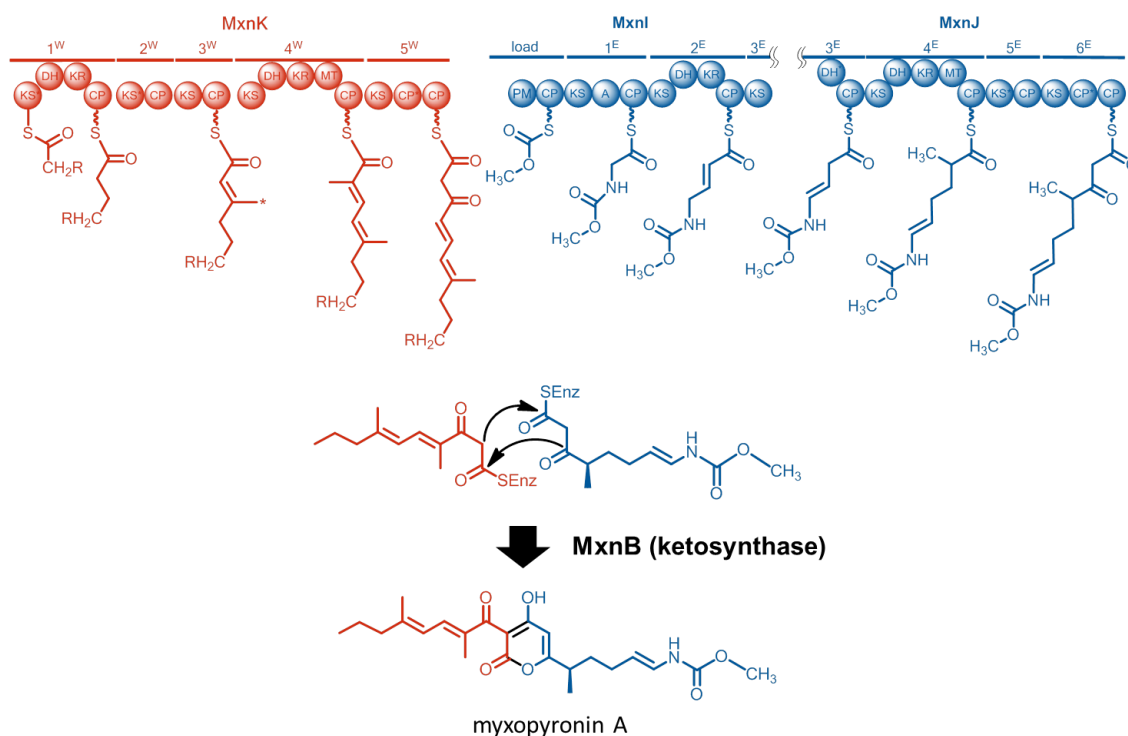


**Figure 6.** Biosynthetic pathway of **myx** [Sucipto et al. 2013]. The western chain (red) is produced by the PKS system MxnK. The eastern chain (blue) is derived from the combined PKS/NRPS system Mxnl/MxnJ. The two chains are condensed by the ketosynthase MxnB *via* intermolecular Claisen condensation.

## 1.4 Mutasynthesis

Approximately 75 percent of the FDA approved drugs for the treatment of infectious diseases have a natural origin [Newman et al. 2003]. Especially bacteria themselves are a rich source for secondary metabolites with antibacterial properties. This is not surprising taking into account their competitive struggle with other bacterial species, forcing them to develop measures for self-defense [von Nussbaum et al. 2006]. The natural compounds are often highly potent and selective but suffer from poor physicochemical properties which have to be improved by medicinal chemistry approaches in order to turn them into clinically applicable drugs [Kennedy 2008; Haebich and von Nussbaum 2009]. Many chiral centers as well as the presence of various functional groups frequently hamper their total synthesis and thus the generation of improved derivatives. These features consequently lead to synthesis routes comprising many steps and often low yields [Prusov 2013]. Furthermore, total

synthesis often involves the application of hazardous and/or expensive chemicals making an industrial scale up difficult [Kennedy 2008, Anderson 2012].

Over the past decades, several alternatives have been developed to generate natural product derivatives, which can compensate for the drawbacks of total synthesis approaches. Two examples are the precursor directed biosynthesis (PDS) and the closely related mutasynthesis that is briefly explained in the following. During biosynthesis, a natural product is usually built in a step by step process involving multimodular enzyme complexes, as illustrated in Fig. 7a. In PDS, synthetic molecules mimicking the naturally used intermediates are fed to a bacterial culture. In case of success, the artificial substrates are incorporated resulting in new derivatives of the respective natural product (Fig. 7b). As the synthetic precursors compete with the natural substrates, incorporation is often insufficient. To circumvent this problem, mutasynthesis has been developed. Herein, the biosynthetic pathway is interrupted by a targeted mutation to prevent formation of the respective native intermediate. A now applied synthetic precursor, structurally adjusted to the subsequent enzymatic steps, will then be rather accepted and incorporated, to yield novel natural product derivatives (Fig. 7c) [Kirschning et al. 2007].

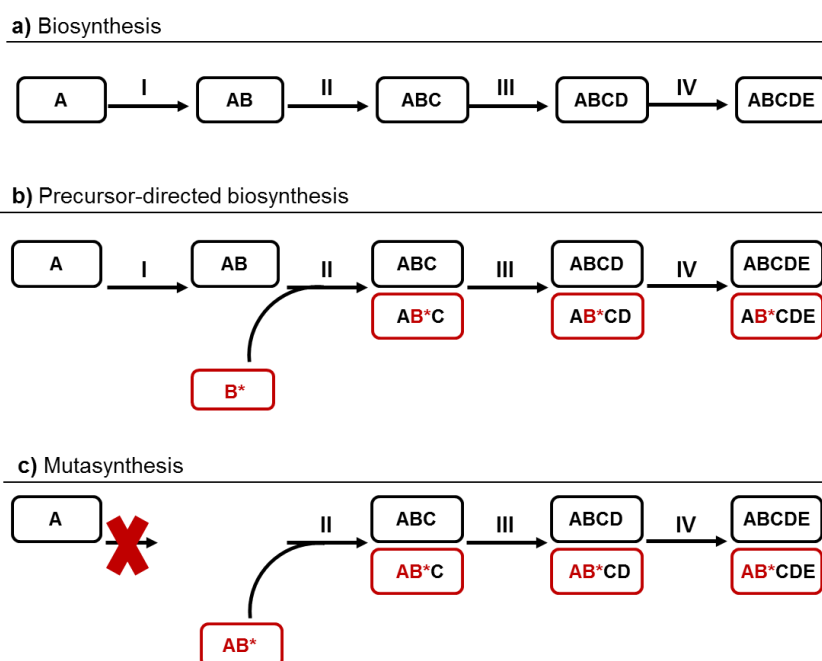


**Figure 7.** Schematic illustration of the multi-step assembly of natural products and their derivatives in a) biosynthesis; b) precursor-directed biosynthesis and c) mutasynthesis. Natural precursors and intermediates are labeled in black, artificial ones in red. Roman numerals designate the respective biosynthetic steps. Adapted from [Kirschning et al. 2007].

Due to the structural requirements for acceptance by the biosynthetic enzymes, PDS and mutasynthesis can certainly not reach the flexibility of total synthesis. Nevertheless several successful examples show that these methods can significantly broaden the chemical space of natural products and yield compounds that are difficult to access *via* chemical synthesis [Zlatopolskiy et al. 2006, Grond et al. 2000, Gregory et al. 2005, Dutton et al. 1991].

## 1.5 *Pseudomonas aeruginosa*

*P. aeruginosa* is a Gram negative rod-shaped bacterium initially discovered in 1900 by the German botanist Walter Migula. It is an opportunistic pathogen which can adapt to many natural environments, growing on plants and animal tissues as well as soil, marshes and coastal marine habitats [Khan et al. 2010, Stover et al. 2000]. *P. aeruginosa* can cause a number of severe diseases, like for instance urinary tract infections in catheterized persons or hospital acquired pneumonia in artificially respiration patients [Bodey et al. 1983]. Moreover it is a leading cause of death in cystic fibrosis patients [Dubern and Diggle 2008]. During the last years *P. aeruginosa* has become a major cause of nosocomial infections [de Bentzmann and Plésiat 2011, Stover et al. 2000] and therefore gained center stage in drug discovery programs. *P. aeruginosa* infections have historically been one of the most hard to treat [O'Shea and Moser 2008]. Being a Gram negative bacterium, the pathogen is naturally equipped with an orthogonal double membrane system that makes it hardly permeable for antibacterial substances. A polysaccharide beset outer membrane hampers the entrance of lipophilic compounds whereas the hydrophobic inner membrane closes the gate for too hydrophilic molecules. In a comprehensive study on the physicochemical requirements of antibiotics, O'Shea mentions a  $\log D_{7.4}$  below 0 and a molecular weight cutoff of approximately 600 Da as prerequisite for molecules to enter *P. aeruginosa* [O'Shea and Moser 2008]. In addition, *P. aeruginosa* possesses diverse efflux pump systems (e.g. MexAB-OprM, Mex-CD-OprJ, MexXY-OprM) with a broad substrate specificity, discharging numerous molecules that successfully entered the cell interior [Masuda et al. 2000]. Moreover *P. aeruginosa* is able to form biofilms which is associated with persistent infections that further complicate antibacterial treatment and hamper the human immune response [Bjarnsholt et al. 2010]. Such biofilms are extracellular polymeric matrices consisting of polysaccharides, extracellular DNA, proteins, lipids and

biosurfactants embedding the bacteria. The formation of biofilms occurs in distinct steps comprising surface attachment and multiplication, microcolony formation, followed by differentiation into a mature, structured biofilm (Fig. 8) [Costerton et al. 1999, Whiteley et al. 2001]. Lowered metabolic activity and prolonged doubling times of cells growing in biofilms decrease the antibacterial effectiveness of many antibiotics [Hoiby et al. 2010]. Furthermore, studies on the gene expression in biofilms show significant differences to free-living cells, causing antibiotic resistances especially to tobramycin, a front-line drug used to treat *P.aeruginosa* infections [Whiteley et al. 2001].

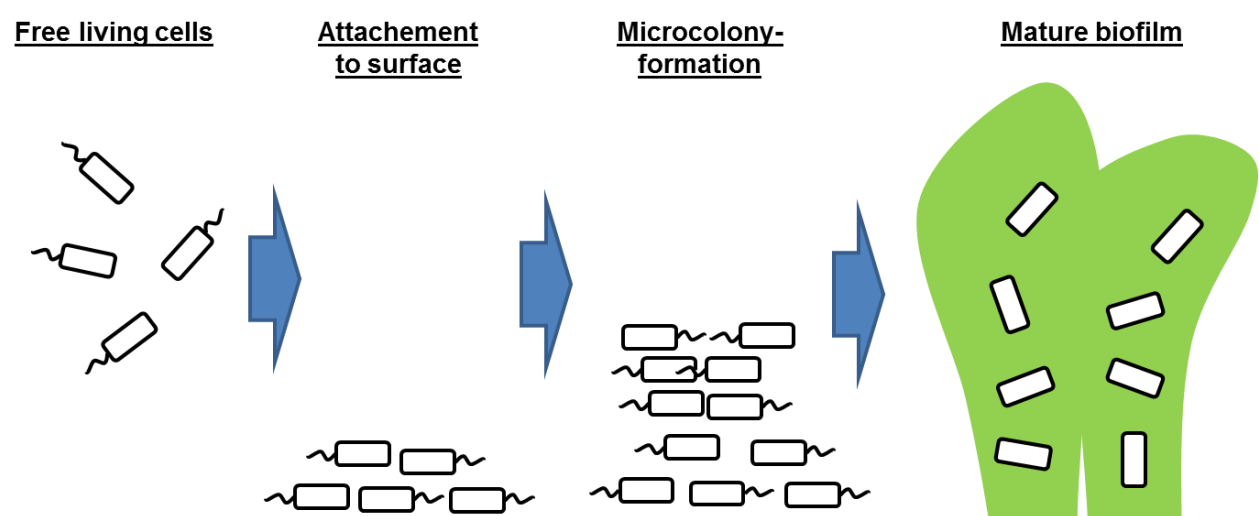


**Figure 8.** Schematic illustration of distinct steps during biofilm formation, adapted from [Costerton et al. 1999].

Besides the described intrinsic insusceptibility, the pathogen can rapidly acquire further antibiotic resistances *via* mutation or horizontal gene transfer rendering the common therapy options ineffective. These mechanisms are even more pronounced among biofilm-growing cells [Driffield et al. 2008, Molin and Tolker-Nielsen 2003].

Taken together new antibiotics are urgently needed to stay forearmed against infections caused by *P. aeruginosa*. In the meantime, the whole genome sequence of *P. aeruginosa* has been elucidated and many virulence mechanisms have been discovered [Stover et al. 2000, de Bentzmann and Plésiat 2011]. This provides new opportunities to develop antibiotics with novel targets to fight *P. aeruginosa* infections. Inhibition of the bacterial quorum sensing system is a promising example which will be described in detail in paragraph 1.6 and 1.7.

## 1.6 Quorum Sensing in *P. aeruginosa*

For a long time, bacteria were regarded as individual and autonomous organisms. The discovery of bacterial cell-to-cell communication systems changed this perspective. Nowadays it is widely accepted that bacteria employ a variety of techniques, termed quorum sensing (QS), enabling a social behavior. In order to communicate, bacteria produce and secrete signal molecules, comparable with human hormones, being detected by the surrounding cells. As the signal strength rises as a function of cell count, the bacterial community can utilize it to assess its cell density [Swift et al. 2001]. Awareness of the population size equips the bacteria with the ability to effectively coordinate group behavior and thus, perform concerted actions. These include for example the production of virulence factors and the formation of biofilms, both decisively contributing to pathogenicity [Whiteley et al. 1999]. Whereas Gram positive bacteria predominantly use small hydrophobic oligopeptides, Gram negative cells apply a number of small, structurally diverse molecules [Miller and Bassler 2001, Federle and Bassler 2003]. Upon binding to their respective receptors, the resulting complex autoinduces the genes that are involved in the production of signal molecules. This positive feedback guarantees a rapidly rising signal when a certain cell-density threshold has been reached [Williams et al. 1992].

QS in *P. aeruginosa* is a tripartite system consisting of two *N*-acylhomoserine-lactone (AHL) dependent circuits (*las* and *rhl*) and a 2-alkyl-4-quinolone (AQ) system (Fig. 9). In the *las* system, LasI conducts the synthesis of *N*-(3-oxo-dodecanoyl)-*L*-homoserine lactone (3-oxo-C12-HSL). 3-Oxo-C12-HSL interacts with the LasR receptor, a transcriptional regulator, which activates target promoters [Gambello and Iglewsky 1991, Passador et al. 1993, Dubern and Diggle 2008]. Furthermore LasR activation is associated with the production of the virulence factors elastase and alkaline protease [Gambello and Iglewsky 1991, Dubern and Diggle 2008]. The processes in the closely related *rhl* system are similar. Herein RhlI directs the synthesis of *N*-(butanoyl)-*L*-homoserine lactone (C4-HSL) which activates the transcriptional regulator RhlR, followed by activation of target promoters [Ochsner et al. 1994, Ochsner and Reiser 1995, Dubern and Diggle 2008]. Moreover, production of the virulence factors pyocyanin, LecA, elastase, rhamnolipids, hydrogen cyanide and alkaline protease increases upon activation of RhlR [Dubern and Diggle 2008].

Besides the described AHL-systems that are widespread among Gram negative bacteria, *P. aeruginosa* is additionally equipped with an AQ system, termed *pqs*, that

exclusively exists in certain *Pseudomonas* and *Burkholderia* strains [Pesci et al. 1999, Diggle et al. 2006]. It regulates several virulence phenotypes for e.g. biofilm formation, elastase production and membrane vesicle formation [Pesci et al. 1999, Heeb et al. 2011, O'Connell et al. 2013].

2-Heptyl-3-hydroxy-4-quinolone (*Pseudomonas* quinolone signal, short form PQS) and its precursor 2-heptyl-4-quinolone (HHQ) are the two main signal molecules in the *pqs* system. The enzymatic machinery responsible for their biosynthesis underlies the expression of the *pqsABCDE* operon. The characteristic feedback loop described above for *las* and *rhl*, exists also here [Xiao et al. 2006]. Upon binding of HHQ or PQS to the transcriptional regulator PqsR (formerly termed MvfR for multiple virulence factor regulator), the activated PqsR triggers expression of the *pqsABCDE* operon resulting in rising HHQ and PQS levels. Compared to HHQ, PQS binds with a 100 fold higher affinity to PqsR [Xiao et al. 2006]. Furthermore it is able to chelate Fe(III), a pivotal nutrient for *P. aeruginosa*, potentially facilitating its uptake into the cell [Diggle et al. 2007]. Moreover it has been shown that PQS is able to down-regulate the host innate immune response [Kim et al. 2010].

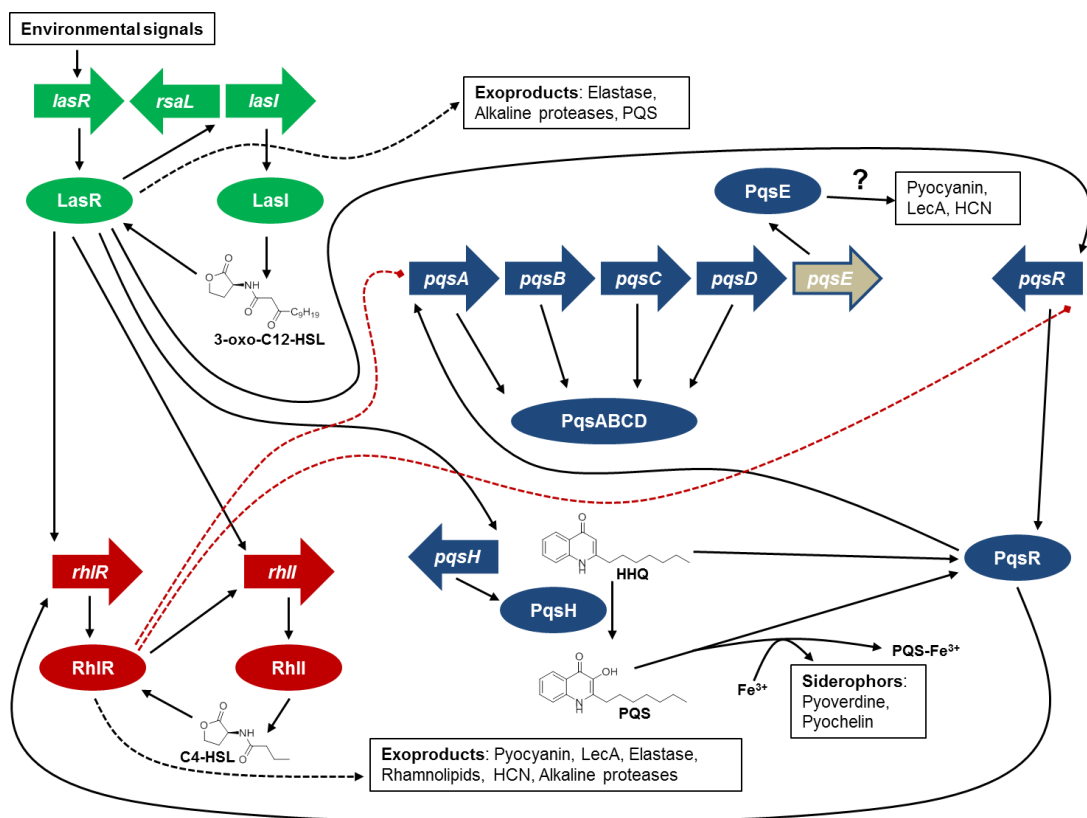


**Figure 9.** Schematic illustration of the quorum sensing system in *P. aeruginosa* [Dubern and Diggle 2008].

The function of PqsE is not entirely clarified. It is encoded by the *pqsABCDE* operon without taking part in the AQ biosynthesis. Nevertheless it controls the production of important virulence factors like elastase and pyocyanin [Yu et al. 2009, Rampioni et al. 2010].

The three QS systems of *P. aeruginosa* are closely linked and thus influence each other. The *las* system is considered superordinate, controlling both, the *rhl* as well as the *pqs* circuit. Whereas activated PqsR triggers expression of *rhlR*, its product RhlR down-regulates expression of the *pqsABCDE* operon. The connection among the systems is further confirmed by a study with several *Pseudomonas aeruginosa* strains, mutated in their distinct QS-pathways including *lasR*<sup>-</sup>, *rhlR*<sup>-</sup>, *pqsR*<sup>-</sup>, *pqsC*<sup>-</sup> and *pqsD*<sup>-</sup> knock-out mutants. All of them were defective in the production of the virulence factor pyocyanin [Gallagher et al. 2002] Taking this into consideration, inhibition of one of the respective QS circuits might also affect the others resulting in extensive effects.

## 1.7 Inhibition of *P. aeruginosa* QS as an anti-virulence strategy

As the name suggests, antibiotics kill bacteria by inhibiting their important cell functions. These mainly include DNA/RNA synthesis, cell wall synthesis, protein biosynthesis, folate synthesis or cell membrane integrity (Fig. 10) [Wright 2010]. Affecting the viability of bacteria creates selection pressure and therefore inevitably leads to resistances against these antibacterial agents, limiting their efficacy and life-span [von Nussbaum et al. 2006]. Hence, there is a continuous need for novel antibiotics.

Recent strategies to break out of this vicious cycle include the development of anti-infectives that attenuate the virulence of bacteria by inhibiting the bacterial cell-to-cell communication systems [O'Connell et al. 2013, Kalia and Purohit 2011]. The basic idea underlying this approach is, that turning infective bacteria into harmless microbes might not cause a selection pressure and consequently does not favor the development of resistant bacteria [Defoirdt et al. 2010, Hentzer et al. 2003, Njoroge and Sperandio. 2009]. As the fitness implications associated with the blockage of QS are not entirely clear, this idea is controversially discussed [Maeda et al. 2012]. Nevertheless, interference with QS might be an attractive attacking point in this

context. Production and secretion of numerous virulence factors in *P. aeruginosa* depend on cell-to-cell communication [Bera et al. 2009]. Therefore, jamming these systems should significantly reduce pathogenicity.

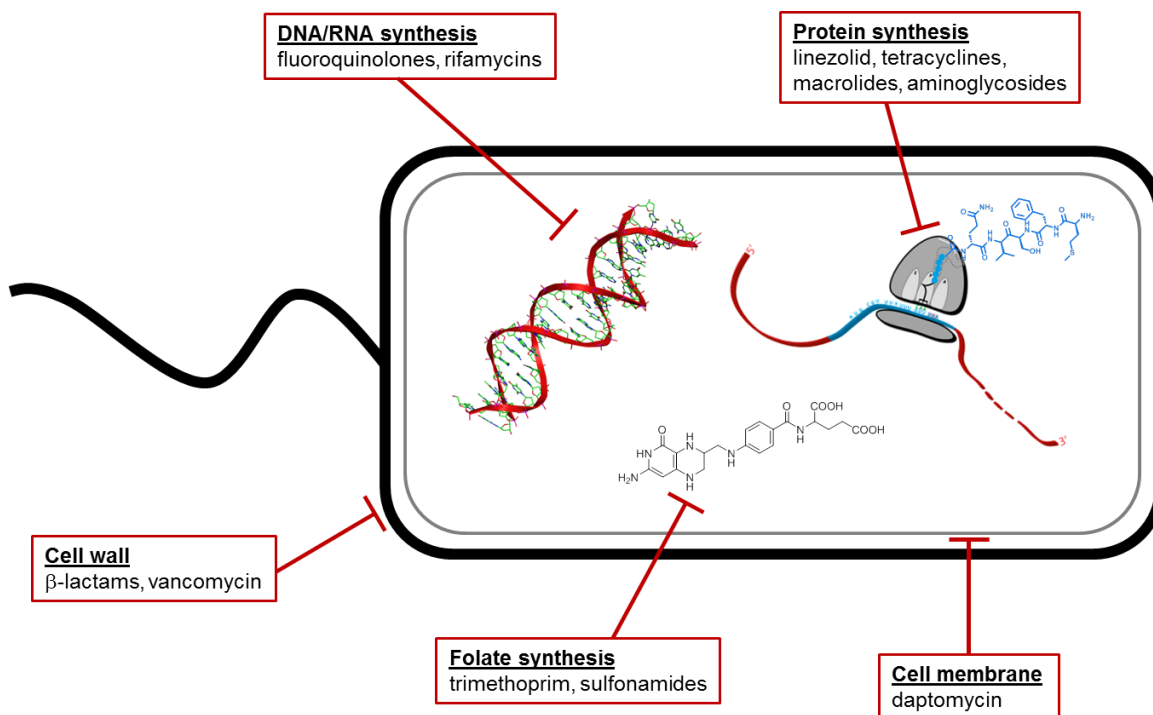


**Figure 10.** Targets of antibiotics, adapted from [Wright 2010].

This theory could already be proven for several QS inhibitors, (Chart 2) of which some should be briefly introduced. The first compounds that delivered the proof of concept regarding QS inhibition as an antimicrobial target, were published by Hentzer et al in 2002, including the halogenated furanone C-30 (**A**). It downregulates the expression of numerous genes associated with QS and consequently reduces virulence factor production. Furthermore *P. aeruginosa* biofilms, grown in the presence of C-30, are much more susceptible to treatment with tobramycin [Hentzer et al. 2002, 2003, Hoiby et al. 2013]. The LasR inhibitor PD12 (**B**) can be regarded as a mimic of the natural ligand 3-oxo-C12-HSL. Its strong antagonistic potency ( $IC_{50}$ : 30 nM determined in a reporter gene assay) is reflected in the ability to decrease pyocyanin and elastase production [Müh et al. 2006]. Our group focusses on inhibition of the *pqs*-QS system in *P. aeruginosa*. In 2012 we described the first PqsR inhibitors, discovered in a ligand-based approach, originating from HHQ. Applied in low micromolar concentrations, **C** was able to reduce the pyocyanin production in *P. aeruginosa* PA14 by about 60-70% without affecting bacterial growth [Lu et al.

2012]. Advancements in this structural class yielded **D**, a potent PqsR antagonist, displaying remarkable abilities in reducing the mortality of *P. aeruginosa* PA14 infected *Caenorhabditis elegans* and *Galleria mellonella* [Lu et al. 2014]. In a related work, our group reported on further PqsR antagonists with more drug like properties (**E,F**) applying fragment-based drug design procedures [Klein et al. 2012, Zender et al. 2013]. Although displaying lower antagonistic activity, these compounds were also able to reduce the pyocyanin and HHQ production in a *P. aeruginosa* culture, while being more suitable for further development due to low molecular weight and favorable physico-chemical properties. In 2012, 2-nitrophenyl methanol derivatives (**G**) were identified in our department as potent PqsD inhibitors. They were capable of reducing the biofilm formation in planktonic *P. aeruginosa* cultures, validating PqsD as a promising drug target [Storz et al. 2012].

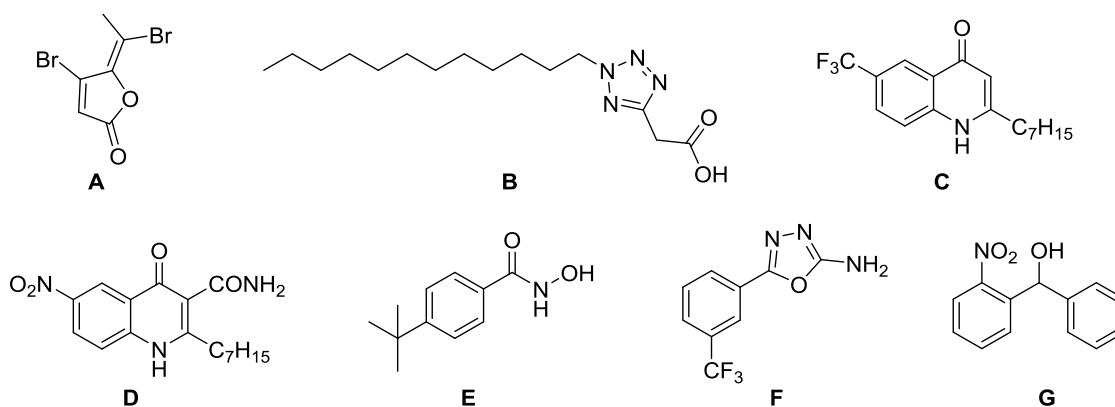


**Chart 2.** Quorum sensing inhibitors targeting the AHL- (**A,B**) or AQ- (**C-G**) mediated QS-systems in *P. aeruginosa*.

## 1.8 AQ Biosynthesis in *P. aeruginosa*

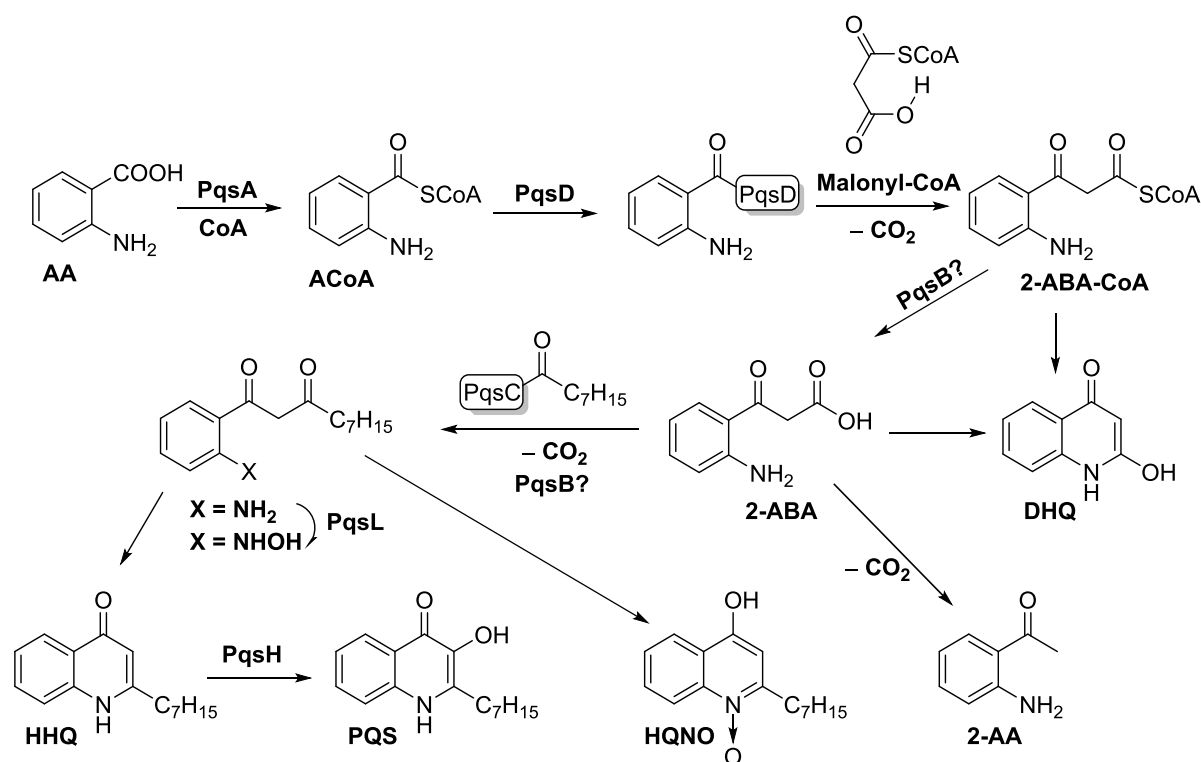
In contrast to the relatively simple *las* and *rhl* related biosynthesis pathways, AQ synthesis is more complex involving several enzymes and intermediates (Scheme 1). The biosynthetic enzymes catalyzing AQ synthesis depend on the expression of the *pqsABCDE* operon. Mutagenesis experiments proved that *pqsA*<sup>-</sup>, *pqsB*<sup>-</sup>, *pqsC*<sup>-</sup> and *pqsD*<sup>-</sup> mutants do not produce Aqs in measurable amounts [Dulcey et al. 2013] In contrast, *pqsE* does not essentially contribute to AQ biosynthesis [Diggle et al. 2003, Déziel et al. 2004, Farrow et al. 2008].

Anthranilic acid (AA) is the starting precursor of AQ biosynthesis. It originates either from the kynurenine pathway or from the alkylquinolone specific anthranilate synthase. The latter is encoded by *phnAB* [Bera et al. 2009]. After activation to its

corresponding coenzyme A (CoA) thioester by PqsA [Coleman et al. 2008] anthraniloyl-CoA (ACoA) is covalently transferred to the Cys112 residue of PqsD. Malonyl-CoA acts as the second substrate of PqsD and is linked to anthranilate under the loss of CO<sub>2</sub>, to yield 2-aminobenzoylacetate (2-ABA) in a two-step reaction *via* its CoA thioester. Once purified, 2-ABA is unstable and rapidly decomposes into 2-amino acetophenone (2-AA) and 2,4-dihydroxyquinoline (DHQ) upon storage at room temperature [Dulcey et al. 2013]. It is propagated that this reaction also happens spontaneously *in vivo* [Zhang et al. 2008].

The aliphatic tail in AQs was identified to originate from octanoic acid. Bound to PqsC, it is transferred to 2-ABA, under loss of CO<sub>2</sub>. The resulting intermediate undergoes spontaneous ring closure yielding HHQ. Oxidation of HHQ by PqsH, a NADH dependent monooxygenase, results in the main *pqs*-QS signaling molecule PQS [Schertzer et al. 2010].

The role of PqsB in the presented pathway still remains to be determined. It seems to be tightly associated to PqsC, hypothetically being involved in its correct folding, but certainly required for PqsC to be active. Only if the two enzymes are present simultaneously, production of HHQ can be accomplished [Dulcey et al. 2013].



**Scheme 1.** Biosynthesis of alkyl-quinolones in *P. aeruginosa*, adapted from [Dulcey et al. 2013].

Until recently it was believed, that HHQ is directly produced by PqsD from ACoA and  $\beta$ -ketodecanoic acid which has indeed been shown to happen *in vitro* [Pistorius et al. 2011]. This reaction was successfully used in several studies to assess the potency of PqsD inhibitors. Despite, Dulcey et al. could recently show by applying  $^{13}\text{C}$ -labeling experiments that  $\beta$ -ketodecanoic acid is not a direct precursor of HHQ *in vivo*.

The production of 4-Hydroxy-2-heptylquinoline-*N*-oxide (HQNO), the *N*-oxide of HHQ, depends on the monooxygenase PqsL [Lépine et al. 2004]. The substrate of PqsL is not known but it was hypothesized to be 2-ABA [Dulcey et al. 2013].

The important functions of PQS and HHQ in cell-to-cell communication as well as their influence on the host have already been described in paragraph 1.6. In addition, also the other agents mediate crucial effects. 2-AA itself is a volatile substance, known to promote phenotypes of *P. aeruginosa* that cause chronic infections while reducing acute virulence [Kesarwani et al. 2011]. It modulates the host immune response in a manner that facilitates persistence while supporting host tolerance [Bandyopadhyaya et al. 2012]. Zhang et al. reported that DHQ exhibits growth inhibitory effects on mouse lung epithelial cells, indicating a contribution of DHQ to the pathogenicity of *P. aeruginosa* [Zhang et al. 2008]. HQNO was described to bear antibacterial activity and thus equips *P. aeruginosa* with a powerful tool to prevail against competitive bacteria [Déziel et al. 2004, Machan et al. 1992].

In conclusion, the biosynthesis of Aqs in *P. aeruginosa* follows a complex scheme. The production of Aqs, 2-AA and DHQ elementarily depends on PqsA and PqsD that synthesize the key intermediate 2-ABA. Hence, an inhibition of these enzymes should have a major impact on cell-to-cell communication.

## 1.9 PqsD as a drug target

PqsD is a key player in the AQ biosynthesis in *P. aeruginosa*, catalyzing the synthesis of the important intermediate 2-ABA (Scheme 1), among others, origin for DHQ, HHQ and PQS biosynthesis [Dulcey et al. 2013]. Recent studies from our group show, that biofilm formation and the production of signal molecules can be decreased by inhibiting PqsD, confirming its suitability as a target for anti-virulence drugs [Storz et al. 2012].

The enzyme consists of 337 amino acids and has a molecular weight (MW) of 36.4 kDa. In solution it primarily exists as a dimer (Fig. 11a) [Bera et al. 2009]. Sequence

alignments suggest that PqsD belongs to the family of  $\beta$ -ketoacyl-ACP synthase (III) type enzymes, like FabH, an enzyme in bacterial fatty acid biosynthesis [Bera et al. 2009, Davies et al. 2000]. This assumption is strongly corroborated by crystal structures of PqsD that reveal a closely related fold to FabH enzymes from several species [Bera et al. 2009]. Furthermore astonishing parallels with chalcone and stilbene synthases can be observed especially in terms of the conserved active site residues. Chalcone and stilbene synthases are plant polyketide synthases that use similar enzymatic mechanisms as bacterial fatty acid synthases [Austin and Noel 2003, Bera et al. 2009].

PqsD is equipped with an about 15 Å deep and rather narrow binding channel with an approximate volume of 650 Å<sup>3</sup>. The channel can be divided into three parts. A positively charged entrance and a mainly hydrophobic middle segment, followed by a polar bottom part, which is delimited by the catalytic residues Cys112, His257 and Asp287 (Fig. 11b).

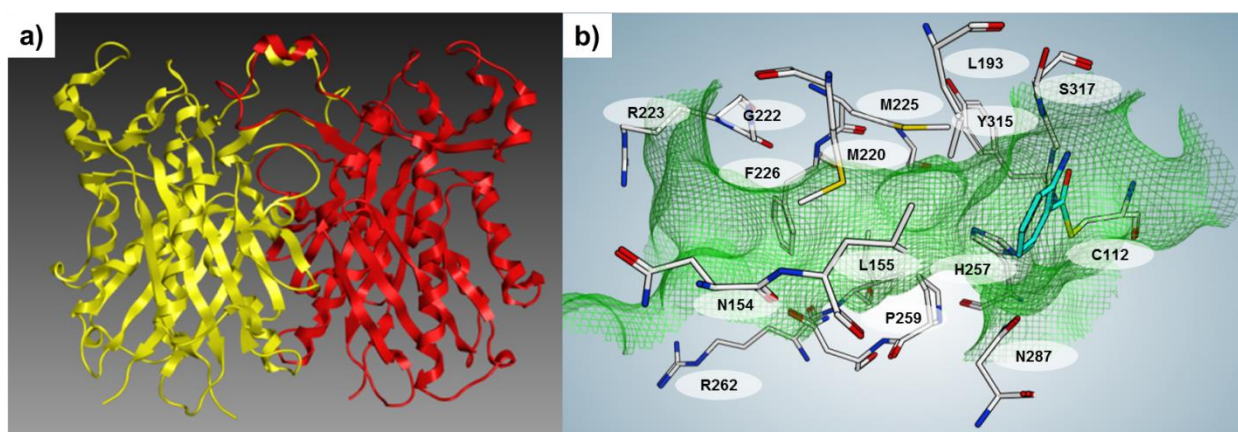


**Figure 11.** a) Secondary structure of PqsD showing a dimer. b) Binding channel of PqsD with covalently bound anthranilate (PDB-ID: 3H77). The channel is illustrated as green mesh. Protein residues and anthranilate are labeled white and turquoise respectively.

## 2 Aim of the Thesis

Bacterial resistances are on the rise and might turn back the clock to the pre-antibiotic era. Their development is just a matter of time which limits the efficacy and life-span of antibacterial agents. This creates a continuous need for new antibiotics to stay forearmed against bacterial infections. Developing substances against already known and exploited targets involves the risk of cross-resistances. It is more promising to find chemical entities that address new targets-(sites) or bearing novel mechanisms of action. This thesis aims at the generation of such antibacterial agents and can be separated into two main parts.

The first task is the development of transcription inhibitors that bind to the RNAP “switch region”, a recently discovered binding site. Two separate approaches are followed. One focusses on the structure-based optimization of a low molecular hit compound, which was discovered in a pharmacophore based virtual screening. Optimization of this compound should follow a rational design process that enables the determination of clear structure-activity relationships (SAR). Besides good target activity, the resulting inhibitors should ideally feature broad-spectrum antibacterial effects, while overcoming existing resistances.

Another approach involves natural  $\alpha$ -pyrone antibiotics from the **myx** and **cor** family. They are already known to inhibit the bacterial RNAP *via* binding to the “switch region”. The total synthesis of these natural products has been achieved but it is laborious and time-consuming. In this work an alternative route for the generation of  $\alpha$ -pyrone antibiotics should be investigated. Thereby mutasynthesis, a combined procedure comprising enzymatic and organic synthesis is used. Initial investigations focus on determination of the substrate specificity of the involved enzymes. The subsequent design of the synthetical precursors should consider the complex crystal-structure of RNAP with **myx**, to enable a targeted introduction of new substituents to generate further interactions while improving the physicochemical properties of potential novel  $\alpha$ -pyrone-derivatives.

The second part of this thesis is dedicated to the development of PqsD inhibitors, a key enzyme in the quorum sensing system of *Pseudomonas aeruginosa*. A blockade of quorum sensing has been shown to reduce the virulence of pathogens without affecting their viability. Therefore it is considered a promising novel mechanism of

action for antibacterial agents that are less prone to resistance development. Starting from an experimental hit, the target affinity should be optimized and the binding mode should be elucidated.

## 3 Results

### 3.1 Novel small molecule inhibitors targeting the “switch region” of bacterial RNAP: Structure-based optimization of a virtual screening hit

J. Henning Sahner, Matthias Groh, Matthias Negri, Jörg Haupenthal, and Rolf W. Hartmann

Reprinted with permission from *Eur. J. Med. Chem.* **2013**, 65, 223-231.

Copyright (2013) Elsevier.

#### Publication A

**Abstract:** Rising resistance against current antibiotics necessitates the development of antibacterial agents with alternative targets. The “switch region” of RNA polymerase (RNAP), addressed by the myxopyronins, could be such a novel target site. Based on a hit candidate discovered by virtual screening, a small library of 5-phenyl-3-ureidothiophene-2-carboxylic-acids was synthesized resulting in compounds with increased RNAP inhibition. Hansch analysis revealed  $\pi$  (lipophilicity constant) and  $\sigma$  (Hammett substituent constant) of the substituents at the 5-phenyl moiety to be crucial for activity. The binding mode was proven by the targeted introduction of a moiety mimicking the enecarbamate side chain of myxopyronin into the hit compound, accompanied by enhanced RNAP inhibitory potency. The new compounds displayed good antibacterial activities against Gram positive bacteria and Gram negative *E. coli* *ToIC*, accompanied by a reduced resistance frequency compared to the established antibiotic rifampicin.

## Introduction

The bacterial RNA polymerase (RNAP) catalyzes the pivotal transcription process and therefore is an attractive drug target for antibacterial agents [1–3]. Due to its high conservation among a wide range of bacteria, inhibitors of the RNAP are applicable against a broad spectrum of bacterial pathogens [4]. The architecture of the bacterial enzyme significantly differs from eukaryotic RNAP, facilitating a selective blockade of the essential bacterial cell function [5,6]. This is exemplified by a wide range of compounds which selectively effect the prokaryotic RNAP [2]. Several classes of inhibitors targeting bacterial RNAP are known [1,3], but at the current state the clinically used compounds are limited to lately approved fidaxomicin and members of the rifamycin family [2,7]. For example rifampicin is used in combination with other antibacterials, in the first line therapy of tuberculosis [3,8]. In the meantime some resistant strains, including multi-resistant *Mycobacterium tuberculosis*, emerged [4,9,10]. This creates an urgent need for the development of new classes of antibacterial agents [2,5,11].

A promising strategy to face resistance is the exploration of novel target sites [6,12]. Recently, the “switch region” has been discovered as an interesting new binding domain of bacterial RNAP [2,4]. Myxopyronin B (**1**), a natural  $\alpha$ -pyrone antibiotic isolated from the myxobacterium *Myxococcus fulvus* [13], and its synthetic derivative desmethyl myxopyronin B (**2**) [14], have been demonstrated to target this region [4,15]. Due to the different binding mode compared to the rifamycin antibiotics, compounds binding to the “switch region” are expected to overcome existent resistance [4]. Studies concerning the activity of myxopyronins towards rifamycin resistant strains of *S. aureus* have confirmed, that the “switch region” inhibitors do not exhibit cross-resistance to the rifamycins [16,17]. Although the natural compound myxopyronin B (**1**) is highly active *in vitro* ( $IC_{50} = 0.35 \mu\text{M}$ ; minimal inhibitory concentration =  $0.8 \mu\text{g/mL}$  for *E. coli TolC*), its use as a drug is hampered by insufficient physicochemical properties [18,19]. Therefore small molecule inhibitors possessing a higher *in vivo* efficacy should be developed.

Another project of our group is focused on the optimization of novel RNAP inhibitors of the benzamidobenzoic acid type, identified by a virtual screening, based on the flexible alignment of known inhibitors. Besides good *in vitro* activity these compounds also possess antibacterial effects [20]. In a previous study Fishwick et al. developed inhibitors of bacterial RNAP, using a structure-based *de novo* design approach.

These compounds, predicted to bind to the “switch region”, possessed inhibitory activity against *E. coli* RNAP, but displayed no antibacterial properties [21]. Very recently Buurmann et al. reported on the first synthetic RNAP inhibitors which have been shown to target the “switch region”. Although these compounds were highly active ( $IC_{50}$  as low as 4.4  $\mu$ M), they showed only weak antibacterial effects [22]. In a further work compounds supposed to interact with the “switch region” were identified by virtual screening, but the putative hits were not experimentally validated [23].

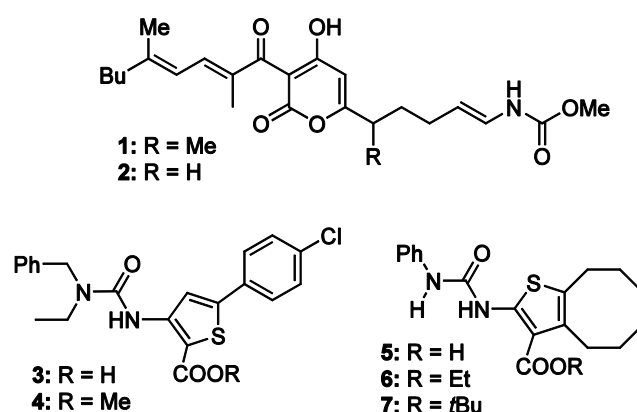


**Chart 1.** Myxopyronins **1** and **2**, hit compound **3**, its ester **4** and *S. aureus* RNAP inhibitors **5**, **6** and **7**.

Recently, we identified novel RNAP inhibitors also following a virtual screening approach. A homology model of *E. coli* RNAP was used to set up a 3D-pharmacophore model, which included ligand features from **1** and **2**, but also protein-derived characteristics, matching the “switch region”. Finally, a pharmacophore-based virtual screening of the ChEMBL library (~42.000 compounds) was performed resulting in a selection of 70 virtual hits. *In vitro* activity determination using a *E. coli* RNAP inhibition assay led to the identification of hit compound **3** showing a moderate inhibitory activity with an  $IC_{50}$  value of 75  $\mu$ M and MIC value of 11  $\mu$ g/mL (*E. coli* TolC) [24]. Interestingly, the related ureido cyclooctathiopyrenes reported by Arhin et al. for example the acid **5** and especially the esters **6** and **7** have been described to inhibit *S. aureus* RNAP, but their binding site was not further investigated. They showed antibacterial effects against several *S. aureus* strains but not against other Gram positive or Gram negative bacteria [25]. As we expect our compounds to bind to the “switch region” of RNAP, which is highly conserved among various bacterial strains [4], we considered compound **3** to be a good starting point for the development of novel antibacterials with broad spectrum activity.

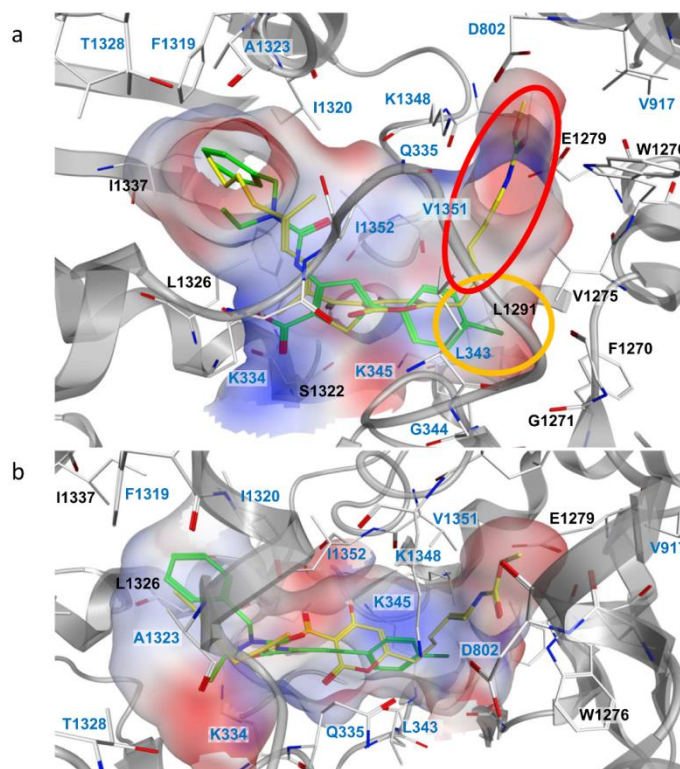


**Figure 1.** Binding mode of desmethyl-myxopyronin **2** (yellow) and compound **3** (green) as front- (a) and top-view (b).

### Molecular Modeling and Optimization Strategy

To find out whether the SAR of the ureido cyclooctathiophenes is reasonable to be considered in our study, compounds **5**, **6** and **7** were subjected to the virtual screening using our 3D-pharmacophore model. None of them was recognized. This is in accordance with the observation of Buurmann et al. that these ureido cyclooctathiophenes failed to dock to the “switch region” of the RNAP [22]. In both crystal structures of *T. thermophilus* RNAP with **1** (PDB ID: 3DXJ) [4] and **2** (PDB ID: 3EQL) [15] the myxopyronins adopt a U-shaped conformation filling the “switch region” binding pocket. According to the docking pose (Figure 1) hit compound **3** is predicted to bind in a tilted conformation. The thiophene core is placed on the top of the entrance to the switch-2 binding cavity, anchored by atomic interactions (H-bond or ion-pair) of its carboxylic acid moiety with Lys334. Such an interaction is not possible with the corresponding ester **4**. The 4-chlorophenyl ring occupies the lower part of the enecarbamate-binding pocket of myxopyronins. Thereby, the chloro atom is fitted into a small negatively-charged site delimited by Leu343, Gly344 and Lys345 ( $\beta'$  subunit) at one side, and Phe1270, Gly1271, Val1275 and Leu1291 ( $\beta$  subunit) on the other side (red area of the electrostatic potential surface in the orange circle in

Figure 1a) The ureido moiety, stabilized by an intramolecular hydrogen-bond (Chart 2) with the carboxylic acid group, overlaps with the dienone side chain of myxopyronins, pointing the lipophilic substituents ethyl and benzyl into the hydrophobic pocket delimited by Leu1326 and Ile1337 ( $\beta$  subunit) and Phe1319, Ile1320, Ala1323, Thr1328, Ile1352 ( $\beta'$  subunit). Based on this binding mode, **3** was divided into the carboxy-thiophene-core and two variable fragments for structure-activity exploration and optimization: the substituted phenyl ring (**A**), and the ureido group (**B**) as depicted in chart 2.

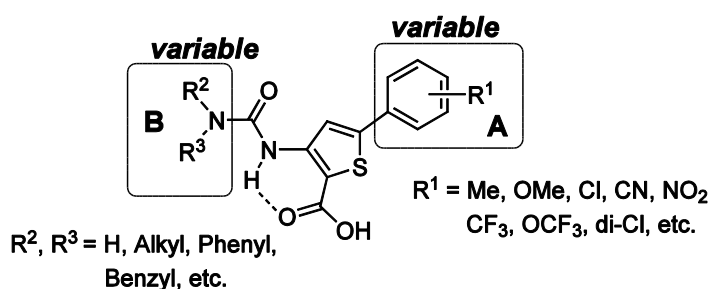
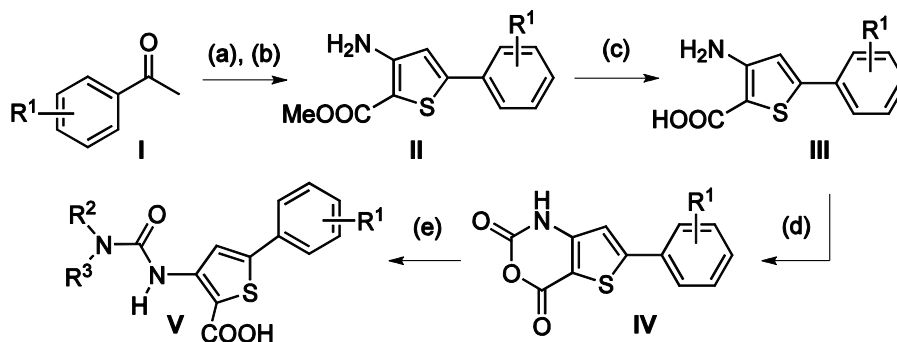


**Chart 2.** Optimization strategy of 5-aryl-3-ureidothiophene-2-carboxylic acids.

## Chemistry

The synthesis of the 5-aryl-3-ureidothiophene-2-carboxylic acids (Scheme 1) started from readily available acetophenones (**I**) which were converted to the 5-aryl thiophene anthranilic acid methylesters (**II**) via an Arnold-Vilsmaier-Haack reaction followed by a cyclization using methylmercaptoacetate [26]. The esters (**II**) were then hydrolysed under basic conditions to afford the thiophene anthranilic acids (**III**) which were converted into the thiaisatoic anhydrides (**IV**) [27,28]. The anhydrides (**IV**) were reacted with various primary and secondary amines giving rise to the 5-aryl-3-ureidothiophene-2-carboxylic acids (**V**) [29]. Compounds **5**, **6** and **7** were synthesized as previously described [25]. Compound **4** was obtained by methylation of compound **3**.



**Scheme 1.** Synthesis of 5-aryl-3-ureidothiophene-2-carboxylic acids (**V**). Reagents and conditions: (a)  $\text{POCl}_3$ , DMF, 50 °C to rt, then  $\text{NH}_2\text{OH}\cdot\text{HCl}$ , up to 150 °C, 75–90%. (b) Methylthioglycolate, NaOMe, MeOH, reflux, 65–85%. (c) KOH, MeOH, THF,  $\text{H}_2\text{O}$ , reflux, 40–80%. (d)  $\text{COCl}_2$ , THF, 50–70%. (e) Amine,  $\text{H}_2\text{O}$ , 100 °C then at 0 °C conc. HCl, 40–80%.

## Results and Discussion

As expected, the ester of **3**, compound **4** did not show *E. coli* RNAP inhibition. Interestingly, not only the esters **6** and **7**, but also the free acid **5** were inactive (Table S2 in Supporting Information). During the hit optimization process of the discovered 5-phenyl-3-ureidothiophene-2-carboxylic-acids, two aims were pursued: Firstly, the putative binding mode of hit compound **3** was investigated by chemical modifications of the substituents on ring **A**. Thereby the Topliss' logical was followed to optimize the hydrophobic and electronic effects [30]. Secondly, the hydrophobic pocket of the “switch region”, occupied by the dienone side chain of myxopyronins, was explored by varying the substitution pattern of the ureido moiety **B**.

The removal of the chlorine (ring **A**) decreased activity as well as its exchange by a methoxy or methyl group. The introduction of the strongly electron-withdrawing and lipophilic trifluoromethyl group was accompanied by a slight increase in activity. Whereas a more hydrophilic, electron-withdrawing nitro group (**12**) was tolerated, but did not enhance the activity, a cyano group at the same position (**13**) led to a decreased inhibitory effect. An additional chloro substituent improved activity independent of the position of both substituents. This correlates well with the distribution of favorable interaction contour plots for chloro atoms within the subpocket of the “switch region” as computed with Molecular Operating Environment (MOE) [31] (Figure 2) localized close to positions 2, 3 and 4. The most active compounds in this series were the 3,4 di-chloro compound **18** and **22** with a

trifluoromethyl and a chloro substituent present in positions 3 and 4. Regarding quantitative structure-activity relationship (QSAR) an excellent correlation was observed when  $\pi$  and  $\sigma$  were used in a multiparameter regression analysis. The obtained Hansch equation (Equation 1:  $\text{pIC}_{50} = 3.71 + 0.34 \times \pi + 0.60 \times \sigma$  ( $n = 16$ ,  $R^2 = 0.95$ ,  $\text{RMSE} = 0.071$ )) clearly indicates that highly lipophilic and strongly electron-withdrawing groups result in the most potent compounds (Figure 3).

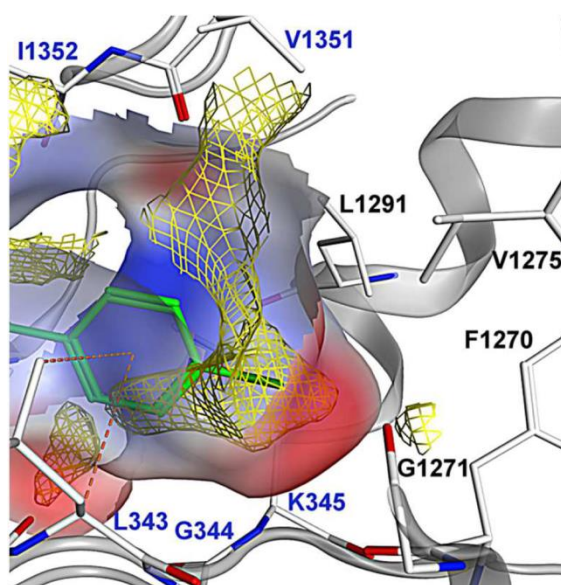


**Figure 2.** Small subpocket of the “switch region” with contour graphics (yellow grid) indicating regions where chlorine has interaction energies within isovalues of  $-4$  kcal/mol.

In order to elucidate the influence of the substitution pattern of ring **A** on the inhibitory potency, *ab initio* geometry optimizations for compounds **3**, **9**, **13** and **18** were carried out and molecular electrostatic potentials (MEP) were visualized (Figure 4). As shown by a larger blue area on ring **A** the electrostatic potential was less negative for the potent compound **18**, followed by **13**, **3** and the inactive compound **9**. As seen in the docking poses of compound **3** and **18** ring **A** is sandwiched between Leu343, Val1351, Ile1352 and the alkyl chain of Lys345, almost perpendicular to the  $\alpha$ -pyrone ring of myxopyronin (Figure 1 and 5). CH- $\pi$  and van der Waals interactions are formed between ring **A** and these residues. The introduction of inductive electron-withdrawing substituents on ring **A** leads to a less polarized/negative potential as shown in the MEP maps (progressively less negative potential – Figure 4). The increase in potency seen for electron-withdrawing groups might depend on stronger London dispersion forces resulting from more balanced electron redistribution at both sides of the ring. The fact that lipophilic (e.g. Cl,  $\text{CF}_3$ ) substituents outreach

hydrophilic ones (e.g. CN) fits well with the presence of several apolar residues in the surrounding, i.e. Phe1270, Val1275, Leu1291, Val1351, Ile1352, Val1353 (Figure 2).

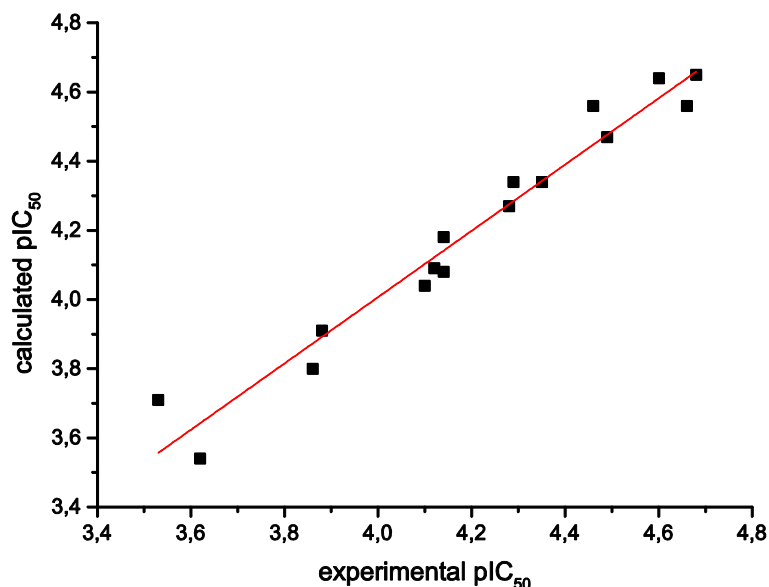


**Figure 3.** Comparison of experimentally determined and calculated activities (based on Equation 1) of compounds **3** and **8–22**.

Within the small negatively charged subpocket (Figure 1 (orange circle) and Figure 2) the chloro derivatives **3** and especially **18** are favored due to a complementary electrostatic surface (blue at chloro atom). The more negative potential (green at nitrogen or oxygen) on the methoxy in **9** and cyano group in **13** probably causes electrostatic repulsions and is consequently associated with a drop in activity. Subsuming, the substitution pattern of ring **A** finetunes charge density distribution of the phenyl system and the thiophene core, enabling enhanced interactions with the target protein.

To proof the binding mode proposed in Figure 1, compound **23** was synthesized [40]. It was deduced from the docking pose, that position 3 at the phenyl ring **A** should be appropriate for an elongation into the pocket occupied by the enecarbamate chain of myxopyronins (red circle in Figure 1). As a linker a C<sub>4</sub> unit has been considered to be suitable for the positioning of a carbamate group. For synthetic reasons we introduced a saturated chain as the corresponding myxopyronin analogue has been described to show a similar biological activity as **1** [14]. The resulting compound **23** that contains a mimic of the myxopyronin enecarbamate chain indeed possessed

increased activity compared to the parent compound **3** (Table 2). Nevertheless the putative new interactions (Figure S2 in Supporting Information) would suggest an even higher gain in activity. We suppose that the entropic penalty for the binding of the highly flexible chain has a negative effect on affinity. Furthermore, it can be rationalized that the positive inductive effect of the introduced alkylcarbamate chain negatively affects the electronic properties of ring **A** according to equation 1. The fact that **23** is more active than **3**, despite these two negative effects, corroborates the validity of the docking pose.

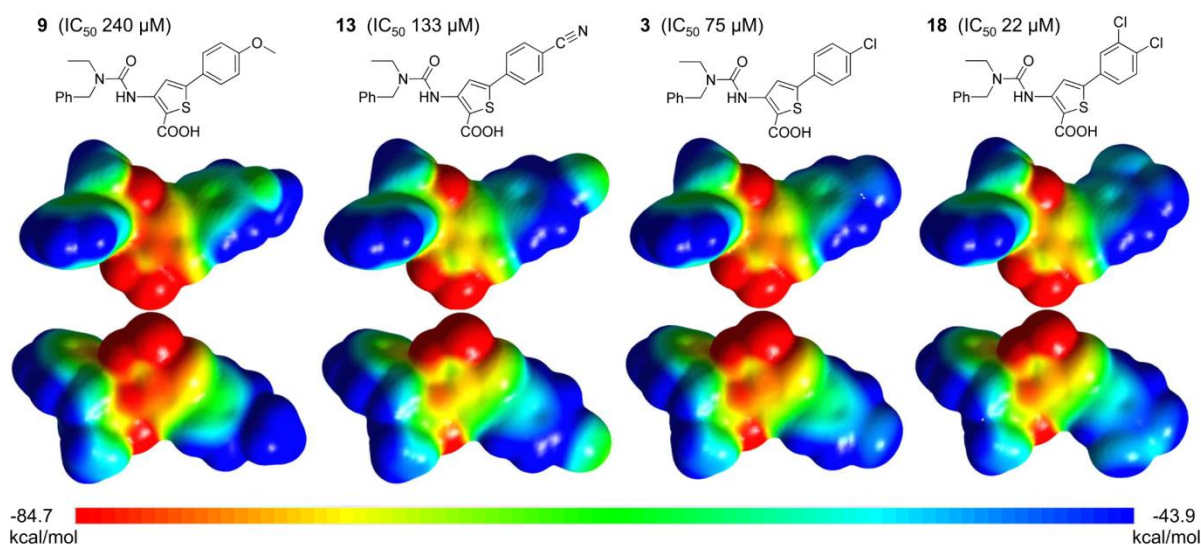


**Figure 4.** *Ab initio* molecular electrostatic potential (MEP) of compounds **3**, **9**, **13** and **18**.

Turning our interest to the ureido motif **B**, we retained the 3,4 di-chloro ring **A**. The unsubstituted ureido compound **24** ( $R^2=R^3=H$ ) displayed low affinity compared to **18** containing two lipophilic alkyl chains. This was concordant with the proposed binding mode since **B** is located in a highly lipophilic cavity where hydrophobic contacts, Van der Waals and CH- $\pi$  interactions, prevail. As depicted in Figure 5 the urea moiety does not form hydrogen-bonds with surrounding residues, but acts as a planar linker for the obligatory hydrophobic groups. Within the compound series derived from primary alkyl amines an increased activity was observed for chain elongation. For example the *n*-hexyl derivative **28** displayed the highest potency compared to smaller substituents. Besides long aliphatic chains, aromatic residues (phenyl, benzyl or phenethyl) were also suitable. The introduction of a second chain at the nitrogen was in general accompanied by an increasing activity.



**Table 1.** Inhibitory activities against *E. coli* RNA polymerase *in vitro* and antibacterial activities.

Cpd	R <sup>1</sup>	Inhibition of <i>E. coli</i> RNAP <sup>a</sup>	MIC (μg/mL) <sup>b,c</sup>	Cpd	R <sup>2</sup>	R <sup>3</sup>	Inhibition of <i>E. coli</i> RNAP <sup>a</sup>	MIC (μg/mL) <sup>b,c</sup>
3	4-Cl	75 μM	11	24	H	H	26%	>25
8	H	292 μM	17	25	H	<i>i</i> -Propyl	26%	15
9	4-OCH <sub>3</sub>	240 μM	15	26	H	<i>n</i> -Butyl	91 μM	13
10	4-CH <sub>3</sub>	137 μM	21	27	H	<i>n</i> -Pentyl	35 μM	10
11	4-CF <sub>3</sub>	51 μM	21	28	H	<i>n</i> -Hexyl	19 μM	>25
12	4-NO <sub>2</sub>	73 μM	23	29	H	Phenyl	25 μM	12
13	4-CN	133 μM	25	30	H	Benzyl	45 μM	10
14	4-OCF <sub>3</sub>	45 μM	21	31	H	Phenethyl	26 μM	8
15	3-Cl	72 μM	9	32	Methyl	Phenyl	45 μM	9
16	3-CF <sub>3</sub>	53 μM	38	33	Methyl	Benzyl	12%	5
17	3-NO <sub>2</sub>	80 μM	22	34	Ethyl	Phenyl	36 μM	16
18	3,4-di-Cl	22 μM	10	18	Ethyl	Benzyl	22 μM	10
19	2,4-di-Cl	32 μM	8	35	<i>n</i> -Propyl	Benzyl	14 μM	>25
20	2,5-di-Cl	35 μM	9	36	<i>n</i> -Propyl	Phenethyl	12 μM	>25
21	3,5-di-Cl	25 μM	n.d.	37	<i>n</i> -Butyl	Phenyl	14 μM	>25
22	3-CF <sub>3</sub> ,4-Cl	21 μM	12	38	<i>n</i> -Butyl	Benzyl	9 μM	>50
1	myx B	0.35 μM	0.8	39	<i>n</i> -Butyl	Phenethyl	7 μM	>25
	rifampicin	0.03 μM	5	40	Benzyl	Benzyl	6 μM	>25

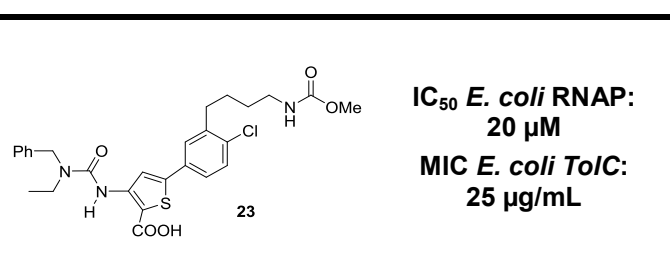
<sup>a</sup> IC<sub>50</sub> values [μM] or inhibition at 100 μM [%] of *E. coli* RNA polymerase; <sup>b</sup> Minimal inhibitory concentration in *E. coli* *ToIC*; <sup>c</sup> >: MIC-determination was limited due to insufficient solubility of the tested compounds. n.d. = not determined

In addition to the RNAP *in vitro* inhibition, the effect of **18** on RNA synthesis was investigated in a whole-cell assay with *E. coli* *ToIC* using radiolabeled <sup>3</sup>H-uridine. At a concentration of 100 μM the RNA level was reduced by 60% after 40 minutes. (Figure S2).

Further biological evaluation was carried out by determination of minimal inhibitory concentrations (MIC) in *E. coli* *ToIC* (Table 1), which is defective in the multidrug AcrAB-ToIC efflux system. Most of the compounds active against the bacterial enzyme displayed growth inhibitory effects in the range of 5–25 μg/mL. Their antibacterial activity is comparable to that of the reference drug rifampicin (5 μg/mL

*E. coli TolC*). The effect on the bacterial growth reflects that the ureidothiophene-carboxylic acids can diffuse across the asymmetric bilayer to gain access to the cell interior, as described for lipophilic antibacterials including macrolides and rifamycins [32]. However, the most potent RNAP inhibitors **35–40** - the compounds with the highest lipophilicity in that class - showed lower antibacterial potency against *E. coli TolC*. These results can be explained by the fact that the outer membrane of Gram negative bacteria is well known to be a potent barrier, hindering too lipophilic compounds from entering the cell [33,34].

**Table 2.** Structure and biological data of **23**.



To explore the spectrum of bacteria possessing susceptibility to selected compounds, MIC values in two Gram positive and two Gram negative strains were determined (Table 3). While the Gram positive strains (*B. subtilis*, *S. aureus*) were in general sensitive, wild type Gram negative bacteria (*E. coli K12*, *P. aeruginosa*) were not affected. For *B. subtilis* and *S. aureus* similar inhibitory effects compared to *E. coli TolC* were observed. Considering that the RNAP “switch region” is highly conserved among various bacterial strains, we assume that the unequal antibacterial potencies are due to differences in cell wall permeability between Gram negative and Gram positive bacteria.

The fact that most compounds were potent against the *TolC* mutant of *E. coli* and almost ineffective against *E. coli K12* suggests that drug-efflux, deactivated in *E. coli TolC*, is responsible for the lack of antibacterial potency in Gram negative bacteria.

An essential requirement for an effective antibacterial agent is that its potency is not reduced by the occurrence of resistant strains. Spontaneous resistance towards myxopyronin B in *S. aureus* occurs at a frequency of  $8 \times 10^{-8}$ , similar to that of rifampicin [17]. The determination of the *in vitro* resistance frequencies in *E. coli TolC* at 2 x MIC revealed a significant (>500-fold) lower value for **15** ( $<4.2 \times 10^{-11}$ )

compared to rifampicin ( $8.3 \times 10^{-8}$ ) and myxopyronin B ( $7.1 \times 10^{-8}$ ). This phenomenon can be explained by the fact that **15** occupies only a part of the “switch region” whereas myxopyronin fills a larger area, including the narrow enecarbamate binding pocket. Especially mutations in this part, which lead to resistance against myxopyronin [4,35], should not affect the antibacterial activity of our compounds. Another mechanism that can contribute to the low resistance frequency can be the effect on an additional target. This will be investigated in further experiments. Our finding indicates, that the probability of occurring resistant strains, is reduced with our compounds compared to existing drugs. This makes these compounds promising candidates for further optimization as novel antibacterials.

**Table 3.** Antibacterial activities of selected 5-aryl-3-ureidothiophene-2-carboxylic acids.

Cpd	MIC <sup>a</sup> <i>E. coli</i> ToIC ( $\mu\text{g/mL}$ )	MIC <sup>a</sup> <i>E. coli</i> K12 ( $\mu\text{g/mL}$ )	MIC <sup>a</sup> <i>P. aeruginosa</i> ( $\mu\text{g/mL}$ )	MIC <sup>a</sup> <i>B. subtilis</i> ( $\mu\text{g/mL}$ )	MIC <sup>a</sup> <i>S. aureus</i> ( $\mu\text{g/mL}$ )
14	21	>100	>100	20	9
15	9	>100	>100	12	21
18	10	>25	>25	11	8
19	8	>50	> 50	10	12
22	12	>50	>50	20	5
27	10	>25	>25	8	>25
29	12	>50	>50	12	6
31	8	>25	>25	7	6
38	>50	>50	>50	>50	>50
40	>25	>25	>25	>25	3
1	0.8	>25	>25	0.9	0.5
rifampicin	10	7	13	4.8	0.02
myxopyronin B	0.8	>25	>25	0.9	0.5

<sup>a</sup> >: MIC-determination was limited due to insufficient solubility of the tested compounds

## Conclusions

With the aim to develop antibacterial substances with broad-spectrum activity, we have chosen the “switch region” of bacterial RNAP as a target site, as it is conserved among various bacterial strains [4]. In a previous work we had discovered hit compound **3** via virtual screening using a 3D-pharmacophore model [24], based on the cocrystal structures of myxopyronins **1** and **2** in the “switch region” [4,15]. In this paper the SAR of compound **3** was explored and the inhibitory potency was

optimized following a rational approach (Hansch, Topliss) supported by computational methods (docking studies, MEPs). Furthermore, the binding mode was experimentally validated by mimicking the natural ligand myxopyronin via introduction of a carbamate sidechain into compound **3**. The new inhibitors show activity against Gram positive (*B. subtilis*, *S. aureus*) and Gram negative (*E. coli TolC*) bacterial strains accompanied by outstanding low resistance frequencies. In contrast, other synthetic RNAP inhibitors possess weak bacterial growth inhibitory activity [21,22] or have only narrow spectrum activity among the *S. aureus* genus [25]. The lack of activity towards Gram negative wild type strains, is most likely due to poor penetration and/or drug efflux. Therefore further optimization is required. Improving the physicochemical properties by introduction of hydrophilic or ionisable groups could enhance cellular availability in Gram negative bacteria. Ring **A** seems to be inappropriate since equation 1 shows the importance of lipophilic substituents in this part. In our opinion, the ureido-motif **B** is so far underexploited and should be utilized. As it is known, that the introduction of polar groups can have negative impact on the activity unless they contribute to favourable enthalpic interactions [36,37], this issue has to be taken into consideration. In the binding area of **B** the polar amino acids (Ser1324, Thr 1329) and some backbone regions could be addressed for such interactions. Thus, clinically applicable, broad spectrum antibacterial agents, that are urgently needed to combat infectious diseases, could finally be obtained. The present work lays the foundation for future structure-based design and expansion of the chemical space in this class.

## Experimental Procedures

### Chemistry

**Materials and methods.** Starting materials were purchased from commercial suppliers and used without further purification. Column flash chromatography was performed on silica gel (40–63  $\mu\text{M}$ ), and reaction progress was monitored by TLC on TLC Silica Gel 60 F<sub>254</sub> (Merck). All moisture-sensitive reactions were performed under nitrogen atmosphere using oven-dried glassware and anhydrous solvents. <sup>1</sup>H and <sup>13</sup>C NMR spectra were recorded on a Bruker Fourier spectrometer (300 or 75 MHz) at ambient temperature with the chemical shifts recorded as  $\delta$  values in ppm units by reference to the hydrogenated residues of deuteriated solvent as internal standard. Coupling constants (*J*) are given in Hz and signal patterns are indicated as

follows: s, singlet; d, doublet; dd, doublet of doublets; t, triplet; m, multiplet, br., broad signal. The melting points (m.p.) were determined using a Stuart Scientific SMP3. The purity of the final compounds was  $\geq 95\%$  as measured by HPLC. The Surveyor LC system consisted of a pump, an autosampler, and a PDA detector. Mass spectrometry was performed on a MSQ electrospray mass spectrometer (ThermoFisher, Dreieich, Germany). The system was operated by the standard software Xcalibur. A RP C18 NUCLEODUR 100-5 (125 mm x 3 mm) column (Macherey-Nagel GmbH, Dühren, Germany) was used as the stationary phase. All solvents were HPLC grade. In a gradient run the percentage of acetonitrile (containing 0.1% trifluoroacetic acid) was increased from an initial concentration of 0% at 0 min to 100% at 15 min and kept at 100% for 5 min. The injection volume was 10  $\mu\text{L}$ , and flow rate was set to 800  $\mu\text{L}/\text{min}$ . MS analysis was carried out at a spray voltage of 3800 V and a capillary temperature of 350  $^{\circ}\text{C}$  and a source CID of 10 V. Spectra were acquired in positive mode from 100 to 1000  $m/z$  at 254 nm for the UV trace.

#### **General Procedure for the synthesis of ureidothiophene-2-carboxylic acids.**

**General procedure for the synthesis of 5-Aryl-3-amino-2-carboxylic acid methylester (II).**  $\text{POCl}_3$  (26.1 g, 0.17 mol) was added dropwise to DMF (24.9 g, 0.34 mol) maintaining the temperature beyond 25  $^{\circ}\text{C}$  (cooling in ice bath) and stirred for additional 15 min. The acetophenone **I** (85.0 mmol) was added slowly and the temperature was kept between 40 and 60  $^{\circ}\text{C}$ . After complete addition, the mixture was stirred for 30 minutes at room temperature. Hydroxylamine hydrochloride (23.6 g, 0.34 mol) was carefully added portionwise (exothermic reaction!) and the reaction was stirred for additional 30 min without heating. After cooling to room temperature, the mixture was poured into ice water (300 mL). The precipitated  $\beta$ -chloro-cinnamionitrile was collected by filtration, washed with  $\text{H}_2\text{O}$  (2 x 50 mL) and dried under reduced pressure over  $\text{CaCl}_2$ . In the next step sodium (1.93 g, 84.0 mmol.) was dissolved in MeOH (85 mL) and methylthioglycolate (6.97 g, 65.6 mmol) was added to the stirred solution. The  $\beta$ -chloro-cinnamionitrile (61.1 mmol) was added and the mixture was heated to reflux for 30 min. After cooling to room temperature, the mixture was poured into ice water (300 mL). The precipitated solid was collected by filtration, washed with  $\text{H}_2\text{O}$  (2 x 50 mL) and dried under reduced pressure over  $\text{CaCl}_2$ . If necessary, recrystallisation from EtOH was performed.

**General procedure for the synthesis of 5-Aryl-3-amino-2-carboxylic acid (III).**

The 5-Aryl-3-amino-2-carboxylic acid methyl ester (16.6 mmol) was added to a solution of KOH (60 mL, 0.6M in H<sub>2</sub>O) and MeOH (60 mL). The mixture was heated to reflux for 3 h, concentrated, and washed with EtOAc (2 x 50 mL). The aqueous layer was cooled with ice and acidified by addition of a saturated aqueous solution of KHSO<sub>4</sub>. The precipitated solid was collected by filtration, washed with H<sub>2</sub>O (2 x 30 mL) and dried under reduced pressure over CaCl<sub>2</sub>.

**General procedure for the synthesis of 5-Aryl-2-thiaisatoic-anhydrid (IV).**

To a solution of the 5-Aryl-3-amino-2-carboxylic acid (III) (5.28 mmol) in THF (50 mL) a solution of phosgene (6.10 mL, 20 wt% in toluene, 11.6 mmol) was added dropwise over a period of 30 min. The reaction mixture was stirred for 2 h at room temperature, followed by the addition of saturated aqueous solution of NaHCO<sub>3</sub> (30 mL) and H<sub>2</sub>O (50 mL). The resulting mixture was extracted with EtOAc/THF (1:1, 3 x 100 mL). The organic layer was washed with saturated aqueous NaCl (100 mL), dried (MgSO<sub>4</sub>) and concentrated. The crude material was suspended in a mixture of *n*-hexane/EtOAc (2:1, 50 mL) heated to 50 °C and after cooling to room temperature separated via filtration.

**General procedure for the synthesis of of 5-Aryl-3-ureidothiophene-2-**

**carboxylic acid (V).** The 5-Aryl-2-thiaisatoic-anhydrid (IV) (0.46 mmol) was suspended in water (7.5 mL) and the appropriate amine (4.60 mmol) was added. The reaction mixture was stirred, heated to 100 °C and then cooled to room temperature. The reaction mixture was poured into a mixture of concentrated HCl and ice (1:1) and extracted with EtOAc/THF (1:1, 60 mL). The organic layer was washed with aqueous HCl (2M), followed by saturated aqueous NaCl (2 x 50 mL), dried (MgSO<sub>4</sub>) and concentrated. The crude material was suspended in a mixture of *n*-hexane/EtOAc (2:1, 20 mL) heated to 50 °C and after cooling to room temperature separated via filtration.

**Spectroscopic data of final compounds.** Spectroscopic data of final compounds can be found in the Supporting Information. Compound **3** is presented as example.

5-(4'-Chlorophenyl)-3-[(*N*-ethylbenzylamino)carbonylamino]-thiophen-2-carboxylic acid (**3**). Yellow powder, m.p. 173–174 °C. <sup>1</sup>H NMR (300 MHz, DMSO-*d*<sub>6</sub>): δ = 1.16 (t, *J* = 7.1 Hz, 3 H), 3.39 (q, *J* = 7.1 Hz, 2 H), 4.58 (s, 2 H), 7.24–7.38 (m, 5 H), 7.50 (d,

$J = 8.5$  Hz, 2 H), 7.71 (d,  $J = 8.5$  Hz, 2 H), 8.29 (s, 1 H), 10.06 (s, 1 H), 13.40 (br. s, 1 H, COOH) ppm.  $^{13}\text{C}$  NMR (75 MHz, DMSO- $d_6$ ):  $\delta = 13.1, 41.8, 49.3, 107.2, 117.8, 127.1, 127.1, 127.4, 128.5, 129.3, 131.5, 133.8, 138.1, 146.1, 146.7, 153.0, 165.6$  ppm.

## Biology

**Transcription assay.** *E. coli* RNA polymerase holo enzyme was purchased from Epicentre Biotechnologies (Madison, WI). Final concentrations in a total volume of 30  $\mu\text{L}$  were one unit of RNA polymerase (0.5  $\mu\text{g}$ ) which were used along with 60 nCi of [5,6- $^3\text{H}$ ]-UTP, 400  $\mu\text{M}$  of ATP, CTP and GTP as well as 100  $\mu\text{M}$  of UTP, 20 units of RNase inhibitor (RiboLock, Fermentas), 10 mM DTT, 40 mM Tris-HCl (pH 7.5), 150 mM KCl, 10 mM  $\text{MgCl}_2$  and 0.1% CHAPS. As a DNA template 3500 ng of religated pcDNA3.1/V5-His-TOPO were used per reaction [38]. Prior to starting the experiment, the compounds were dissolved in DMSO (final concentration during experiments: 2%). Dilution series of compounds were prepared using a liquid handling system (Janus, Perkin Elmer, Waltham, MA). The components described above (including the inhibitors) were preincubated in absence of NTPs and DNA for 10 min at 25  $^\circ\text{C}$ . Transcription reactions were started by the addition of a mixture containing DNA template and NTPs and incubated for 10 min at 37  $^\circ\text{C}$ . The reaction was stopped by the addition of 10% TCA, followed by a transfer of this mixture to a 96 well Multiscreen GFB plate (Millipore, Billerica, MA) and incubation for 45 min at 4  $^\circ\text{C}$ . The plate underwent several centrifugation and washing steps with 10% TCA and 95% ethanol to remove residual unincorporated  $^3\text{H}$ -UTP. After that the plate was dried (30 min, 50  $^\circ\text{C}$ ) and 30  $\mu\text{L}$  of scintillation fluid (Optiphase Supermix, Perkin Elmer) was added to each well. After 10 min the wells were assayed for presence of  $^3\text{H}$ -RNA by counting using a Wallac MicroBeta TriLux system (Perkin Elmer). To obtain inhibition values for each sample, their counts were related to DMSO controls.

**RNA synthesis assay.** *E. coli TolC* was cultured in lysogeny broth (LB) medium.  $^3\text{H}$ -uridine (1  $\mu\text{Ci}/\text{mL}$ ) was added during the logarithmic growth phase and 3 min before the addition of compound **18** at 100  $\mu\text{M}$  (0.5% DMSO). 300  $\mu\text{L}$  of the cultured bacteria were harvested 40 min after addition of the inhibitors and supplemented with 2 volumes of 10% TCA. After 45 min at 4  $^\circ\text{C}$  the precipitates were collected and washed using a 96 well glass fiber filter plate (Multiscreen GFB) (Millipore, Billerica, MA). After adding Optiphase Supermix (Perkin Elmer, Waltham, MA) the

quantification of radioactivity was performed using a Wallac MicroBeta TriLux system (Perkin Elmer).

**Determination of IC<sub>50</sub> values.** For the determination of IC<sub>50</sub> values three different concentrations of a compound were chosen (two samples for each concentration) including data points above and below the IC<sub>50</sub> value. The calculation of the IC<sub>50</sub> value was performed by plotting the percent inhibition vs. the concentration of inhibitor on a semi-log plot. From this the molar concentration causing 50% inhibition was calculated. At least three independent determinations were performed for each compound.

**Minimal inhibitory concentration (MIC) determinations.** MIC values in *E. coli ToIC* were performed with all compounds. Selected compounds were additionally tested in *E. coli K12*, *Bacillus subtilis subsp. subtilis*, *Pseudomonas aeruginosa PAO1* and *Staphylococcus aureus subsp. aureus* (Newman strain). As a bacteria start OD<sub>600</sub> 0.03 was used in a total volume of 200 µL in lysogeny broth (LB) containing the compounds predissolved in DMSO (maximal DMSO concentration in the experiment: 1%). Final compound concentrations prepared from serial dilutions ranged from 0.02 to 100 µg/mL (double values for each concentration) depending on their antibacterial activity and the observation of compound precipitation in the growth medium. The ODs were determined after addition of the compounds and again after incubation for 18 h at 37 °C and 50 rpm (200 rpm for *PAO1*) in 96 well plates (Sarstedt, Nümbrecht, Germany) using a FLUOStar Omega (BMG labtech, Ortenberg, Germany). Given MIC values are means of two independent determinations (three if MIC <10 µg/mL) and are defined as concentrations at which bacterial growth was no more detectable.

**Determination of resistance frequency.** The amount of *E. coli ToIC* cells per mL was determined by plating bacteria dilutions on LB agar plates following colony counting. Different amounts of cells were incubated in LB in presence of the 2 x MIC of rifampicin, myxopyronin B and compound **18** in parallel (16 h, 37 °C, 50 rpm) following LB exchange, re-cultivation and growth control. A threshold was determined at which bacterial growth and hence resistance development occurred following calculation of the resistance frequency.

## Computational Chemistry

**Docking Calculations.** Selected compounds were docked into the “switch region” of the *E. coli* RNAP homology model using Goldv5.0 [24].

**Molecular Electrostatic Potential.** For compounds **3**, **9**, **13**, and **18** *ab initio* geometry optimizations were performed choosing as basis set HF/6-31+ G (d,p) by means of the Gaussian 03 software, and the molecular electrostatics potential map (MEP) was plotted using GaussView, version 3.0, the 3D molecular graphics package of Gaussian [39]. Electrostatic potential surfaces were generated mapping the electrostatic potentials onto molecular electron densities at an isovalue of 0.0004 e/A°. The MEP maps are color-coded, ranging from -85 (red) to -44 (blue) kcal/mol).

**QSAR model.** The QSAR model (Equation 1) was obtained using the software Molecular Operating Environment (MOE) v. 2010.10.

**Acknowledgments:** The authors thank Jeannine Jung and Jannine Ludwig for performing the *in vitro* tests. We also appreciate Ailke Gerstner for her help in performing the synthesis. Furthermore we are grateful to K. Gerth (Helmholtz Centre for Infection Research (HZI) in Braunschweig) for kindly providing myxopyronin B. J. Henning Sahner gratefully acknowledges a scholarship from the “Stiftung der Deutschen Wirtschaft” (SDW).

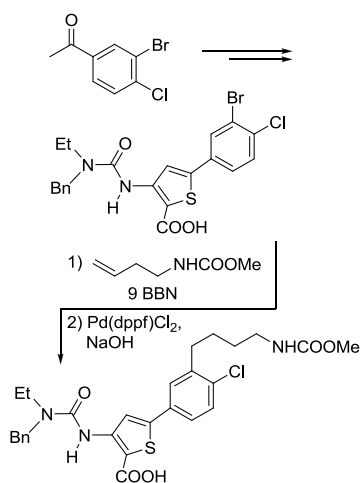
## References

- [1] A. Srivastava; M. Talaue, S. Liu, D. Degen, R.Y. Ebricht, E. Sineva, A. Chakraborty, S.Y. Druzhinin, S. Chatterjee, J. Mukhopadhyay, Y.W. Ebricht, A. Zozula, J. Shen, S. Sengupta, R.R. Niedfeldt, C. Xin, T. Kaneko, H. Irschik, R. Jansen, S. Donadio, N. Connell, R.H. Ebricht, New target for inhibition of bacterial RNA polymerase: 'switch region', *Curr. Opin. Microbiol.* 14 (2011) 532–543.
- [2] I. Chopra, Bacterial RNA polymerase: a promising target for the discovery of new antimicrobial agents, *Curr. Opin. Invest. Dr.* 8 (2007) 600–607.
- [3] R. Mariani, S. I. Maffioli, Bacterial RNA polymerase inhibitors: an organized overview of their structure, derivatives, biological activity and current clinical development status, *Curr. Med. Chem.* 16 (2009) 430–454.
- [4] J. Mukhopadhyay, K. Das, S. Ismail, D. Koppstein, M. Jang, B. Hudson, S. Sarafianos, S. Tuske, J. Patel, R. Jansen, H. Irschik, E. Arnold, R.H. Ebricht, The RNA polymerase “switch region” is a target for inhibitors. *Cell* 135 (2008) 295–307.
- [5] P. Cramer, Multisubunit RNA polymerases, *Curr. Opin. Struc. Biol.* 12 (2002) 89–97.

- [6] R.H. Ebright, RNA polymerase: structural similarities between bacterial RNA polymerase and eukaryotic RNA polymerase II, *J. Mol. Biol.* 304 (2000) 687–698.
- [7] I. Artsimovitch, J. Seddon, P. Sears, Fidaxomicin is an inhibitor of the initiation of bacterial RNA synthesis, *Clin. Infect. Dis.* 55 (suppl 2) (2012), S127–S131.
- [8] T. Schaberg, M. Forßbohm, B. Hauer, D. Kirsten, R. Kropp, R. Loddenkemper, K. Magdorf, H. Rieder, D. Sagebiel, R. Urbanczik, Richtlinien zur medikamentösen Behandlung der Tuberkulose im Erwachsenen- und Kindesalter. *Pneumologie* 55 (2001) 494–511.
- [9] A. Pablos-Méndez, M.C. Raviglione, A. Laszlo, N. Binkin, H.L. Rieder, F. Bustreo, D.L. Cohn, C.S. Lambregts-van Weezenbeek, S.J. Kim, P. Chaulet, P. Nunn, Global surveillance for antituberculosis-drug resistance, 1994-1997. World Health Organization-International Union against Tuberculosis and Lung Disease Working Group on Anti-Tuberculosis Drug Resistance Surveillance, *New Engl. J. Med.* 338 (1998) 1641–1649.
- [10] M.A. Espinal, A. Laszlo, L. Simonsen, F. Boulahbal, S.J. Kim, A. Reniero, S. Hoffner, H.L. Rieder, N. Binkin, C. Dye, R. Williams, M.C. Raviglione, Global trends in resistance to antituberculosis drugs. World Health Organization-International Union against Tuberculosis and Lung Disease Working Group on Anti-Tuberculosis Drug Resistance Surveillance, *New Engl. J. Med.* 344 (2001) 1294–1303.
- [11] L.B. Rice, Unmet medical needs in antibacterial therapy, *Biochem. Pharmacol.* 71 (2006) 991–995.
- [12] Q. Al-Balas, N.G. Anthony, B. Al-Jaidi, A. Alnimr, G. Abbott, A.K. Brown, R.C. Taylor, G.S. Besra, T.D. McHugh, S.H. Gillespie, B.F. Johnston, S.P. Mackay, G.D. Coxon, Identification of 2-aminothiazole-4-carboxylate derivatives active against *Mycobacterium tuberculosis* H37Rv and the  $\beta$ -ketoacyl-ACP synthase mtFabH, *PLoS ONE* 4 (2009) e5617.
- [13] H. Irschik, K. Gerth, G. Höfle, W. Kohl, H. Reichenbach, The myxopyronins, new inhibitors of bacterial RNA synthesis from *Myxococcus fulvus* (Myxobacterales), *J. Antibiot.* 36 (1983) 1651–1658.
- [14] T. Doundoulakis, A.X. Xiang, R. Lira, K.A. Agrios, S.E. Webber, W. Sisson, R.M. Aust, A.M. Shah, R.E. Showalter, J.R. Appleman, K.B. Simonsen, Myxopyronin B analogs as inhibitors of RNA polymerase, synthesis and biological evaluation, *Bioorg. Med. Chem. Lett.* 14 (2004) 5667–5672.
- [15] G.A. Belogurov, M.N. Vassilyeva, A. Sevostyanova, J.R. Appleman, A.X. Xiang, R. Lira, S.E. Webber, S. Klyuyev, E. Nudler, I. Artsimovitch, D.G. Vassilyev, Transcription inactivation through local refolding of the RNA polymerase structure, *Nature* 457 (2009) 332–335.
- [16] A. O'Neill, B. Oliva, C. Storey, A. Hoyle, C. Fishwick, I. Chopra, RNA polymerase inhibitors with activity against rifampin-resistant mutants of *Staphylococcus aureus*, *Antimicrob. Agents Ch.* 44 (2000) 3163–3166.
- [17] T.I. Moy, A. Daniel, C. Hardy, A. Jackson, O. Rehrauer, Y.S. Hwang, D. Zou, K. Nguyen, J.A. Silverman, Q. Li, C. Murphy, Evaluating the activity of the RNA polymerase inhibitor myxopyronin B against *Staphylococcus aureus*, *FEMS Microbiol. Lett.* 319 (2011) 176–179.
- [18] D. Haebich, F. von Nussbaum, Lost in transcription - inhibition of RNA polymerase, *Angew. Chem. Int. Edit.* 48 (2009) 3397–3400.

- [19] R. O'Shea, H.E. Moser, Physicochemical properties of antibacterial compounds: implications for drug discovery, *J. Med. Chem.* 51 (2008), 51, 2871–2878.
- [20] S. Hinsberger, M. Groh, M. Negri, J. Hauptenthal, R.W. Hartmann, unpublished results.
- [21] M.J. McPhillie, R. Trowbridge, K.R. Mariner, A.J. O'Neill, A.P. Johnson, I. Chopra, C.W.G. Fishwick, Structure-based ligand design of novel bacterial RNA polymerase inhibitors, *ACS Med. Chem. Lett.* 2 (2011) 729–734.
- [22] E.T. Buurman, M.A. Foulk, N. Gao, V.A. Laganas, D.C. McKinney, D.T. Moustakas, J.A. Rose, A.B. Shapiro, P.R. Fleming, Novel rapidly diversifiable antimicrobial RNA polymerase switch region inhibitors with confirmed mode of action in *Haemophilus influenzae*, *J. Bacteriol.* 194 (2012) 5504–5512.
- [23] Y.S. Li, L. Zhou, X. Ma, H. Song, X.Y. Tang, Pharmacophore modeling and structure-based virtual screening for a novel “switch region” target of bacterial RNA polymerase, *Med. Chem. Res.* (2011), 1–11.
- [24] M. Negri, J. Hauptenthal, R.W. Hartmann, unpublished results.
- [25] F. Arhin, O. Bélanger, S. Ciblat, M. Dehbi, D. Delorme, E. Dietrich, D. Dixit, Y. Lafontaine, D. Lehoux, J. Liu, G.A. McKay, G. Moeck, R. Reddy, Y. Rose, R. Srikumar, K.S.E. Tanaka, D.M. Williams, P. Gros, J. Pelletier, T.R. Parr, A.R. Far, A new class of small molecule RNA polymerase inhibitors with activity against rifampicin-resistant *Staphylococcus aureus*, *Bioorg. Med. Chem.* 14 (2006) 5812–5832.
- [26] H. Hartmann, J. Liebscher, A simple method for the synthesis of 5-aryl-3-amino-2-alkoxycarbonylthiophenes, *Synthesis* (1984) 275–276.
- [27] F. Fabis, S. Jolivet-Fouchet, M. Robba, H. Landelle, S. Rault, Thiaisatoic anhydrides: efficient synthesis under microwave heating conditions and study of their reactivity, *Tetrahedron* 54 (1998) 10789–10800.
- [28] L. Foulon, E. Braud, F. Fabis, J.C. Lancelot, S. Rault, Synthesis and combinatorial approach of the reactivity of 6- and 7-arylthieno [3,2-*d*][1,3] oxazine-2,4-diones, *Tetrahedron* 59 (2003) 10051–10057.
- [29] F.X. Le Foulon, E. Braud, F. Fabis, J.C. Lancelot, S. Rault, Solution-phase parallel synthesis of a 1140-member ureidothiophene carboxylic acid library, *J. Comb. Chem.* 7 (2005) 253–257.
- [30] J.G. Topliss, Utilization of operational schemes for analog synthesis in drug design, *J. Med. Chem.* 15 (1972) 1006–1011.
- [31] Molecular Operating Environment (MOE), 2011.10; Chemical Computing Group Inc., 1010 Sherbooke St. West, Suite #910, Montreal, QC, Canada, H3A 2R7 (2011).
- [32] H. Nikaido, Molecular basis of bacterial outer membrane permeability revisited, *Microbiol. Mol. Biol. R.* 67 (2003) 593–656.
- [33] C.M. Morris, A. George, W.W. Wilson, F.R. Champlin, Effect of polymyxin B nonapeptide on daptomycin permeability and cell surface properties in *Pseudomonas aeruginosa*, *Escherichia coli*, and *Pasteurella multocida*, *J. Antibiot.* 48 (1995) 67–72.
- [34] H. Nikaido, Outer membrane of *Salmonella typhimurium*. Transmembrane diffusion of some hydrophobic substances, *Biochim. Biophys. Acta* 433 (1976) 118–132.

- [35] A. Srivastava, D. Degen, Y.W. Ebricht, R.H. Ebricht, Frequency, spectrum, and fitness costs of resistance to myxopyronin in *Staphylococcus aureus*: myxopyronin resistance has non-zero fitness cost, *Antimicrob. Agents Ch.* 56 (2012) 6250–6255.
- [36] S. Cabani, P. Gianni, V. Mollica, L. Lepori, Group contributions to the thermodynamic properties of non-ionic organic solutes in dilute aqueous solution, *J. Solution Chem.* 10 (1981) 563–595.
- [37] E. Freire, Do enthalpy and entropy distinguish first in class from best in class?, *Drug Discov. Today* 13 (2008) 869–874.
- [38] J. Hauptenthal, K. Hüsecken, M. Negri, C.K. Maurer, R.W. Hartmann, Influence of DNA template choice on transcription and inhibition of *E. coli* RNA polymerase, *Antimicrob. Agents Ch.* 56 (2012) 4536–4539.
- [39] H.B. Schlegel, G.E. Scuseria, M.A. Robb, J.R. Cheeseman, gaussian 03, revision c.02. Gaussian Inc.: Wallingford CT 2004.
- [40] Compound **23** was synthesized via the following route:



## 3.2 Binding mode characterization of novel RNA polymerase inhibitors using a combined chemical and NMR approach

Martina Fruth, Alberto Plaza, Stefan Hinsberger, J. Henning Sahner, Jörg Hauptenthal, Markus Bischoff, Rolf Jansen, Rolf Müller, and Rolf W. Hartmann

Reprinted with permission from *ACS Chem. Biol.* **2014**, *9*, 2656-2663

Copyright (2014) American Chemical Society.

### Publication B

**Abstract:** The bacterial RNA polymerase (RNAP) represents a validated target for the development of broad-spectrum antibiotics. However, the medical value of RNAP inhibitors in clinical use is limited by the prevalence of resistant strains. To overcome this problem, we focused on the exploration of alternative target sites within the RNAP. Previously, we described the discovery of a novel RNAP inhibitor class containing an ureidothiophene-2-carboxylic acid core structure. Herein, we demonstrate that these compounds are potent against a set of methicillin-resistant *Staphylococcus aureus* (MRSA) strains (MIC: 2–16  $\mu\text{g ml}^{-1}$ ) and rifampicin-resistant *Escherichia coli* TolC strains (MIC: 12.5–50  $\mu\text{g ml}^{-1}$ ). Additionally, an abortive transcription assay revealed that these compounds inhibit the bacterial transcription process during the initiation phase. Furthermore, the binding mode of the ureidothiophene-2-carboxylic acids was characterized by mutagenesis studies and ligand-based NMR spectroscopy. Competition saturation transfer difference (STD) NMR experiments with the described RNAP inhibitor myxopyronin A (**Myx**) suggest that the ureidothiophene-2-carboxylic acids compete with **Myx** for the same binding site in the RNAP “switch region”. INPHARMA (interligand NOE for pharmacophore mapping) experiments and molecular docking simulations provided a binding model in which the ureidothiophene-2-carboxylic acids occupy the region of the **Myx** western chain binding site and slightly occlude that of the eastern chain. These results demonstrate that the ureidothiophene-2-carboxylic acids are a highly attractive new class of RNAP inhibitors that can avoid the problem of resistance.

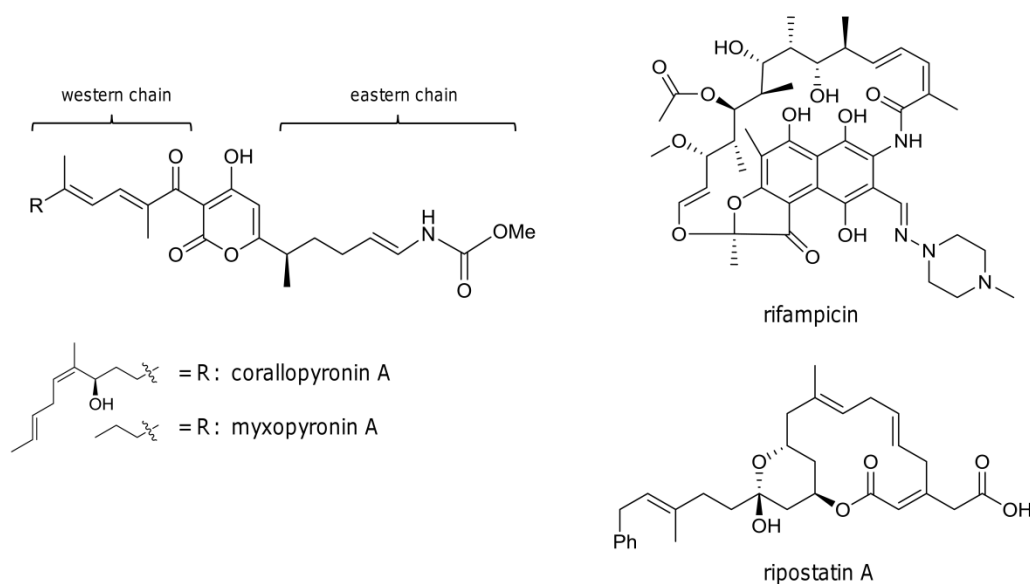
## Introduction

Antimicrobial resistance has become a global health concern due to the widening gap between the rapid spread of resistant pathogens (1) and the shortage of effective treatment options (2, 3). Thus, the development of novel and potent anti-infectives is urgently needed. A validated but hitherto underexploited target for the development of broad-spectrum antibiotics is the bacterial RNA polymerase (RNAP). Up to date, rifamycins and fidaxomicin are the only RNAP inhibitors used in clinical practice (4–8). Rifampicin (**Rif**) (Figure 1), a member of the rifamycin family, plays a fundamental role in tuberculosis treatment as a first-line agent in combination with isoniazid (9). However, its use is limited due to the prevalence of **Rif**-resistant *Mycobacterium tuberculosis* (MTB) strains (10, 11). Resistance to the class of rifamycins arises from point mutations in the *rpoB* gene encoding for the RNAP  $\beta$  subunit (12).

A strategy to overcome the problem of resistance is to explore alternative target sites, which are distant from the **Rif** binding pocket. Therefore, we applied a virtual screening approach addressing the RNAP “switch region” (18). This target site resides at the base of the RNAP clamp, a domain of the  $\beta'$  subunit and coordinates the opening and closing of the RNAP active centre cleft. The “switch region” is not overlapping with the **Rif** binding site and is highly conserved among Gram-positive and Gram-negative bacteria grading it as an attractive target for the identification of novel broad-spectrum antibiotics (13–15). Using a homology model of *E. coli* RNAP a 3D-pharmacophore model was established, which incorporates protein-derived properties of the “switch region” as well as ligand features from **Myx**, a well-known “switch region” binder (16–18) (Figure 1). The virtual screening based on this model identified a hit compound containing an ureidothiophene-2-carboxylic acid core, which served as starting point for activity-guided optimization (18). This class of compounds (Figure 1) showed promising *in vitro* RNAP transcription inhibition and antibacterial activity against Gram-positive bacteria (*S. aureus*, *B. subtilis*) and *E. coli* TolC. Moreover, they possessed a significantly lower resistance frequency compared to **Rif** or **Myx** (18). Present work described here revealed that the ureidothiophene-2-carboxylic acids are also active against several clinical MRSA isolates and **Rif**-resistant spontaneous *E. coli* TolC mutants. Thus, the ureidothiophenes are considered promising candidates for further development.

Here, we established the mode of binding of the ureidothiophenes by using a combination of site-directed mutagenesis and ligand-based NMR methods including STD NMR and INPHARMA. As common methods like SPR or protein based NMR approaches are not feasible to detect binding of small molecules to RNAP due to its large size (core enzyme: ~ 380 kDa), the two ligand-based NMR spectroscopic methods applied herein represent excellent alternatives as they do not impose restrictions on the size of the target protein (19, 20). Besides, to gain deeper insight into the mode of action of the ureidothiophene-2-carboxylic acids an abortive transcription assay was performed.

(a)



(b)

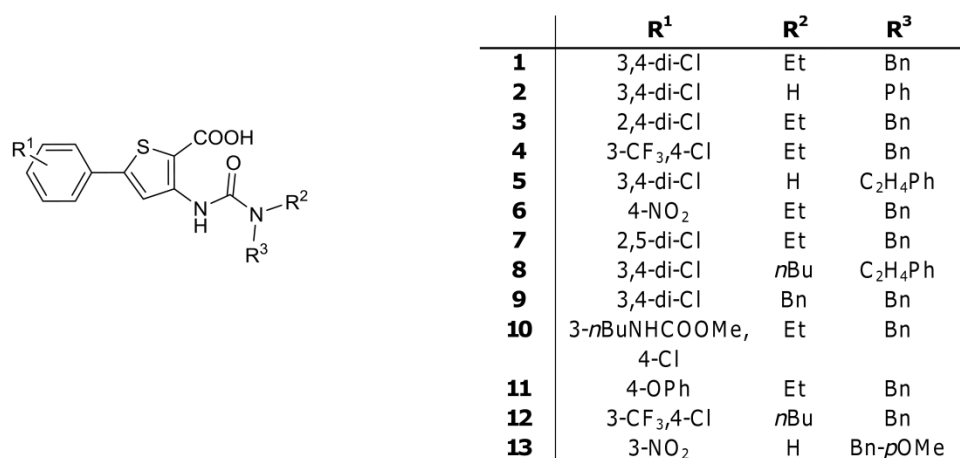


**Figure 1.** (a) RNAP inhibiting natural products, (b) ureidothiophene-2-carboxylic acid derivatives

## Results and discussion

**Antibacterial Activity.** First of all, the activity of the ureidothiophene-2-carboxylic acid derivatives against resistant strains, including **Rif**-resistant *E. coli* TolC and multidrug-resistant *S. aureus*, was assessed by broth microdilution methods (Table 1a and 1b).

**Table 1.** (a) MIC value determination in clinical *Staphylococcus aureus* (MRSA) isolates; (b) MIC value determination in **Rif**-resistant *E. coli* TolC mutants

(a)

MRSA		MIC [ $\mu\text{g ml}^{-1}$ ]			
Isolate	Type <sup>a</sup>	2	9	Myx	Rif
USA300 Lac	CA-MRSA	8	2	1	0.0156
COL	HA-MRSA	16	2	1	0.0078–0.0156
5191	LA-MRSA	16	2	0.5–1	0.0078–0.0156
R44	LA-MRSA	8	2	1	0.0156

(b)

Strain	MIC [ $\mu\text{g ml}^{-1}$ ]							
	1	3	4	5	6	7	Myx	Rif
<i>Ec</i> TolC	12.5–25	12.5–25	25	12.5	25	25	1.25	8
<i>Ec</i> TolC $\beta$ Q513L <sup>b</sup>	12.5	12.5–25	25	12.5	25–50	25	1.25	>100
<i>Ec</i> TolC $\beta$ H526Y <sup>b</sup>	12.5	12.5–25	25	12.5	50	25	1.25	>100

<sup>a</sup> CA-MRSA, community acquired MRSA; HA-MRSA, hospital acquired MRSA; LA-MRSA, livestock-associated MRSA

<sup>b</sup> **Rif**-resistant *E. coli* TolC strains with mutations in the *rpoB* gene encoding for the RNAP  $\beta$  subunit.

Spontaneous **Rif**-resistant *E. coli* TolC mutants with single point mutations in the *rpoB* gene causing high level resistance to **Rif**, were still susceptible towards the ureidothiophene-2-carboxylic acids. These results indicate that the ureidothiophenes show no cross-resistance with **Rif** as intended by our approach to address the RNAP “switch region”. Moreover, the compounds display potent activity against a set of methicillin-resistant *Staphylococcus aureus* (MRSA) isolates with differing antimicrobial resistance patterns (Table S1), such as the community acquired MRSA strain USA300 Lac (21), the early hospital acquired MRSA strain COL (22) and the livestock-associated MRSA CC398 isolates 5191 (23) and R44 (24). Compound **9** (Figure 1) was found to be the most potent. It exhibited a MIC value of  $2 \mu\text{g ml}^{-1}$  in all screened MRSA strains, which is similar to that of the reference compound **Myx** (Table 1a).

**Abortive Transcription Assay.** It has been shown that **Myx** inhibits the transcription initiation (14). Since the ureidothiophene-2-carboxylic acids were designed to bind to the same binding site than **Myx**, it can be assumed that these compounds may also inhibit the initiation of the transcription cycle. To confirm this hypothesis, an HPLC-based abortive transcription assay (25) was performed. Inhibition of transcription initiation was measured by quantification of abortive transcripts that are usually formed during the initiation phase (26, 27). As illustrated in Figure 2, compounds **1** and **6** (Figure 1) induced a drastic reduction of abortive transcript formation. As expected, this data demonstrate that the ureidothiophenes interfere with the transcription process during the initiation phase.

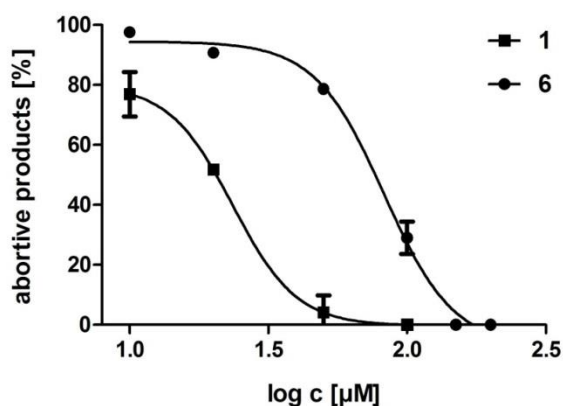


**Figure 2.** Abortive Transcription Assay. Dose-dependent inhibition of **1** and **6** on abortive product formation (ApUp<sup>3</sup>H-C) using ApU and <sup>3</sup>H-CTP as substrates. Standard deviations from two independent experiments are indicated by error bars.

**Mutagenesis studies.** The ureidothiophene-2-carboxylic acids were designed as RNAP inhibitors that bind into the “switch region”. Recent docking studies suggest that these compounds bind in a tilted conformation overlapping with the **Myx** western chain but do not extend in the binding region of the eastern chain (18). To corroborate these findings, several amino acid substitutions in the “switch region” were introduced (Figure S1). Subsequently, the effects of these mutations on both the RNAP transcription inhibition and the antibacterial activity were examined. As expected, mutations in the binding pocket of the **Myx** eastern chain including RNAP  $\beta$  V1275M and  $\beta$  E1279K, did not impair the antibacterial activity of the ureidothiophene-2-carboxylic acid series against *E. coli* TolC (Table S2). Surprisingly, substitution of amino acids located in the proposed binding site such as RNAP  $\beta$  S1322,  $\beta$  L1291,  $\beta'$  K345,  $\beta'$  K334 and  $\beta'$   $\Delta$ 334–5 neither had a significant effect on the antibacterial activity against *E. coli* TolC nor on the *in vitro* activity (Table S2, S3).

**Characterization of the Binding Mode by STD NMR, INPHARMA and Molecular Docking.** All together, the above mentioned results raise the question whether the RNAP “switch region” is indeed the binding site of the ureidothiophene compound series as obtained from our molecular docking experiments. Thus, we performed competition STD NMR (28) experiments where the representative compound **6** (Figure 1) was titrated into a 100:1 complex of **Myx**/RNAP. Difference spectra were monitored for a change in intensity of signals belonging to either **6** or **Myx** during the titration. As shown in Figure 3, stepwise addition of **6** to the complex **Myx**/RNAP diminished the signal intensities of **Myx** concomitant with steady increases in signal intensities belonging to **6**. In fact, addition of three equivalents of **6** resulted in a ~70% uniform decrease in intensity for signals belonging to **Myx** (see Figure 3C). By addition of five equivalents of **6** the signals of **Myx** were almost unnoticeable. Consequently, **6** and **Myx** bind the “switch region” of RNAP in a competitive manner.

Additionally, competition STD NMR experiments were performed between **6** and two other described “switch region” binders, coralopyronin A (**Cor**) and ripostatin A (**Rip**) (29, 30) (Figure 1). **Cor** is a structural analog of **Myx** whereas **Rip** is a cyclic macrolide. So far no crystal structures for these natural products have been reported. Nevertheless, isolation and sequencing of **Cor**- and **Rip**-resistant mutants show that the binding pocket of **Rip** and **Cor** overlap with that of **Myx** (14). As illustrated in

Figure S2, an overall reduction of the **Cor** and **Rip** STD signals is observed upon the addition of **6**, further indicating that **6** binds into the RNAP “switch region”.

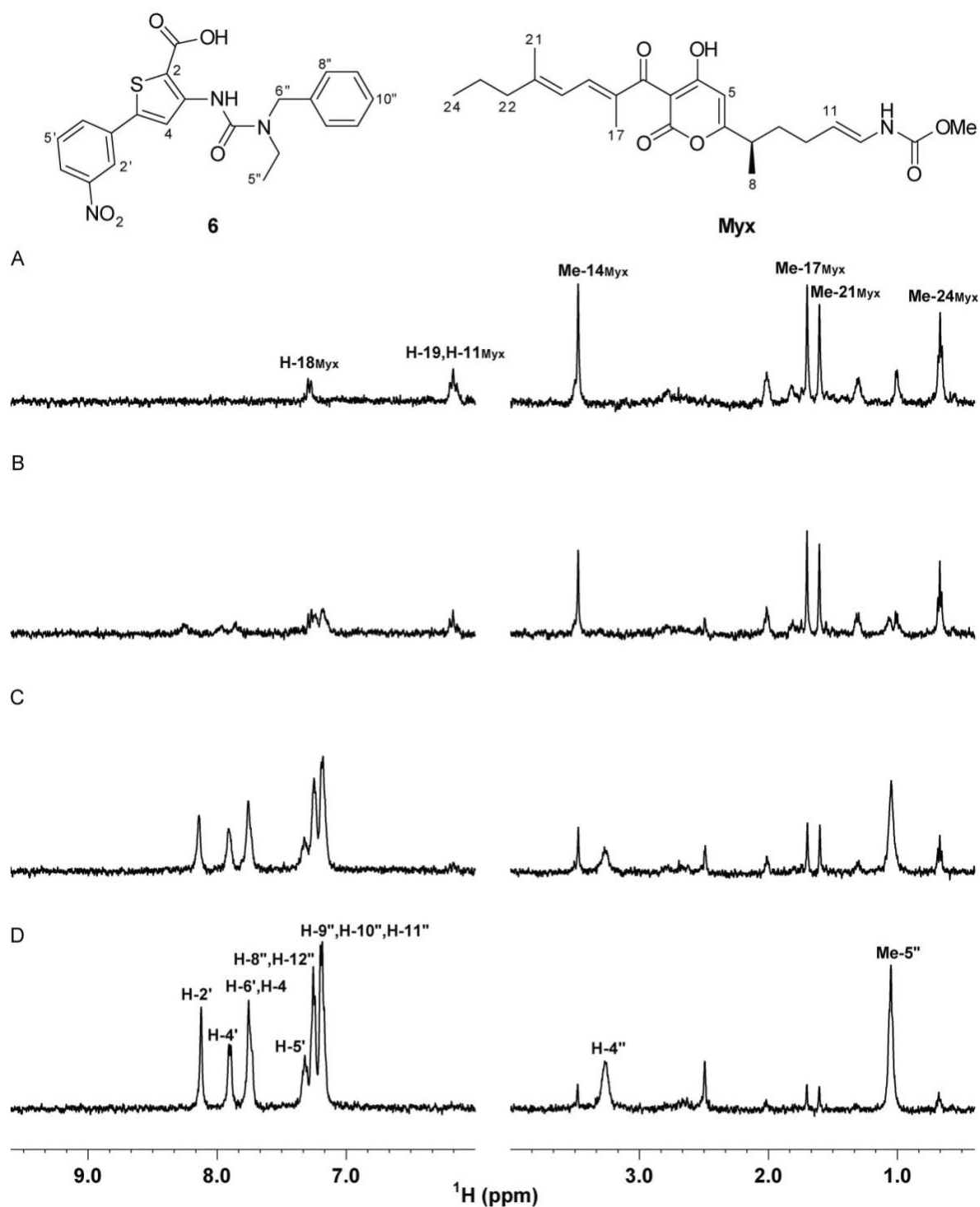


**Figure 3.** STD NMR competition experiments of **6** and **Myx** binding to core RNAP. (A) Expanded  $^1\text{H}$  STD NMR spectrum of **Myx** (250  $\mu\text{M}$ ) in the presence of core RNAP (2.5  $\mu\text{M}$ ). (B-D) STD NMR spectra of the same sample upon addition of (B) 1, (C) 3 and (D) 5 equivalents of **6**.

The INPHARMA method was used to exclude allosteric effects on the displacement of **Myx** by **6** (31). This method is based on the observation of protein-mediated NOE transfer between two ligands binding competitively to the same protein binding pocket. Additionally, we qualitatively analyzed the INPHARMA correlations (32, 33) to determine the binding orientation of **6** in the “switch region” of RNAP relative to that of **Myx**. To this respect, 2D-NOESY experiments were performed for a mixture of RNAP/**Myx**/**6** in a concentration ratio of 1:150:150 at mixing times ranging from 20 to 600 ms. Interligand NOE signals were not detected between **6** and **Myx** in absence of RNAP at mixing times as high as 200 ms, thus excluding a direct interaction between **6** and **Myx**. Due to the size of the receptor (~380 kDa) and to avoid “long” spin-diffusion pathways contributing to the interligand signals, 2D NOESY experiments acquired with a mixing time of 70 ms were chosen to analyze spin-diffusion-mediated interligand NOE interactions (34). In particular, INPHARMA correlations of different intensities were observed between protons of the aromatic rings of **6** and protons Me-24, H-23, H-22, Me-21, Me-17, and H-10 of **Myx** (Figure 4 and Table 2).

Interestingly, besides the weak INPHARMA correlations from H-10 no other signals were observed from protons belonging to the eastern chain of **Myx**. These results corroborate that **6** and **Myx** bind competitively to the “switch region” of RNAP, and furthermore indicate that **6** occupies the region of the **Myx** western chain binding site and slightly occludes that of the eastern chain. Additionally, the strongest INPHARMA correlations were observed from Me-24<sub>Myx</sub> to the protons of both, phenyl and benzyl rings of **6** (Figure 4), suggesting that these two rings and Me-24<sub>Myx</sub> occupy the same area in the binding site. This can only be accomplished if **6** binds to the RNAP “switch region” in two different poses. In one pose, the phenyl ring is residing at a similar site to that of Me-24<sub>Myx</sub> while in the second pose the benzyl moiety is placed at the Me-24<sub>Myx</sub> position. Unfortunately, overlapping of proton signals for Me-5” of **6** and Me-8<sub>Myx</sub> prevents us from using diagnostic INPHARMA correlations from the latter to further corroborate this hypothesis. To circumvent this problem, an ureidothiophene analogue (**13**) without the ethyl group at the position of R<sup>2</sup> (Figure 1) was synthesized. Additionally, a methoxy group was introduced to the benzyl ring of **13** to avoid the signal overlap of H-18<sub>Myx</sub> with H-8”/H-12” of **6**.

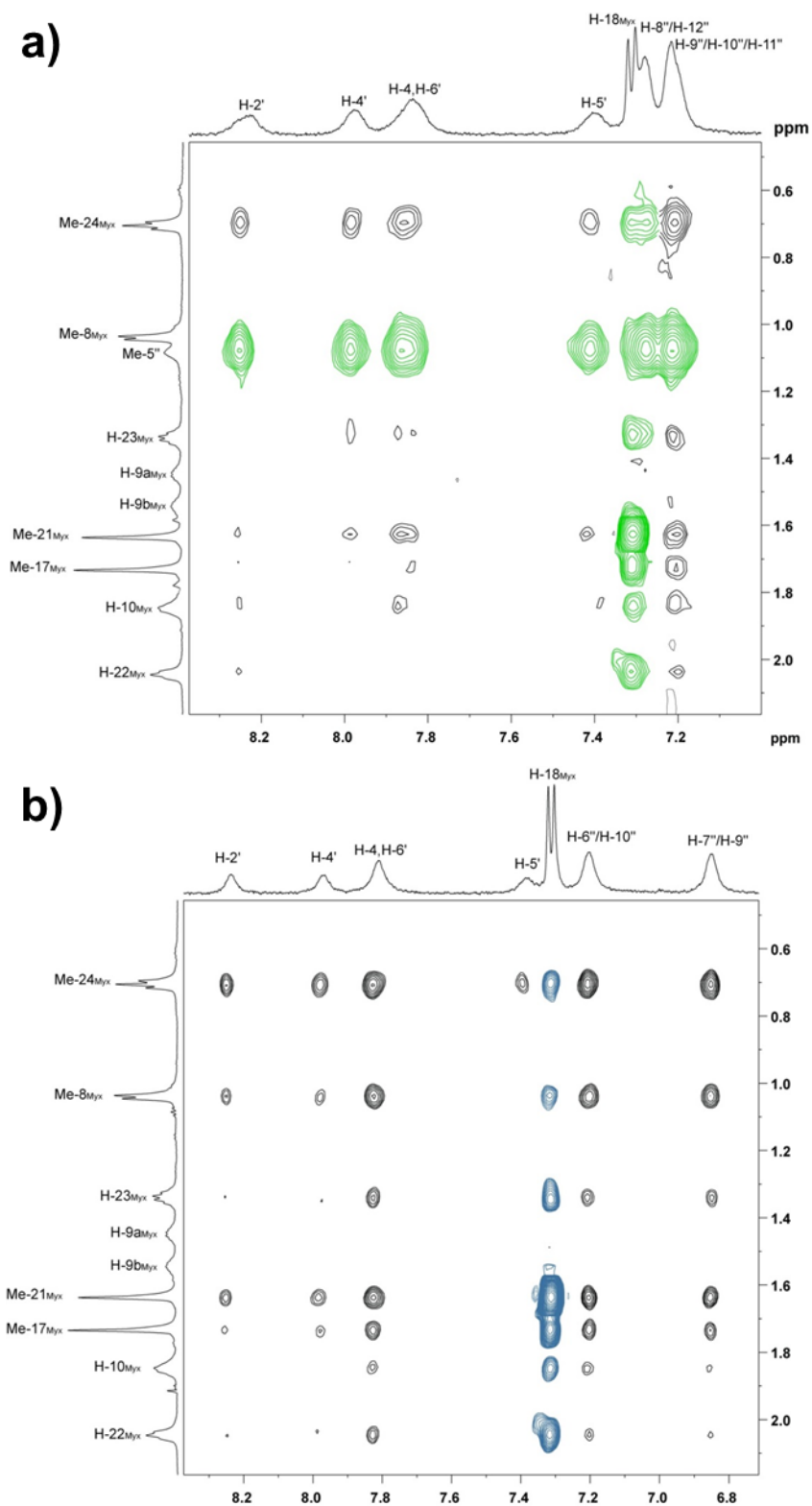


**Figure 4.** NOESY spectra (a) of a mixture of RNAP (2.5  $\mu\text{M}$ ), **Myx** (375  $\mu\text{M}$ ) and **6** (375  $\mu\text{M}$ ) and (b) of a mixture of RNAP (2.5  $\mu\text{M}$ ), **Myx** (375  $\mu\text{M}$ ) and **13** (375  $\mu\text{M}$ ). Signals are assigned in the 1D spectra. The numbering of the atoms of **Myx** and **6** corresponds to that shown in Figure 3, numbering of **13** is shown in the SI (Figure S4). Black peaks represent the interligand transferred NOEs (INPHARMA NOEs) mediated by the hydrogen atoms of RNAP. Overlapping signals are colored in green and intramolecular transferred NOEs from **13** are colored in blue.

**Table 2.** Observed INPHARMA signals between the hydrogen atoms of **Myx** and **6** and **13**, respectively

Myx	Compound 6	Compound 13
<b>Me-24</b>	H-2', H-4', H-5', H-4/6' <sup>a</sup> , H-4'', H-9''–11''	H-2', H-4', H-5', H-4/6' <sup>a</sup> , H-6''/10'', H-7''/9'', MeO-8''
<b>H-23</b>	H-4', H-4/6' <sup>a</sup> , H-9''–11''	H-2', H-4', H-4/6' <sup>a</sup> , H-6''/10'', H-7''/9'', 8''MeO-8''
<b>H-22</b>	H-2', H-4/6' <sup>a</sup> , H-9''–11''	H-2', H-4', H-4/6' <sup>a</sup> , H-6''/10'', H-7''/9'', MeO-8''
<b>Me-21</b>	H-2', H-4', H-5', H-4/6' <sup>a</sup> , H-9''–11''	H-2', H-4', H-4/6' <sup>a</sup> , H-6''/10'', H-7''/9'', MeO-8''
<b>Me-17</b>	H-4/6' <sup>a</sup> , H-9''–11''	H-2', H-4', H-4/6' <sup>a</sup> , H-6''/10'', H-7''/9'', MeO-8''
<b>H-10</b>	H-2', H-4/6' <sup>a</sup> , H-8''–12''	H-4/6' <sup>a</sup> , H-6''/10'', H-7''/9'', MeO-8''
<b>Me-8</b>	–	H-2', H-4', H-4/6' <sup>a</sup> , H-6''/10'', H-7''/9'', MeO-8''

<sup>a</sup> indicates overlapping signals

As a matter of fact, a 2D NOESY spectrum of the mixture RNAP/**13/Myx** clearly showed strong interligand NOE interactions from Me-8<sub>Myx</sub> to the protons of the phenyl ring and benzyl moiety indicating that all these three residues are located near the same protein protons (Figure 4b and Table 2). Also, Me-24<sub>Myx</sub> showed strong INPHARMA correlations to protons of both aromatic rings of **13**. Taken together, these results suggest that both, **6** and **13**, can bind to the “switch region” of RNAP in two different poses with inverted orientations (*vide supra*). Moreover, the INPHARMA data indicate that **6** and **13** partially occlude the **Myx** binding site in a region that ranges from Me-24<sub>Myx</sub> to Me-8<sub>Myx</sub>.

To further evaluate the binding mode of **6** and **13** in the “switch region” of RNAP, we performed molecular docking studies using MOE (*Molecular Operating Environment*) (31) based on the INPHARMA results. The obtained docking poses with inverted orientations for **6** and **13** that correlated best with the STD and INPHARMA results are illustrated in Figure 5.

In poses A and C the NO<sub>2</sub>-substituted phenyl ring is positioned in the upper hydrophobic region of the **Myx** western chain pocket whereas the benzyl ring occupies the lower part of the eastern chain pocket of **Myx**. In docking poses B and D the same area of the “switch region” is occupied by **6** and **13**, but the benzyl and the phenyl ring bind in inverted orientations compared to poses A and C.

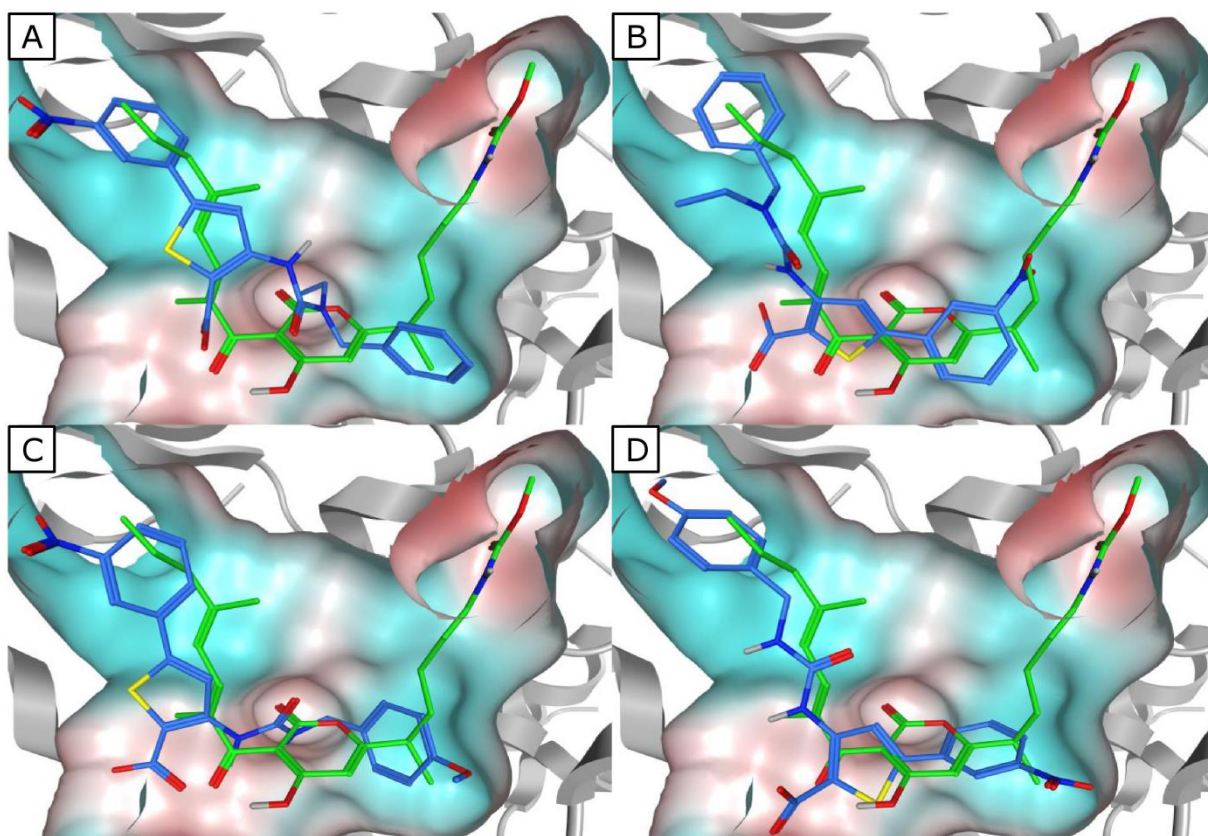


**Figure 5.** Proposed binding modes of **6** (A, B) and **13** (C, D) in the RNAP “switch region”. Since there is no high-resolution crystal structure of the *E. coli* RNAP “switch region” available, an *E. coli* homology model (18) was used. The binding mode of **Myx** (green) is shown to illustrate its relative orientation to **6** and **13** (blue). Hydrophobic and hydrophilic areas of the pocket are colored turquoise and red, respectively.

Recently we could demonstrate that the ureidothiophene-2-carboxylic acids are capable of inhibiting the  $\sigma$ :core assembly which would indicate that these compounds could also bind to the  $\sigma$ :core interface (36). Existence of a second binding site is also

supported by the fact that titrating **Myx** into a **6**/RNAP complex did not result in the displacement of the STD signals of **6** (data not shown). Further evidence of a second binding site for the ureidothiophenes was achieved by monitoring the dose-dependent effect of **6** to quench the intrinsic fluorescence of RNAP core enzyme. Graphical representation of the results displayed a monophasic curve progression for **Myx** (14) and **Rif** whereas **6** showed a biphasic character of the curve indicating that **6** can bind to more than one binding site. Besides that these compounds can bind in two orientations, a second binding site within RNAP could also contribute to the fact, that amino acid substitutions in the “switch region” do not impair the inhibitory activity of the ureidothiophene-2-carboxylic acids.

### Conclusion

In summary, we have shown that the ureidothiophene-2-carboxylic acids possess good antibacterial activity against different clinically relevant MRSA isolates and **Rif**-resistant *E. coli* TolC strains indicating the absence of cross-resistance with existing antibiotics. On the basis of the STD NMR and INPHARMA data, these compounds bind competitively to **Myx** in the RNAP “switch region”. The structural information provided by the transfer NOE experiments along with molecular docking studies allowed us to propose a plausible binding mode for the ureidothiophene-2-carboxylic acids, which occupy the same area of the “switch region” as the **Myx** western chain and the 2-pyrone core. Moreover, our results confirm that our pharmacophore-based virtual screening approach has been successful in identifying easily accessible small molecule RNAP inhibitors that bind to the intended target site, the RNAP “switch region”, thus providing the potential to avoid the problem of resistance. In closing, these results provide useful insights into the structural requirements for optimized interactions with the target site and may thus facilitate structure-based optimization of this inhibitor class.

### Methods

**Plasmids.** For purification of *E. coli* wild type core RNAP the plasmid pVS10 was used which encodes the *E. coli* *rpoA-rpoB-rpoC* [His6] and *rpoZ* ORFs under control of a T7 promoter (37). Amino acid substitutions in the *E. coli* RNAP subunits were constructed by site-directed mutagenesis on the basis of pVS10, pRL663 and pIA458

containing a fragment from  $\beta$  *SdaI* to  $\beta'$  *BsmI* (17) and were verified by sequencing. Detailed information about the plasmids are provided in the SI.

**Selection of Rif- and Myx-resistant *E. coli* TolC spontaneous mutants.** The procedure was performed as described earlier (38).

**Protein Purification.** Wild type and altered RNAP core enzymes were purified as described previously (37) without the DNA-affinity chromatography step.

**MIC determination.** 3–4 isolated colonies of *E. coli* TolC transformed with a pRL663 or pRL706 derivative or colonies of spontaneous myxopyronin-resistant *E. coli* TolC mutants were transferred into 5 ml MHB containing 200  $\mu\text{g ml}^{-1}$  ampicillin and incubated over night at 37 °C with shaking. The turbidity of the bacterial suspension was adjusted to that of a McFarland standard 0.5 (OD 600  $\sim$  = 0,1 for  $10^8$  cfu  $\text{ml}^{-1}$ ) and was then diluted by a factor of 1:100 with sterile MHB ( $10^6$  cfu  $\text{ml}^{-1}$ ). Aliquots of 100  $\mu\text{l}$  bacterial suspension were subcultured in 100  $\mu\text{l}$  MHB containing the compounds dissolved in DMSO in different concentrations in a 96-well plate in triplicates and incubated at 37 °C for 18 h with shaking (50 rpm). Final DMSO concentration in the experiment was 1 %. For testing *E. coli* TolC transformed with a pRL663 and pRL706 derivative, the MHB was supplemented with IPTG (1 mM). Given MIC values are means of at least two independent determinations (three if  $\text{MIC} < 10 \text{ mg mL}^{-1}$ ) and are defined as the lowest concentration of the compounds that inhibit visible growth of the tested isolates.

MICs for MRSA isolates were determined by broth microdilution as recommended by the Clinical and Laboratory Standards Institute (39). Antibiotic resistance profiles of the MRSA isolates were determined using the Vitek 2 automated antimicrobial susceptibility testing system (bioMérieux, Marcy l'Étoile, France).

**Transcription assay.** The assay was performed as described previously (18, 40, 41) with minor modifications. Final concentrations in a total volume of 30  $\mu\text{L}$  were 56 nM wild type or mutant core RNAP, respectively. An equimolar amount of  $\sigma^{70}$  was used along with 60 nCi of [5,6- $^3\text{H}$ ]-UTP, 400  $\mu\text{Mol}$  ATP, CTP and GTP as well as 100  $\mu\text{M}$  of UTP, 20 units of RNase inhibitor (RiboLock, Fermentas), 10 mM DTT, 40 mM tris-HCl (pH 7.5), 150 mM KCl, 10 mM  $\text{MgCl}_2$  and 0.1% CHAPS. As a DNA template 3500 ng of religated pcDNA3.1/V5-His-TOPO was used per reaction. Prior to starting the experiment, core enzyme was preincubated with  $\sigma^{70}$  for 10 min at 25 °C to allow

formation of the holo enzyme. Subsequent steps are performed as described previously (18).

**HPLC-based Abortive Transcription Assay.** The assay was performed as described previously (42).

**NMR Spectroscopy.** STD NMR data were recorded at 290 K on a Bruker Avance 500 NMR instrument equipped with a cryogenically cooled 5 mm inverse triple resonance gradient probe. Experiments were recorded with the carrier set at  $-2$  ppm for on-resonance irradiation and 40 ppm for off-resonance irradiation. Control spectra were recorded under identical conditions. Selective protein saturation (2 s) was accomplished using a train of 50 ms Gauss-shaped pulses, each separated by a 1 ms delay, at an experimentally determined optimal power (50 dB on our probe); a T1 $\rho$  filter (15 ms) was incorporated to suppress protein resonances. Experiments were recorded using a minimum of 256 scans and 32 K points. On- and off-resonance spectra were processed independently and subtracted to provide a difference spectrum. 2D NOESY (INPHARMA) experiments were recorded at 290 K on a Bruker Ascend 700 NMR instrument equipped with a cryogenically cooled 5 mm inverse triple resonance gradient probe. Samples containing 150:150:1 **Myx/6**/core RNAP and **Myx/13**/core RNAP were prepared in deuterated buffer (20 mM NaPO<sub>4</sub> and 50 mM NaCl, pH 6.8). 2D NOESY experiments were acquired using standard pulse sequences with water suppression (WATERGATE), 96 scans as 2048x400 data points at mixing times ranging from 20–800 ms.

**Computational Chemistry.** The virtual binding modes of compounds **6** and **13** were created using MOE (*Molecular Operating Environment*). The model of *E. coli* RNAP in complex with myxopyronin A, which was used as receptor in the following docking experiments, was created by superposition of 3DXJ (*T. thermophilus* RNAP in complex with myxopyronin A) (14) and an *E. coli* RNAP homology model (18). After removal of the *T. thermophilus* protein the remaining receptor-ligand complex was energy minimized using the LigX module of MOE (standard settings) tethering receptor and ligand (strength: 10). Employing the docking module of MOE, compounds **6** and **13** were docked into the myxopyronin binding site. “Triangle Matcher” was chosen as placement method and “London dG” was selected as scoring function. “Rotate bonds” and “Remove duplicates” functions were switched on and 30 hits were retained. Implying the results of the NMR experiments a

pharmacophore containing two aromatic features (radius F1: 2 Å, F2: 1.5 Å) was used to guide the docking. Furthermore the same docking was performed with an additional forcefield refinement. The docking results were searched for the poses which correlated best with the NMR results. These were further refined using the LigX module (standard settings) tethering the receptor (strength: 5000) to afford the final binding modes.

## Acknowledgements

The authors thank R.-H. Ebricht for providing pRL663 and pRL706 derivatives and I. Artsimovitch for providing pVS10 and pIA derivatives. Furthermore, we thank J. Jung, J. Ludwig and K. Hilgert for excellent technical support.

## References

- (1) Mattelli, A., Roggi, A., and Carvalho, A. (2014) Extensively drug-resistant tuberculosis: epidemiology and management. *Clin. Epidemiol.* 6, 111–118.
- (2) Conly, J.-M., and Johnston, B.-L. (2005) Where are all the new antibiotics? The new antibiotic paradox. *Can. J. Infect. Dis. Med. Microbiol.* 16, 159–160.
- (3) EDCCD/EMEA Joint Technical Report. The bacterial challenge: time to react. (2009) EMEA/576176/2009.
- (4) Artsimovitch, I., and Vassylyev, D.-G. (2006) Is it easy to stop RNA polymerase? *Cell Cycle* 5, 399–404.
- (5) Chopra, I. (2007) *Bacterial RNA polymerase: a promising target for the discovery of new antimicrobial agents*. *Curr. Opin. Invest. Drugs* 8, 600–607.
- (6) Villain-Guillot, P., Bastide, L., Gualtieri, M., and Leonetti, J.-P. (2007) *Progress in targeting bacterial transcription*. *Drug Discov. Today* 12, 200–208.
- (7) Mariani, R., and Maffioli, S.-J. (2009) *Bacterial RNA polymerase inhibitors: an organized overview of their structure, derivatives, biological activity and current clinical development status*. *Curr. Med. Chem.* 16, 430–454.
- (8) Venugopal, A.-A., and Johnson, S. (2012) Fidaxomicin: A Novel Macrocyclic Antibiotic Approved for Treatment of *Clostridium difficile* Infection. *Clin. Infect. Dis.* 54, 568–574.
- (9) Mitchison, D. (2000) Role of individual drugs in the chemotherapy of tuberculosis. *Int. J. Tuberc. Lung Dis.* 4, 796–806.
- (10) Espinal, M.-A., Laszlo, A., Simonsen, L., Boulahbal, F., Kim, S.-J., Reniero, A., Hoffner, S., Rieder, H.-L., Binkin, N., Dye, C., Williams, R., and Raviglione, M.-C. (2001) Global trends in resistance to antituberculosis drugs. World Health Organization-International Union against tuberculosis and lung disease working group on anti-tuberculosis drug resistance surveillance. *N. Engl. J. Med.* 344, 1294–1303.
- (11) Mukinda, F.-K., Theron, D., van der Spuy, G.-D., Jacobson, K.-R., Roscher, M., Streicher, E.-M., Musekiwa, A., Coetzee, G.-J., Victor, T.-C., Marais, B.-J., Nachega, J.-B., Warren, R.-M.,

- and Schaaf, H.-S. (2012) Rise in rifampicin-mono-resistant tuberculosis in Western Cape, South Africa. *Int. J. Tuberc. Lung. Dis.* 16, 196–202.
- (12) Jin, D.-J., and Gross, C.-A. (1988) Mapping and Sequencing of Mutations in the *Escherichia coli* rpoB Gene that Lead to Rifampicin Resistance. *J. Mol. Biol.* 202, 45–58.
- (13) Chopra, I. (2007) Bacterial RNA polymerase: a promising target for the discovery of new antimicrobial agents. *Curr. Opin. Invest. Drugs* 8, 600–607.
- (14) Mukhopadhyay, J., Das, K., Ismail, S., Koppstein, D., Jang, M., Hudson, B., Sarafianos, S., Tuske, S., Patel, J., Jansen, R., Irschik, H., Arnold, E., and Ebright, R.-H. (2008) The RNA polymerase “switch region” is a target for inhibitors. *Cell* 135, 295–307.
- (15) Srivastava, A., Talaue, M., Liu, S., Degen, D., Ebright, R.-Y., Sineva, E., Chakraborty, A., Druzhinin, S.-Y., Chatterjee, S., Mukhopadhyay, J., Ebright, Y.-W., Zozula, A., Shen, J., Sengupta, S., Niedfeldt, R.-R., Xin, C., Kaneko, T., Irschik, H., Jansen, R., Donadio, S., Connell, N., and Ebright, R.-H. (2011) New target for inhibition of bacterial RNA polymerase: ‘switch region’. *Curr. Opin. Microbiol.* 14, 532–543.
- (16) Irschik, H., Gerth, K., Hofle, G., Kohl, W., and Reichenbach, H. (1983) The myxopyronins, new inhibitors of bacterial RNA synthesis from *Myxococcus fulvus* (Myxobacterales). *J. Antibiot.* 36, 1651–1658.
- (17) Belogurov, G., Vassilyeva, M., Sevostyanova, A., Appleman, J., Xiang, A., Lira, R., Webber, S., Klyuyev, S., Nudler, E., Artsimovitch, I., and Vassilyev, D. (2009) Transcription inactivation through local refolding of the RNA polymerase structure. *Nature* 45, 332–335.
- (18) Sahner, J.-H., Groh, M., Negri, M., Hauptenthal, J., and Hartmann, R.-W. (2013) Novel small molecule inhibitors targeting the “switch region” of bacterial RNAP: structure-based optimization of a virtual screening hit. *Eur. J. Med. Chem.* 65, 223–231.
- (19) Fejzo, J., Lepre, C., and Xie, X. (2003) Application of NMR Screening in Drug Discovery. *Curr. Top. Med. Chem.* 3, 81–97.
- (20) Meyer, B., and Peters, T. (2003) NMR Spectroscopy Techniques for Screening and Identifying Ligand Binding to Protein Receptors. *Angew. Chem. Int. Ed.* 42, 864–890.
- (21) Voyich, J.-M., Braughton, K.-R., Sturdevant, D.-E., Whitney A.-R., Saïd-Salim, B., Porcella, S.-F., Long, R.-D., Dorward, D.-W., Gardner, D.-J., Kreiswirth, B.-N., Musser, J.-M., and DeLeo, F.-R. (2005) Insights into mechanisms used by *Staphylococcus aureus* to avoid destruction by human neutrophils. *J. Immunol.* 175, 3907–3919.
- (22) Kornblum, J., Hartman, B.-J., Novick, R.-P., and Tomasz, A. (1986) Conversion of a homogeneously methicillin-resistant strain of *Staphylococcus aureus* to heterogeneous resistance by Tn551-mediated insertional inactivation. *Eur. J. Clin. Microbiol.* 5, 714–8.
- (23) Ballhausen, B., Jung, P., Kriegeskorte, A., Makgotlho, P.-A., Ruffing, U., von Müller, L., Köck, R., Peters, G., Herrmann, M., Ziebuhr, W., Becker, K., and Bischoff, M. (2014) LA-MRSA CC398 differ from classical community acquired-MRSA and hospital acquired-MRSA lineages: functional analysis of infection and colonization processes. *Int. J. Med. Microbiol.* Epub Jun 27, 2014. DOI: 10.1016/j.ijmm.2014.06.006.
- (24) Ruffing, U., Akulenko, R., Bischoff, M., Helms, V., Herrmann, M., and von Müller, L. (2012) Matched-cohort DNA microarray diversity analysis of methicillin sensitive and methicillin

- resistant *Staphylococcus aureus* isolates from hospital admission patients. *PLoS One* 7, e52487.
- (25) Hüsecken, K., Negri, M., Fruth, M., Boettcher, S., Hartmann, R.-W., and Haupenthal, J. (2013) Peptide-based investigation of the *Escherichia coli* RNA polymerase  $\sigma^{70}$ : core interface as target site. *ACS Chem. Biol.* 8, 758–766.
- (26) McClure, W.-R., Cech, C.-L., and Johnston, D.-E. (1978) A steady state assay for the RNA polymerase initiation reaction. *J. Biol. Chem.* 253, 8941.
- (27) Vo, N.-V., Hsu, L.-M., Kane, C.-M., and Chamberlin, M.-J. (2003) *In Vitro* Studies of Transcript Initiation by *Escherichia coli* RNA Polymerase. 2. Formation and Characterization of Two Distinct Classes of Initial Transcribing Complexes. *Biochemistry* 42, 3787–3797.
- (28) Mayer, M., and Meyer, B. (2001) Group Epitope Mapping by Saturation Transfer Difference NMR To Identify Segments of a Ligand in Direct Contact with a Protein Receptor. *J. Am. Chem. Soc.* 123, 6108–6117.
- (29) Irschik, H., Jansen, R., Höfle, G., Gerth, K., and Reichenbach, H. (1985) The coralopyronins, new inhibitors of bacterial RNA synthesis from *Myxobacteria*. *J. Antibiot.* 38, 145–152.
- (30) Irschik, H., Augustiniak, H., Gerth, K., Höfle, G., and Reichenbach, H. (1995) The Ripostatins, Novel Inhibitors of Eubacterial RNA Polymerase Isolated from Myxobacteria. *J. Antibiot.* 48, 787–792.
- (31) Sánchez-Pedregal, V.-M., Reese, M., Meiler, J., Blommers, M.-J.-J., Griesinger, C., and Carlomagno, T. (2005) The INPHARMA Method: Protein-Mediated Interligand NOEs for Pharmacophore Mapping. *Angew. Chem.* 117, 4244–4247.
- (32) Bartoschek, S., Klabunde, T., Defossa, E., Dietrich, V., Stengelin, S., Griesinger, C., Carlomagno, T., Focken, I., and Wendt, K.-U. (2010) Drug Design for G-Protein-Coupled Receptors by a Ligand-Based NMR-Method. *Angew. Chem.* 49, 1426–1429.
- (33) Krimm, I. (2012) INPHARMA-based identification of ligand binding site in fragment-based drug design. *Med. Chem. Commun.* 3, 605–610.
- (34) Orts, J., Griesinger, C., and Carlomagno, T. (2009) The INPHARMA technique for pharmacophore mapping: A theoretical guide to the method. *J. Mag. Res.* 200, 64–73.
- (35) *Molecular Operating Environment*, 2010.10; Chemical Computing Group Inc., 1010 Sherbooke St. West, Suite #910, Montreal, QC, Canada, H3A 2R7, (2010).
- (36) Hüsecken, K., unpublished results.
- (37) Belogurov, G.-A., Vassilyeva, M.-N., Svetlov, V., Klyuyev, S., Grishin, N.-V., Vassilyev, D.-G., and Artsimovitch, I. (2007) Structural Basis for Converting a General Transcription Factor into an Operon-Specific Virulence Regulator. *Mol. Cell* 26, 117–129.
- (38) Elgaher, W.-A.-M., Fruth, M., Groh, M., Haupenthal, J., and Hartmann, R.-W. (2014) Expanding the scaffold for bacterial RNA polymerase inhibitors: design, synthesis and structure–activity relationships of ureidoheterocyclic-carboxylic acids. *RSC Adv.* 4, 2177–2194.
- (39) Methods for Dilution Antimicrobial Susceptibility Tests for Bacteria That Grow Aerobically. Approved standard - Ninth edition. CLSI document M07-A9. Clinical and Laboratory Standards Institute, 950 West Valley Road, Suite 2500, Wayne, PA 19087, USA, 2012.

- (40) Haupenthal, J., Hüsecken, K., Negri, M., Maurer, C.-K., and Hartmann, R.-W. (2012) Influence of DNA Template Choice on Transcription and Inhibition of *Escherichia coli* RNA Polymerase. *Antimicrob. Agents Chemother.* 56, 4536–4539.
- (41) Hinsberger, S., Hüsecken, K., Groh, M., Negri, M., Haupenthal, J., and Hartmann, R.-W. (2013) Discovery of Novel Bacterial RNA Polymerase Inhibitors: Pharmacophore-Based Virtual Screening and Hit Optimization. *J. Med. Chem.* 56, 8332–8338.
- (42) Hüsecken, K., Negri, M., Fruth, M., Boettcher, S., Hartmann, R.-W. and Haupenthal, J. (2013) Peptide-Based Investigation of the *Escherichia coli* RNA Polymerase  $\sigma^{70}$ :Core Interface As Target Site. *ACS Chem. Biol.* 8, 758–766.

### 3.3 Advanced Mutasynthesis Studies on Natural $\alpha$ -Pyrone Antibiotics from *Myxococcus fulvus*

J. Henning Sahner, H. Sucipto, Silke C. Wenzel, Matthias Groh, Rolf W. Hartmann, and Rolf Müller

Reprinted with permission from *ChemBioChem* **2015**, DOI: 10.1002/cbic.

201402666

Copyright (2015) John Wiley and Sons.

#### Publication C

**Abstract:** Myxopyronin is a natural  $\alpha$ -pyrone antibiotic isolated from the soil bacterium *Myxococcus fulvus* Mx f50. Myxopyronin is able to inhibit the bacterial RNA polymerase (RNAP) by binding to a part of the enzyme not targeted by the clinically used rifamycins. This mode of action makes myxopyronins promising molecules for the development of novel broad-spectrum antibacterials. Herein we describe the derivatization of myxopyronins using an advanced mutasynthesis approach as a first step towards this goal. Site-directed mutagenesis of the biosynthetic machinery was used to block myxopyronin biosynthesis at different stages. The resulting mutants were fed with distinct precursors mimicking biosynthetic intermediates to restore production. Mutasynthons incorporation and production of novel myxopyronin derivatives was analyzed by HPLC-MS/MS. This work sets the stage for accessing numerous myxopyronin derivatives thus significantly expanding the chemical space of the class of  $\alpha$ -pyrone antibiotics.

## Introduction

The current development of bacterial resistances against clinically used antibiotics is alarming. Resistant *Mycobacterium tuberculosis* (MTB) strains for example represent a major health threat and approximately 1.5 million patients die from tuberculosis infections each year.<sup>[1]</sup> Over the last decades multi-drug resistant tuberculosis strains (MDR-TB) evolved, which are resistant to the first line TB drugs rifampicin and isoniazid.<sup>[2]</sup> These strains gave rise to the increasingly prevalent extensively drug resistant tuberculosis strains (XDR-TB). These strains are additionally resistant towards at least one of the second line TB drugs.<sup>[3,4]</sup> Rifampicin is the most prominent anti TB drug. It binds at the active site of the bacterial RNA polymerase (RNAP), inhibiting the initiation of RNA synthesis and thus the transcription process.<sup>[5,6]</sup> Consequently, widespread occurrence of rifampicin resistance dramatically hampers tuberculosis therapy.<sup>[7]</sup> This situation stresses the importance of the development of new antibiotics that can overcome existing resistances. However, developing substances addressing already known and exploited targets involves the risk of cross-resistances. It is more promising to identify inhibitors of novel targets and binding sites to avoid such effects.<sup>[8-10]</sup> Recently the switch region of the bacterial RNAP was discovered as a new binding site. It is targeted by the natural  $\alpha$ -pyrone antibiotic myxopyronin (Chart 1),<sup>[11]</sup> which was isolated from the terrestrial myxobacterium *Myxococcus fulvus* Mx f50.<sup>[12,13]</sup> It was shown that rifampicin resistant mutants exhibit no cross-resistance to myxopyronin which makes myxopyronins a promising starting point for drug development.<sup>[14]</sup> Corallopyronins, which are structurally closely related to myxopyronins (Chart 1), represent further members of the  $\alpha$ -pyrone class of antibiotics..

Despite the close structural similarity between myxopyronins and corallopyronins, there are remarkable differences in their pharmacodynamic profiles. Whereas corallopyronin completely blocks RNA synthesis *in vitro*, myxopyronin only achieves inhibition to a certain extent even at high concentrations.<sup>[15]</sup> Nevertheless, myxopyronin shows a lower minimal inhibitory concentration (MIC) against several pathogens including *M. tuberculosis* H37Rv than corallopyronin (myxopyronin: 1.6  $\mu\text{g/mL}$ ; corallopyronin: 3.1  $\mu\text{g/mL}$ ).<sup>[16]</sup>

The total synthesis of myxopyronin, corallopyronin and several derivatives has been reported.<sup>[17-19]</sup> Due to the complexity of the compounds the described procedures are laborious, comprise many steps with relatively low final yields and are not economically viable.

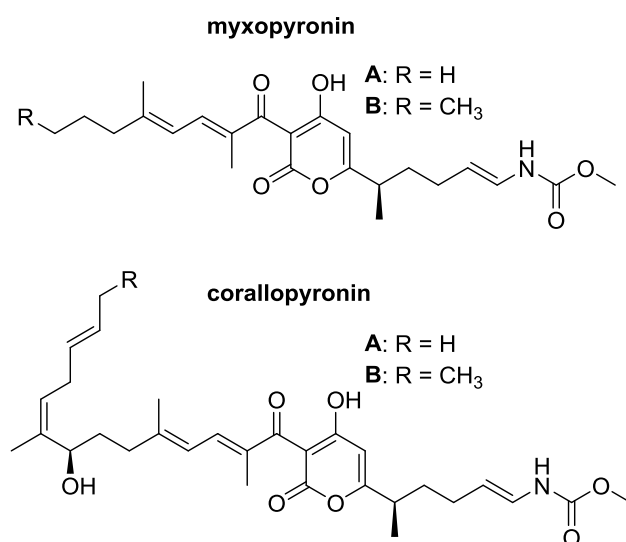


**Chart 1.** Natural  $\alpha$ -pyrone antibiotics myxopyronin A/B and corallopyronin A/B.

Mutasynthesis represents an attractive approach for the generation of derivatives of complex natural products, without the necessity of multi-step organic synthesis.<sup>[20-23]</sup> In this method, small and chemically relatively simple precursors (mutasynthons), mimicking biosynthetic intermediates, are added to the culture of a mutagenized microbe, in which natural product biosynthesis was blocked at a certain stage. The mutasynthons enter the cells and are incorporated into the modified biosynthetic pathway resulting structurally diverse compounds. Currently, most successful examples in the literature target precursor biosynthesis such as the 3-amino-5-hydroxybenzoic acid (AHBA) moiety of ansamitocins.<sup>[24,25]</sup> The technology has rarely been used to incorporate more advanced biosynthetic intermediates or even complex parts of the final molecule.

Recently, the biosynthetic pathways of myxopyronin (Figure 1a) and corallopyronin were elucidated, establishing the basis for mutasynthesis approaches.<sup>[26,27]</sup> The natural products are composed of a central pyrone core decorated with two sidechains (“western” (green) and “eastern” (blue), Figure 1a). The western and

eastern moieties originate from two enzymatic machineries that independently catalyze the assembly of each chain (here described for myxopyronins). The western chain is generated by the polyketide synthase (PKS) MxnK and the carbamate containing eastern chain is produced by the hybrid PKS / non-ribosomal peptide synthetase (NRPS) system MxnI/MxnJ. Such multimodular megasynthetases catalyze the stepwise assembly of simple precursors into complex molecules by using a distinct set of catalytic domains ordered in modules. Each module incorporates one specific unit into the growing biosynthetic intermediate. After chain assembly, both halves are connected by the ketosynthase MxnB *via* intermolecular Claisen-condensation resulting in the characteristic  $\alpha$ -pyrone core structure.

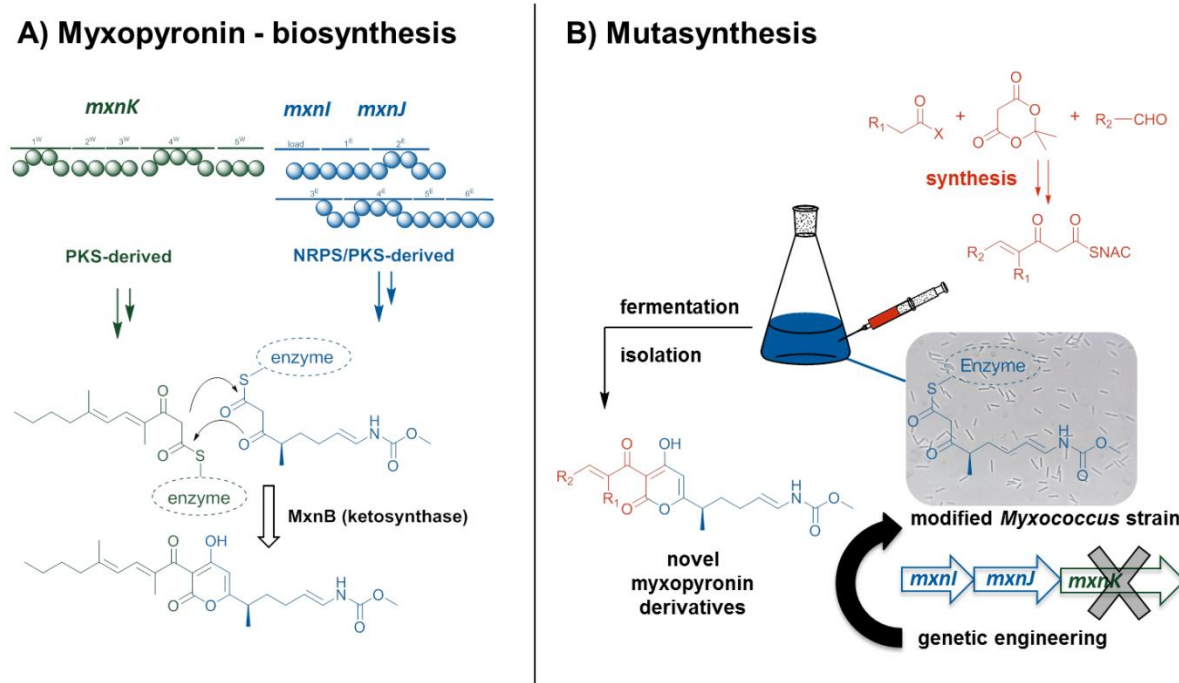


**Figure 1.** a) Biosynthetic pathway of myxopyronin.<sup>[26]</sup> The western chain (green) is produced by the PKS system MxnK. The eastern chain (blue) is derived from the combined PKS/NRPS system MxnI/MxnJ. The two chains are connected by the ketosynthase MxnB. b) Mutasynthesis approach. Synthetic western chains (red) are fed to a *M. fulvus*  $\Delta$ *mxnK* culture, incapable of producing the native western chain. During fermentation, the synthetic precursors are combined with the native eastern chain to yield novel myxopyronin derivatives.

The physicochemical properties of myxopyronin are more complex than those of common clinically used antibiotics.<sup>[7,28]</sup> Its high lipophilicity causes decreasing MIC values in the presence of serum albumin. The compound also features a conjugated

double bond system which makes it unstable and sensitive to UV light.<sup>[7,29]</sup> Moreover, myxopyronin is highly flexible causing a significant entropic penalty when binding to its target site which probably reduces its potency. The present work focuses on setting the stage for the advanced mutasynthesis-based development of new myxopyronin derivatives (Figure 1b), which could potentially overcome these problems and ideally display higher inhibitory potency. So far the coralloyronin producer was not amenable to the genetic modifications required for mutasynthesis and we therefore focused our work on myxopyronin. The major aim of this study was to elucidate the structural requirements for the mutasynthons to be taken up by the producing strain and to be accepted by the myxopyronin biosynthetic machinery. Due to the high structural similarity between myxopyronin and coralloyronin it is expected that our results will be transferable to the coralloyronin system.

### Results and discussion

Myxopyronin adopts a U-shaped conformation inside the switch region of the bacterial RNAP (Figure 2). The eastern chain extends into a narrow channel delimited by V1037, W1038, E1041 of the RNAP  $\beta$ -subunit and K1097, V1099, D1100, H805, K1463, V1466, I1467 of the  $\beta'$ -subunit. Its polar carbamate function forms several crucial water mediated hydrogen bonds with D1100, K1463 ( $\beta'$ ) and W1038 ( $\beta$ ). Initial structure activity relationship (SAR) studies show that slight variations in the eastern part of the molecule result in a dramatic loss of inhibitory activity, with one exception. The derivative lacking the (*R*)-methyl group, right next to the  $\alpha$ -pyrone core (desmethyl-myxopyronin), possesses the thus far highest activity, approximately three times that of the natural product.<sup>[19]</sup>

The western chain of myxopyronins provides wider scope for structural variations. It is only composed of hydrophobic functionalities that do not significantly contribute to interactions with the RNAP switch region. Nevertheless, interactions with several polar amino acids and protein backbones are addressable in this region. Establishment of a single specific hydrogen bond could therefore result in improved RNAP inhibitors. Moreover, the larger RNAP binding pocket in this area provides the option to introduce bulkier groups, which would resemble coralloyronins that are significantly larger in the western chain part. Thus, we focused on the production of myxopyronin derivatives with modified western chains. *N*-acetyl cysteamine (NAC)

thioesters were chosen as substrates for feeding experiments as they mimic carrier protein (CP) bound biosynthetic intermediates of the assembly line. In general, the application of NAC thioesters for mutasynthesis approaches with PKS/NRPS assembly lines is well established. They are known to enter cells and to be accepted as substrates by biosynthetic enzymes.<sup>[20]</sup>

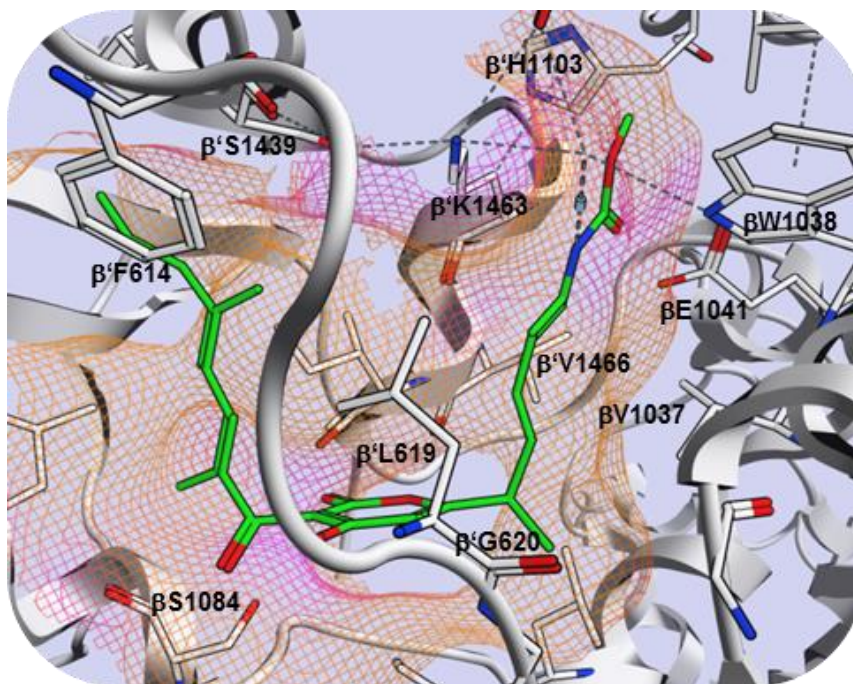


**Figure 2.** Crystal structure of myxopyronin inside the switch region of *Thermus thermophilus* RNAP (PDB-ID; 3DXJ).<sup>[11]</sup>

In a first attempt we aimed to synthesize mimics of the fully matured western chain intermediate, which should directly enter the chain condensation reaction catalyzed by MxnB. Synthesis of the required  $\beta$ -keto NAC-thioesters from the corresponding  $\beta$ -ketoacids is intractable due to the instability of the free acids or undesired side products under coupling conditions.<sup>30</sup> Therefore, we developed a synthetic route which involves dioxinones as protected  $\beta$ -ketoacid equivalents. The majority of the desired  $\beta$ -keto NAC thioesters was obtained according to the synthesis route shown in Scheme 1. The first step involves an acylation of Meldrum's acid (**I**)<sup>[31]</sup> followed by a rearrangement, yielding dioxinone **II**.<sup>[32]</sup> After conversion to the dioxinone phosphonate **III**,<sup>[33]</sup> the resulting compound was coupled with the appropriate aldehyde in a Horner-Wadsworth-Emmons reaction to yield the unsaturated dioxinone **IV**.<sup>[34]</sup> Final conversion with NAC-H gave rise to the desired  $\beta$ -keto-NAC-thioester **V**.<sup>[30]</sup>

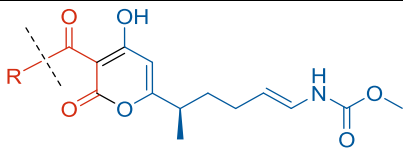
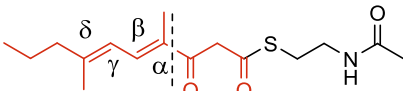
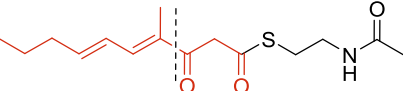
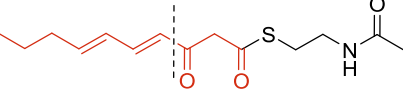
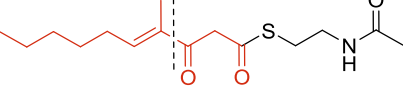
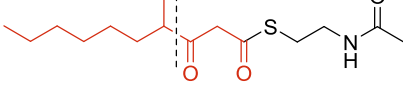
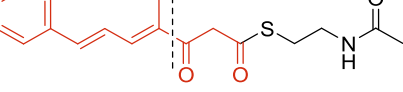
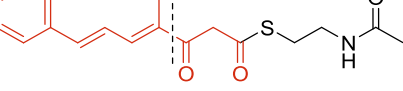
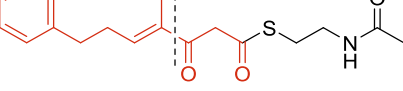
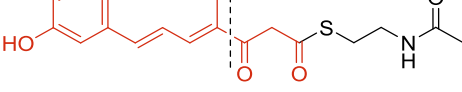
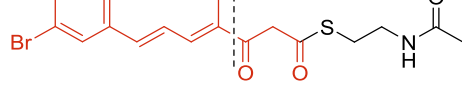
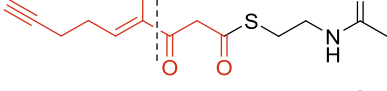
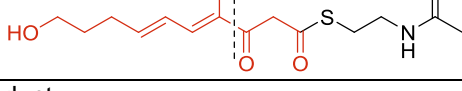


chain condensation reaction catalyzed by MxnB. While removal of the methyl group in the  $\delta$ -position (**2**) was tolerated and resulted in the production of the novel derivative **W2**, additional elimination of the methyl in the  $\alpha$ -position (**3**) did not yield the expected product. Compound **4** lacking the  $\delta$ -methyl and the  $\gamma$ -double bond was accepted again whereas the completely saturated precursor **5** was not incorporated. From these results we concluded, that the  $\alpha$ -methyl group as well as the  $\alpha$ -double bond are essential for substrate acceptance and pyrone ring formation by MxnB. Hence, these structural features were included in all further synthesized mutasynthons to maximize the probability of incorporation.

Next we evaluated if mutasynthons with terminal phenyl substituents are incorporated. Such aromatic systems allow an easy introduction of a variety of functional groups. When attached at the appropriate positions of the ring, these groups can be used to engineer new and specific interactions with bacterial RNAP. A closer look at the complex-crystal structure of bacterial RNAP with myxopyronin (PDB-ID: 3DXJ) revealed that the pocket accepting the western part should be wide enough to adapt to this dramatic structural change. Compound **6** was initially tested as a prototype for this purpose and resulted in production of the desired derivative **W6** (compare Figure 3). Replacement of the  $\alpha$ -methyl group by an ethyl function (**7**) or omitting of the  $\gamma$ -double bond (**8**) allowed for incorporation as well.

Molecular modelling studies with the myxopyronin derivative **W6** suggested that a hydroxyl function in the *meta* position of the phenyl ring might lead to a water mediated H-bond with W1434 ( $\beta'$ -subunit). Moreover, the additional hydrophilic function could lead to improved physicochemical properties. For this purpose, compound **9** was synthesized and successful incorporation yielding derivative **W9** was achieved. Encouraged by these promising results a precursor with a bromo-substituent instead the hydroxyl function (**10**) was synthesized and fed, which enabled the production of the expected myxopyronin analog (**W10**). Such a brominated derivative provides extended possibilities for further derivatization, e.g. under Suzuki<sup>35</sup> or Buchwald Hartwig<sup>36</sup> conditions, to access a broader chemical space.

**Table 1.** Synthetic western side chain mimics. If accepted, the red part of the structure is included in the final myxopyronin derivative.

Entry	Formula	Myx derivative
		
1		<b>W1</b>
2		<b>W2</b>
3		n.p.
4		<b>W4</b>
5		n.p.
6		<b>W6</b>
7		<b>W7</b>
8		<b>W8</b>
9		<b>W9</b>
10		<b>W10</b>
11		<b>W11</b>
12		<b>W12</b>
	n.p. no product	

We next intended to introduce a terminal alkyne functionality to create the possibility for subsequent synthetic modifications of the expected mutasynthesis product. The

resulting myxopyronin analog could for example react with different azides under mild conditions (click-chemistry)<sup>[37]</sup> to generate triazole containing myxopyronin derivatives with various substitution patterns. A corresponding mutasynthon (**11**) was synthesized and successfully incorporated resulting in the production of myxopyronin derivative **W11**. Inspired by coralopyronin, we finally synthesized a mutasynthon bearing a terminal hydroxyl group (**12**) at the same position as in the coralopyronin western chain. So far there is no x-ray structure of a coralopyronin – RNAP complex. Due to the close similarity to myxopyronin and several mutagenesis studies,<sup>[38]</sup> its binding mode can be assumed to be analogous to myxopyronin's. The additional alkyl chain of coralopyronin likely extends into an adjacent lipophilic pocket interacting with  $\beta$ -L1326 (Figure 4).<sup>[11,16]</sup> The hydroxyl function presumably contributes to its activity by forming a hydrogen-bond with the protein. A corresponding myxopyronin derivative (**W12**) might therefore benefit from an additional interaction similar to coralopyronin and was obtained after feeding of **12** to a  $\Delta$ *mxnK* culture.

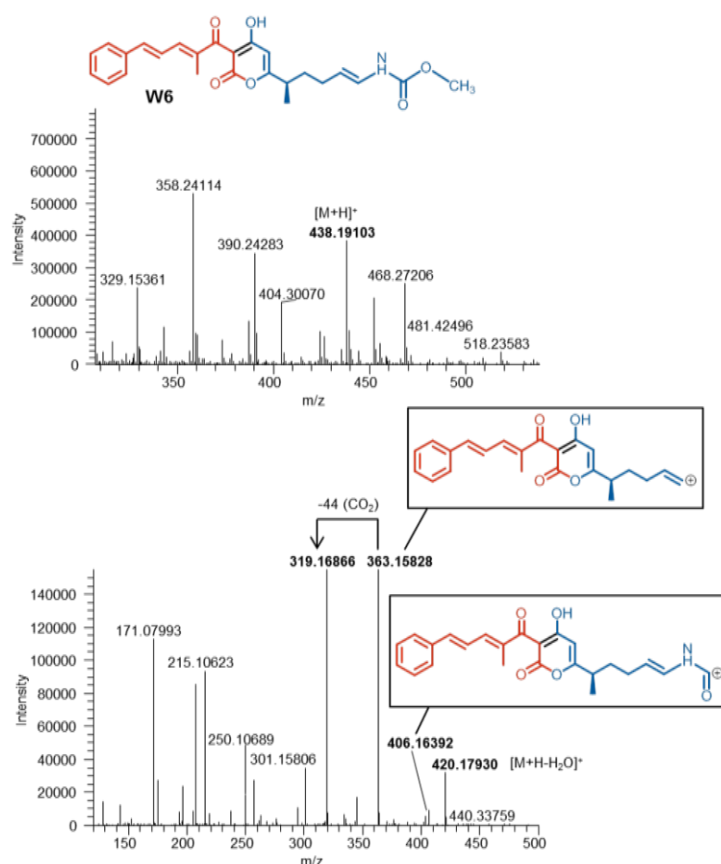


**Figure 3.** **W6** detected in an extract from a culture of Mx f50  $\Delta$ *mxnK* after feeding **6**. Top: MS spectrum; bottom: fragment spectrum of the parent ion  $m/z$  438.19  $[M+H]^+$  (Table 2).

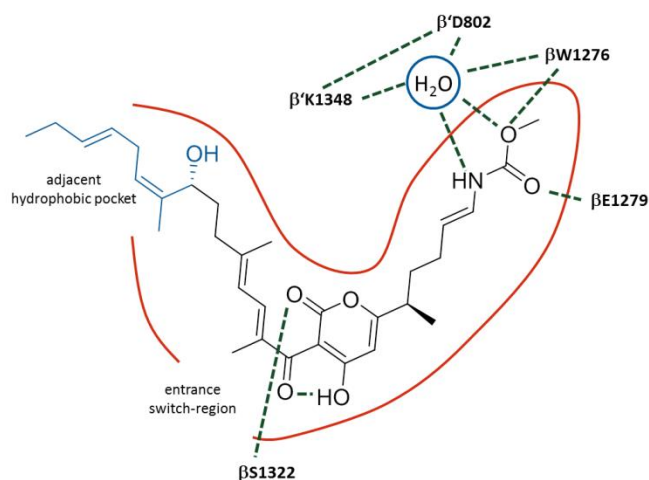
**Table 2.** Characterization of novel myxopyronin analogs with representative fragmentation patterns observed

	Chemical formula	Calculated mass <i>m/z</i> [M+H] <sup>+</sup>	Observed mass <i>m/z</i> [M+H] <sup>+</sup>	Fragmentation due to losses of			
				H <sub>2</sub> O ( <i>m/z</i> = 18)	CH <sub>3</sub> OH ( <i>m/z</i> = 32)	H <sub>2</sub> N-CO <sub>2</sub> CH <sub>3</sub> ( <i>m/z</i> = 75)	H <sub>2</sub> N-CO <sub>2</sub> CH <sub>3</sub> , CO <sub>2</sub> ( <i>m/z</i> = 119)
<b>Myx</b>	C <sub>23</sub> H <sub>32</sub> NO	418.22241	418.22217	400.211	386.195	343.18988	299.20017
<b>W1</b>	C <sub>23</sub> H <sub>32</sub> NO	418.22241	418.22227	400.211	386.195	343.18981	299.20007
<b>W2</b>	C <sub>22</sub> H <sub>30</sub> NO	404.20676	404.20666	386.195	372.180	329.17446	285.18464
<b>W4</b>	C <sub>22</sub> H <sub>32</sub> NO	406.22241	406.22250	388.210	374.195	331.18951	287.19987
<b>W6</b>	C <sub>25</sub> H <sub>28</sub> NO	438.19111	438.19103	420.179	406.163	363.15828	319.16866
<b>W7</b>	C <sub>26</sub> H <sub>30</sub> NO	452.20676	452.20686	434.195	420.181	377.17400	333.18430
<b>W8</b>	C <sub>25</sub> H <sub>30</sub> NO	440.20676	440.20659	422.195	408.179	365.17410	321.18438
<b>W9</b>	C <sub>25</sub> H <sub>28</sub> NO	454.18602	454.18643	436.174	n.o. <sup>[a]</sup>	379.15314	335.16345
<b>W10</b>	C <sub>25</sub> H <sub>26</sub> NO	516.10163	516.10175	498.090	484.075	441.06942	397.07952
<b>W11</b>	C <sub>21</sub> H <sub>26</sub> NO	388.17546	388.17557	n.o. <sup>[a]</sup>	n.o. <sup>[a]</sup>	313.14233	269.15311
<b>W12</b>	C <sub>22</sub> H <sub>30</sub> NO	420.20167	420.20148	402.190	n.o. <sup>[a]</sup>	345.16920	301.17982
<b>W13</b>	C <sub>23</sub> H <sub>32</sub> NO	418.22241	418.22232	400.211	386.195	343.18984	299.19999
<b>W14</b>	C <sub>26</sub> H <sub>30</sub> NO	452.20676	452.20670	434.197	420.180	377.17516	333.18508
<b>W16</b>	C <sub>23</sub> H <sub>32</sub> NO	418.22241	418.22235	400.211	386.195	343.18972	299.20000
<b>W17</b>	C <sub>22</sub> H <sub>30</sub> NO	404.20676	404.20675	386.196	372.182	329.17496	285.18512
<b>W18</b>	C <sub>25</sub> H <sub>28</sub> NO	438.19111	438.19118	420.180	406.164	363.15886	319.16910

<sup>[a]</sup> n.o. not observed

First attempts to isolate sufficient quantities of the new myxopyronin derivatives generated *via* mutasynthesis experiments failed due to the relatively low production yields. In general, possible bottlenecks might be caused by limited uptake of the  $\beta$ -keto NAC thioesters, their fast degradation after feeding to the culture or inefficient incorporation into the biosynthetic process. Closer analysis of culture extracts after fermentation revealed that only trace amounts of the mutasynthons are left, indicating that precursor degradation/instability might be a limiting factor. Therefore we decided to increase the chemical stability of the mutasynthons and to re-design the myxopyronin mutasynthesis approach. In the experiments described above, western chain biosynthesis was completely blocked and complementation was achieved by feeding mimics of fully matured western chain intermediates. Thus,  $\beta$ -keto thioesters were required as mutasynthons to enable the final pyrone ring formation *via* Claisen-condensation. In order to circumvent the usage of rather unstable  $\beta$ -keto thioesters, which do also not allow for long-term storage, we aimed to block and complement

western chain biosynthesis at earlier stages. This would enable feeding experiments with simplified and more stable mutasynthons (see Figures S2a and S2b in SI). Therefore, two additional mutants were generated by site-directed mutagenesis to inactivate the carrier protein domains from modules 1 and 4 (CP-1<sup>W</sup> or CP-4<sup>W</sup>). In both cases, the CP active site serine required for posttranslational modification<sup>[39]</sup> was mutated to alanine resulting in the mutant strains  $\Delta$ CP-1<sup>W</sup> or  $\Delta$ CP-4<sup>W</sup>, respectively. Interestingly, western chain biosynthesis was not completely abolished as trace amounts of myxopyronin A could still be detected in culture extracts of both mutants. We reasoned that in case of  $\Delta$ CP-1<sup>W</sup> butyryl-CoA might act as starter unit, which is directly elongated and incorporated into the assembly process at module 3. However, the production of myxopyronin A by  $\Delta$ CP-4<sup>W</sup> is difficult to explain with standard PKS biochemistry. One possible scenario might involve an additional (iterative) elongation round without keto reduction by module 1<sup>W</sup> and subsequent modification of the  $\beta$ -keto moiety possibly on CP-2<sup>W</sup> (or CP-1<sup>W</sup>) to introduce the methyl branch.

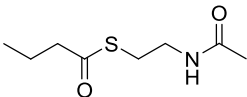
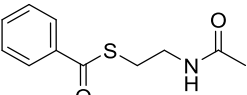
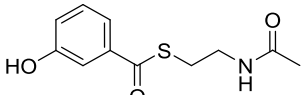
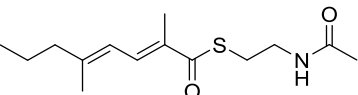
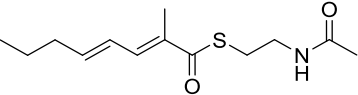
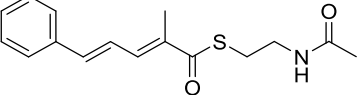


**Figure 4.** Schematic illustration of myxopyronin (black) and coralloyronin (black + blue) inside the RNAP switch region. Adapted from Mukhopadhyay et al.<sup>[11]</sup>

Although myxopyronin biosynthesis was not completely inhibited, feeding experiments with simplified and more stable mutasynthons were performed. Cultures of the  $\Delta$ CP-1<sup>W</sup> mutant were supplemented with precursors **13–15** and myxopyronin production was analyzed by HPLC-MS/MS. As expected, myxopyronin A was produced after feeding of compound **13** in larger quantities than in the control without feeding. Precursor **14** was also accepted resulting in detection of myxopyronin

derivative **W14**. Interestingly **15**, carrying a hydroxyl group in the *meta* position, did not result in the production of a hydroxylated myxopyronin-derivative as observed previously when the  $\beta$ -keto thioester (**9**) was used for feeding. It is possible that selectivity issues of downstream catalytic domains in the PKS are the cause, which are circumvented in feeding experiments with fully matured western chain mimics like precursor **9**.

**Table 3.** Synthetic western side chain mimics.

Entry	Formula	Myx derivative
13		<b>W13 (= W1)</b>
14		<b>W14</b>
15		<b>n.p.</b>
16		<b>W16 (= W1)</b>
17		<b>W17</b>
18		<b>W18</b>

n.p. no product

Mutant strain  $\Delta$ CP-4<sup>W</sup> was analyzed by using extended NAC-thioesters **16–18** to mimic module 4<sup>W</sup> intermediates. All substrates are accepted and the respective myxopyronin derivatives could be detected *via* HPLC-MS/MS analysis (increased levels of myxopyronin A in the  $\Delta$ CP-4<sup>W</sup> culture fed with **16** compared to the control). Although the NAC-thioesters without a  $\beta$ -keto function were more stable, the yield of final products was still too low for product isolation (1-10  $\mu$ g/L) to allow for bioactivity testing. Detection of large amounts of substrates in the culture supernatants suggested that insufficient uptake into the cells is a limiting factor. To address this bottleneck modified feeding procedures, including the addition of detergents like polyethylenglycol (PEG), Tween or DMSO to increase cell permeability as well as increasing the number of feeding points were evaluated. However, improved myxopyronin production yields could not be observed. Additional experiments to

improve the final yield will be carried out to fully exploit the established mutasynthesis systems and to access compound material from the culture extracts after biotechnological process optimization. With regard to this bottleneck, engineering the efflux pumps of the producer strain might hold promise to improve precursor uptake. Furthermore, we focus on establishing a heterologous production system, potentially giving rise to higher yields.

### Conclusion

Mutasynthesis represents a powerful approach to produce libraries of natural product derivatives, which are difficult to access by purely synthetic routes. Here we established the basis of such an approach for the bacterial RNAP inhibitor myxopyronin. Mutants of the native myxopyronin producer *M. fulvus* Mx f50 were generated to completely block or at least significantly reduce native western chain assembly. Intriguingly most of the synthesized mutasynthons can be successfully incorporated *via* the established mutasynthesis systems. This indicates that the participating enzymes display relatively high tolerance for variations in the substrate structure. The substrate specificity of MxnB, which is responsible for the last step of myxopyronin biosynthesis, could be evaluated. The mutant with an entirely dysfunctional MxnK required the feeding of  $\beta$ -keto NAC thioesters (**1–12**) to generate the final products. On the one hand, these substrates allow the highest degree of flexibility concerning structural variations of the resulting myxopyronin derivatives, due to the late stage of incorporation. On the other hand their synthesis is more laborious and the compounds are relatively unstable. Mutants expressing a partially functional western-chain assembly line enabled feeding experiments with shorter precursors without a  $\beta$ -keto function. These mutasynthons are more stable and easier to synthesize in large quantities. However, the variability in terms of tolerated structural variations is more restricted compared to the  $\beta$ -keto mutasynthons. Although productivity is currently too low to allow for full characterization of the products and thus clearly has to be improved, the established mutasynthesis systems provide a comprehensive basis for upcoming studies to generate various new myxopyronin derivatives. This will allow us to further exploit this promising class of  $\alpha$ -pyrone antibiotics. The broad western-chain substrate-tolerance in the final condensation reaction even allows the exploration of the coralopyronin chemical space *via* the ‘myxopyronin mutasynthesis system’. The resulting compounds could

be streamlined to improve their physicochemical properties and potentially overcome the problems of existing antibiotic resistances.

## Experimental Section

**Bacterial Strains and Culturing Conditions.** Bacterial strains and plasmids used during this study are listed in Table S1. *Myxococcus fulvus* Mx f50 wild type and mutants were grown in Casitone Yeast (CY) medium (0.3% casitone, 0.1% yeast extract, 0.1% CaCl<sub>2</sub> x 2 H<sub>2</sub>O) supplemented with 5 x 10<sup>-4</sup> g L<sup>-1</sup> vitamin B12 after autoclaving. For liquid cultures, the strains were grown at 30 °C and 105 rpm on an orbital shaker and harvested after 3 days. *E. coli* strains were cultured in lysogeny broth (LB) medium (1 % tryptone, 0.5% yeast extract, 0.5% NaCl) at 37 °C. Appropriate antibiotic selection at a final concentration of 100 µg mL<sup>-1</sup> ampicillin or 50 µg mL<sup>-1</sup> kanamycin was added whenever necessary.

**DNA preparations and PCR.** *M. fulvus* Mx f50 genomic DNA was prepared either via the Phenol Chloroform Isoamyl alcohol extraction method<sup>[40]</sup> or by using the Genra Puregene Genomic DNA Purification Kit (Qiagen) according to the manufacturer's protocol. Plasmid DNA was either purified by standard alkaline lysis<sup>[40]</sup> or by using the GeneJet Plasmid Miniprep Kit (Thermo Fisher Scientific). The PCR reactions were carried out in a peqSTAR 96 Universal Gradient thermocycler (Peqlab): initial denaturation (3 min, 95 °C); 30 cycles of denaturation (30 s, 95 °C), annealing (30 s, 53 or 57 °C) and elongation (varied based on PCR product length 1 kb min<sup>-1</sup>, 72 °C); and final extension (10 min, 72 °C). DNA fragments were separated by agarose gel electrophoresis and isolated using the peqGold Gel Extraction (Peqlab). The PCR products were cloned into the pJET1.2 blunt (Thermo Fisher Scientific) vector and sequenced using the primers pJET1.2For/pJET1.2Rev, respectively. Primer sequences are listed in Table S2.

**General procedure for site directed mutagenesis of *mxnK* by in frame deletion and by point mutation.** In general, construction of in-frame deletion mutants was carried out by amplifying 1000–1250 bp homology regions on each side of the desired deletion area by PCR. Each fragment was subcloned to the pJET1.2 blunt vector and sequenced using the primers pJET1.2For and pJET1.2Rev. After sequence verification the homology regions were cloned into the pSWU41 vector,<sup>[41]</sup>

which contains a neomycin phosphotransferase (*nptII*) and levansucrose (*sacB*) gene cassette, by using restriction sites indicated in Table S2. The resulting constructs were subsequently electroporated into *M. fulvus* Mx f50. *M. fulvus* Mx f50 was grown in baffled flask with CY medium until an OD<sub>600</sub> between 0.6-0.9 was reached. Cells were then harvested from 2–4 mL culture ( $1-2 \times 10^9$  cells mL<sup>-1</sup>) by centrifugation at 12500 rpm for 1 min at room temperature. After two washing steps with 1 mL H<sub>2</sub>O at room temperature, cells were resuspended in 65 µL H<sub>2</sub>O. Plasmid DNA (1–2 µg) was mixed with the cell suspension, and electroporation was carried out under the following conditions: 25 µF, 400 Ω, 650 V using 0.1 cm electroporation cuvettes and a GenePulser XCell device (Bio-Rad). 1 mL CY medium was directly added to the cell suspension immediately after electroporation and the cells were transferred into a 2 mL centrifuge tube. After 6–8 h cultivation at 30 °C and 800 rpm on a thermomixer, the cells were mixed with 2 mL CY soft agar (CY medium containing 0.7 % agar) and plated on CY agar plates (CY medium containing 1.7% agar) supplemented with 50 µg mL<sup>-1</sup> kanamycin or 6.25 µg mL<sup>-1</sup> oxytetracycline. The plates were incubated at 30 °C for 7-10 days until colonies became visible.

For the construction of markerless double crossover mutants the following strategy was applied: After verification of the single crossover mutants (kanamycin-resistant mutants) by PCR (integration via two different homology regions was possible), a selected single crossover mutant was grown in CY medium in the absence of antibiotics. After 3–4 days 1 mL of the well-grown culture was transferred into 50 mL fresh medium to start another cultivation cycle at 30 °C for 3–4 days. This procedure was repeated for three times to increase the possibility for a second crossover event, which would result in the loss of the inactivation plasmid. Depending on the homology region used for the second crossover this can yield either the wild type genotype ('revertant') or the expected double crossover mutant strain, in which the targeted region is deleted. To select for clones in which a second crossover took place, a counter selection system based on the *sacB* gene was used.<sup>[41]</sup> For this, different dilutions of the cell population were plated on CY agar supplemented with 6% sucrose for counter selection. After 7–10 days, first colonies appeared, which were then grown in liquid culture (CY medium) to isolate genomic DNA for genotypic verification and to extract the cultures for phenotypic analysis as described below.

**Inactivation of *mxnK* by in-frame deletion.** To disrupt *mxnK* by in-frame deletion, a gene inactivation plasmid harbouring two fragments, which are 1001 bp and 1262 bp

in size and homologous to the upstream and downstream area of the chromosomal target region, was constructed. These fragments were amplified from *M. fulvus* Mx f50 genomic DNA by PCR using the primers mxn54/mxn55 and mxn56/mxn57. After hydrolysis of the upstream fragment (mxn54/mxn55 product) with *Bam*HI and *Not*I, and the downstream fragment (mxn56/57 product) with *Not*I and *Sac*I, the fragments were ligated into pSWU41 hydrolyzed with *Bam*HI and *Sac*I to generate pHSU-mxn18. All subcloning steps were performed using *E. coli* HS996. For genotypic analysis of the single crossover, a set of different PCRs using the primer combinations mxn68/mxn69, mxn70/mxn72 and mxn73/mxn71 was carried out to verify the correct integration of the inactivation plasmid. For genotypic analysis of the putative double crossover mutants PCRs using the primers mxn68/mxn71 were carried out. Further confirmation of the deletion mutant was obtained by Southern Blot analysis (Figure S1).

**Inactivation of *mxnK* by point mutation at CP-1<sup>W</sup>.** To disrupt *mxnK* by point mutation, a gene inactivation plasmid harbouring 2445 bp fragment was constructed. The fragment was amplified from *M. fulvus* Mx f50 genomic DNA by overlap PCR using the primers mxn169/mxn170 and mxn171/mxn172. After hydrolysis of the fragment with *Pvu*I and *Not*I, it was ligated into pSWU41 hydrolyzed with *Pvu*I and *Not*I to generate pHSU-mxn48. For genotypic analysis of the single crossover, a set of different PCRs using the primer combinations mxn185/mxn70 and pSWU41-F/mxn187 was carried out to verify the correct integration of the inactivation plasmid. For genotypic analysis of the double crossover, PCR using primer combination mxn189/mxn205 was performed and the amplified product was sequenced.

**Inactivation of *mxnK* by point mutation at CP-4<sup>W</sup>.** To disrupt *mxnK* by point mutation, a gene inactivation plasmid harbouring 2486 bp fragment was constructed. The fragment was amplified from *M. fulvus* Mx f50 genomic DNA by overlap PCR using the primers mxn174/mxn175 and mxn176/mxn177. After hydrolysis of the fragment with *Pvu*I and *Not*I, it was ligated into pSWU41 hydrolyzed with *Pvu*I and *Not*I to generate pHSU-mxn49. For genotypic analysis of the single crossover, a set of different PCRs using the primer combinations mxn191/mxn70, pSWU41-F/mxn193 and mxn195/mxn70 was carried out to verify the correct integration of the inactivation plasmid. For genotypic analysis of the double crossover, PCR using primer

combination mxn195/mxn206 was performed and the amplified product was sequenced.

**Feeding for mutasynthesis experiments.** A pre-culture of *M. fulvus* Mx f50ΔmxnK or *M. fulvus* Mx f50ΔCP-1<sup>W</sup> or *M. fulvus* Mx f50ΔCP-4<sup>W</sup> was grown in CY medium at 30 °C until an OD<sub>600</sub> between 0.3–0.6. The pre-culture was used to inoculate 20 mL CY medium ( $7.2 \times 10^6$  cells mL<sup>-1</sup>). Cultivation was carried out for further 12–24 hours before feeding the substrate mimics. *N*-acetyl-cysteamine (SNAC)-esters mimicking western chain 1-12 were fed to *M. fulvus* Mx f50ΔmxnK cultures to a final concentration of 20-100 μm. While 13-15 were fed to *M. fulvus* Mx f50ΔCP-1<sup>W</sup>, 16-18 were fed to *M. fulvus* Mx f50ΔCP-4<sup>W</sup>. They were grown for another 48 hours before the cells were harvested. The supernatant was extracted twice with an equal volume of ethyl acetate. After evaporation of the organic phase, the residue was dissolved in 100 μl methanol. Analysis of the crude extract from the cultures using LC-MS showed the formation of novel myxopyronin analogs. Further measurements by high-resolution mass spectrometry confirmed the incorporation of the precursors, showing the same type of fragmentation pattern.

**HPLC-MS/MS analysis.** All measurements were performed on a Dionex Ultimate 3000 RSLC system using a Waters BEH C18, 50 x 2.1 mm, 1.7 μm dp column by injection of five μl methanolic sample. Separation was achieved by a linear gradient with (A) H<sub>2</sub>O + 0.1 % FA to (B) ACN + 0.1 % FA at a flow rate of 600 μl min<sup>-1</sup> and 45 °C. The gradient was initiated by a 0.33 min isocratic step at 5 % B, followed by an increase to 95 % B in 9 min to end up with a 1 min flush step at 95 % B before reequilibration with initial conditions. UV and MS detection were performed simultaneously. Coupling the HPLC to the MS was supported by an Advion Triversa Nanomate nano-ESI system attached to a Thermo Fisher Orbitrap. Mass spectra were acquired in centroid mode ranging from 200–2000 m/z at a resolution of R = 30000.

### Acknowledgements

The authors would like to thank Thomas Hoffmann and Eva Luxenburger for their help in performing the HPLC-MS measurements. JHS gratefully acknowledges a scholarship from the “Stiftung der Deutschen Wirtschaft” (SDW).

## References

- [1] WHO: Global Tuberculosis Report **2014**: WHO/HTM/TB/2014.08.
- [2] T. Dalton, P. Cegielski, S. Akkslip, L. Asencios, J. C. Caoili, S.-N. Cho, V. V. Erokhin, J. Ershova, M. T. Gler, B. Y. Kazenyy, H. J. Kim, K. Kliiman, E. Kurbatova, C. Kvanovsky, V. Leimane, M. van der Walt, L. E. Via, G. V. Volchenkov, M. A. Yagui, H. Kang, Global PETTS investigators, *Lancet* **2012**, *380*, 1406-1417.
- [3] WHO: Guidelines for the programmatic Management of Drug-Resistant Tuberculosis: emergency update. **2008**, WHO/HTM/TB/2008.402.
- [4] M. Zignol, W. van Gemert, D. Falzon, C. Sismanidis, P. Glaziou, K. Floyd, M. Raviglione, *B. World Health Organ.* **2012**, *90*, 111-119.
- [5] E. A. Campbell, N. Korzheva, A. Mustaev, K. Murakami, S. Nair, A. Goldfarb, S. A. Darst, *Cell* **2001**, *104(6)*, 901-912.
- [6] I. Chopra, *Curr. Opin. Investig. D.* **2007**, *8(6)*, 600-607.
- [7] D. Haebich, F. von Nussbaum, *Angew. Chem. Int Ed.* **2009**, *48(19)*, 3397-3400.
- [8] C. T. Barrett, J. F. Barrett, *Curr. Opin. Biotech.* **2003**, *14(6)*, 621-626.
- [9] J. Wang, A. Galgoci, S. Kodali, K. B. Herath, H. Jayasuriya, K. Dorso, F. Vicente, A. González, D. Cully, D. Bramhill, S. Singh, *J. Biol. Chem.* **2003**, *278(45)*, 44424-44428.
- [10] A.R.M. Coates, G. Halls, Y. Hu, *Br. J. Pharmacol* **2011**, *163*, 184-194.
- [11] J. Mukhopadhyay, K. Das, S. Ismail, D. Koppstein, M. Jang, B. Hudson, S. Sarafianos, S. Tuske, J. Patel, R. Jansen, H. Irschik, E. Arnold, R. H. Ebright, *Cell* **2008**, *135(2)*, 295-307.
- [12] H. Irschik, K. Gerth, G. Höfle, W. Kohl, H. Reichenbach, *J. Antibiot.* **1983**, *36(12)*, 1651-1658.
- [13] W. Kohl, H. Irschik, H. Reichenbach, G. Höfle, *Liebigs Ann. Chem.* **1983**, 1656-1667.
- [14] A. O'Neill, B. Oliva, C. Storey, A. Hoyle, C. Dishwick, I. Chopra, *Antimicrob. Agents Ch.* **2000**, *44(11)*, 3163-3166.
- [15] H. Irschik, R. Jansen, G. Höfle, K. Gerth, H. Reichenbach, *J. Antibiot.* **1985**, *38(2)*, 145-152.
- [16] A. Srivastasa, M. Talaue, S. Liu, D. Degen, R. Y. Ebright, E. Sineva, A. Chakraborty, S. Y. Druzhinin, S. Chatterjee, J. Mukhopadhyay, Y. W. Ebright, A. Zozula, J. Shen, S. Sengupta, R. R. Niedfeldt, C. Xin, T. Kaneko, H. Irschik, R. Jansen, S. Donadio, N. Conell, R. H. Ebright, *Curr. Opin. Microbiol.* **2011**, *14(5)*, 532-543.
- [17] A. Rentsch, M. Kalesse, *Angew. Chem. Int Ed.* **2012**, *51(45)*, 11381-11384.
- [18] R. Lira, A. X. Xiang, T. Doundoulakis, W. T. Biller, K. A. Agrios, K. B. Simonsen, S. E. Webber, W. Sisson, R. M. Aust, A. M. Shah, R. E. Showalter, V. N. Banh, K. R. Steffy, J. R. Appleman, *Bioorg. Med. Chem. Lett.* **2007**, *17(24)*, 6797-6800.
- [19] T. Doundoulakis, A. X. Xiang, R. Lira, K. A. Agrios, S. E. Webber, W. Sisson, R. M. Aust, A. M. Shah, R. E. Showalter, J. R. Appleman, K. B. Simonsen, *Bioorg. Med. Chem. Lett.* **2004**, *14(22)*, 5667-5672.
- [20] A. Kirschning, F. Taft, T. Knobloch, *Org. Biomol. Chem.* **2007**, *5(20)*, 3245-3259.
- [21] C. J. Dutton, S. P. Gibson, A. C. Goudie, K. S. Holdom, M. S. Pacey, J. C. Ruddock, *J. Antibiot.* **1991**, *44(3)*, 357-365.
- [22] S. J. Daum, J. R. Lemke, *Ann. Rev. Microbiol.* **1979**, *33*, 241-265.

- [23] W. T. Shier, K. L. Rinehart Jr., D. Gottlieb, *P. Natl. Acad. Sci. USA*. **1969**, *63*(1), 198-204.
- [24] T. Knobloch, G. Dräger, W. Collisi, F. Sasse, A. Kirschning, *J. Org. Chem.* **2012**, *8*, 861-869.
- [25] K. Harmrolfs, L. Mancuso, B. Drung, F. Sasse, A. Kirschning, *J. Org. Chem.* **2014**, *10*, 535-543.
- [26] H. Sucipto, S. C. Wenzel, R. Müller, *ChemBioChem* **2013**, *14*(13), 1581-1589.
- [27] Ö. Erol, T. F. Schäberle, A. Schmitz, S. Rachid, C. Gurgui, M. El Omari, F. Lohr, S. Kehraus, J. Piel, R. Müller, G. M. König, *ChemBioChem* **2010**, *11*, 1253-1265.
- [28] R. O'Shea, H. E. Moser, *J. Med. Chem.* **2008**, *51*(10), 2871-2878.
- [29] T. I. Moy, A. Daniel, C. Hardy, A. Jackson, O. Rehrauer, Y. S. Hwang, D. Zou, K. Nguyen, J. A. Silverman, Q. Li, C. Murphy, *FEMS Microbiol. Lett.* **2011**, *319*(2), 176-179.
- [30] I. H. Gilbert, M. Ginty, J. A. O'Neill, T. J. Simpson, J. Staunton, C. L. Willis, *Bioorg. Med. Chem. Lett.* **1995**, *5*(15), 1587-1590.
- [31] Y. Oikawa, K. Sugano, O. Yonemitsu, *J. Org. Chem.* **1978**, *43*(10), 2087-2088.
- [32] B. M. Trost, J. P. N. Papillon, T. Nussbaumer, *J. Am. Chem. Soc.* **2005**, *127*(50), 17921-17937.
- [33] R. K. Boeckman Jr., T. M. Kamenecka, S. G. Nelson, J. R. Pruitt, T. E. Barta, *Tetrahedron Lett.* **1991**, *32*(23), 2581-2584.
- [34] T. Yoshinari, K. Ohmori, M. G. Schrems, A. Pfaltz, K. Suzuki, *Angew. Chem. Int Ed.* **2010**, *49*(5), 881-885.
- [35] a) N. Miyaura, K. Yamada, A. Suzuki, *Tetrahedron Lett.* **1979**, *20*(36), 3437-3440. b) N. Miyaura, A. Suzuki, *J. Chem. Commun.* **1979**, *0* (19), 866-867.
- [36] a) J. Louie, J. F. Hartwig, *Tetrahedron Lett.* **1995**, *36*(21), 3609-3612. b) A. S. Guram, R. A. Rennels, S. L. Buchwald, *Angew. Chem. Int Ed.* **1995**, *34*(12), 1348-1350.
- [37] a) V. V. Rostovtsev, L. G. Green, V. V. Fokin, K. B. Sharpless, *Angew. Chem. Int Ed.* **2002**, *41*(14), 2596-2599. b) C. W. Tornøe, C. Christensen, M. Meldal, *J. Org. Chem.* **2002**, *67*(9), 3057-3064.
- [38] K. Mariner, M. McPhillie, R. Trowbridge, C. Smith, A. J. O'Neill, C. W. G. Fishwick, I. Chopra, *Antimicrob. Agents Ch.* **2011**, *55*(5), 2413-2416.
- [39] R. H. Lambalot, A. M. Gehring, R. S. Flugel, P. Zuber, M. LaCelle, M. A. Marahiel, R. Reid, C. Khosla, C. T. Walsh, *Chem. Biol.* **1996**, *3*(11), 923-936.
- [40] J. Sambrook and D. W. Russell in *Molecular cloning: A laboratory manual*, Cold Spring Harbor Laboratory Press, Cold Spring Harbor, New York, **2001**.
- [41] S. S. Wu, D. Kaiser, *J. Bacteriol.* **1996**, *178*, 5817-5821.

### 3.4 Combining *in Silico* and Biophysical Methods for the Development of *Pseudomonas aeruginosa* Quorum Sensing Inhibitors: An Alternative Approach for Structure-Based Drug Design

J. Henning Sahner, Christian Brengel, Michael P. Storz, Matthias Groh, Alberto Plaza, Rolf Müller, and Rolf W. Hartmann

Reprinted with permission from *J. Med. Chem.* **2013**, 56(21), 8656–8664.

Copyright (2013) American Chemical Society.

#### Publication D

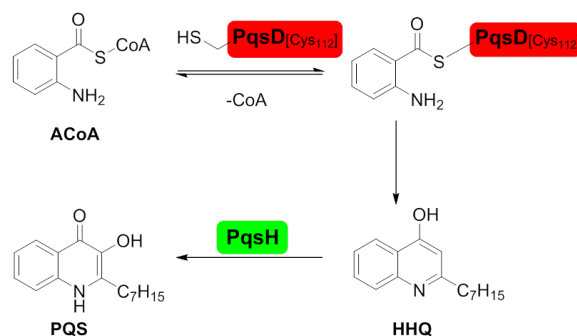
**Abstract:** The present work deals with the optimization of an inhibitor of PqsD, an enzyme essential for *Pseudomonas aeruginosa* quorum sensing apparatus. Molecular docking studies, supported by biophysical methods (surface plasmon resonance, isothermal titration calorimetry, saturation transfer difference NMR), were used to illuminate the binding mode of the 5-aryl-ureidothiophene-2-carboxylic acids. Enabled to make profound predictions, structure-based optimization led to increased inhibitory potency. Finally a covalent inhibitor was obtained. Binding to the active site was confirmed by LC-ESI-MS and MALDI-TOF-MS experiments. Following this rational approach, potent PqsD inhibitors were efficiently developed within a short period of time. This example shows that a combination and careful application of *in silico* and biophysical methods represents a powerful complement to co-crystallography.

## Introduction

Structure-based drug design is a rational strategy to develop bioactive molecules without the necessity of performing many rounds of modifications to derive structure activity relationships (SAR). Frequently data from X-ray co-crystallography are used to accelerate the lead optimization process. Although this method is undeniably efficient, there are some drawbacks: a co-crystal structure does not necessarily represent the biological state, as it results in a single “frozen” conformation that is affected by the crystallization conditions.<sup>1,2</sup> Furthermore, especially the ligand may not be well defined even at high resolution.<sup>3</sup> In some cases, attempts of co-crystallizing ligands and their targets were not successful forcing the research groups to make use of alternative strategies. The described problems can be overcome by the use of biophysical methods such as surface plasmon resonance (SPR), nuclear magnetic resonance (NMR) and isothermal titration calorimetry (ITC). An advantage of SPR, NMR and ITC is that they can be performed in aqueous solution, which can be considered almost “physiological” conditions.

In the forefront of this work, compound **1** (Figure 1a) was identified as an inhibitor of PqsD. The target protein PqsD, is a key player in the quorum sensing system of *P. aeruginosa*. It mediates the formation of heptyl-4-hydroxy-quinoline (HHQ) which is the precursor of *Pseudomonas* quinolone signal (PQS) (Scheme 1). Both molecules are potent virulence factors and function as signal molecules of *P. aeruginosa*, coordinating group behavior like the formation of biofilms.<sup>4,5</sup> The substrate channel of PqsD is about 15 Å long and rather narrow.<sup>6</sup> The channel can be divided into three parts. A positively charged entrance followed by a mainly hydrophobic middle segment, ending in a polar bottom part. The latter is delimited by the catalytic residues Cys112, His257 and Asp287. Suppression of PqsD activity has been shown recently by our group to inhibit biofilm formation.<sup>7</sup> This makes PqsD an attractive target for the therapy of chronic *P. aeruginosa* infections, especially in immunosuppressed individuals.<sup>8-10</sup>

Herein, we report on the optimization of **1** supported by biophysical methods and molecular docking. The approach described in the following, represents a hit to lead optimization process that does not involve co-crystallographic structure determination.



**Scheme 1. Biosynthesis of signaling molecules HHQ and PQS in *Pseudomonas aeruginosa*.** Anthranilate is transferred to PqsD via thio-esterification of ACoA with Cys112. The next step is a condensation with acetyl carrier protein (ACP) bound β-ketodecanoic acid to form HHQ, which is finally transformed to PQS by PqsH.

## Results and discussion

The  $IC_{50}$  value of compound **1** (Figure 1a) against PqsD was determined in a functional enzyme assay<sup>11</sup> to be 6  $\mu$ M. The same compound has recently been reported as a weak inhibitor of bacterial RNA polymerase ( $IC_{50}$ : 241  $\mu$ M)<sup>12</sup>, a classical target for antibacterial therapy. While targeting quorum sensing an antibacterial effect is not desired to avoid selection pressure inevitably leading to the development of resistant strains.<sup>13</sup> Thus, other potential hit candidates from the 5-aryl-ureidothiophene-2-carboxylic acid class, displaying poor selectivity, were not considered for further optimization (see Table S1 in Supporting Information).

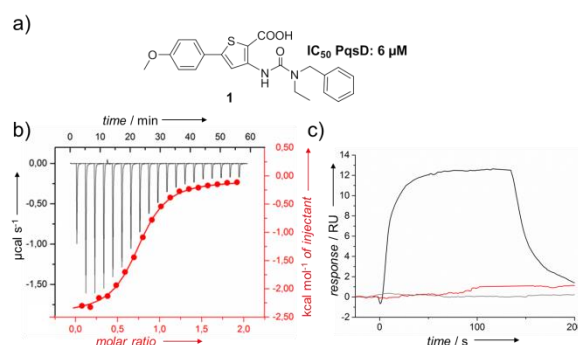


**Figure 1. a)** Compound **1**. Biophysical characterization of **1**: **b)** Thermogram (red) and titration curve (black) obtained from ITC of PqsD with **1**; **c)** SPR experiment: ACoA binds to PqsD (black). ACoA binding is inhibited by preincubation with **1** (red). The reference signal is shown in grey.

Attempts to obtain a co-crystal-structure of **1** and PqsD, using soaking techniques, were not successful. Therefore, a combination of biophysical methods and molecular docking was used to elucidate the binding mode of **1**. To exclude a non-specific binding behavior (e.g. *via* aggregation), **1** was examined in an isothermal titration

calorimetry (ITC) experiment to ensure stoichiometric binding. Thereby an equimolar binding ratio ( $0.82 \pm 0.05$ ) with a  $K_D$  of  $6.3 \pm 2.6 \mu\text{M}$  was determined (Figure 1b), confirming that the discovered class of compounds represents a promising starting point for further optimization.

In order to clarify the binding site on PqsD, SPR experiments were conducted. It was shown, that the natural substrate ACoA can no longer bind to the enzyme when PqsD was preincubated with **1** (Figure 1c). This result indicates that **1** binds inside the ACoA-channel, thus blocking the first step of the catalytic reaction.

From docking simulations with **1**, two putative binding modes with similar scoring values but reverse orientations were obtained. In the first pose (Figure 2; orange), the ureido *N*-ethyl-benzyl moiety points to the bottom of the pocket (delimited by Cys112, His257 and Asn287), whereas in the second pose (Figure 2; green), the methoxy-group is placed in this position.

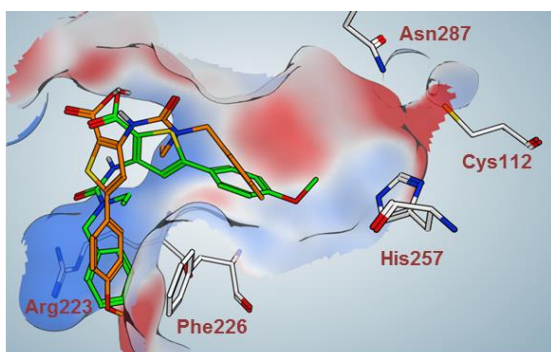


**Figure 2.** Docking poses of **1** within the ACoA channel of PqsD: (orange; Vina-Score:  $8.3 \text{ kcal mol}^{-1}$ ) (green; Vina-Score:  $8.2 \text{ kcal mol}^{-1}$ ).

To get a reliable starting point for a structure-based optimization, discrimination between the two poses was necessary. Therefore, we designed an SPR competition experiment with model compounds **1–3** from the 5-aryl-ureidothiophene-2-carboxylic acid class, differently substituted in the ureido and aryloxy parts (Figure 3b). As competitor compounds the 2-nitrophenyl-methanols **A** and **B** were used (Figure 3a). They were recently reported as PqsD inhibitors<sup>7</sup> and were shown to interact with the catalytic residues, especially Cys112, at the bottom of the ACoA-channel.<sup>14</sup>

As illustrated in Figure 3a, the presence of **A** and **B** should influence the binding of the ureidothiophene model compounds depending on their substitution pattern. Compared with **2**, **1** bears a large substituent at the ureido part, whereas **3** is elongated in the aryloxy part, at the opposite site. If the ureido part points to the

bottom of the pocket, one would expect that **1** is more sterically hindered than **2** and **3**, when the competitors are present. In contrast, the longer aryloxy part of **3** should lead to a reduced binding if the ureidothiophenes bind in the reversed orientation. In the absence of a competitor compound, **1–3** displayed comparable responses (Figure 3c). When the sterically less demanding 2-nitrophenyl-methanol derivative **A** was present, a reduction of affinity was observed exclusively for **3** bearing a bulky phenyl substituent in the aryloxy part. In contrast, the ethyl-benzyl moiety at the ureido motif of **1** did not prevent a binding. These results fit to the docking prediction with the aryloxy part pointing into the pocket (Figure 2, green). In competition with **B**, the binding affinity of all three compounds was reduced as expected from the docking results. (see Figure S1 and S2) Thus a deeper insight into the position of the new inhibitors in the binding channel was provided.

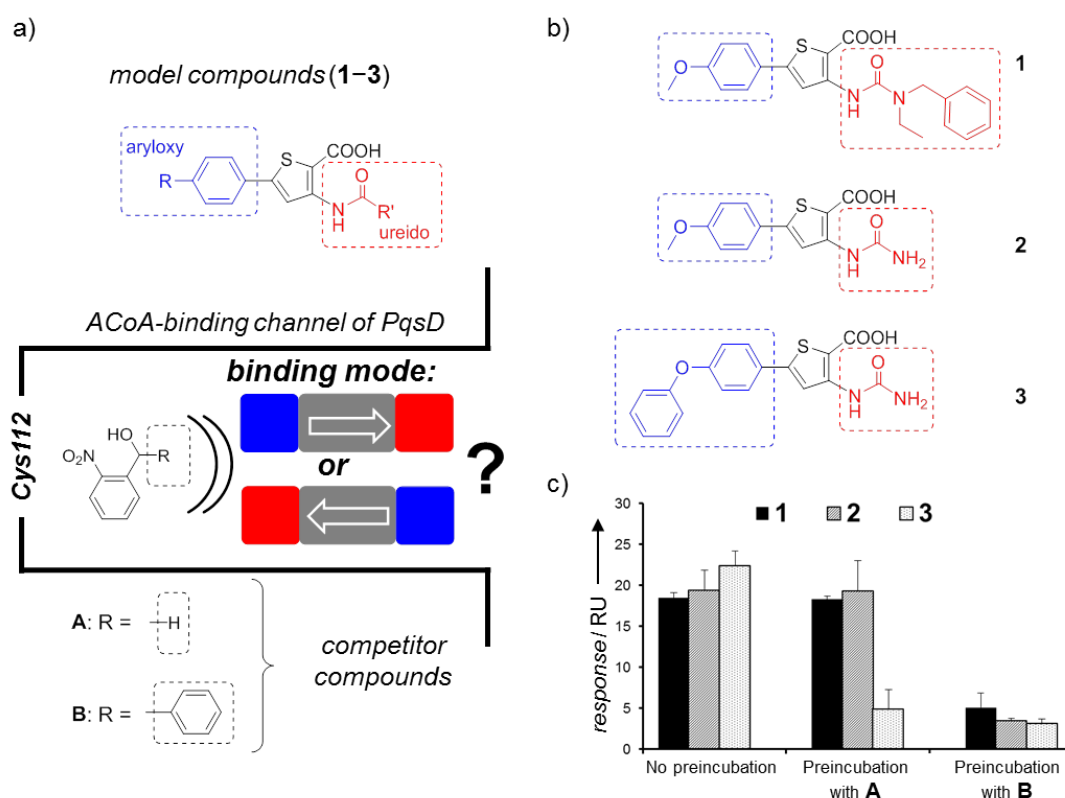


**Figure 3.** a) Schematic illustration of the SPR competition experiments: PqsD was preincubated with competitor compounds **A** and **B** binding to the ACoA-channel, delimited by Cys112. The model compounds **1–3** were subsequently added and the influence of **A** or **B** on their binding behaviors was investigated. The results shed light on the binding mode of the aryl-ureidothiophene-2-carboxylic acids. b) Structures of the model compounds **1–3** c) Results from SPR-competition experiments suggest the aryloxy-moiety to point into the pocket.

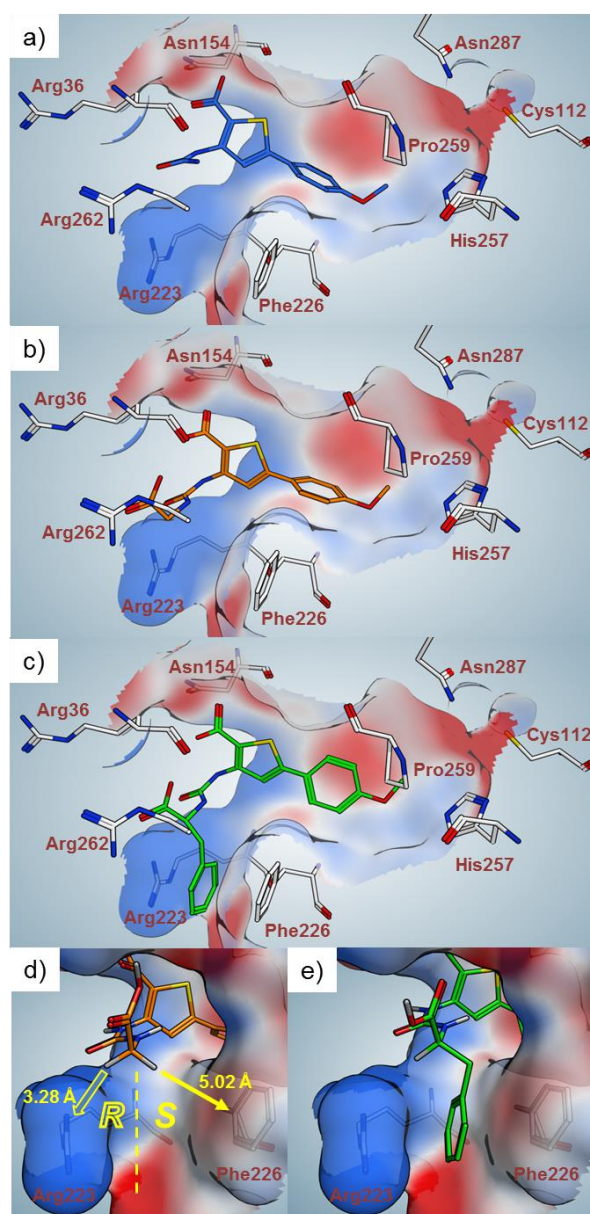


**Figure 4.** **a)** Docking pose of **2**, the starting point for structure-based optimization. **b)** Docking pose of glycine derivative **4**. **c)** Docking pose of optimized compound **7**. **d)** Illustration of the limited space in the narrow cleft formed by Arg223 and Phe226. **e)** Close-up of the benzyl moiety of **7**, perfectly fitting into the narrow cleft.

As the starting point for structure activity exploration compound **2** was chosen, a truncated derivative of the initial hit **1**. It displays comparable ligand efficiency (LE, Table 1) whilst being more suitable for further modification at the ureido motif. The docking pose of **2** (Figure 4a) suggests an anchoring of the ureido moiety by interaction of the carbonyl oxygen with Arg223. To validate this assumption, binding of **2** to the R223A mutant, that should display weaker affinity, was investigated by SPR. The response of compound **2** was reduced to 6 response units (RU) in

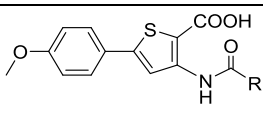
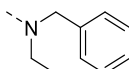
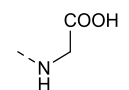
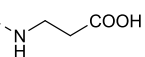
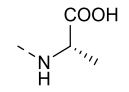
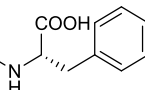
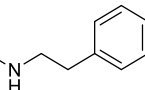
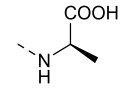
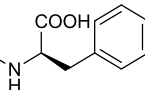
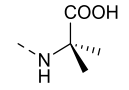
comparison to 25 RU for the wild type enzyme (see Figure S4), confirming this hypothesis. Arg262, placed in the upper part of the binding pocket, should be a potential interaction partner for a negatively charged moiety. The introduction of a carboxylate resulting in compounds **4** and **5** (Table 1) indeed led to an increased activity, confirming this prediction. In the docking pose, the introduced carboxylic acid moiety of **4** is located closely to Arg262 enabling the formation of a new interaction (Figure 4b). Based on the finding that **4** is more active than **5**, we concluded that a methylene linker is more appropriate than a longer spacer unit. This allowed making use of  $\alpha$  amino acids for simple variations in the next steps, taking advantage of their hydrophilicity to increase the polarity of the inhibitors, as low lipophilicity is an important requirement for drugs targeting Gram negative bacteria. A study of O'Shea et al. shows that almost all antibiotics, effective against *P. aeruginosa*, possess a  $\text{clogD}_{7.4}$  value below 0.<sup>15</sup> While our hit compound **1** ( $\text{logD}_{7.4}$ : 2.58) did not meet this criterion, amino acid derivative **4** ( $\text{logD}_{7.4}$ : -1.62) did

As illustrated in Figure 4b, docking simulations predict that the glycine derivative **4** is anchored by an interaction of the carboxylate group with Arg262. The narrow cleft, subjacent to the  $\alpha$ -position of **4** and delimited by Arg223 and Phe226, is supposed to be addressable by expansion of **4**. A targeted approach should replace the *pro-S* hydrogen since the space adjacent to the *pro-R* hydrogen is blocked by Arg223, which could lead to a sterical clash (Figure 4d). Following this strategy, the introduction of *S*-amino acid residues improved the activity resulting in up to submicromolar  $\text{IC}_{50}$  values in case of the *S*-alanine and *S*-phenylalanine derivative **6** and **7** (Figure 4b-e). Compound **8**, the counterpart of **7** that lacks the COOH group next to the ureido moiety displays a significantly weaker inhibition. This again highlights the importance of the carboxylic acid group, which is in accordance with our binding hypothesis.

In order to complete the picture, the *R*-enantiomers **9** and **10** were investigated. In both cases the activity decreased dramatically. These data corroborate the highly selective three-dimensional interaction formed by the *S*-enantiomeric moieties with the target enzyme. To evaluate whether the decreased activity of the *R*-enantiomer **9** is due to a sterical clash, as expected, or associated with the absence of the *S*-methyl group of **6**, the dimethyl compound **11** was investigated. The fact that **11** was less active than **4** and **6** confirms the prediction of a sterical collision.

To test for selectivity towards bacterial RNA polymerase, the most potent derivatives **6** and **7** were tested for inhibition of this enzyme. Both displayed only slight inhibitory potency (~10–20%) at a concentration of 200  $\mu\text{M}$ .

**Table 1.** Inhibition of PqsD *in vitro*, ligand efficiencies and  $\text{clogD}_{7.4}$  values of compounds **1–11**

				
Cpd	R	$\text{IC}_{50}$ PqsD	$\text{LE}^{[a]}$	$\text{clogD}_{7.4}^{[b]}$
<b>1</b>		<b>6 <math>\mu\text{M}</math></b>	<b>0.25</b>	<b>2.58</b>
<b>2</b>		<b>170 <math>\mu\text{M}</math></b>	<b>0.26</b>	<b>0.15</b>
<b>4</b>		<b>7 <math>\mu\text{M}</math></b>	<b>0.30</b>	<b>-1.62</b>
<b>5</b>		<b>37 <math>\mu\text{M}</math></b>	<b>0.25</b>	<b>-1.47</b>
<b>6</b>		<b>2 <math>\mu\text{M}</math></b>	<b>0.32</b>	<b>-1.27</b>
<b>7</b>		<b>0.5 <math>\mu\text{M}</math></b>	<b>0.28</b>	<b>0.59</b>
<b>8</b>		<b>58 <math>\mu\text{M}</math></b>	<b>0.21</b>	<b>2.61</b>
<b>9</b>		<b>54 <math>\mu\text{M}</math></b>	<b>0.24</b>	<b>-1.27</b>
<b>10</b>		<b>26 <math>\mu\text{M}</math></b>	<b>0.19</b>	<b>0.59</b>
<b>11</b>		<b>56 <math>\mu\text{M}</math></b>	<b>0.23</b>	<b>-0.93</b>

<sup>[a]</sup> Ligand efficiency calculated as  $\text{LE} = 1.4 \times (\text{pIC}_{50}/\text{HAC})$

<sup>[b]</sup>  $\text{clogD}_{7.4}$  calculated with ACDLabs Percepta 2012

Saturation transfer difference (STD) NMR<sup>16</sup> was used to identify the binding epitopes of **7** (Figure S5). Strong STD enhancements were observed for all protons of **7** with the methylene linker protons exhibiting the strongest enhancements. This is

consistent with the docking simulations, which predict these methylene protons to be positioned at the entrance of the narrow subpocket delimited by Arg223 and Phe226. Moreover, the fact that the other protons of **7** also displayed strong STD enhancements suggests that **7** is nearly completely surrounded by PqsD.

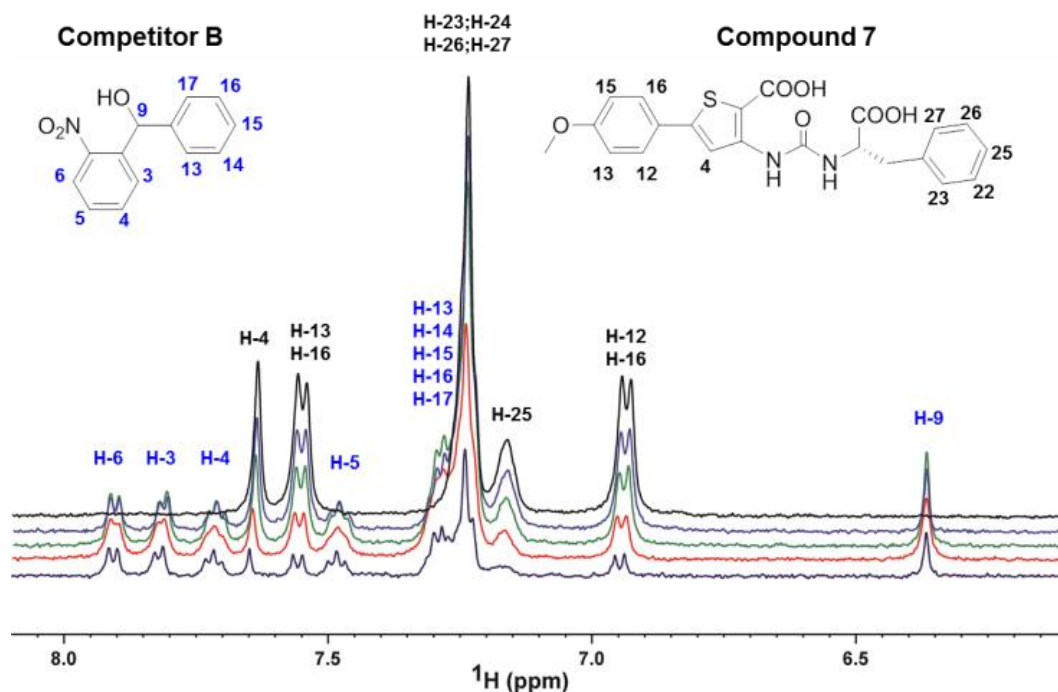


**Figure 5.** Competition of **7** and **B** binding to PqsD by STD NMR. Expanded  $^1\text{H}$  STD NMR spectrum of **7** (1 mM) in the presence of PqsD (10  $\mu\text{M}$ ) (black curve). STD NMR spectra recorded on the same sample after addition of 0.5 (purple), 1.0 (green), 2.0 (red) and 3.0 (blue) equivalents of compound **B**. Signals of **7** are labeled in black, from **B** in blue.

To confirm that the optimized inhibitors bind in a similar way as the model compounds **1–3**, the SPR-competition experiment with **A** and **B** was conducted for compound **7**. As expected, the binding response was only significantly reduced in the presence of **B** (Figure S3). In addition, we performed an STD-NMR competition experiment to validate the SPR results. Increasing amounts of compound **B** were added to a 100:1 complex of **7**/PqsD (Figure 5). Difference spectra were monitored for a change in intensity of signals belonging to either **7** or **B** during titration. As seen in the spectral expansions showing the aromatic region, stepwise addition of up to 3.0 equivalents of **B** with respect to **7** resulted in a uniform decrease in intensity for signals corresponding to **7** while signals ascribable to **B** appeared and steadily increased. This confirms that **7** binds deep inside the ACoA-channel of PqsD.

Finally, we focused on the substituted 5-aryl ring that is predicted to be located near the active site within the ACoA channel (Figure 4). As already shown with phenoxy compound **3** ( $IC_{50} = 20 \mu\text{M}$ ), larger substituents are tolerated in this part of the binding pocket. As Cys112 is pivotal for the catalytic activity of PqsD, a covalent trapping of this amino acid should lead to an effective blockade of the enzymatic machinery. For that purpose a  $\beta$ -chloroacetyl moiety was introduced, as an “electrophilic warhead”,<sup>17</sup> at the appropriate position, linked to the 5-aryl ring *via* an amide function (Figure 6a).

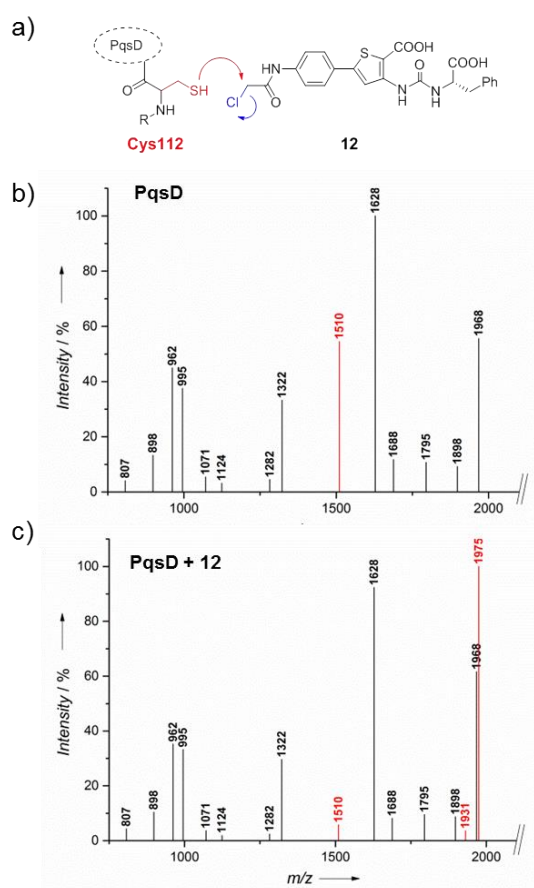


**Figure 6.** a) Schematic illustration of the proposed trapping of Cys112 by the introduced electrophilic warhead of **12**. MALDI-TOF-MS after tryptic digestion. The mass of the fragment containing Cys112 is highlighted in red b) PqsD c) PqsD after incubation with **12**. Signals below 3% intensity were removed for the sake of clarity (raw data is shown in Figure S6 and S7).

The resulting compound **12** ( $\text{clogD}_{7.4}$ :  $-0.59$ ) displays an  $IC_{50}$  value of  $2 \mu\text{M}$ . The covalent binding of **12** to PqsD was demonstrated by LC-ESI-MS. The PqsD peak ( $m/z = 36687.5 [M+H]^+$ ) shifted after preincubation with **12** to the calculated adduct mass ( $m/z = 37153.1 [M+H]^+$ ) (Figure S8). To evaluate whether indeed Cys112 is targeted by **12**, the tryptically digested protein was analyzed by MALDI-TOF-MS. The

signal of the fragment containing Cys112, with a calculated  $m/z = 1510.8 [M+H]^+$ , was found in the reference sample without inhibitor. In the sample treated with **12**, this signal was absent while two new peaks at  $m/z = 1975.9$  and  $1931.9 [M+H]^+$  appeared (Figure 6b,c). The former fits to the Cys112 fragment with covalently bound **12**. The latter refers to its fragmentation product missing a carboxylic acid moiety. Taking into account that a long residence time at the active site is considered important for *in vivo* potency of the inhibitor,<sup>18</sup> covalently binding compound **12** carries the potential of strong biological effects.

## Conclusions

In conclusion, we optimized the PqsD inhibitor **1**, following a novel approach. First, an equimolar binding behavior to the target protein PqsD was determined by ITC. The binding mode was elucidated by examination of three model compounds (**1–3**) in SPR competition experiments. To the best of our knowledge, this is the first example of such an approach. These findings allowed profound docking calculations guiding our subsequent structure-based optimization process. This approach culminated in an irreversible inhibitor, which covalently binds to the active site of PqsD as predicted. The optimization of activity was accompanied by reduced lipophilicity (Table 1), caused by the introduction of amino acids at the ureido motif. According to the literature, this should facilitate permeation into Gram negative cells.<sup>15</sup>

For several drug targets, inhibitors with known binding sites and the protein crystal structures are available. In such cases, the presented approach of determining the binding mode can be helpful to guide a structure-based design of new inhibitors, especially if co-crystallization fails.

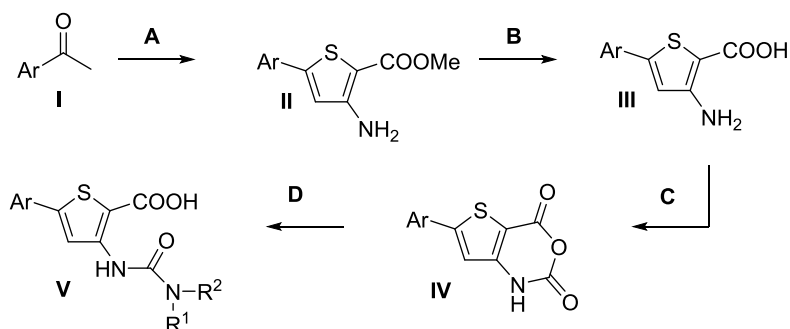
While we mainly focused on the inhibitory potency at this early point of development, structural variations leading to more drug-like properties (e.g. bio-isosteric exchange of the carboxylic groups) remains a challenging task and will be an element of future work. Additional efforts will also include studies on intracellular activity and inhibition of biofilm formation in *P. aeruginosa*. In the present study, shortcomings of *in silico* docking simulations (prediction of multiple binding modes) were compensated by the use of biophysical methods. This rational approach represents a powerful complement to X-ray co-crystallography and should be applicable to many drug targets with known ligands.

## Experimental section

**Materials and Methods.** Starting materials were purchased from commercial suppliers and used without further purification. Column flash chromatography was performed on silica gel (40–63  $\mu\text{M}$ ), and reaction progress was monitored by TLC on TLC Silica Gel 60 F<sub>254</sub> (Merck). All moisture-sensitive reactions were performed under nitrogen atmosphere using oven-dried glassware and anhydrous solvents. <sup>1</sup>H and <sup>13</sup>C NMR spectra were recorded on Bruker Fourier spectrometers (500/300 or 176/126/75 MHz) at ambient temperature with the chemical shifts recorded as  $\delta$  values in ppm units by reference to the hydrogenated residues of deuteriated solvent as internal standard. Coupling constants (*J*) are given in Hz and signal patterns are indicated as follows: s, singlet; d, doublet; dd, doublet of doublets; t, triplet; m, multiplet, br., broad signal. The purity of the final compounds was >95% except for **12** (90%) measured by HPLC. The Surveyor LC system consisted of a pump, an autosampler, and a PDA detector. Mass spectrometry was performed on a MSQ electrospray mass spectrometer (ThermoFisher, Dreieich, Germany). The system was operated by the standard software Xcalibur. A RP C18 NUCLEODUR 100-5 (125 mm x 3 mm) column (Macherey-Nagel GmbH, Dühren, Germany) was used as the stationary phase. All solvents were HPLC grade. In a gradient run the percentage of acetonitrile (containing 0.1% trifluoroacetic acid) was increased from an initial concentration of 0% at 0 min to 100% at 15 min and kept at 100% for 5 min. The injection volume was 10  $\mu\text{L}$ , and flow rate was set to 800  $\mu\text{L}/\text{min}$ . MS analysis was carried out at a spray voltage of 3800 V and a capillary temperature of 350 °C and a source CID of 10 V. Spectra were acquired in positive mode from 100 to 1000 *m/z* at 254 nm for the UV trace.

## Chemistry

**General synthesis procedures.** Experimental details on synthesis of **12** can be found in the Supporting Information.



**Scheme S1:** Synthesis of 5-aryl-3-ureidothiophene-2-carboxylic acids.

Method A, general procedure for the synthesis of 5-aryl-3-amino-2-carboxylic acid methylester (**II**):<sup>19</sup>

$\text{POCl}_3$  (26.1 g, 0.17 mol) was added dropwise to DMF (24.9 g, 0.34 mol) maintaining the temperature below 25 °C (cooling in ice bath) and stirred for additional 15 min. The acetophenone **I** (85.0 mmol) was added slowly and the temperature was kept between 40 and 60 °C. After complete addition, the mixture was stirred for 30 minutes at room temperature. Hydroxylamine hydrochloride (23.6 g, 0.34 mol) was carefully added portionwise (exothermic reaction!) and the reaction was stirred for additional 30 min without heating. After cooling to room temperature, the mixture was poured into ice water (300 mL). The precipitated  $\beta$ -chloro-cinnamionitrile was collected by filtration, washed with  $\text{H}_2\text{O}$  (2 x 50 mL) and dried under reduced pressure over  $\text{CaCl}_2$ . In the next step sodium (1.93 g, 84.0 mmol.) was dissolved in MeOH (85 mL) and methylthioglycolate (6.97 g, 65.6 mmol) was added to the stirred solution. The  $\beta$ -chloro-cinnamionitrile (61.1 mmol) was added and the mixture was heated to reflux for 30 min. After cooling to room temperature, the mixture was poured in ice water (300 mL). The precipitated solid was collected by filtration, washed with  $\text{H}_2\text{O}$  (2 x 50 mL) and dried under reduced pressure over  $\text{CaCl}_2$ . If necessary, recrystallisation was performed from EtOH.

Method B, general procedure for the synthesis of 5-aryl-3-amino-2-carboxylic acid (**III**):

The 5-aryl-3-amino-2-carboxylic acid methyl ester **II** (16.6 mmol) was added to a solution of KOH (60 mL, 0.6M in H<sub>2</sub>O) and MeOH (60 mL). The mixture was heated to reflux for 3 h, concentrated, and washed with EtOAc (2 x 50 mL). The aqueous layer was cooled with ice and acidified with a saturated aqueous solution of KHSO<sub>4</sub>. The precipitated solid was collected by filtration, washed with H<sub>2</sub>O (2 x 30 mL) and dried under reduced pressure over CaCl<sub>2</sub>.

Method C, general procedure for the synthesis of 5-aryl-2-thiaisatoic-anhydrid (**IV**):<sup>20,21</sup>

To a solution of the 5-aryl-3-amino-2-carboxylic acid (**III**) (5.28 mmol) in THF (50 mL) a solution of phosgene (6.10 mL, 20 wt% in toluene, 11.6 mmol) was added dropwise over a period of 30 min. The reaction mixture was stirred for 2 h at room temperature, followed by the addition of saturated aqueous solution of NaHCO<sub>3</sub> (30 mL) and H<sub>2</sub>O (50 mL). The resulting mixture was extracted with EtOAc/THF (1:1, 3 x 100 mL). The organic layer was washed with saturated aqueous NaCl (100 mL), dried (MgSO<sub>4</sub>) and concentrated. The crude material was suspended in a mixture of *n*-hexane/EtOAc (2:1, 50 mL) heated to 50 °C and after cooling to room temperature separated *via* filtration.

Method D, general procedure for the synthesis of of 5-aryl-3-ureidothiophene-2-carboxylic acid (**V**):<sup>22</sup>

The 5-aryl-2-thiaisatoic-anhydrid (**IV**) (0.46 mmol) was suspended in water (7.5 mL) and the appropriate amine (4.60 mmol) was added. The reaction mixture was stirred, heated to 100 °C and then cooled to room temperature. The reaction mixture was poured into a mixture of concentrated HCl and ice (1:1) and extracted with EtOAc/THF (1:1, 60 mL). The organic layer was washed with aqueous HCl (2M), followed by saturated aqueous NaCl (2 x 50 mL), dried (MgSO<sub>4</sub>) and concentrated. The crude material was suspended in a mixture of *n*-hexane/EtOAc (2:1, 20 mL) heated to 50 °C and after cooling to room temperature separated *via* filtration.

Spectroscopic data of final compounds and intermediates can be found in the Supporting Information. Compound **7** is presented as example.

**(S)-3-(3''-(1-Carboxy-2-phenylethyl)ureido)-5-(4'-methoxyphenyl)thiophene-2-carboxylic acid (7).**

<sup>1</sup>H NMR (DMSO-*d*<sub>6</sub>, 300 MHz): δ = 12.84 (br. s., 2 H, COOH), 9.42 (s, 1 H), 8.15 (d, *J* = 7.9 Hz, 1 H), 8.09 (s, 1 H), 7.69–7.51 (m, *J* = 8.8 Hz, 2 H), 7.37–7.25 (m, 4 H), 7.25–7.17 (m, 1 H), 7.03–6.97 (m, *J* = 8.8 Hz, 2 H), 4.56–4.28 (m, 1 H), 3.79 (s, 3 H, OCH<sub>3</sub>), 3.11 (dd, *J* = 13.9, 4.6 Hz, 1 H), 2.88 (dd, *J* = 13.9, 9.8 Hz, 1 H) ppm. <sup>13</sup>C NMR (DMSO-*d*<sub>6</sub>, 75 MHz): δ = 173.6, 164.6, 160.1, 153.7, 147.1, 145.9, 137.7, 129.0, 128.2, 127.1, 126.4, 125.4, 116.7, 114.7, 105.8, 55.3, 54.4, 36.9 ppm.

**Biology and Biophysics**

**General procedure for expression and purification of recombinant PqsD WT and R223A mutant in *E. coli*.** His6-tagged PqsD (H6-PqsD) and mutants were expressed in *E. coli* and purified using a single affinity chromatography step. Briefly, *E. coli* BL21 (λDE3) cells containing the pET28b(+)/pqsD (kindly provided by Prof. Rolf Müller) were grown in LB medium containing 50 µg/mL kanamycin at 37 °C to an OD<sub>600</sub> of approximately 0.8 units and induced with 0.2 mM IPTG for 16 h at 16 °C. The cells were harvested by centrifugation (5,000 rpm, 10 min, 4 °C) and the cell pellet was resuspended in 100 mL binding buffer (10 mM Na<sub>2</sub>HPO<sub>4</sub>, 2 mM KH<sub>2</sub>PO<sub>4</sub> pH 7.4, 3 mM KCl, 137 mM NaCl, 20 mM imidazole, 10% glycerol (v/v)) and lysed by sonication for a total process time of 2.5 min. Cell debris were removed by centrifugation (18500 rpm, 40 min, 4 °C) and the supernatant was filtered through a syringe filter (0.20 µm). The clarified lysate was immediately applied to a Ni-NTA column, washed with binding buffer and eluted with 500 mM imidazole. The protein containing fractions were buffer-exchanged into 125 mM Na<sub>2</sub>HPO<sub>4</sub>, 50 mM KH<sub>2</sub>PO<sub>4</sub> pH 7.6, 50 mM NaCl, 10% glycerol (v/v), using a PD10 column and judged pure by SDS-PAGE analysis. Then protein was stored in aliquots at –80 °C.

**Screening assay procedure for *in vitro* PqsD inhibition.**<sup>11</sup> The assay was performed monitoring enzyme activity by measuring HHQ formed by condensation of anthraniloyl-CoA and β-ketodecanoic acid. The reaction mixture contained MOPS buffer (0.05 M, pH 7.0) with 0.005% (w/v) Triton X-100, 0.1 µM of the purified enzyme and inhibitor. The test compounds were dissolved in DMSO and diluted with buffer. The final DMSO concentration was 0.5%. After 10 min preincubation at 37 °C, the reaction was started by the addition anthraniloyl-CoA to a final concentration of 5 µM

and  $\beta$ -ketodecanoic acid to a final concentration of 70  $\mu$ M. Reactions were stopped by addition of MeOH containing 1  $\mu$ M amitriptyline as internal standard for LC/MS-MS analysis. HHQ was quantified using a HPLC-MS/MS mass spectrometer (ThermoFisher, Dreieich, Germany) in ESI mode. Ionization of HHQ and the internal standard amitriptyline was optimized in each case. The solvent system consisted of 10 mM ammonium acetate (A) and acetonitrile (B), both containing 0.1% trifluoroacetic acid. The initial concentration of B in A was 45%, increasing the percentage of B to 100% in 2.8 min and keeping it at 98% for 0.7 min with a flow of 500  $\mu$ L/min. The column used was a NUCLEODUR-C18, 100-3/125-3 (Macherey & Nagel, Dueren, Germany). Control reactions without the inhibitor, but including identical amounts of DMSO, were performed in parallel and the amount of HHQ produced was set to 100%. All reactions were performed in triplicates.

**RNAP-transcription assay.** *E. coli* RNA polymerase holo enzyme was purchased from Epicentre Biotechnologies (Madison, WI). Final concentrations in a total volume of 30  $\mu$ L were one unit of RNA polymerase (0.5  $\mu$ g) which were used along with 60 nCi of [5,6- $^3$ H]-UTP, 400  $\mu$ M of ATP, CTP and GTP as well as 100  $\mu$ M of UTP, 20 units of RNase inhibitor (RiboLock, Fermentas), 10 mM DTT, 40 mM Tris-HCl (pH 7.5), 150 mM KCl, 10 mM MgCl<sub>2</sub> and 0.1% CHAPS. As a DNA template 3500 ng of religated pcDNA3.1/V5-His-TOPO were used per reaction.<sup>23</sup> Prior to starting the experiment, the compounds were dissolved in DMSO (final concentration during experiments: 2%). Dilution series of compounds were prepared using a liquid handling system (Janus, Perkin Elmer, Waltham, MA). The components described above (including the inhibitors) were preincubated in absence of NTPs and DNA for 10 min at 25 °C. Transcription reactions were started by the addition of a mixture containing DNA template and NTPs and incubated for 10 min at 37 °C. The reaction was stopped by the addition of 10% TCA, followed by a transfer of this mixture to a 96 well Multiscreen GFB plate (Millipore, Billerica, MA) and incubation for 45 min at 4 °C. The plate underwent several centrifugation and washing steps with 10% TCA and 95% ethanol to remove residual unincorporated  $^3$ H-UTP. After that the plate was dried (30 min, 50 °C) and 30  $\mu$ L of scintillation fluid (Optiphase Supermix, Perkin Elmer) was added to each well. After 10 min the wells were assayed for presence of  $^3$ H-RNA by counting using a Wallac MicroBeta TriLux system (Perkin Elmer). To obtain inhibition values for each sample, their counts were related to DMSO controls.

**Surface plasmon resonance.** SPR binding studies were performed using a Reichert SR7500DC instrument optical biosensor (Reichert Technologies, Depew, NY, USA) and CMD500M (carboxymethyl dextrane-coated) sensor chips obtained from XanTec (XanTec Bioanalytics, Düsseldorf, Germany).

**Immobilization of wild type PqsD and R223A mutant.** PqsD was immobilized on a CMD500M sensor chip at 12 °C using standard amine coupling analogous to the manufacturers' instructions. PqsD was diluted into sodium acetate buffer (10 mM, pH 4.5) to a final concentration of 100 µg/mL. PqsD was immobilized at densities between 5000-6000 RU for binding studies and for mutagenesis studies. The PqsD mutant was immobilized analogously to the wild type.

**Competition studies.** The competition studies were performed at a constant flow rate of 50 µL/min in instrument running buffer (50 mM MOPS, pH 8.0, 150 mM NaCl, 5% DMSO (v/v), 0.1% Triton X 100 (v/v)). 10 mM stock solutions of compounds **1**, **2** and **3** in DMSO were directly diluted to a concentration of 500 µM (50 mM MOPS, pH 8.0, 150 mM NaCl, 0.1% Triton X-100 (v/v)) and then diluted to a final concentration of 100 µM in running buffer (50 mM MOPS, pH 8.0, 150 mM NaCl, 5% DMSO (v/v), 0.1% Triton X 100 (v/v)). Final concentration of DMSO was retained at 5% (v/v). Before the compounds were injected, 6 warm-up blank injections were performed. Buffer blank injections and DMSO calibration were included for double referencing.

**ACoA competition.** PqsD was preincubated with compound **1**, therefore **1** was added to the running buffer (100 µM). The sensor chip surface was flushed for several hours at a constant flow rate of 50 µL/min until the baseline was stable. Afterwards the flow rate was decreased to 10 µL/min and ACoA was injected (100 µM) twice for 120 s association and 15 min dissociation times.

**Competitor competition.** PqsD was preincubated with compounds **A** or **B**, therefore the competitor compound was added to the running buffer (100 µM). The sensor chip surface was flushed for several hours at a constant flow rate of 50 µL/min until the baseline was stable. Afterwards the flow rate was decreased to 10 µL/min and compound **1**, **2** or **3** were injected (100 µM) twice for 120 s association and 300 s dissociation times. Due to a slow  $k_{\text{off}}$  rate of the competitor compounds,  $k_{\text{D}}$  values referring to the concentrations do not play a decisive role during the competition experiment.

**Studies with R223A mutant.** The experiments were performed at a constant flow rate of 50  $\mu\text{L}/\text{min}$  in instrument running buffer (50 mM MOPS, pH 8.0, 150 mM NaCl, 5% DMSO (v/v), 0.1% Triton X 100 (v/v)) at 12  $^{\circ}\text{C}$ . 10 mM stock solutions of compounds **1** or **2** in DMSO were diluted to a concentration of 100  $\mu\text{M}$  analogous to the binding studies. Before the compound was injected, twelve warm-up blank injections were performed. The obtained data were referenced against blank injections and DMSO calibration. The compounds were injected twice for 120 s association and 300 s dissociation time. Scrubber software was used for processing and analysing data.

**Isothermal titration calorimetry.** ITC experiments were carried out using an ITC200 instrument (Microcal Inc., GE Healthcare). Concentration of the ligand in DMSO stock solutions was 20 mM. Final ligand concentrations were achieved by diluting 1:20 (v/v) in the experimental buffer resulting in a final DMSO concentration of 5% (v/v). Protein concentration was determined by measuring the absorbance at 280 nm using a theoretical molarity extinction coefficient of  $17,780 \text{ M}^{-1} \text{ cm}^{-1}$ . DMSO concentration in the protein solution was adjusted to 5% (v/v). ITC measurements were routinely performed at 25  $^{\circ}\text{C}$  in PBS-buffer, pH 7.4, 10% glycerol (v/v), 5% DMSO (v/v). The titrations were performed on 100  $\mu\text{M}$  PqsD-His6 in the 200  $\mu\text{L}$  sample cell using 2  $\mu\text{L}$  injections of 1.0 mM ligand solution every 180 s. Raw data were collected and the area under each peak was integrated. To correct for heats of dilution and mixing the final baseline consisting of small peaks of the same size at the end of the experiment was subtracted. The experimental data were fitted to a theoretical titration curve (one site binding model) using MicroCal Origin 7 software, with  $\Delta\text{H}$  (enthalpy change in  $\text{kcal mol}^{-1}$ ),  $K_{\text{A}}$  (association constant in  $\text{M}^{-1}$ ), and  $N$  (number of binding sites) as adjustable parameters. Thermodynamic parameters were calculated from equation:

$$\Delta\text{G} = \Delta\text{H} - T\Delta\text{S} = RT \ln K_{\text{A}} = -RT \ln K_{\text{D}}$$

where  $\Delta\text{G}$ ,  $\Delta\text{H}$ , and  $\Delta\text{S}$  are the changes in free energy, enthalpy, and entropy of binding, respectively,  $T$  is the absolute temperature, and  $R = 1.98 \text{ cal mol}^{-1} \text{ K}^{-1}$ . For compound **1** four independent experiments were performed.

**Saturation transfer difference NMR.** All NMR data were recorded at 298 K on a Bruker Avance 500 NMR instrument equipped with a cryogenically cooled z-shielded gradient probe. Experiments were recorded with the carrier set at -2 ppm for on-

resonance irradiation and 40 ppm for off-resonance irradiation. Control spectra were recorded under identical conditions on samples containing free compound **7** to test for artifacts. Selective protein saturation (3 s) was accomplished using a train of 50 ms Gauss-shaped pulses, each separated by a 1 ms delay, at an experimental determined optimal power (50 dB on our probe); a T1 $\rho$  filter (15 ms) was incorporated to suppress protein resonances. Experiments were recorded using a minimum of 512 scans and 32K points. On- and off-resonance spectra were processed independently, and subtracted to provide a difference spectrum. Samples containing **7** and PqsD at final concentrations of 1 mM and 10  $\mu$ M, respectively, were prepared in 20 mM sodium phosphate, 50 mM NaCl, and 5 mM MgCl<sub>2</sub>, pH 7.0.

**LC-ESI-MS.** PqsD (25  $\mu$ M) was preincubated with compound **12** (25  $\mu$ M) for 30 min at 37°C in Tris-HCl buffer (0.05 M, pH 8.0) with 0.5% DMSO. Dithiothreitol was added and the samples were analyzed by HPLC-ESI. All ESI-MS-measurements were performed on a Dionex Ultimate 3000 RSLC system using an Aeris Widepore XB-C8, 150 x 2.1 mm, 3.6  $\mu$ m dp column (Phenomenex, USA). Separation of 2  $\mu$ l sample was achieved by a linear gradient from (A) H<sub>2</sub>O + 0.05% TFA to (B) ACN + 0.05% TFA at a flow rate of 250  $\mu$ l/min and 45 °C. The gradient was initiated by a 1.0 min isocratic step at 15% B, followed by an increase to 80% B in 4.5 min to end up with a 6 min step at 80% B before re-equilibration with initial conditions. UV spectra were recorded by a DAD in the range from 200 to 600 nm. The LC flow was split to 75  $\mu$ l/min before entering the maXis 4G hr-ToF mass spectrometer (Bruker Daltonics, Bremen, Germany) using the standard Bruker ESI source. In the source region, the temperature was set to 180°C, the capillary voltage was 4000 V, the dry-gas flow was 6.0 l/min and the nebulizer was set to 1.1 bar. Mass spectra were acquired in positive ionization mode ranging from 600 – 1800 m/z at 2.5 Hz scan rate. Protein masses were deconvoluted by using the Maximum Entropy algorithm (Copyright 1991-2004 Spectrum Square Associates, Inc.).

**MALDI-TOF-MS.** PqsD (10  $\mu$ M) was preincubated with compound **12** (10  $\mu$ M) for 60 min at 37°C using identical buffer composition as in the screening assay procedure (0.05 M MOPS, pH 7.0 with 0.005 % (w/v) Triton X-100 and 0.5 % DMSO). The buffer was exchanged by an NH<sub>4</sub>HCO<sub>3</sub> buffer (0.05 M, pH 8.1) in three diafiltration steps. Diafiltration was performed at 1200 g for 6 min at 4°C in Nanosep® Centrifugal Devices (MWCO = 10K) of Pall Corporation (Port Washington, NY, USA). The protein

was digested with trypsin overnight and dithiothreitol was added.  $\alpha$ -Cyano-4-hydroxycinnamic acid was used as matrix component. Analyzes of the peptides were performed on a 4800 TOF/TOF Analyzer mass spectrometer (Applied Biosystems, Darmstadt, Germany) in positive reflector mode using a pulsed 200 Hz solid state Nd:YAG laser with a wavelength of 355 nm. Laser energy was set to 2000–2300 units for standards and to 2700–3200 units for real samples. Source 1 voltage was set to 20 kV with a grid voltage of 16 kV. Reflector detector voltage was 2.19 kV. Spectra of standard peptides used for wide range calibration ranging from 0.8 to 4 kDa (des-arg1-bradykinin, angiotensin I, glu1-fibrinopeptide B, ACTH 1–17 clip, ACTH 18–39 clip and ACTH 7–38 clip) were measured with a delay time of 600 ns. One single mass spectrum was formed from 20 subspectra per spot using 25 accepted laser impulses each. From the standard peptides exclusively monoisotopic ions were used with a minimum signal-to-noise (S/N) ratio of 20 and a resolution >10000. Mass tolerance was set to 0.3 Da with maximum outlier of 5 ppm. Accepted calibration settings were used to measure real sample spectra in the range of 1 to 3.5 kDa with a minimum S/N range of 10 and a resolution >8000. An internal algorithm defined the isotope cluster area subsequently named intensity (I), based on the peptides' molecular weight and their general elemental composition. MALDI-TOF-MS resulted in pmfs consisting of mass-intensity spectra ( $m/z$ - $I_{\text{abs, ai}}$ ).

### Molecular Modeling

**Docking.** Inhibitors were built in Molecular Operating Environment (MOE).<sup>24</sup> The receptor was derived from the co-crystal structure of anthraniloyl coenzyme A with PqsD (PDB Code: 3H77)<sup>6</sup> ACoA, the covalently bound anthranilate and H<sub>2</sub>O were removed and Cys112 was restored considering its conformation in 3H76.<sup>6</sup> AutoDockTools V.1.5.6 was used to add polar hydrogens and to save the protein in the appropriate file format for docking with Vina. For docking AutoDockVina was used.<sup>25</sup> The docking parameters were kept at their default values. The docking grid was sized 18 Å x 24 Å x 24 Å, covering the entire ACoA channel.

### Acknowledgements

The authors thank Carina Scheid for technical assistance, Patrick Fischer for his help performing the synthesis, Dr. K. Hollemeyer for MALDI-TOF investigations and Michael Hoffmann for LC-ESI-MS measurements. J.H. Sahner gratefully acknowledges a scholarship from the Stiftung der Deutschen Wirtschaft (SDW).

## References

- (1) Wagner, G.; Hyberts, S. G.; Havel, T. F. NMR structure determination in solution: a critique and comparison with X-ray crystallography. *Annu. Rev. Biophys. Biomol. Struct.* **1992**, *21*, 167–198.
- (2) Davis, A. M.; Teague, S. J.; Kleywegt, G. J. Application and limitations of X-ray crystallographic Data in structure-based ligand and drug design. *Angew. Chem. Int. Ed.* **2003**, *42*, 2718–2736.
- (3) Boström, J. Reproducing the conformations of protein-bound ligands: a critical evaluation of several popular conformational searching tools. *J. Comp-Aided Mol. Des.* **2001**, *15*, 1137–1152.
- (4) Xiao, G.; Dézièl, E.; He, J.; Lépine, F.; Lesic, B.; Castonguay, M.-H.; Milot, S.; Tampakaki, A. P.; Stachel, S. E.; Rahme, L. G. MvfR, a key *Pseudomonas aeruginosa* pathogenicity LTTR-class regulatory protein, has dual ligands. *Mol. Microb.* **2006**, *62*, 1689–1699.
- (5) For a recent review see: Dubern, J.-F.; Diggle, S. P. Quorum sensing by 2-alkyl-4-quinolones in *Pseudomonas aeruginosa* and other bacterial species. *Mol. Biosyst.* **2008**, *4*, 882–888.
- (6) Bera, A.K.; Atanasova, V.; Robinson, H.; Eisenstein, E.; Coleman, J. P.; Pesci, E. C.; Parsons, J. F. Structure of PqsD, a *Pseudomonas* quinolone signal biosynthetic enzyme, in complex with anthranilate. *Biochemistry* **2009**, *48*, 8644–8655.
- (7) Storz, M. P.; Maurer, C. K.; Zimmer, C.; Wagner, N.; Brengel, C.; de Jong, J. C.; Lucas, S.; Müsken, M.; Häussler, S.; Steinbach, A.; Hartmann, R. W. Validation of PqsD as an anti-biofilm target in *Pseudomonas aeruginosa* by development of small-molecule inhibitors. *J. Am. Chem. Soc.* **2012**, *134*, 16143–16146.
- (8) Gomez, M. I.; Prince, A. Opportunistic infections in lung disease: *Pseudomonas* infections in cystic fibrosis. *Curr. Opin. Pharmacol.* **2007**, *7*:244–251.
- (9) Hakki, M.; Limaye, A. P.; Kim, H. W.; Kirby, K. A.; Corey, L.; Boeckh, M. Invasive *Pseudomonas aeruginosa* infections: high rate of recurrence and mortality after hematopoietic cell transplantation. *Bone Marrow Transpl.* **2007**, *39*, 687–693.
- (10) Asboe, D.; Gant, V.; Aucken, H. M.; Moore, D. A.; Umasankar, S.; Bingham, J. S.; Kaufmann, M. E.; Pitt, T. L. Persistence of *Pseudomonas aeruginosa* strains in respiratory infection in AIDS patients. *AIDS* **1998**, *12*, 1771–1775.
- (11) Pistorius, D.; Ullrich, A.; Lucas, S.; Hartmann, R. W.; Kazmaier, U.; Müller, R. Biosynthesis of 2-alkyl-4(1H)-quinolones in *Pseudomonas aeruginosa*: potential for therapeutic interference with pathogenicity. *ChemBioChem* **2011**, *12*, 850–853.
- (12) Sahner, J. H.; Groh, M.; Negri, M.; Haupenthal, J.; Hartmann, R. W. Novel small molecule inhibitors targeting the “switch region” of bacterial RNAP: structure-based optimization of a virtual screening hit. *Eur. J. Med. Chem.* **2013**, *65*, 223–231.
- (13) Hentzer, M.; Givskov, M. Pharmacological inhibition of quorum sensing for treatment of chronic bacterial infections. *J. Clin. Invest.* **2003**, *112*, 1300–1307.
- (14) Storz, M. P.; Brengel, C.; Weidel, E.; Hoffmann, M.; Empting, M.; Steinbach, A.; Müller, R.; Hartmann, R. W. unpublished results.

- (15) O'Shea, R.; Moser, H.E. Physicochemical properties of antibacterial compounds: implications for drug discovery. *J. Med. Chem.* **2008**, *51*, 2871–2878.
- (16) Mayer, M.; Meyer, B. Characterization of ligand binding by saturation transfer difference NMR spectroscopy. *Angew. Chem. Int. Ed.* **1999**, *38*, 1784–1788.
- (17) Henise, J. C.; Taunton, J. Irreversible Nek2 kinase inhibitors with cellular activity. *J. Med. Chem.* **2011**, *54*, 4133–4146.
- (18) Copeland, R. A.; Pompliano, D. L.; Meek, T. D. Drug-target residence time and its implications for lead optimization. *Nat. Rev. Drug Discov.* **2006**, *5*, 730–739.
- (19) Hartmann, H.; Liebscher, J. A simple method for the synthesis of 5-aryl-3-amino-2-alkoxycarbonylthiophenes. *Synthesis* **1984**, 275–276.
- (20) Fabis, F.; Jolivet-Fouchet, S.; Robba, M.; Landelle, H.; Rault, S. Thiaisatoic anhydrides: efficient synthesis under microwave heating conditions and study of their reactivity. *Tetrahedron* **1998**, *54*, 10789–10800.
- (21) Foulon, L.; Braud, E.; Fabis, F.; Lancelot, J.C.; Rault, S. Synthesis and combinatorial approach of the reactivity of 6-and 7-arylthieno [3, 2-d][1, 3] oxazine-2, 4-diones. *Tetrahedron* **2003**, *59*, 10051–10057.
- (22) Le Foulon, F.X.; Braud, E.; Fabis, F.; Lancelot, J.C.; Rault, S. Solution-phase parallel synthesis of a 1140-member ureidothiophene carboxylic acid library. *J. Comb. Chem.* **2005**, *7*, 253–257.
- (23) Haupenthal, J.; Hüsecken, K.; Negri, M.; Maurer, C.K.; Hartmann, R.W. Influence of DNA template choice on transcription and inhibition of *E. coli* RNA polymerase. *Antimicrob. Agents Ch.* **2012**, *56*, 4536–4539.
- (24) Molecular Operating Environment (MOE), 2010.10; Chemical Computing Group Inc., 1010 Sherbooke St. West, Suite #910, Montreal, QC, Canada, H3A 2R7, **2010**.
- (25) Trott, O.; Olson, A. J. AutoDock Vina: improving the speed and accuracy of docking with a new scoring function, efficient optimization, and multithreading. *J. Comput. Chem.* **2009**, *31*, 455–461.

### 3.5 Exploring the chemical space of ureidothiophene-2-carboxylic acids as inhibitors of the quorum sensing enzyme PqsD from *Pseudomonas aeruginosa*

J. Henning Sahner, Martin Empting, Ahmed Kamal, Elisabeth Weidel, Matthias Groh, Carsten Börger, and Rolf W. Hartmann

This manuscript was submitted for publication to *Eur. J. Med. Chem.*

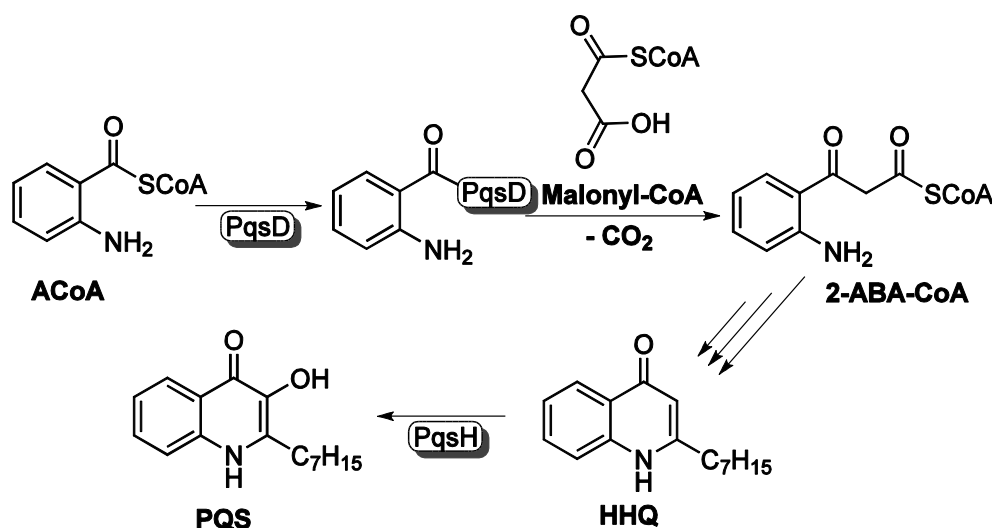
#### Publication E

**Abstract:** *P. aeruginosa* employs a quorum sensing (QS) communication system that makes use of small diffusible molecules. Among other effects, the QS system coordinates the formation of biofilm which decisively contributes to difficulties in the therapy of *Pseudomonas* infections. The present work deals with the structure-activity exploration of ureidothiophene-2-carboxylic acids as inhibitors of PqsD, a key enzyme in the biosynthetic pathway of signal molecules in the *Pseudomonas* QS system. We describe an improvement of the inhibitory activity by successfully combining features from two different PqsD inhibitor classes. Furthermore the functional groups, which are responsible for the inhibitory potency, were identified. Moreover, the inability of the new inhibitors, to prevent signal molecule formation in whole cell assays, is discussed.

## Introduction

Antibiotic therapy is characterized by the everlasting competition between the generation of novel antibacterial substances and the development of the respective bacterial resistances.[1,2] One outstanding example is the opportunistic pathogen *P. aeruginosa* which is responsible for severe infections and is a leading cause of death in cystic fibrosis patients.[3] Its ability to rapidly form resistances against the currently used antibiotics necessitates new approaches for antibacterial treatment.[4,5] Typically, antibiotics affect bacterial viability and thus cause a selection pressure that inevitably leads to the development of resistances.[6] In recent years several research groups have been trying to break out of this vicious cycle by reducing the virulence of the pathogens instead of affecting their viability. One approach is the inhibition of the bacterial cell-to-cell communication systems like QS.[7] In QS, bacterial cells release a variety of small diffusible molecules which can be detected by other bacteria. This kind of molecular signaling allows the bacterial population to assess its cell density and coordinate group behavior. The *Pseudomonas* QS system consists of two *N*-acylhomoserine lactone (AHL) regulatory circuits (*las* and *rhl*) linked to an 2-alkyl-4-quinolone (AQ) system.[3] Whereas the AHL systems are widespread among Gram negative bacteria,[8] our group focuses on the so called *Pseudomonas* quinolone signal quorum sensing (PQS-QS) system, an AQ system that exclusively exists in *P. aeruginosa* and some *Burkholderia* strains.[9] It is involved in the production of a number of virulence factors that contribute to their pathogenicity.[10] Moreover, it takes part in regulating the formation of biofilms, a main cause for bacterial resistance against conventional antibiotics in clinical use.[11] The *pqsABCDE* operon, whose expression is controlled by the transcriptional regulator PqsR (MvfR), directs the AQ biosynthesis in *P. aeruginosa*. Molecules, produced upon activity of this operon are among others, 2-heptyl-3-hydroxy-4-quinolone (*Pseudomonas* quinolone signal, PQS) and its biosynthetic precursor 2-heptyl-4-quinolone (HHQ).[12] HHQ and PQS themselves activate PqsR leading to an auto-induction of the *pqsABCDE* operon.[13,14] Besides, they can modulate the innate immune response of mammalian cells, affecting the first defense barrier of the host.[15,16,17] Compounds, interfering with the PQS-QS system have proven to be promising candidates for drug development. Treatment with antagonists of the PqsR receptor enabled the survival of *P. aeruginosa* infected *Galleria mellonella* larvae.[18] Furthermore we could show that inhibitors of the

enzyme PqsD, a key player in the AQ biosynthesis (Scheme 1), are able to reduce biofilm in *P. aeruginosa* cultures.[19] It was recently reported by Dulcey et al., that PqsD produces 2-aminobenzoylacetate-coenzyme A (2-ABA-CoA), a highly active intermediate in the HHQ biosynthesis, by converting anthraniloyl-coenzyme A (ACoA) with malonyl CoA. Firstly, ACoA is covalently transferred to C112 of PqsD, followed by the reaction with malonyl-CoA. Further conversion of the intermediate 2-ABA-CoA in several enzymatic steps finally results in HHQ and PQS (Scheme 1).[17] Interestingly, PqsD is also capable of directly producing HHQ by converting ACoA with  $\beta$ -ketodecanoic acid.[20] In the recent past we frequently used this enzymatic reaction to assess the activity of PqsD inhibitors.[19,21–25] For compounds interfering with the first enzymatic step, the formation of the PqsD-CoA complex, this is still a valid method.[23,24]



**Scheme 1.** Biosynthetic pathway of the signal molecules HHQ and PQS according to Dulcey et al. [15].

In a recent work, we reported on the class of ureidothiophene-2-carboxylic acids as potent inhibitors of PqsD. Biophysical methods were used to confirm a binding hypothesis derived from molecular docking studies. This approach enabled the structure-based optimization of a screening hit compound resulting in a series of highly active molecules (e.g. **A** and **B** in Chart 1).[21] According to our docking pose and the results from SPR competition experiments, the most active derivative **B** occupies an area, spanning from the entrance of the binding channel to the active site, leaving a gap of about 6 Å to the bottom of the pocket where the catalytic residues are located. Its carboxylic acid groups are supposed to interact with Asn154

and Arg262 respectively anchoring the inhibitor in the binding channel of PqsD. The phenylalanine residue perfectly fits into a narrow pocket at the channel's entrance delimited by Arg 223 and Phe226 and (Figure 1).

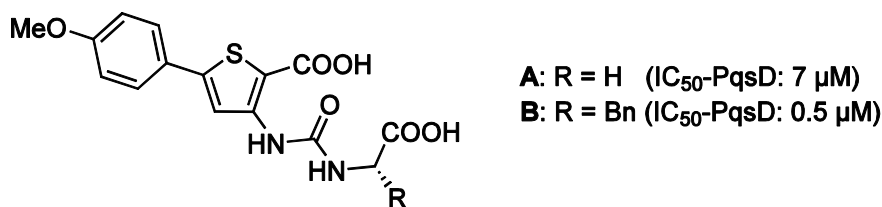


**Chart 1.** Structures of the PqsD inhibitors **A** and **B**.

In this work we describe further exploration of the chemical space, the structure activity relationships (SAR) and the intracellular effects of this class of inhibitors.

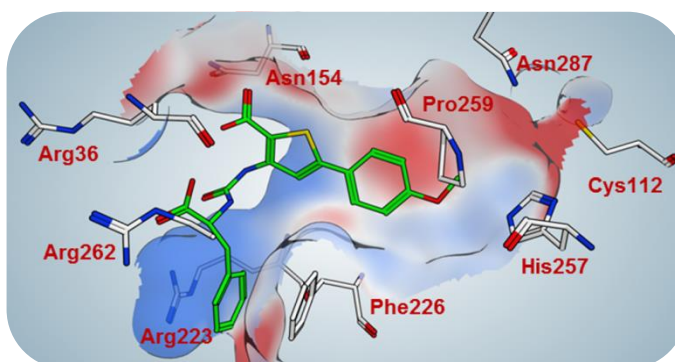


**Figure 1.** Docking pose of **B** inside the binding channel of PqsD.

### Results and discussion

According to our binding hypothesis, the carboxylate group of the amino acid part in **A** and **B** interacts with Arg262 at the entrance of the PqsD binding channel (Figure 1). The natural substrate anthraniloyl CoA (ACoA) builds several ion bridges between its phosphoric acid groups and the arginins on the surface of the protein. Such interactions are considered very potent in literature.[26,27] Inspired by ACoA we replaced the carboxylic acid moiety by a phosphoric acid group (**1**). In comparison to the glycine derivative **A** the activity did not increase. Based on these findings, the phosphoric acid was not considered for further optimization due to synthetic reasons.

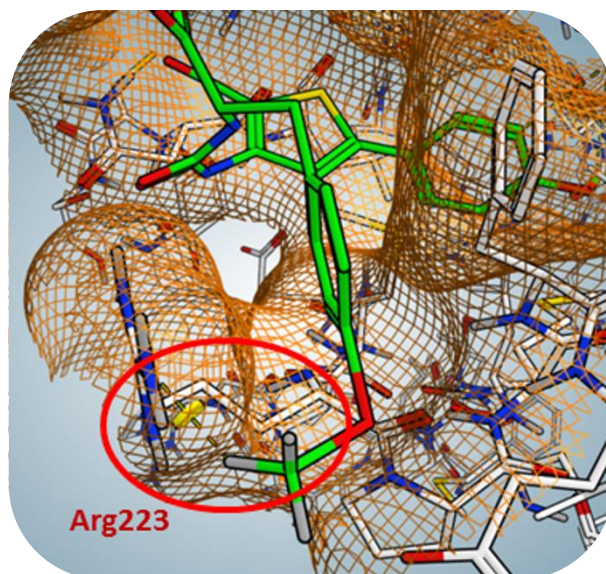


**Figure 2.** Illustration of the proposed clash between the additional methoxy group and the protein residue Arg223.

The so far most active inhibitor **B** carries a phenylalanine substituent at the ureido motif. In order to fine-tune the electronic properties of the aromatic system we investigated electron donating and electron withdrawing substituents in *para*-position. In case of an electron donating hydroxyl function (**2**), the activity dropped to 29  $\mu\text{M}$  similar to an additional methoxy group (**3**;  $\text{IC}_{50}$ : 31  $\mu\text{M}$ ). In case of the latter this is probably due to steric reasons, which is in good agreement with our binding hypothesis (Figure 2).

Introduction of an electron withdrawing and lipophilic chlorine substituent (**4**) also resulted in decreased inhibitory potency (14  $\mu\text{M}$ ). As both kinds of substituents with inverse electronic properties were detrimental to the activity, we considered the unsubstituted ring as most favorable. In the next step we shortened (**5**) and prolonged (**6**) the linker between the  $\alpha$ -position and the phenyl ring. In the crystal structure, the entrance to the sub-pocket, delimited by Arg223 and Phe226 and Glu227 is narrow and therefore requires a special conformation. This conformation is obviously only provided by the compound with the methylene linker as both, **5** and **6** displayed significantly weaker inhibitory potency. As a last trial to explore the SAR at this part of the molecule, readily available (*S*)-amino acids were introduced. None of the resulting compounds (**7-11**) outperformed the potency of **B**.

**Table 1.** Inhibitory activities of **1–11** against *P. aeruginosa* PqsD *in vitro*.

Entry	R	Inhibition of PqsD <sup>a</sup>
<b>1</b>		7.0 ± 0.7 μM
<b>2</b>		29.0 ± 0.01 μM
<b>3</b>		31.3 ± 3.7 μM
<b>4</b>		13.8 ± 1.1 μM
<b>5</b>		~50% @ 50 μM
<b>6</b>		33.7 ± 1.5 μM
<b>7</b>		31.9 ± 3.0 μM
<b>8</b>		19.0 ± 2.6 μM
<b>9</b>		13.2 ± 0.9 μM
<b>10</b>		5.0 ± 0.9 μM
<b>11</b>		30.3 ± 0.3 μM

<sup>a</sup> IC<sub>50</sub> values of PqsD

We proceeded, retaining the phenylalanine residue at the ureido-motif, as the most promising moiety and subsequently focused on the opposite side of the molecule. Firstly parts of the methoxy equipped ring of **B** were removed to determine the essential functional groups. Demethylation, resulting in hydroxyl compound **12** decreased the activity. Further omitting this OH-group (**13**) however partially restored it. This leads to the assumption that the oxygen of the methoxy group contributes to the activity to a certain extent, presumably as a hydrogen bond acceptor. In absence of an appropriate interaction partner the hydrogen bond donor of **13** is surrounded by highly ordered water molecules, leading to an entropic loss and, therefore, a lowered activity. Removal of the entire methoxyphenyl ring (**14**) results in a total loss of inhibitory potency. To reveal the bioactive conformation and the orientation of the methoxyphenyl ring towards the thiophene, **15** and **16** were investigated. The methyl

group of **15** increased the  $IC_{50}$  to  $8 \mu\text{M}$  suggesting an ortho-effect and thus an unfavorable perpendicular orientation of the two rings or a steric clash of the additional substituent. Rigidification by an ethylene linker (**16**), which directly connects the two aromatic systems causing a planar structure (Figure 3), did not improve the activity as well. The tight shape of the PqsD binding channel that demands certain flexibility from entering inhibitors can once more be an explanation for these findings.

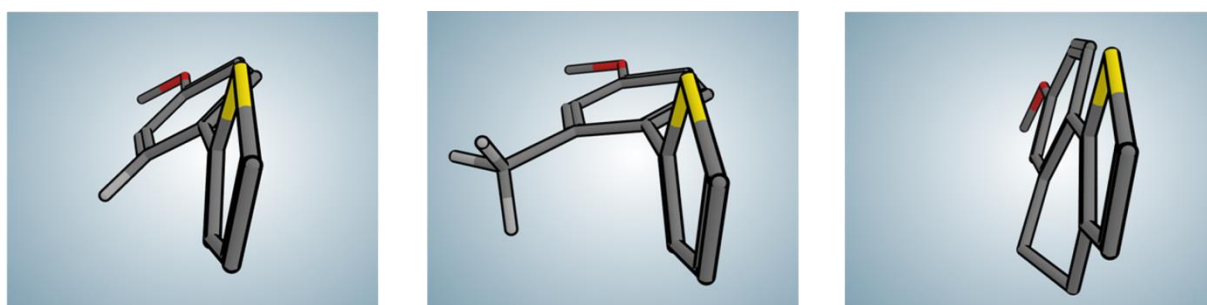


**Figure 3.** Energy minimized conformations showing the orientation between the phenyl ring and the thiophene core of **B**, **15** and **16**.

**Table 2.** Inhibitory activities of **12–17** against *P. aeruginosa* PqsD *in vitro*.

Entry	Structure	Inhibition of PqsD <sup>a</sup>
<b>12</b>		$21.6 \pm 3.9 \mu\text{M}$
<b>13</b>		$3.8 \pm 1.4 \mu\text{M}$
<b>14</b>		no inhibition @ $50 \mu\text{M}$
<b>15</b>		$7.5 \pm 1.8 \mu\text{M}$
<b>16</b>		$23.7 \pm 0.02 \mu\text{M}$
<b>17</b>		$11.5 \pm 2.0 \mu\text{M}$

<sup>a</sup>  $IC_{50}$  values of PqsD

The proposed interaction between the carboxylic acid at the thiophene core with Asn154 was corroborated by compound **17**. Removal of the carboxylic group decreased the activity by about twentyfold.

By the application of SPR competition experiments in the above mentioned earlier work,[21] we were able to narrow down the position of the ureidothiophene-2-carboxylic acids within the binding channel compared to known PqsD inhibitors from the 2-(nitrophenyl)-methanol class (**C** and **D** in Chart 2). Whereas the shorter compound **C** (Figure 4a turquoise) did not affect the binding affinity of **B**, the longer derivative **D** (Figure 4b yellow) prevented binding of **B** (data not shown), fitting to our binding hypothesis.

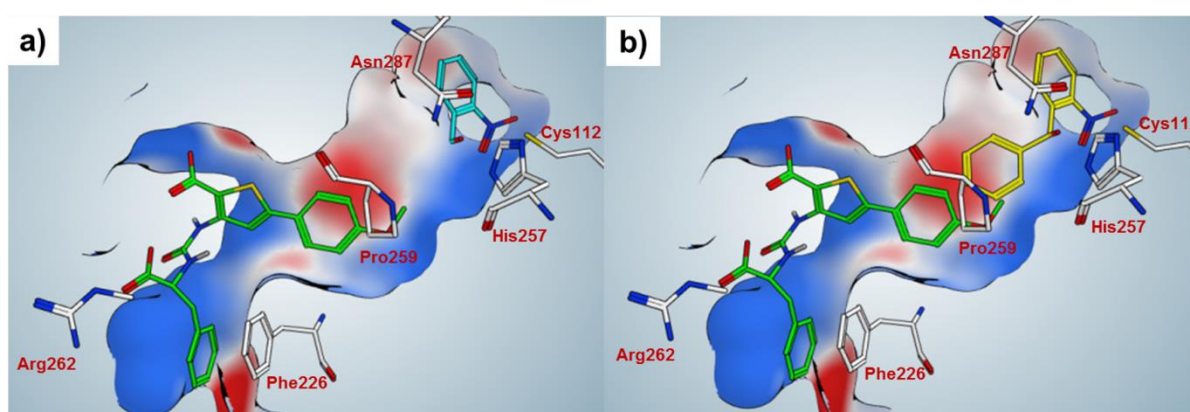


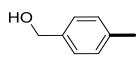
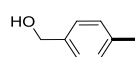
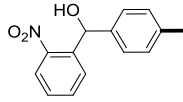
**Figure 4.** a) Docking pose of **B** (green) and **C** (turquoise). b) Docking pose of **B** (green) and **D** (yellow).

According to the docking pose, a linkage of the two inhibitor classes in order to combine their interactions with PqsD should be possible. We decided to enlarge the unsubstituted compound **13** step by step to achieve a full combination with **D**. Due to the absence of strong interactions with the protein, docking studies never delivered an unambiguous orientation of the aryl ring at the thiophene core within the pocket. Even though an attachment in 3-position (**18,19**) should be favorable according to the dockings with compound **B** (compare Figure 4), expansion in 4-position (**20–22**) lead to better results. We hypothesized that this is once again due to the tight shape of the binding channel which hampers the entrance of the stronger tilted compounds **18** and **19**.

Whereas the introduction of the first phenyl ring (**20**) did not result in better inhibition, elongation with a hydroxy-methyl function (**21**), which is supposed to mimic the one

of **C** and **D** increased the activity by twentyfold compared to **13** (factor three compared to **B**).

**Table 3.** Inhibitory activities of **18–22** against *P. aeruginosa* PqsD *in vitro*.

Entry	3-Position	4-Position	Inhibition of PqsD <sup>a</sup>
<b>18</b>		H	14.1 ± 0.03 μM
<b>19</b>		H	19.4 ± 0.02 μM
<b>20</b>	H		2.7 ± 0.5 μM
<b>21</b>	H		0.14 ± 0.03 μM
<b>22</b>	H		0.36 ± 0.06 μM

<sup>a</sup> IC<sub>50</sub> values of PqsD

Attachment of the second, nitro-substituted ring (**22**) forfeits parts of the activity gain. A possible explanation could be that the final compound is large and inflexible and, is therefore, incapable of adapting to conformational changes which would be necessary to retain the sum of interactions of the respective single compounds **B** and **D**.

To confirm, that the nitro-substituted ring of **22** reaches deep into the binding channel, SPR experiments were performed. Firstly, the binding responses of **B**, **21** and **22** towards PqsD were recorded in the absence of ACoA. In a second experiment, the PqsD loaded sensor chip was treated with ACoA. According to the catalytic mechanism of PqsD this results in the anthranilate-PqsD complex, in which the anthranilic acid is covalently bound to Cys112. Subsequently the binding responses of **B**, **21** and **22** to this complex were determined. Only the signals of **22** showed significant differences between treated and untreated PqsD (Figure S1 in supporting information). Since this behavior is typical for the 2-nitrophenylmethanol derivatives,[22] occupation of the same binding site can be assumed.

Although the inhibitors displayed high potency in the cell free enzyme assay, none of them was able to reduce the HHQ levels in a whole cell *P. aeruginosa* assay. These

findings can be attributed to different reasons like permeation- or efflux problems. Several steps were taken to achieve an intracellular activity.

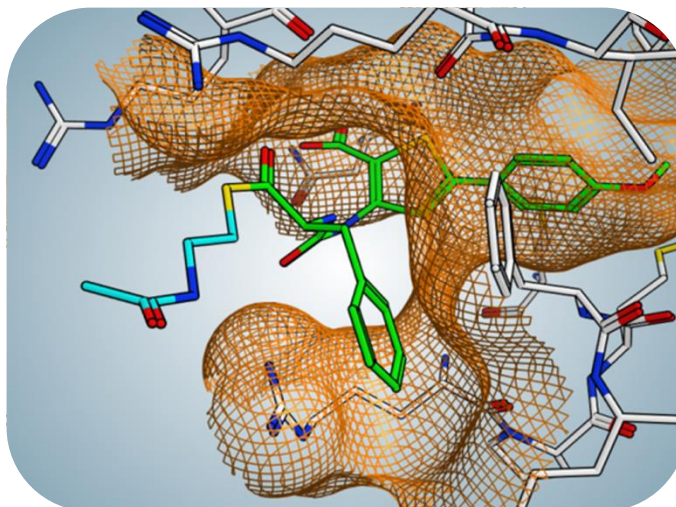


**Figure 5.** Docking pose of **B** (green) extended with the NAC moiety (blue) present in **24**, illustrating how the additional residue is directed outside the binding channel of PqsD.

Fluoroquinolone and  $\beta$ -lactam antibiotics are mostly zwitterionic. According to several reports in literature, this feature significantly contributes to their transport into the cell, which was shown especially for the  $\beta$ -lactams.[28,29] Inspired by that we introduced *S*-histidine instead of *S*-phenylalanine, using the imidazole ring as a bioisostere of the phenyl ring while gaining a basic function and therefore a potentially positive charge at the same time. The resulting compound **23** displayed weak activity against PqsD (40% inhibition at 50  $\mu$ M) but showed for the first time significant but very moderate reduction of HHQ levels in the whole cell assay (Reduction of HHQ at 250  $\mu$ M: 16 $\pm$ 5 %). In a second attempt, we made use of an *N*-acetyl thioester (NAC-ester) which is frequently used in mutasynthesis programs. The NAC adducts thereby serve as mimics of coenzyme A esters which improve their acceptance as precursors in biosynthesis and might also facilitate the entrance into bacterial cells in comparison to the free acids.[30] The carboxylic acid moiety of the phenylalanine was considered more suitable for the attachment of an NAC unit than the one at the thiophene core. It is presumably positioned at the entrance of the pocket (Figure 5) directing the additional substituent outside the binding channel of PqsD, and therefore avoiding steric hindrance. Thus an intracellular cleavage of the thioester to set the active form free might not be mandatory. The resulting compound **24** (Chart 3) still displayed reasonable activity ( $IC_{50}$ : 32  $\mu$ M) but turned out to be inactive in the whole-cell assay. We further examined the introduction of a cell penetrating peptide (**25**) at the same

position. Again, the inhibitory activity on the cell free level could be retained, but no inhibitory effect in the whole cell assay was observed at the test concentration.

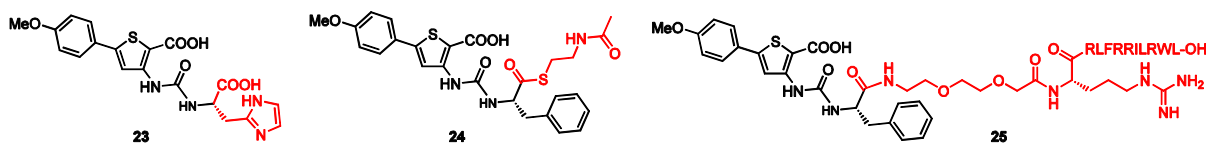


**Chart 3.** Structures of compound **23–25**, carrying moieties (highlighted in red) which should facilitate the entrance into Gram-negative cells.

## Conclusions

In conclusion, we further explored the chemical space of the ureidothiophene-2-carboxylic acids as inhibitors of PqsD. The pharmacophore of the inhibitor class was determined and the essentiality of several functional groups was clarified. Moreover, two inhibitor classes could be successfully merged without having access to structural information of protein-ligand x-ray structures. The resulting compounds display higher inhibitory activity by profiting from the combined interactions with the protein. Following this approach, the most potent PqsD inhibitors described so far were obtained. Although the potency in cell free assay was high, an intracellular activity could not be achieved even by attachment of a cell penetrating peptide. We assume that the class of inhibitors is subject to efflux causing natural resistance of *P. aeruginosa* towards the newly developed antibacterial agents. Therefore, we consider the ureidothiophene-2-carboxylic acids to be not eligible for further development in the field of *Pseudomonas* quorum sensing inhibitors. The problem could eventually be solved by a combined application with efflux pump inhibitors, or by using pharmaceutical technological methods, but this is beyond the frame of this work. Nevertheless, important interactions of functional groups with the protein were revealed that can be used to improve the inhibitory activity of other PqsD inhibitors with better intracellular effects.

## Experimental procedures

### Chemistry

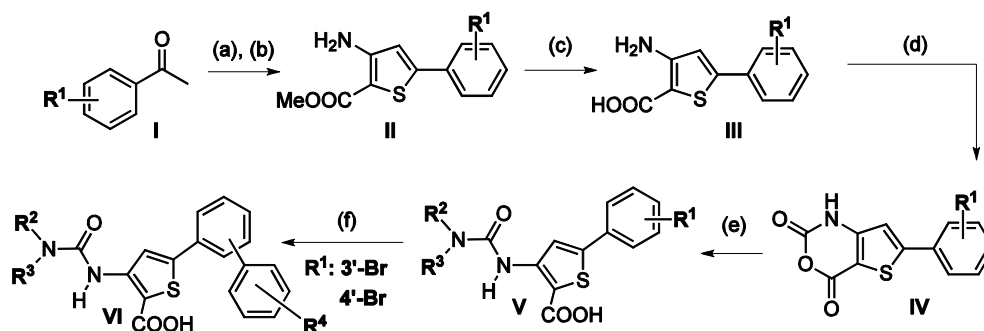
**Materials and methods.** Starting materials were purchased from commercial suppliers and used without further purification. Column flash chromatography was

performed on silica gel (40–63  $\mu\text{M}$ ), and reaction progress was monitored by TLC on TLC Silica Gel 60 F<sub>254</sub> (Merck). All moisture-sensitive reactions were performed under nitrogen atmosphere using oven-dried glassware and anhydrous solvents. Preparative RP-HPLC was carried out on a Waters Corporation setup containing a 2767 sample manager, a 2545 binary gradient module, a 2998 PDA detector and a 3100 electron spray mass spectrometer. Purification was performed using a Waters XBridge column (C18, 150 x 19 mm, 5  $\mu\text{m}$ ), a binary solvent system A and B (A = water with 0.1% formic acid; B = MeCN with 0.1% formic acid) as eluent, a flow rate of 20 mL/min and a gradient of 60% to 95% B in 8 min were applied. <sup>1</sup>H and <sup>13</sup>C NMR spectra were recorded on a Bruker Fourier spectrometer (500/300 or 125/75 MHz) at ambient temperature with the chemical shifts recorded as  $\delta$  values in ppm units by reference to the hydrogenated residues of deuterated solvent as internal standard. Coupling constants (*J*) are given in Hz and signal patterns are indicated as follows: s, singlet; d, doublet; dd, doublet of doublets; t, triplet; m, multiplet, br., broad signal. Purity of the final compounds was determined by HPLC. The Surveyor LC system consisted of a pump, an autosampler, and a PDA detector. Mass spectrometry was performed on a MSQ electrospray mass spectrometer (ThermoFisher, Dreieich, Germany). The system was operated by the standard software Xcalibur. A RP C18 NUCLEODUR 100-5 (125 mm x 3 mm) column (Macherey-Nagel GmbH, Dühren, Germany) was used as the stationary phase. All solvents were HPLC grade. In a gradient run the percentage of acetonitrile (containing 0.1% trifluoroacetic acid) was increased from an initial concentration of 0% at 0 min to 100% at 15 min and kept at 100% for 5 min. The injection volume was 10  $\mu\text{L}$ , and flow rate was set to 800  $\mu\text{L}/\text{min}$ . MS analysis was carried out at a spray voltage of 3800 V and a capillary temperature of 350 °C and a source CID of 10 V. Spectra were acquired in positive mode from 100 to 1000 m/z at 254 nm for the UV trace.

### **Synthesis and spectroscopic details.**

The synthesis of most of the 5-aryl-3-ureidothiophene-2-carboxylic acids (Scheme 2) started from readily available acetophenones (**I**) which were converted to the 5-aryl thiophene anthranilic acid methylesters (**II**) *via* an Arnold-Vilsmaier-Haack reaction followed by a cyclization using methylmercaptoacetate [31]. The esters (**II**) were then hydrolysed under basic conditions to afford the thiophene anthranilic acids (**III**) which

were converted into the thiaisatoic anhydrides (**IV**) [32,33]. The anhydrides (**IV**) were reacted with various amines giving rise to the 5-aryl-3-ureidothiophene-2-carboxylic acids (**V**) [34]. Further substituents at the 5-aryl ring were introduced using boronic acids or esters respectively *via* Suzuki coupling yielding **VI** [35].



**Scheme 2.** Synthesis of 5-aryl-3-ureidothiophene-2-carboxylic acids **V** or **VI** respectively. Reagents and conditions: (a) POCl<sub>3</sub>, DMF, 50 °C to rt, then NH<sub>2</sub>OH·HCl, up to 150 °C. (b) Methylthioglycolate, NaOMe, MeOH, reflux. (c) KOH, MeOH, THF, H<sub>2</sub>O, reflux. (d) COCl<sub>2</sub>, THF. (e) Amine, H<sub>2</sub>O, 100 °C then at 0 °C conc. HCl. (f) Na<sub>2</sub>CO<sub>3</sub>, Pd(PPh<sub>3</sub>)<sub>4</sub>, boronic acid or ester, THF, H<sub>2</sub>O, toluene, 80 °C.

Further details on the synthesis and spectroscopic data of final compounds and intermediates can be found in the supporting information.

## Biology

**General procedure for expression and purification of recombinant PqsD WT and R223A mutant in *E. coli*.** His<sub>6</sub>-tagged PqsD (H6-PqsD) and mutants were expressed in *E. coli* and purified using a single affinity chromatography step. Briefly, *E. coli* BL21 (λDE3) cells containing the pET28b(+)/pqsD (kindly provided by Prof. Rolf Müller, Helmholtz Institute for Pharmaceutical Research Saarland (HIPS), Saarbrücken, Germany) were grown in LB medium containing 50 µg/mL kanamycin at 37 °C to an OD<sub>600</sub> of approximately 0.8 units and induced with 0.2 mM IPTG for 16 h at 16 °C. The cells were harvested by centrifugation (5,000 rpm, 10 min, 4 °C) and the cell pellet was resuspended in 100 mL binding buffer (10 mM Na<sub>2</sub>HPO<sub>4</sub>, 2 mM KH<sub>2</sub>PO<sub>4</sub> pH 7.4, 3 mM KCl, 137 mM NaCl, 20 mM imidazole, 10% glycerol (v/v)) and lysed by sonication for a total process time of 2.5 min. Cell debris were removed by centrifugation (18500 rpm, 40 min, 4 °C) and the supernatant was filtered through a syringe filter (0.20 µm). The clarified lysate was immediately applied to a Ni-NTA column, washed with binding buffer and eluted with 500 mM imidazole. The protein

containing fractions were buffer-exchanged into 125 mM Na<sub>2</sub>HPO<sub>4</sub>, 50 mM KH<sub>2</sub>PO<sub>4</sub> pH 7.6, 50 mM NaCl, 10% glycerol (v/v), using a PD10 column and judged pure by SDS-PAGE analysis. Then protein was stored in aliquots at –80 °C.

**Screening assay procedure for *in vitro* PqsD inhibition** [20]. The assay was performed monitoring enzyme activity by measuring HHQ formed by condensation of anthraniloyl-CoA and β-ketodecanoic acid. The reaction mixture contained MOPS buffer (0.05 M, pH 7.0) with 0.005% (w/v) Triton X-100, 0.1 μM of the purified enzyme and inhibitor. The test compounds were dissolved in DMSO and diluted with buffer. The final DMSO concentration was 0.5%. After 10 min preincubation at 37 °C, the reaction was started by the addition anthraniloyl-CoA to a final concentration of 5 μM and β-ketodecanoic acid to a final concentration of 70 μM. Reactions were stopped by addition of MeOH containing 1 μM amitriptyline as internal standard for LC/MS-MS analysis. HHQ was quantified using a HPLC-MS/MS mass spectrometer (ThermoFisher, Dreieich, Germany) in ESI mode. Ionization of HHQ and the internal standard amitriptyline was optimized in each case. The solvent system consisted of 10 mM ammonium acetate (A) and acetonitrile (B), both containing 0.1% trifluoroacetic acid. The initial concentration of B in A was 45%, increasing the percentage of B to 100% in 2.8 min and keeping it at 98% for 0.7 min with a flow of 500 μL/min. The column used was a NUCLEODUR-C18, 100-3/125-3 (Macherey Nagel, Dühren, Germany). Control reactions without the inhibitor, but including identical amounts of DMSO, were performed in parallel and the amount of HHQ produced was set to 100%.

**Determination of extracellular HHQ and PQS levels.** For determination of extracellular levels of HHQ produced by PA14, cultivation was performed in the following way: cultures (initial OD<sub>600</sub> = 0.02) were incubated with or without inhibitor (final DMSO concentration 1%, v/v) at 37 °C, 200 rpm and a humidity of 75% for 16 h in 24-well Greiner BioOne (Frickenhausen, Germany) Cellstar plates containing 1.5 mL of LB medium per well. For HHQ analysis, according to the method of Lepine et al.,[36] 500 μL of the cultures supplemented with 50 μL of a 10 μM methanolic solution of the internal standard (IS) 5,6,7,8-tetradeutero-2-heptyl-4(1*H*)-quinolone (HHQ-d<sub>4</sub>) were extracted with 1 mL of ethyl acetate. After centrifugation (18,620 g, 12 min), 400 μL of the organic phase were evaporated to dryness and redissolved in methanol. UHPLC-MS/MS analysis was carried out as described in detail by Storz et

al.[19] The monitored ions were (mother ion [m/z], product ion [m/z], scan time [s], scan width [m/z], collision energy [V], tube lens offset [V]): HHQ: 244, 159, 0.5, 0.01, 30, 106; HHQ-d<sub>4</sub>(IS): 248, 163, 0.1, 0.01, 32, 113. For each sample, cultivation and sample work-up were performed in triplicates. Inhibition values of HHQ formation were normalized to OD<sub>600</sub>.

### Surface Plasmon Resonance

**General.** SPR binding studies were performed using a Reichert SR7500DC instrument optical biosensor (Reichert Technologies, Depew, NY, USA) and CMD500M sensor chips obtained from XanTec (XanTec Bioanalytics, Düsseldorf, Germany). Scrubber 2 software (Version 2.0c, 2008, BioLogic Software) was used for proceeding and analyzing the data. Changes in refractive index due to DMSO dependent solvent effects were corrected by use of a calibration curve (seven solutions, 4.25%–5.75% DMSO in buffer).

**Immobilization of His<sub>6</sub>-PqsD.** PqsD (38 kDA, >90% pure based on SDS-PAGE) was immobilized at an level of 5919 RU on a CMD500M (carboxymethyl-dextran-coated) sensor chip at 18 °C analogous to the method described by Henn et al. [37].

**Binding studies.** The ACoA preincubation studies were performed as previously described using a constant flow rate of 25 µL/min and HEPES buffer as instrument running buffer (10 mM HEPES, pH 7.4, 150 mM NaCl, 5% DMSO (v/v), 0.05% Polysorbat 20 (v/v)) [20]. ACoA (100 µM) was injected for approximately 40 minutes with a constant flow of 5 µL/min to reach saturation of the ACoA binding site. Afterwards, the flow rate was increased to 50 µL/min for 30 min in order to flush all CoA away. Once the baseline is stable again the compounds were consecutively injected and the responses at equilibrium were compared to those obtained with the untreated surface. Experiments were performed in duplicate. For **B** a concentration series of 250, 125 and 62.5 µM were used. Since stronger binding signal was observed for **21**, the concentration series was decreased to 100, 50 and 25 µM, whereas a series of 25, 12.5, and 6.25 µM was measured for **22**. The compounds were injected for 120 s association times and 300 s dissociation times.

## Computational Chemistry

**Docking.** Inhibitors were built in MOE. The receptor was derived from crystal structure of PqsD in complex with ACoA (PDB Code: 3H77)[10] The residuals of CoA, the covalently bound anthranilate and H<sub>2</sub>O were removed and Cys112 was restored considering its conformation in 3H76.[10] AutoDockTools V.1.5.6 was used to add polar hydrogens and to save the protein in the appropriate file format for docking with Vina. AutoDockVina was used for docking calculations.[38] The docking parameters were kept at their default values. The docking grid was sized 18 Å x 24 Å x 24 Å, covering the entire ACoA channel.

## Acknowledgments

The authors thank Carina Scheidt and Simone Amman for performing the *in vitro* tests. We also appreciate Patrick Fischer's help in performing the synthesis. Furthermore we thank Dr. Werner Tegge (Helmholtz Centre for Infection Research (HZI), Braunschweig, Germany) for kindly providing the cell penetrating peptide. J. Henning Sahner gratefully acknowledges a scholarship from the "Stiftung der Deutschen Wirtschaft" (SDW). This project was funded by BMBF through grant 1616038B.

## References

- [1] J. Davies, Bacteria on the rampage, *Nature* 383 (1996) 219–220.
- [2] C. Walsh, Molecular mechanisms that confer antibacterial drug resistance, *Nature* 406 (2000) 775–781.
- [3] J.-F. Dubern, S. P. Diggle, Quorum sensing by 2-alkyl-4-quinolones in *Pseudomonas aeruginosa* and other bacterial species, *Mol Biosyst.* 4, 882–888.
- [4] N. Bagge, O. Ciofu, L. T. Skovgaard, N. Høiby, Rapid development in vitro and in vivo of resistance to ceftazidime in biofilm-growing *Pseudomonas aeruginosa* due to chromosomal  $\beta$ -lactamase, *APMIS* 108 (2000) 589–600.
- [5] A. R. M. Coates, G. Halls, Y. Hu, Novel classes of antibiotics or more of the same?, *Brit. J. Pharmacol.* 163 (2011) 184–194.
- [6] F. von Nussbaum, M. Brands, B. Hinzen, S. Weigand, D. Haebich, Antibacterial natural products in medicinal chemistry - Exodus of revival?, *Angew. Chem. Int. Ed.* 45 (2006), 5072–5129.
- [7] For a recent review see: S. Scutera, M. Zucca, D. Savoia, Novel approaches for the design and discovery of quorum-sensing inhibitors, *Expert Opin. Drug. Discov.* 9 (2014), 353–366.
- [8] S. Swift, J. A. Downie, N. A. Whitehead, A. M. Barnard, G. P. Salmond, P. Williams, Quorum sensing as a population-density-dependent determinant of bacterial physiology, *Org. Biomol.*

Chem. 12 (2001) 6094–6104.

- [9] S. Diggle, P. Lumjiaktase, F. Dipilato, K. Winzer, M. Kunakorn, D. A. Barrett, S. R. Chhabra, M. Cámara, P. Williams, Functional genetic analysis reveals a 2-alkyl-4-quinolone signaling system in the human pathogen *Burkholderia pseudomallei* and related bacteria, *Chem. Biol.* 13 (2006) 701–710.
- [10] A. K. Bera, V. Atanasova, H. Robinson, E. Eisenstein, J. P. Coleman, E. C. Pesci, J. F. Parsons, Structure of PqsD, a *Pseudomonas* quinolone signal biosynthetic enzyme, in complex with anthranilate, *Biochemistry* 48 (2009) 8644–8655.
- [11] L. Yang, M. Nilsson, M. Gjermansen, M. Givskov, T. Toker-Nielsen, Pyoverdine and PQS mediated subpopulation interactions involved in *Pseudomonas aeruginosa* biofilm formation, *Mol. Microbiol.* 74 (2009) 1380–1392.
- [12] L. Gallagher, S. L. McKnight, M. S. Kuznetsova, E. C. Pesci, C. Manoil, Functions required for extracellular quinolone signaling by *Pseudomonas aeruginosa*, *J. Bacteriol.* 184 (2002) 6472–6480.
- [13] D. S. Wade, M. Worth Calfee, E. R. Rocha, E. A. Ling, E. Engstrom, J. P. Coleman, E. C. Pesci, Regulation of *Pseudomonas* quinolone signal synthesis in *Pseudomonas aeruginosa*, *J. Bacteriol.* 187 (2005) 4372–4380.
- [14] G. Xiao, E. Déziel, J. He, F. Lépine, B. Lesic, M.-H. Castonguay, S. Milot, A. P. Tampakaki, S. E. Stachel, L. G. Rahme, MvfR, a key *Pseudomonas aeruginosa* pathogenicity LTTR-class regulatory protein, has dual ligands, *Mol. Microbiol.* 62 (2006) 1689–1699.
- [15] A. Bandyopadhyaya, M. Kesarwani, Y.-A. Que, J. He, K. Padfield, R. Tompkins, L. G. Rahme, The quorum sensing volatile molecule 2-amino acetophenon modulates host immune response in a manner that promotes life with unwanted guests, *PLoS Pathog.* 8 (2012) p. e1003024.
- [16] K. Kim, Y. U. Kim, B. H. Koh, S. S. Hwang, S.-H. Kim, F. Lépine, Y.-H. Cho, G. R. Lee, HHQ and PQS, two *Pseudomonas aeruginosa* quorum-sensing molecules, down regulate the innate immune responses through the nuclear factor- $\kappa$ B pathway, *Immunology* 129 (2010) 578–588.
- [17] C. E. Dulcey, V. Dekimpe, D.-A. Fauvelle, S. Milot, M.-C. Groleau, N. Doucet, L. G. Rahme, F. Lépine, E. Déziel, The end of an old hypothesis: The *Pseudomonas* signaling molecules 4-hydroxy-2-alkylquinolines derive from fatty acids, not 3-ketofatty acids, *Chem. Biol.* 20 (2013) 1481–1491.
- [18] C. Lu, C. K. Maurer, B. Kirsch, A. Steinbach, R. W. Hartmann, Overcoming unexpected functional inversion of a PqsR antagonist in *Pseudomonas aeruginosa*: An in vivo potent antivirulence agent targeting pqs quorum sensing, *Angew. Chem. Int. Ed.* 53 (2014) 1109–1112.
- [19] M. P. Storz, C. K. Maurer, C. Zimmer, N. Wagner, C. Brengel, J. C. de Jong, S. Lucas, M. Müsken, S. Häussler, A. Steinbach, R. W. Hartmann, Validation of PqsD as an anti-biofilm target in *Pseudomonas aeruginosa* by development of small-molecule inhibitors, *J. Am. Chem. Soc.* 134 (2012) 16143–16146.
- [20] D. Pistorius, A. Ullrich, S. Lucas, R. W. Hartmann, U. Kazmaier, R. Müller, Biosynthesis of 2-

- alkyl-4(1H)-quinolones in *Pseudomonas aeruginosa*: Potential for therapeutic interference with pathogenicity, *ChemBioChem* 12 (2011) 850–853.
- [21] J. H. Sahner, C. Brengel, M. P. Storz, M. Groh, A. Plaza, R. Müller, R. W. Hartmann, Combining in silico and biophysical methods for the development of *Pseudomonas aeruginosa* quorum sensing inhibitors: An alternative approach for structure-based drug design, *J. Med. Chem.* 56 (2013) 8656–8664.
- [22] E. Weidel, J. C. de Jong, C. Brengel, M. P. Storz, A. Braunshausen, M. Negri, A. Plaza, A. Steinbach, R. Müller, R. W. Hartmann, Structure optimization of 2-Benzamidobenzoic acids as PqsD inhibitors for *Pseudomonas aeruginosa* infections and elucidation of binding mode by SPR, STD NMR, and molecular docking, *J. Med. Chem.* 56 (2013) 6146–6155.
- [23] M. Storz, G. Allegretta, B. Kirsch, M. Empting, R. W. Hartmann, From in vitro to in cellulo: structure-activity relationship of (2-nitrophenyl)methanol derivatives as inhibitors of PqsD in *Pseudomonas aeruginosa*, *Org. Biomol. Chem.* 12 (2014) 6094–6104.
- [24] M. Storz, C. Brengel, E. Weidel, M. Hoffmann, K. Hollemeyer, A. Steinbach, R. Müller, M. Empting, R. W. Hartmann, Biochemical and biophysical analysis of chiral PqsD inhibitor revealing tight-binding behavior and enantiomers with contrary thermodynamic signatures, *ACS Chem. Biol.* 8 (2013) 2794–2801.
- [25] S. Hinsberger, Johannes C. de Jong, M. Groh, J. Haupenthal, R. W. Hartmann, Benzamidobenzoic acids as potent PqsD inhibitors for the treatment of *Pseudomonas aeruginosa* infections, *Eur. J. Med. Chem.* 76 (2014) 343–351.
- [26] F. A. Cotton, V. W. Day, E. E. Hazen Jr., S. Larsen, S. T. K. Wong, Structure of bis(methylguanidinium) monohydrogen orthophosphate. A model for the arginine-phosphate interactions at the active site of staphylococcal nuclease and other phosphohydrolytic enzymes, *J. Am. Chem. Soc.* 96 (1974) 4471–4478.
- [27] A. S. Woods, S. Ferré, Amazing stability of the arginine-phosphate electrostatic interaction, *J. Proteom Res.* 4 (2005) 1397–1402.
- [28] H. Nikaido, E. Y. Rosenberg, J. Foulds, Porin channels in *Escherichia coli*: Studies with  $\beta$ -lactams in intact cells, *J. Bacteriol.* 153 (1983) 232–240.
- [29] F. Yoshimura, H. Nikaido, Diffusion of  $\beta$ -lactam antibiotics through the porin channels of *Escherichia coli* K-12, *Antimicrob. Agents Ch.* 27 (1985) 84–92.
- [30] A. Kirschning, F. Taft, T. Knobloch, Total synthesis approaches to natural product derivatives based on the combination of chemical synthesis and metabolic engineering, *Org. Biomol. Chem.* 5 (2007) 3245–3259.
- [31] H. Hartmann, J. Liebscher, A simple method for the synthesis of 5-aryl-3-amino-2-alkoxycarbonylthiophenes, *Synthesis* (1984) 275–276.
- [32] F. Fabis, S. Jolivet-Fouchet, M. Robba, H. Landelle, S. Rault, Thiaisatoic anhydrides: Efficient synthesis under microwave heating conditions and study of their reactivity, *Tetrahedron* 54 (1998) 10789–10800.
- [33] L. Foulon, E. Braud, F. Fabis, J.C. Lancelot, S. Rault, Synthesis and combinatorial approach of the reactivity of 6- and 7-arylthieno [3,2-d][1,3] oxazine-2,4-diones. *Tetrahedron* 59 (2003) 10051–10057.

- [34] F.X. Le Foulon, E. Braud, F. Fabis, J.C. Lancelot, S. Rault, Solution-phase parallel synthesis of a 1140-member ureidothiophene carboxylic acid library. *J. Comb. Chem.* 7 (2005) 253–257.
- [35] N. Miyaura, K. Yamada, A. Suzuki. A new stereospecific cross-coupling by palladium-catalyzed reaction of 1-alkenylboranes with 1-alkenyl or 1-alkynyl halides. *Tetrahedron Lett.* 20 (1979) 3437–3440.
- [36] F. Lépine, S. Milot, E. Déziel, J. He, L. G. Rahme, Electrospray/mass spectrometric identification and analysis of 4-hydroxy-2-alkylquinolines (HAQs) produced by *Pseudomonas aeruginosa*, *J. Am. Soc. Mass. Spectrom.* 15 (2004) 862–869.
- [36] F. Lépine, S. Milot, E. Déziel, J. He, L. G. Rahme, Electrospray/mass spectrometric identification and analysis of 4-hydroxy-2-alkylquinolines (HAQs) produced by *Pseudomonas aeruginosa*, *J. Am. Soc. Mass. Spectrom.* 15 (2004) 862–869.
- [37] C. Henn, S. Boettcher, A. Steinbach, R. W. Hartmann, Catalytic enzyme activity on a biosensor chip: Combination of surface plasmon resonance and mass spectrometry, *Anal. Biochem.* 428 (2012) 28–30.
- [38] O. Trott, A. J. Olson, AutoDock Vina: Improving the speed and accuracy of docking with a new scoring function, efficient optimization, and multithreading, *J. Comput. Chem.* 31 (2009) 455–461.

## 4 Final Discussion

As stated in chapter two, the prior goal of this thesis was the generation of anti-infectives with novel target sites and/or new mechanisms of action to overcome existing bacterial resistances. Measures of rational drug design should thereby guide the development process to systematically obtain potent chemical entities.

For the sake of clarity, the numbering of compounds was annotated with the letter of the respective manuscript from which it originates. For example: Compound “**3**” from manuscript **A** is termed “**A/3**” in the following paragraphs.

### 4.1 Structure activity relationships (SAR)

Deriving SAR from the biological data of a set of derivatives is the most important instrument in medicinal chemistry. It reveals the relationship between structural features and pharmacological activity for a series of derivatives [Wermuth et al. 1998] and thus, directs a rational drug optimization process.

#### 4.1.1 Small molecule RNAP inhibitors

Publication **A** deals with the development of small molecule inhibitors from the class of 5-aryl-3-ureidothiophene-2-carboxylic acids targeting the “switch region” of bacterial RNAP. The hit compound **A/3** ( $IC_{50} = 75 \mu M$ ) was found in a pharmacophore based virtual screening. The performed structural modifications can be divided into two parts (Fig. 12). First, the substitution pattern of the 5-aryl moiety was modified following the Topliss’ logical. Whereas the introduction of hydrophilic or electron donating groups (EDG) lead to reduced inhibitory potencies, lipophilic or electron withdrawing groups (EWG) caused constant to enhanced activities. The best results were obtained by the introduction of two lipophilic EWGs. To gain a deeper insight into the underlying principle of the substituent effects on the biological activity, a multi-parameter Hansch regression analysis was performed. The results impressively highlighted the relation between the two factors and underlined the importance of  $\pi$  (lipophilicity constant) and  $\sigma$  (Hammett parameter) for the biological activity. The obtained Hansch analysis represents a valuable support for further rational derivatization and should be considered in following optimization programs. The second part of publication **A** focused on the modification of the substituents at

the ureido motif at the opposite site of the molecule. Thereby space demanding lipophilic moieties were found to be favored in this position, which is in good agreement with the propagated docking pose that predicts this part of the molecule to reach into a rather large and hydrophobic part of the “switch region”.

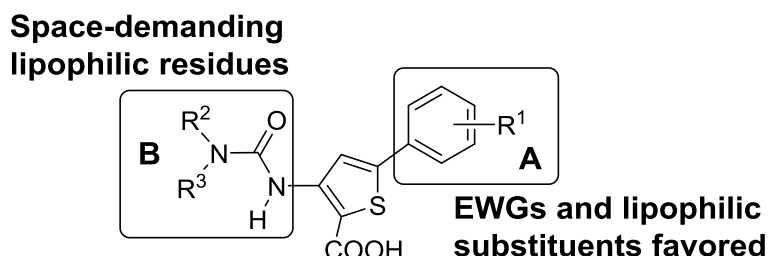


**Figure 12.** Summary of the observed SARs of small molecule RNAP inhibitors from the class of ureidothiophene-2-carboxylic acids.

#### 4.1.2 Myxopyronin derivatives *via* mutasynthesis

Publication **C** addresses the generation of novel **myx** derivatives using mutasynthesis as an alternative method to total synthesis. In this case, two kinds of structural requirements have to be taken into account. Besides the introduction of new substituents that can form further interactions with the RNAP “switch region”, the substrate specificity of the participating biosynthetic enzymes needs to be considered. Therefore, the design process of mutasynthons followed a two-step process, firstly evaluating the flexibility of the biosynthesis and secondly the targeted introduction of putative interaction partners.

In the beginning, the substrate specificity of MxnB, the ketosynthase which catalyzes the last step in the **myx** biosynthesis, was investigated. Starting with the natural precursor, functional groups were systematically removed to determine the key functions, decisive for substrate acceptance. The results revealed that MxnB is sensitive to modifications close to the molecular position at which the intermolecular Claisen condensation takes place. The  $\alpha$ -methyl group and the  $\alpha$ -double bond turned out to be essential for incorporation (Fig. 13). These findings were considered in the design process of all further precursors to maximize the probability of incorporation.

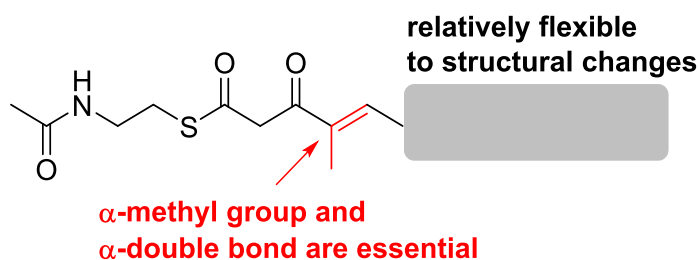


**Figure 13.** Basic structure of the applied  $\beta$ -keto thioester mutasynthons highlighting the functional groups, essential for incorporation by MxnB.

Afterwards functional groups were introduced into the precursors that should enable additional interactions of putative **myx** analogs with the RNAP “switch region”. Thereby the mentioned complex-crystal structure (PDB-ID: 3DXJ) was used to guide the design process. Initial investigations included the incorporation of a phenyl ring (**C/6–C/8**) at the end of the chain. Such an aromatic ring could serve as a platform for the introduction of various substituents that, if connected to the appropriate position, could form additional contacts with the protein and thus, increase the binding affinity. After successful incorporation of the phenyl containing substrates **C/6–C/8** by MxnB, this idea was successfully exemplified for a hydroxyl function (**C/9**) and a bromo-substituent (**C/10**), which were accepted as well. Moreover the short derivative **C/11** carrying an endstanding alkyne moiety, as well as a **cor** inspired hydroxylated precursor **C/12** were successfully incorporated. Further studies involved accession of the biosynthetic pathway at an earlier stage, using *M. fulvus* mutants whose western chain assembly line was interrupted by targeted point mutation. The design of the appropriate precursors (**C/13–C/18**) was guided by the established  $\beta$ -keto-substrates. Except for **C/15**, all substrates were successfully incorporated indicating that the other involved enzymes can also adapt to structural modifications of the biosynthetic intermediates.

In conclusion, high substrate flexibility is an essential requirement to enable the generation of comprehensive libraries by mutasynthesis. This is fulfilled by the investigated **myx** biosynthesis pathway. Whereas the substrate specificity of the biosynthetic enzymes could be elucidated, the SAR of the produced **myx** analogs remains theory until their successful isolation and biological evaluation.

### 4.1.3 Ureidothiophene-2-carboxylic acids as PqsD inhibitors

Publication **D** and **E** cover the development of potent PqsD inhibitors. **D/1** (= **A/9**) served as a starting point of this work, originating from the RNAP project presented in publication **A**. In accordance with the Hansch equation in **A**, **D/1** hardly inhibits RNAP. As a bactericidal effect is undesired while targeting the quorum sensing system, selectivity toward RNAP is a crucial prerequisite. Therefore the methoxy function was retained in favor of selectivity, even though other derivatives with for e.g. chloro substituents displayed better inhibitory potency against PqsD (compare Table S1 in the Supporting information of Publication **D** (section 6.4.2)). Molecular docking, complemented by competition SPR experiments delivered a reliable binding mode (compare section 4.2) that could be used to perform a structure-based optimization.

After validation of the binding mode, **D/2**, a truncated version of **D/1** was chosen as the starting point. Despite lower activity it bears comparable ligand efficiency to **D/1** while being more suitable for further modifications. According to the predicted binding mode, the ureido motif serves as an anchor, interacting with R223. This was verified by SPR studies with the R223A mutant. Subsequently  $\alpha$ -amino acids were introduced to target R262 with an additional carboxylic function and to extend the structure into a narrow sub-pocket at the entrance of the PqsD substrate channel. (*S*)-Phenylalanine (**D/6**) turned out to have the highest potential in this position. Molecular docking studies suggested a perfect fit of the benzyl moiety to the sub-pocket. Neither introduction of substituents at the phenyl ring (**E/2–E/4**), nor a variation of the linker-length (**E/5,E/6**) as well as its replacement by other residues (**E/7–E/11**) improved the inhibitory potency. The crucial role of the carboxylic group introduced with the amino acid is highlighted by **D/8**, lacking this group and consequently possessing 100 fold lower activity compared to **D/6**. Interestingly the (*R*)-configured derivatives (**D/9,D/10**) displayed approximately 50 fold weaker activity in favor of a selective interaction of the (*S*)-configured analogs.

The validated docking pose even enabled the rational design of a covalent inhibitor (**D/12**). As predicted, the targeted introduction of a  $\beta$ -chloroacetyl moiety allowed a nucleophilic attack by the key residue C112 (Fig. 14). A proposed interaction between the carboxylic acid function at the thiophene core and N254 was confirmed by the decarboxylated counterpart of **D/6**, **E/17**, displaying a 20 fold impaired  $IC_{50}$  value.

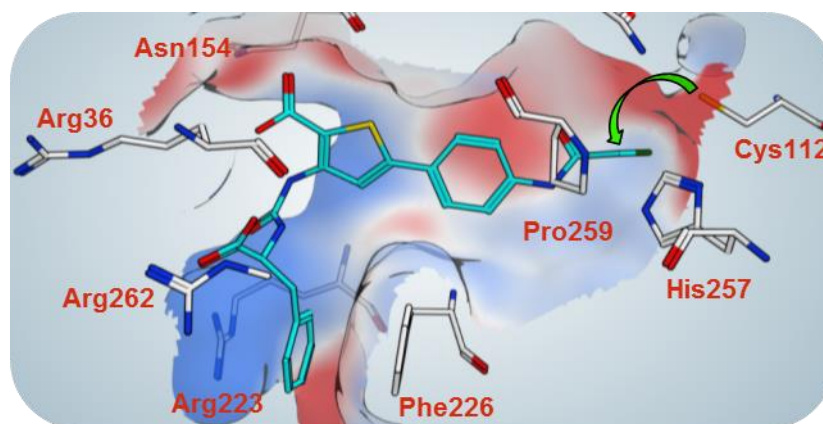


**Figure 14.** Illustration of the proposed binding mode of **D/12** based on the docking pose of **D/6**, highlighting the proposed attack of C112 at the  $\beta$ -chloroacetyl moiety.

Freezing the bioactive conformation is a widely used strategy in medicinal chemistry to increase the activity of drugs [Fang et al. 2014]. The underlying idea is to reduce the loss of entropy upon binding of the ligand. Therefore the rigidified analogs of **D/6**, **E/15** and **E/16** were investigated. Whereas the methylated compound **E/15** favors a perpendicular orientation of the 5'-ring to the thiophene core, the ethylene linker of **E/16** holds the two rings in one plain. The fact that both compounds display low activity permits two explanations. Either the appropriate conformation cannot be adopted by both, or the additional substituents cause sterical clashes with the protein. To draw a final conclusion, further rigidified derivatives need to be examined.

Further studies focused on the 5'-aryl-ring. Whereas removal of the methoxy group (**E/12**, **E/13**) was tolerated, omitting of the entire 5'-ring (**E/14**) lead to a complete loss of activity.

In order to gain further interactions, the structures of two inhibitor classes, namely the 2-nitrophenyl methanols [Storz et al. 2012, 2013, 2014] and the ureidothiophene-2-carboxylic acids [Sahner et al. 2013] were combined. SPR competition experiments allowed a determination of the overlapping contact sites of both classes. Following from these results, structural features of the 2-nitrophenyl methanol derivative (**E/D**) were stepwise attached to the 5'aryl ring of **E/13**. Introduction in *para* position (**E/20–E/22**) turned out to be superior compared to an attachment at the *meta* position (**E/18**, **E/19**). This can be explained by the shape of the narrow substrate

channel that necessitates a relatively straight or flexible ligand structure. Thus, the *meta*-substituted compounds are probably too strongly tilted to enter the binding site.

Taken together, investigations on the SAR in Publication **D** and **E** revealed, that nearly all structural features of **D/6** contribute to its biological activity. However, it is not clear yet whether they are the most favorable functional groups or if they can be bioisosterically replaced. Nevertheless, **D/6** establishes a solid basis for further modifications. **E/21** and **E/22** give a hint how additional interactions can be achieved to improve the affinity to the target protein.

## 4.2 Binding mode validation

Publications **A**, **B** and **D** describe distinct methods to validate the binding mode of the respective synthesized inhibitors. In case of the RNAP “switch region” inhibitors (Publication **A**), we decided to perform a chemically driven verification. The binding pose, predicted by molecular docking suggested a structure extension into the narrow channel representing the contact site of myxopyronin’s eastern chain. Therefore a moiety mimicking this part of **myx** was introduced at the appropriate position of the synthetic small molecule inhibitor. The fact that this dramatic structural change was tolerated and the resulting compound (**A/23**) displays increased activity compared to the parent compound **A/3**, is a strong hint, that the predicted binding mode is correct. Nevertheless, it cannot be excluded, that the additional substituent can form interactions at another part of the protein. Thus, such a chemically driven confirmation of the binding mode should ideally be complemented by generation and sequencing of spontaneous mutants or mutagenesis studies. Due to low solubility of **A/23** this was not possible in that particular case. In Publication **B**, competition STD NMR experiments unambiguously proved that **myx** and the ureidothiophene-2-carboxylic acids compete for the same binding site. Furthermore the results revealed that the ureidothiophenes are able to bind to the “switch region” in two reverse orientations and besides have a second target site on RNAP.

The binding mode of the PqsD inhibitors (Publication **D**) was verified using SPR. SPR is mainly used to assess the binding affinity of ligands to their respective targets. However, competition experiments involving ligands with known binding sites render it a powerful tool to determine the binding position of new molecules. Hence, 2-nitrophenyl methanol derivatives, known to bind deep inside the binding channel

interacting with the active site residues were used as competitors. Thereby the ureidothiophenes could be identified as channel blockers binding about 6 Å distant from the bottom of the binding pocket. The availability of model compounds, carrying different substitution pattern on both sites of the molecule, even enabled the determination of the ligand orientation inside the binding channel. These results served as cross-validation of several binding poses predicted by molecular docking studies.

In conclusion, combinations of biophysical experiments (NMR, SPR) complemented by docking studies are straightforward methods to elucidate the binding mode of a ligand. However, they cannot be used in every case, as ligands with known binding sites and a crystal structure of the protein are required, but not always available. Nevertheless, given that these requirements are fulfilled, the presented methods can pave the way for a structure-based design process, especially if co-crystallization efforts fail.

### 4.3 Intracellular activity

Sustainable permeation into the cell interior is a prerequisite for intracellular activity of anti-infectives. A study of O'Shea and Moser shows, that Gram negative bacteria are much more difficult to access than Gram positive cells, due to their orthogonal double membrane system and the equipment with broad spectrum efflux pumps [O'Shea and Moser 2008].

The results of this work clearly confirm these findings. The synthesized RNAP inhibitors (Publication **A** and **B**) exhibit potent antibacterial effects against the Gram positive pathogen *S. aureus* and *B. subtilis* (MIC values as low as 2 µg/mL). In contrast, the Gram negative wildtype strains *E. coli* K12 and *P. aeruginosa* were insusceptible regarding the applied inhibitors. Taking into consideration the low micromolar MIC values determined with *E.coli* TolC, efflux pumps might be a bottleneck for antibacterial activity of the novel compounds. Results from a continuative study corroborate this hypothesis as a combined application of the ureidothiophenes with the efflux pump inhibitor PAβN improved their antibacterial effects [Elgaher et al. 2013]. Besides potential efflux, the synthesized inhibitors do not meet the required physicochemical criteria. The majority of drugs entering Gram negative cells bear  $\text{clogD}_{7.4}$  values below 0. None of the compounds **A1–A/40**

reaches down to this region. Hence, if a Gram negative activity is desired, further structural variations leading to optimized physicochemical properties need to be accomplished. The latter is challenging taking into account the predominant lipophilic character of the RNAP “switch region”, limiting the introduction of hydrophilic moieties. Thus, even though the “switch region” is highly conserved among a wide range of bacteria, it might not be suitable for efficient antibiotics against Gram negative strains.

The PqsD inhibitors described in Publication **D** and **E** address a target in *P. aeruginosa* and can therefore only perform their task by reaching the cell interior. As these compounds are based on the RNAP inhibitors described above, structural changes accompanied by improved physicochemical properties are required to accomplish this goal. The replacement of *N*-ethyl-benzylamine by  $\alpha$ -amino acids contributed to both, decreasing the  $\text{clogD}_{7.4}$  to an acceptable range between  $-1.6$  and  $0.6$  (**D/4–D/6**). However, a reduction of HHQ levels in a whole cell assay could not be achieved. Even the introduction of moieties that are known to increase the permeation into Gram negative cells (for example a *N*-acetylcysteamine (NAC) thioester (**E/24**) or a cell penetrating peptide (**E/25**)), was not successful. These results lead to the hypothesis that the ureidothiophene core structure is responsible for the recognition and subsequent elimination by efflux pumps, a problem which can only be overcome by even more drastical structure variations or for example a combined application with efflux pump inhibitors.

## 4.4 Overcoming existing resistances

Rising emergence of bacterial resistances towards established antibiotics creates a continuous need for novel anti-infectives. Publication **A** addresses this task by the development of small molecule RNAP inhibitors that target the “switch region”, a so far underexploited binding site of this macromolecule. The “switch region” was unambiguously proven as a binding site of the obtained ureidothiophenes by competition STD and INPHARMA NMR experiments (publication **B**). The new inhibitors, display a  $>1500$  fold lower resistance frequency (exemplarily shown for compound **A/15**) as the clinically used rifampicin and the natural product **myx A**. This phenomenon can be explained by the fact that **A/15** occupies only a part of the binding pocket area that is covered by **myx**. Especially mutations in the narrow side pocket, contact site of the **myx** eastern chain and thus leading to **myx** resistance

[Mukhopadhyay et al. 2008, Srivastava et al. 2012], should not affect the antibacterial activity of our compounds. Another mechanism that can contribute to the low resistance frequency might be the effect on another target site. Results from an intrinsic fluorescence quenching assay corroborate this hypothesis showing a concentration dependent curve with a biphasic character (compare Figure S2b in supporting information of publication **B**) indicating a second binding site on RNAP.

In summary it can be stated that lower sensitivity of the new RNAP inhibitors to resistance development might be a significant advantage in daily clinical administration. Furthermore their potent antibacterial activity, especially against MRSA isolates and rifampicin resistant *E. coli* TolC strains, underscores their high potential for drug development.

## 4.5 Total/semi-synthesis vs. mutasynthesis

Publication **C** deals with the production of “unnatural, natural”  $\alpha$ -pyrone antibiotics using mutasynthesis. As stated in the introduction (paragraph 1.4), mutasynthesis can be a powerful alternative to total synthesis. However, its practicability as well as its efficiency should in each case be critically compared with approaches involving total- or semi-synthesis [Kirschning et al. 2007]. The first bottleneck, while aiming for the production of comprehensive libraries, might be a narrow substrate specificity of the involved biosynthetic enzymes. In the case of **myx**-derivatives this especially includes the ketosynthase MxnB, catalyzing the Claisen-condensation between the two independently assembled chains, yielding the characteristic  $\alpha$ -pyrone core. Several artificial  $\beta$ -keto thioester precursors with variations compared to the native substrate were accepted by MxnB, confirming that a wide range of structurally diverse **myx** analogs can be covered by mutasynthesis. Apparently only the  $\alpha$ -methyl group and the  $\alpha$ -double bond are essential for incorporation. Initial trials to isolate mutasynthesis products failed due to low yields. This hurdle has to be cleared to make mutasynthesis an efficient method that can compete with total synthesis of **myx** derivatives. E.g. expression of the biosynthesis pathway in a heterologous system, producing higher amounts of the desired derivatives, could be a solution. An alternative option is provided by an enzymatic *in vitro* synthesis of  $\alpha$ -pyrone-analogs, currently explored in our group [Sucipto and Sahner et al., manuscript in preparation]. Herein, two artificial chains (western and eastern) are connected by purified MxnB,

supplemented with the appropriate carrier proteins (CP). Making use of this method, a reduction of losses associated with the complicated isolation and purification processes one is facing during mutasynthesis can be achieved. Furthermore, given that the required enzymes can be obtained in good yields, the culture size is no longer a determinant for the outcome of the production.

## 4.6 Ureidothiophene-2-carboxylic acids

This thesis reports on ureidothiophene-2-carboxylic acids as inhibitors of the bacterial enzymes RNAP and PqsD. They excel by an established synthesis, allowing relatively easy modifications and thus, being interesting for medicinal chemistry approaches. As the name suggests, the compounds include a thiophene core, decorated with a carboxylic acid group in 2 and a ureido moiety in 3 position. Several reports in literature describe a very similar motif (substituted 2-aminothiophene-3-carbonyl) as a cause for promiscuous activity precluding selectivity [Baell and Holloway 2010, Soelaiman et al. 2003, Broom et al. 2006, Huth et al. 2005]. Both structural features only differ by the position of the sulfur inside the ring (Fig. 15). The close structural analogy suggests a similar behavior and thus promiscuity of the inhibitors developed in this work.

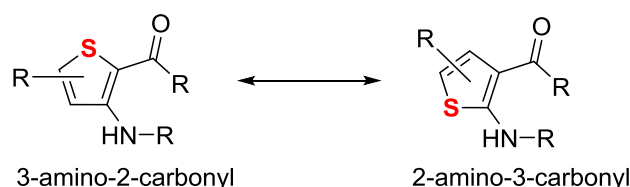


**Figure 15.** Comparison of a 3-amino-2-carbonyl thiophene with 2-amino-3-carbonyl thiophene illustrating their close structural relation.

The results in this thesis prove that it is absolutely possible to obtain selective inhibitors that feature a 3-amino-2-carbonyl-thiophene motif. It was clearly shown that RNAP inhibition can only be achieved if a 5'aryl substituent at the thiophene core is decorated with lipophilic EWGs. In contrast the PqsD inhibitor **D/1** is equipped with an electron donating methoxy functionality and consequently displays almost no RNAP inhibition (selectivity factor: 40). Furthermore, a very sharp SAR can be observed for the PqsD inhibitors themselves. Slight structural changes at the amino acid residue, not involving the thiophene core, cause a drastical reduction of the inhibitory potency.

Taken together, chemical entities comprising a thiophene core equipped with amino and carbonyl function might be at higher risk of being promiscuous binders. Nevertheless, selective inhibitors can be obtained by introduction of the appropriate substituents, ideally guided by structure-based design.

## 4.7 Summary and outlook

### 4.7.1 Small molecule RNAP inhibitors (Publication A and B)

Based on a virtual screening hit, ureidothiophenes-2-carboxylic acids have been discovered as potent “switch region” inhibitors of the bacterial RNAP. They excel at good bactericidal effects against Gram positive strains and the Gram negative efflux mutant *E. coli* TolC. Furthermore the novel inhibitors exhibit an outstandingly low resistance frequency compared to established antibiotics. Especially the most potent compound **A/40** is very lipophilic ( $\log P > 6$ ) and thus lacks drug-likeness and acceptable water solubility. The introduction of hydrophilic substituents is challenging due to the overall high lipophilicity of the “switch region”. However, some polar amino acids as well as accessible backbone atoms might be addressable, enabling the formation of additional interactions and improvement of the physicochemical properties.

An alternative strategy to achieve drug-likeness might be a prodrug-approach. The advantage of such an approach would be that it is independent from the active form of the inhibitor. Hence, a cleavable polar appendage could be attached to the most potent RNAP inhibitor **A/40** for example *via* an ester bond. Upon entrance into the cell it could be cleaved by a non-specific bacterial esterase to set the active form free.

### 4.7.2 “Unnatural natural” myx derivatives (Publication C)

Recently, the biosynthetic pathway of the natural  $\alpha$ -pyrone antibiotic **myx** has been elucidated [Sucipto et al. 2013]. The thereby obtained knowledge was used in this thesis to produce new **myx** analogs using a mutasynthesis approach (Publication C). Firstly, the substrate specificity of the involved biosynthetic enzymes was investigated and the essential structural features for successful precursor incorporation were determined. Taking these findings into consideration we proceeded with the investigation of structurally more diverse substrates. A crystal structure of *Th. thermophilus* RNAP in complex with **myx** (PDB-ID: 3DXJ) guided a

structure based introduction of further functional groups in order to form additional interactions. Moreover, chemical moieties were attached enabling synthetic modification of the novel **myx** analogs (Fig. 16). 15 out of a total of 18 examined precursors were incorporated, rendering mutasynthesis a serious alternative to total synthesis. Future studies might include even more chemically diverse precursors to expand the chemical space of the  $\alpha$ -pyrone antibiotics.

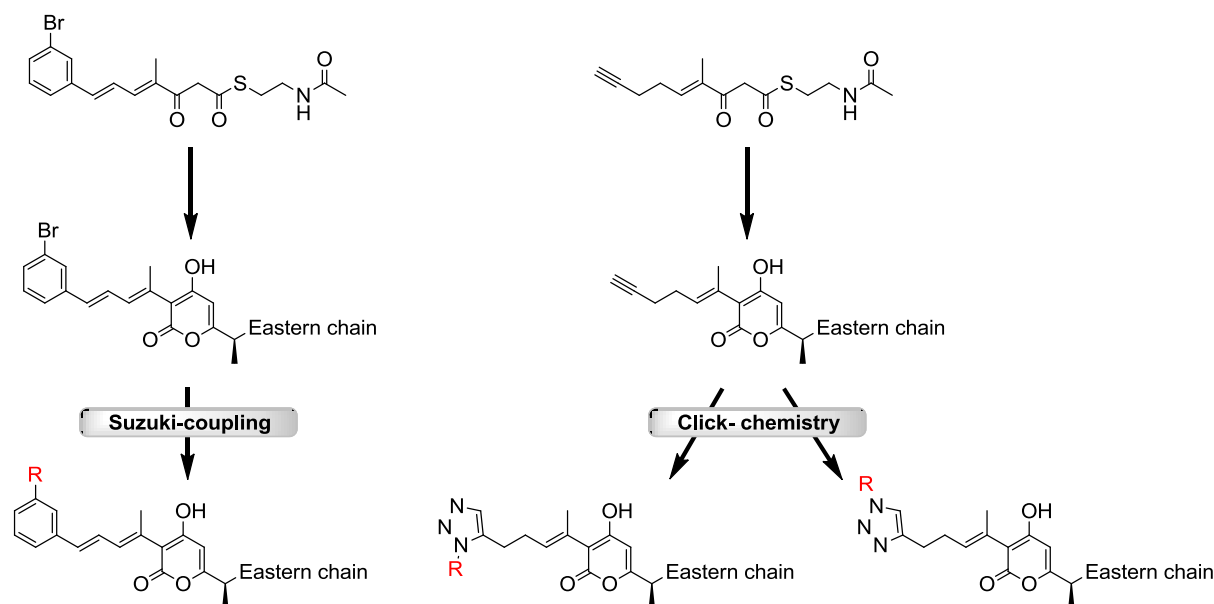


**Figure 16.** Proposal for synthetic modifications of the **myx** analogs **C/W10** and **C/W11**.

Initial trials to isolate the generated **myx** analogs produced by mutasynthesis, failed due to low production yields. This problem needs to be solved to enable isolation of sufficient amounts to determine biological activity and to derive further SAR. In terms of increasing the **myx** (derivative) production, heterologous expression of the biosynthetic gene cluster in a different strain and subsequent mutasynthesis, might be a promising approach. Another strategy could be a scale-up of the *in vitro* condensation experiment presented above (section 4.5). Being successful in expressing and purifying the required enzymes in large amounts, the enzymatic *in vitro* condensation represents an attractive alternative to mutasynthesis, as it is a rather clean process, decreasing yield losses associated with complex purification protocols.

### 4.7.3 PqsD inhibitors (Publication D and E)

In Publication **D**, compound **D/1** was identified as an inhibitor of the *P. aeruginosa* quorum sensing enzyme PqsD with moderate activity ( $IC_{50}$ : 6  $\mu$ M). Its stoichiometric binding to PqsD was confirmed using ITC. SPR competition experiments complemented by computational docking studies were used to determine the binding mode of **D/1**. The validated binding mode enabled a structure based optimization process yielding the potent PqsD inhibitor **D/6** with an  $IC_{50}$  value of 0.5  $\mu$ M. The accuracy of the determined binding mode was underlined by the targeted development of a covalent inhibitor (**D/12**) binding to the protein as predicted, proven by MALDI-ToF and HPLC-MS methods. In Publication **E**, the at that time most potent compound **D/6** (= **E/B**) was further investigated. The systematic design of novel inhibitors revealed the contribution and importance of nearly all of its functional groups. Furthermore, results from SPR competition experiments in combination with docking studies guided a successful merging of two inhibitor classes (Fig. 17). The resulting inhibitors (**E/21** and **E/22**) display higher activity ( $IC_{50}$ : 0.14 and 0.35  $\mu$ M) by profiting from the combined interactions with the protein. Even though being highly active in the cell free enzyme assay, none of the investigated PqsD inhibitors possessed intracellular potency. Several moieties were introduced into the molecule that should facilitate their permeation into *P. aeruginosa* cells but remained unsuccessful. Possible bottlenecks include the transmembrane permeation of the compounds themselves or efflux systems. Continuative studies should focus on solving this problem for example by applying the inhibitors in combination with efflux pump inhibitors.

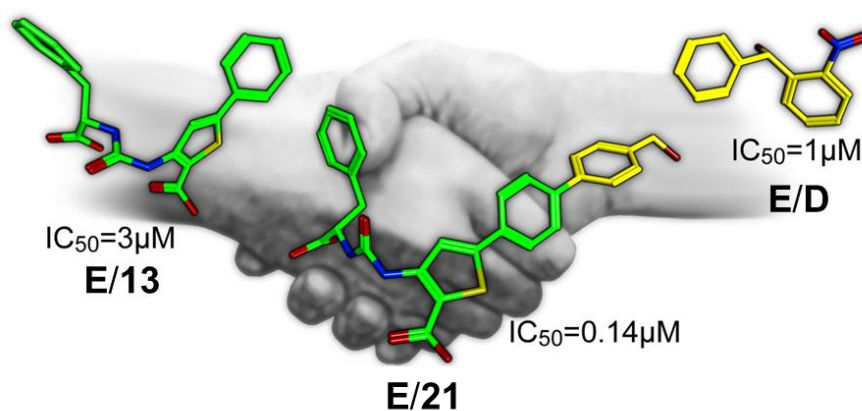


**Figure 17:** Illustration of the merging of two PqsD inhibitor classes. The resulting compound **E/21** contains features of both classes and displays increased inhibitory potency.

## 5 References

- Aloush, V., Navon-Venezia, S., Seigman-Igra, Y., Cabili, S., and Carmeli, Y. (2006). Multidrug-resistant *Pseudomonas aeruginosa*: risk factors and clinical impact. *Antimicrob. Agents Chemother.* **50**, 43–48.
- Anderson, N.G. (2012). *Practical process research and development – A guide for organic chemists* (Oxford, UK: Academic Press).
- Artsimovitch, I., Seddon, J., and Sears, P. (2012). Fidaxomicin is an inhibitor of the initiation of bacterial RNA synthesis. *Clin. Inf. Dis.* **55**, Supplement article S127–S131.
- Artsimovitch, I., Vassilyeva, M.N., Svetlov, D., Svetlov, V., Perederina, A., Igarashi, N., Matsugaki, N., Wakatsuki, S., Tahirov, T.H., and Vassilyev, D.G. (2005). Allosteric modulation of the RNA polymerase catalytic reaction is an essential component of transcription control by rifamycins. *Cell* **122**, 351–363.
- Austin, M.B., and Noel, J.P. (2003). The chalcone synthase superfamily of type III polyketide synthases. *Nat. Prod. Rep.* **20**, 79–110.
- Baell, J.B., and Holloway, G.A. (2010). New substructure filters for removal of pan assay interference compounds (PAINS) from screening libraries and for their exclusion in bioassays. *J. Med. Chem.* **53**, 2719–2740.
- Bandyopadhyaya, A., Kesarwani, M., Que, Y.-A., He, J., Padfield, K., Tompkins, R., and Rahme, L.G. (2012). The quorum sensing volatile molecule 2-amino acetophenon modulates host immune responses in a manner that promotes life with unwanted guests. *PLoS Pathog* **8**, e1003024.
- Baquero, F. (1997). Gram-positive resistance: challenge for the development of new antibiotics. *J. Antimicrob. Chemother.* **39** Suppl A, 1–6.
- Bera, A.K., Atanasova, V., Robinson, H., Eisenstein, E., Coleman, J.P., Pesci, E.C., and Parsons, J.F. (2009). Structure of PqsD, a *Pseudomonas* quinolone signal biosynthetic enzyme, in complex with anthranilate. *Biochemistry* **48**, 8644–8655.
- Bjarnsholt, T., Tolker-Nielsen, T., Høiby, N., and Givskov, M. (2010). Interference of *Pseudomonas aeruginosa* signalling and biofilm formation for infection control. *Expert Rev. Mol. Med.* **12**, e11.
- Bodey, G.P., Bolivar, R., Fainstein, V., and Jadeja, L. (1983). Infections caused by *Pseudomonas aeruginosa*. *Clin. Infect. Dis.* **5**, 279–313.
- Broom, W.J., Auwarter, K.E., Ni, J., Russel, D.E., Yeh, L.-A., Maxwell, M.M., Glicksman, M., Kazantsev, A.G., and Brown, R.H. (2006). Two approaches to drug discovery in SOD1-mediated ALS. *J. Biomol. Screen.* **11**, 729–735.
- Brueckner, F., and Cramer, P. (2008). Structural basis of transcription inhibition by  $\alpha$ -amanitin and implications for RNA polymerase II translocation. *Nat. Struct. Mol. Biol.* **15**, 811–818.
- Buurman, E.T., Foulk, M.A., Gao, N., Laganas, V.A., McKinney, D.C., Moustakas, D.T., Rose, J.A., Shapiro, A.B., and Fleming, P.R. (2012). Novel rapidly diversifiable antimicrobial RNA polymerase switch region inhibitors with confirmed mode of action in *Haemophilus influenzae*. *J. Bacteriol.* **194**, 5504–5512.
- Campbell, E.A., Korzheva, N., Mustaev, A., Murakami, K., Nair, S., Goldfarb, A., and Darst, S.A. (2001). Structural mechanism for rifampicin inhibition of bacterial RNA polymerase. *Cell* **104**, 901–912.
- Chopra, I. (2007). Bacterial RNA polymerase: a promising target for the discovery of new antimicrobial agents. *Curr. Opin. Investig. Drugs* **8**, 600–607.

- Coleman, J.P., Hudson, L.L., McKnight, S.L., Farrow, J.M., Calfee, M.W., Lindsey, C.A., and Pesci, E.C. (2008). *Pseudomonas aeruginosa* PqsA is an anthranilate-coenzyme A ligase. *J. Bacteriol.* *190*, 1247–1255.
- Comas, I., Borrell, S., Roetzer, A., Rose, G., Malla, B., Kato-Maeda, M., Galagan, J., Niemann, S., and Gagneux, S. (2011). Whole-genome sequencing of rifampicin-resistant *Mycobacterium tuberculosis* strains identifies compensatory mutations in RNA polymerase genes. *Nat. Genet.* *44*, 106–110.
- Cooper, M.A. (2002). Optical biosensors in drug discovery. *Nat. Rev. Drug. Discov.* *1*, 515–528.
- Costerton, J.W., Stewart, P.S., and Greenberg, E.P. (1999). Bacterial biofilms: a common cause of persistent infections. *Science* *284*, 1318–1322.
- Cramer, R.D., Patterson, D.E., and Bunce, J.D. (1988). Comparative molecular field analysis (CoMFA). 1. Effect of shape on binding of steroids to carrier proteins. *J. Am. Chem. Soc.* *110*, 5959–5967.
- Dalton, T., Cegielski, P., Akksilp, S., Asencios, L., Campos Caoili, J., Cho, S.-N., Erokhin, V.V., Ershova, J., Gler, M.T., Kazenny, B.Y., et al. (2012). Prevalence of and risk factors for resistance to second-line drugs in people with multidrug-resistant tuberculosis in eight countries: a prospective cohort study. *Lancet* *380*, 1406–1417.
- Darst, S.A. (2004). New inhibitors targeting bacterial RNA polymerase. *Trends Biochem. Sci.* *29*, 159–160.
- Davies, C., Heath, R.J., White, S.W., and Rock, C.O. (2000). The 1.8 Å crystal structure and active-site architecture of beta-ketoacyl-acyl carrier protein synthase III (FabH) from *Escherichia coli*. *Structure* *8*, 185–195.
- Davies, J., and Davies, D. (2010). Origins and evolution of antibiotic resistance. *Microbiol. Mol. Biol. Rev.* *74*, 417–433.
- de Bentzmann, S., and Plésiat, P. (2011). The *Pseudomonas aeruginosa* opportunistic pathogen and human infections. *Environ. Microbiol.* *13*, 1655–1665.
- Defoirdt, T., Boon, N., and Bossier, P. (2010). Can bacteria evolve resistance to quorum sensing disruption? *PLoS Pathog* *6*, e1000989.
- Déziel, E., Lépine, F., Milot, S., He, J., Mindrinos, M.N., Tompkins, R.G., and Rahme, L.G. (2004). Analysis of *Pseudomonas aeruginosa* 4-hydroxy-2-alkylquinolines (HAQs) reveals a role for 4-hydroxy-2-heptylquinoline in cell-to-cell communication. *P. Natl. Acad. Sci. USA.* *101*, 1339–1344.
- Diggle, S.P., Lumjiaktase, P., Dipilato, F., Winzer, K., Kunakorn, M., Barrett, D.A., Chhabra, S.R., Cámara, M., and Williams, P. (2006). Functional genetic analysis reveals a 2-Alkyl-4-quinolone signaling system in the human pathogen *Burkholderia pseudomallei* and related bacteria. *Chem. Biol.* *13*, 701–710.
- Diggle, S.P., Matthijs, S., Wright, V.J., Fletcher, M.P., Chhabra, S.R., Lamont, I.L., Kong, X., Hider, R.C., Cornelis, P., Cámara, M., et al. (2007). The *Pseudomonas aeruginosa* 4-quinolone signal molecules HHQ and PQS play multifunctional roles in quorum sensing and iron entrapment. *Chem. Biol.* *14*, 87–96.
- Diggle, S.P., Winzer, K., Chhabra, S.R., Worrall, K.E., Cámara, M., and Williams, P. (2003). The *Pseudomonas aeruginosa* quinolone signal molecule overcomes the cell density-dependency of the quorum sensing hierarchy, regulates rhl-dependent genes at the onset of stationary phase and can be produced in the absence of LasR. *Mol. Microbiol.* *50*, 29–43.
- Driffield, K., Miller, K., Bostock, J.M., O'Neill, A.J., and Chopra, I. (2008). Increased mutability of *Pseudomonas aeruginosa* in biofilms. *J. Antimicrob. Chemoth.* *61*, 1053–1056.
- Dubern, J.-F., and Diggle, S.P. (2008). Quorum sensing by 2-alkyl-4-quinolones in

*Pseudomonas aeruginosa* and other bacterial species. *Mol. Biosyst.* **4**, 882–888.

Dulcey, C.E., Dekimpe, V., Fauvelle, D.-A., Milot, S., Groleau, M.-C., Doucet, N., Rahme, L.G., Lépine, F., and Déziel, E. (2013). The end of an old hypothesis: the *Pseudomonas* signaling molecules 4-hydroxy-2-alkylquinolines derive from fatty acids, not 3-ketofatty acids. *Chem. Biol.* **20**, 1481–1491.

Dutton, C.J., Gibson, S.P., Goudie, A.C., Holdom, K.S., Pacey, M.S., Ruddock, J.C., Bu'Lock, J.D., and Richards, M.K. (1991). Novel avermectins produced by mutational biosynthesis. *J. Antibiot.* **44**, 357–365.

Ebright, R.H. (2000). RNA polymerase: structural similarities between bacterial RNA polymerase and eukaryotic RNA polymerase II. *J. Mol. Biol.* **304**, 687–698.

Elgaher, W.A.M., Fruth, M., Groh, M., Hauptenthal, J., and Hartmann, R.W. (2013). Expanding the scaffold for bacterial RNA polymerase inhibitors: design, synthesis and structure–activity relationships of ureido-heterocyclic-carboxylic acids. *R. Soc. Chem. Adv.* **4**, 2177–2194.

Erol, O., Schäberle, T.F., Schmitz, A., Rachid, S., Gurgui, C., Omari, El, M., Lohr, F., Kehraus, S., Piel, J., Müller, R., et al. (2010). Biosynthesis of the myxobacterial antibiotic coralopyronin A. *ChemBioChem* **11**, 1253–1265.

Fang, Z., Song, Y., Zhan, P., Zhang, Q., and Liu, X. (2014). Conformational restriction: an effective tactic in “follow-on-”based drug discovery. *Future Med. Chem.* **6**, 885–901.

Farrow, J.M., Sund, Z.M., Ellison, M.L., Wade, D.S., Coleman, J.P., and Pesci, E.C. (2008). PqsE functions independently of PqsR-*Pseudomonas* quinolone signal and enhances the rhl quorum-sensing system. *J. Bacteriol.* **190**, 7043–7051.

Federle, M.J., and Bassler, B.L. (2003). Interspecies communication in bacteria. *J. Clin. Invest.* **112**, 1291–1299.

Gallagher, L.A., McKnight, S.L., Kuznetsova, M.S., Pesci, E.C., and Manoil, C. (2002). Functions required for extracellular quinolone signaling by *Pseudomonas aeruginosa*. *J. Bacteriol.* **184**, 6472–6480.

Gambello, M.J., and Iglewski, B.H. (1991). Cloning and characterization of the *Pseudomonas aeruginosa* lasR gene, a transcriptional activator of elastase expression. *J. Bacteriol.* **173**, 3000–3009.

Gregory, M.A., Petkovic, H., Lill, R.E., Moss, S.J., Wilkinson, B., Gaisser, S., Leadlay, P.F., and Sheridan, R.M. (2005). Mutasynthesis of rapamycin analogues through the manipulation of a gene governing starter unit biosynthesis. *Angew. Chem. Int. Ed.* **44**, 4757–4760.

Grond, S., Papastavrou, I., and Zeeck, A. (2000). Structural diversity of 1-O-acyl  $\alpha$ -L-rhamnopyranosides by precursor-directed biosynthesis with *Streptomyces griseoviridis*. *Eur. J. Org. Chem.* **2000**, 1875–1881.

Grundmann, H., Aires-de-Sousa, M., Boyce, J., and Tiemersma, E. (2006). Emergence and resurgence of meticillin-resistant *Staphylococcus aureus* as a public-health threat. *Lancet* **368**, 874–885.

Haebich, D., and Nussbaum, von, F. (2009). Lost in transcription--inhibition of RNA polymerase. *Angew. Chem. Int. Ed.* **48**, 3397–3400.

Hansch, C. (1969). Quantitative approach to biochemical structure-activity relationships. *Acc. Chem. Res.* **2**, 232–239.

Hansch, C., Maloney, P.P., Fujita, T., and Muir, R.M. (1962). Correlation of biological activity of phenoxyacetic acids with Hammett substituent constants and partition coefficients. *Nature* **194**, 178–180.

Heeb, S., Fletcher, M.P., Chhabra, S.R., Diggle, S.P., Williams, P., and Cámara, M. (2011).

Quinolones: from antibiotics to autoinducers. *FEMS Microbiol. Rev.* **35**, 247–274.

Hentzer, M., Riedel, K., Rasmussen, T.B., Heydorn, A., Andersen, J.B., Parsek, M.R., Rice, S.A., Eberl, L., Molin, S., Høiby, N., et al. (2002). Inhibition of quorum sensing in *Pseudomonas aeruginosa* biofilm bacteria by a halogenated furanone compound. *Microbiology* **148**, 87–102.

Hentzer, M., Wu, H., Andersen, J.B., Riedel, K., Rasmussen, T.B., Bagge, N., Kumar, N., Schembri, M.A., Song, Z., Kristoffersen, P., et al. (2003). Attenuation of *Pseudomonas aeruginosa* virulence by quorum sensing inhibitors. *EMBO J.* **22**, 3803–3815.

Huth, J.R., Mendoza, R., Olejniczak, E.T., Johnson, R.W., Cothron, D.A., Liu, Y., Lerner, C.G., Chen, J., and Hajduk, P.J. (2005). ALARM NMR: a rapid and robust experimental method to detect reactive false positives in biochemical screens. *J. Am. Chem. Soc.* **127**, 217–224.

Høiby, N., Bjarnsholt, T., Givskov, M., Molin, S., and Ciofu, O. (2010). Antibiotic resistance of bacterial biofilms. *Int. J. Antimicrob. Agents* **35**, 322–332.

Irschik, H., Gerth, K., Höfle, G., Kohl, W., and Reichenbach, H. (1983). The myxopyronins, new inhibitors of bacterial RNA synthesis from *Myxococcus fulvus* (Myxobacterales). *J. Antibiot.* **36**, 1651–1658.

Irschik, H., Jansen, R., Höfle, G., Gerth, K., and Reichenbach, H. (1985). The coralopyronins, new inhibitors of bacterial RNA synthesis from Myxobacteria. *J. Antibiot.* **38**, 145–152.

Jakobsen, T.H., Bjarnsholt, T., Jensen, P.Ø., Givskov, M., and Høiby, N. (2013). Targeting quorum sensing in *Pseudomonas aeruginosa* biofilms: current and emerging inhibitors. *Future Microbiol.* **8**, 901–921.

Kalia, V.C., and Purohit, H.J. (2011). Quenching the quorum sensing system: potential antibacterial drug targets. *Crit. Rev. Microbiol.* **37**, 121–140.

Kaul, P.N. (1998). Drug discovery: past, present and future. *Prog. Drug Res.* **50**, 9–105.

Kennedy, J. (2008). Mutasynthesis, chemobiosynthesis, and back to semi-synthesis: combining synthetic chemistry and biosynthetic engineering for diversifying natural products. *Nat. Prod. Rep.* **25**, 25–34.

Kesarwani, M., Hazan, R., He, J., Que, Y.-A., Que, Y., Apidianakis, Y., Lesic, B., Xiao, G., Dekimpe, V., Milot, S., et al. (2011). A quorum sensing regulated small volatile molecule reduces acute virulence and promotes chronic infection phenotypes. *PLoS Pathog* **7**, e1002192.

Khan, N.H., Ahsan, M., Taylor, W.D., and Kogure, K. (2010). Culturability and survival of marine, freshwater and clinical *Pseudomonas aeruginosa*. *Microbes. Environ.* **25**, 266–274.

Kim, K., Kim, Y.U., Koh, B.H., Hwang, S.S., Kim, S.-H., Lépine, F., Cho, Y.-H., and Lee, G.R. (2010). HHQ and PQS, two *Pseudomonas aeruginosa* quorum-sensing molecules, down-regulate the innate immune responses through the nuclear factor-kappaB pathway. *Immunology* **129**, 578–588.

Kirschning, A., Taft, F., and Knobloch, T. (2007). Total synthesis approaches to natural product derivatives based on the combination of chemical synthesis and metabolic engineering. *Org. Biomol. Chem.* **5**, 3245–3259.

Klein, T., Henn, C., de Jong, J.C., Zimmer, C., Kirsch, B., Maurer, C.K., Pistorius, D., Müller, R., Steinbach, A., and Hartmann, R.W. (2012). Identification of small-molecule antagonists of the *Pseudomonas aeruginosa* transcriptional regulator PqsR: biophysically guided hit discovery and optimization. *ACS Chem. Biol.* **7**, 1496–1501.

Kohl, W., Irschik, H., and Reichenbach, H. (1983). Antibiotika aus gleitenden Bakterien, XVII. Myxopyronin A und B – zwei neue Antibiotika aus *Myxococcus fulvus* Stamm Mx f50. *Liebigs Ann. Chem.* 1656–1667.

- Kurabachew, M., Lu, S.H.J., Krastel, P., Schmitt, E.K., Suresh, B.L., Goh, A., Knox, J.E., Ma, N.L., Jiricek, J., Beer, D., et al. (2008). Lipiarmycin targets RNA polymerase and has good activity against multidrug-resistant strains of *Mycobacterium tuberculosis*. *J. Antimicrob. Chemoth.* **62**, 713–719.
- Ladbury, J.E. (2010). Calorimetry as a tool for understanding biomolecular interactions and an aid to drug design. *Biochem. Soc. T.* **38**, 888–893.
- Leeb, M. (2004). Antibiotics: a shot in the arm. *Nature* **431**, 892–893.
- Lépine, F., Milot, S., Déziel, E., He, J., and Rahme, L.G. (2004). Electrospray/mass spectrometric identification and analysis of 4-hydroxy-2-alkylquinolines (HAQs) produced by *Pseudomonas aeruginosa*. *J. Am. Soc. Mass Spectr.* **15**, 862–869.
- Lu, C., Maurer, C.K., Kirsch, B., and Steinbach, A. (2014). Overcoming the unexpected functional inversion of a PqsR antagonist in *Pseudomonas aeruginosa*: an *in vivo* potent antivirulence agent targeting pqs quorum sensing. *Angew. Chem. Int. Ed.* **126**, 1127–1130.
- Lu, C., Kirsch, B., Zimmer, C., de Jong, J.C., Henn, C., Maurer, C.K., Müsken, M., Häussler, S., Steinbach, A., and Hartmann, R.W. (2012). Discovery of antagonists of PqsR, a key player in 2-alkyl-4-quinolone-dependent quorum sensing in *Pseudomonas aeruginosa*. *Chem. Biol.* **19**, 381–390.
- Machan, Z.A., Taylor, G.W., Pitt, T.L., Cole, P.J., and Wilson, R. (1992). 2-Heptyl-4-hydroxyquinoline N-oxide, an antistaphylococcal agent produced by *Pseudomonas aeruginosa*. *J. Antimicrob. Chemoth.* **30**, 615–623.
- Maeda, T., García-Contreras, R., Pu, M., Sheng, L., Garcia, L.R., Tomás, M., and Wood, T.K. (2012). Quorum quenching quandary: resistance to antivirulence compounds. *ISME J.* **6**, 493–501.
- Marshall, G.R., Barry, C.D., Bosshard, H.E., Dammkoehler, R.A., Dunn, D., (1979). The Conformational parameter in drug design: the active analog approach. American Chemical Society, Washington D.C. **112**, 205–226.
- Masuda, N., Sakagawa, E., Ohya, S., Gotoh, N., Tsujimoto, H., and Nishino, T. (2000). Substrate specificities of MexAB-OprM, MexCD-OprJ, and MexXY-oprM efflux pumps in *Pseudomonas aeruginosa*. *Antimicrob. Agents Chemother.* **44**, 3322–3327.
- Mavromoustakos, T., Durdagi, S., Koukoulitsa, C., Simcic, M., Papadopoulos, M.G., Hodoscek, M., and Grdadolnik, S.G. (2011). Strategies in the rational drug design. *Curr. Med. Chem.* **18**, 2517–2530.
- Mayer, M., and Meyer, B. (1999). Characterization of ligand binding by saturation transfer difference NMR spectroscopy. *Angew. Chem. Int. Ed.* **38**, 1784–1788.
- McPhillie, M.J., Trowbridge, R., Mariner, K.R., O'Neill, A.J., Johnson, A.P., Chopra, I., and Fishwick, C.W.G. (2011). Structure-based ligand design of novel bacterial RNA polymerase inhibitors. *ACS Med. Chem. Lett.* **2**, 729–734.
- Miller, M.B., and Bassler, B.L. (2001). Quorum sensing in bacteria. *55*, 165–199.
- Molin, S., and Tolker-Nielsen, T. (2003). Gene transfer occurs with enhanced efficiency in biofilms and induces enhanced stabilisation of the biofilm structure. *Curr. Opin. Biotech.* **14**, 255–261.
- Mukhopadhyay, J., Das, K., Ismail, S., Koppstein, D., Jang, M., Hudson, B., Sarafianos, S., Tuske, S., Patel, J., Jansen, R., et al. (2008). The RNA polymerase “switch region” is a target for inhibitors. *Cell* **135**, 295–307.
- Müh, U., Schuster, M., Heim, R., Singh, A., Olson, E.R., and Greenberg, E.P. (2006). Novel *Pseudomonas aeruginosa* quorum-sensing inhibitors identified in an ultra-high-throughput screen. *Antimicrob. Agents Chemother.* **50**, 3674–3679.
- Newman, D.J., Cragg, G.M., and Snader, K.M. (2003). Natural products as sources of new drugs over the period 1981-2002. *J. Nat. Prod.* **66**, 1022–1037.

- Njoroge, J., and Sperandio, V. (2009). Jamming bacterial communication: new approaches for the treatment of infectious diseases. *EMBO Mol. Med.* *1*, 201–210.
- Nussbaum, von, F., Brands, M., and Hinzen, B. (2006). Antibacterial Natural Products in Medicinal Chemistry—Exodus or Revival? *Angew. Chem. Int. Ed.* *45*, 5072–5129.
- O'Connell, K.M.G., Hodgkinson, J.T., Sore, H.F., Welch, M., Salmond, G.P.C., and Spring, D.R. (2013). Combating multidrug-resistant bacteria: current strategies for the discovery of novel antibacterials. *Angew. Chem. Int. Ed.* *52*, 10706–10733.
- Ochsner, U.A., and Reiser, J. (1995). Autoinducer-mediated regulation of rhamnolipid biosurfactant synthesis in *Pseudomonas aeruginosa*. *P. Natl. Acad. Sci. USA.* *92*, 6424–6428.
- Ochsner, U.A., Koch, A.K., Fiechter, A., and Reiser, J. (1994). Isolation and characterization of a regulatory gene affecting rhamnolipid biosurfactant synthesis in *Pseudomonas aeruginosa*. *J. Bacteriol.* *176*, 2044–2054.
- O'Shea, R., and Moser, H.E. (2008). Physicochemical properties of antibacterial compounds: implications for drug discovery. *J. Med. Chem.* *51*, 2871–2878.
- Passador, L., Cook, J.M., Gambello, M.J., Rust, L., and Iglewski, B.H. (1993). Expression of *Pseudomonas aeruginosa* virulence genes requires cell-to-cell communication. *Science* *260*, 1127–1130.
- Pesci, E.C., Milbank, J.B., Pearson, J.P., McKnight, S., Kende, A.S., Greenberg, E.P., and Iglewski, B.H. (1999). Quinolone signaling in the cell-to-cell communication system of *Pseudomonas aeruginosa*. *P. Natl. Acad. Sci. USA.* *96*, 11229–11234.
- Pistorius, D., Ullrich, A., Lucas, S., Hartmann, R.W., Kazmaier, U., and Müller, R. (2011). Biosynthesis of 2-Alkyl-4(1H)-quinolones in *Pseudomonas aeruginosa*: potential for therapeutic interference with pathogenicity. *ChemBioChem* *12*, 850–853.
- Podlogar, B.L., and Ferguson, D.M. (2000). QSAR and CoMFA: a perspective on the practical application to drug discovery. *Drug Des. Discov.* *17*, 4–12.
- Prusov, E.V. (2013). Total synthesis of antibiotics: recent achievements, limitations, and perspectives. *Appl. Microbiol. Biot.* *97*, 2773–2795.
- Rampioni, G., Pustelny, C., and Fletcher, M.P. (2010). Transcriptomic analysis reveals a global alkyl-quinolone-independent regulatory role for PqsE in facilitating the environmental adaptation of *Pseudomonas aeruginosa* to plant and animal hosts. *Environ. Microbiol.* *12*, 1659–1673.
- Reddy M.R. and Parrill, A.L. (1999). Overview of Rational Drug Design. American Chemical Society, Washington D.C. *719*, 1–11.
- Renaud, J.-P., and Delsuc, M.-A. (2009). Biophysical techniques for ligand screening and drug design. *Curr. Opin. Pharmacol.* *9*, 622–628.
- Rester, U. (2008). From virtuality to reality - virtual screening in lead discovery and lead optimization: a medicinal chemistry perspective. *Curr. Opin. Drug Discov. Devel.* *11*, 559–568.
- Sánchez-Pedregal, V.M., Reese, M., Meiler, J., Blommers, M.J.J., Griesinger, C., and Carlomagno, T. (2005). The INPHARMA method: protein-mediated interligand NOEs for pharmacophore mapping. *Angew. Chem. Int. Ed.* *44*, 4172–4175.
- Schertzer, J.W., Brown, S.A., and Whiteley, M. (2010). Oxygen levels rapidly modulate *Pseudomonas aeruginosa* social behaviours via substrate limitation of PqsH. *Mol. Microbiol.* *77*, 1527–1538.
- Soelaiman, S., Wei, B.Q., Bergson, P., Lee, Y.-S., Shen, Y., Mrksich, M., Shoichet, B.K., and Tang, W.-J. (2003). Structure-based inhibitor discovery against adenylyl cyclase toxins from pathogenic bacteria that cause anthrax and whooping cough. *J. Biol. Chem.* *278*, 25990–25997.

- Srivastava, A., Talaue, M., Liu, S., Degen, D., Ebright, R.Y., Sineva, E., Chakraborty, A., Druzhinin, S.Y., Chatterjee, S., Mukhopadhyay, J., et al. (2011). New target for inhibition of bacterial RNA polymerase: 'switch region'. *Curr. Opin. Microbiol.* *14*, 532–543.
- Storz, M.P., Allegretta, G., Kirsch, B., Empting, M., and Hartmann, R.W. (2014). From in vitro to in cellulose: structure-activity relationship of (2-nitrophenyl)methanol derivatives as inhibitors of PqsD in *Pseudomonas aeruginosa*. *Org. Biomol. Chem.* *12*, 6094–6104.
- Storz, M.P., Brengel, C., Weidel, E., Hoffmann, M., Hollemeyer, K., Steinbach, A., Müller, R., Empting, M., and Hartmann, R.W. (2013). Biochemical and biophysical analysis of a chiral PqsD inhibitor revealing tight-binding behavior and enantiomers with contrary thermodynamic signatures. *ACS Chem. Biol.* *8*, 2794–2801.
- Storz, M.P., Maurer, C.K., Zimmer, C., Wagner, N., Brengel, C., de Jong, J.C., Lucas, S., Müsken, M., Häussler, S., Steinbach, A., et al. (2012). Validation of PqsD as an anti-biofilm target in *Pseudomonas aeruginosa* by development of small-molecule inhibitors. *J. Am. Chem. Soc.* *134*, 16143–16146.
- Stover, C.K., Pham, X.Q., Erwin, A.L., Mizoguchi, S.D., Warrener, P., Hickey, M.J., Brinkman, F.S., Hufnagle, W.O., Kowalik, D.J., Lagrou, M., et al. (2000). Complete genome sequence of *Pseudomonas aeruginosa* PAO1, an opportunistic pathogen. *Nature* *406*, 959–964.
- Sucipto, H., Wenzel, S.C., and Müller, R. (2013). Exploring chemical diversity of  $\alpha$ -pyrone antibiotics: molecular basis of myxopyronin biosynthesis. *ChemBioChem* *14*, 1581–1589.
- Swift, S., Allan Downie, J., Whitehead, N.A., Barnard, A.M.L., Salmond, G.P.C., and Williams, P. (2001). Quorum sensing as a population-density-dependent determinant of bacterial physiology. *Adv. Microb. Physiol.* *45*, 199–270.
- Topliss, J.G. (1972). Utilization of operational schemes for analog synthesis in drug design. *J. Med. Chem.* *15*, 1006–1011.
- Topliss, J.G. (1977). A manual method for applying the Hansch approach to drug design. *J. Med. Chem.* *20*, 463–469.
- Tupin, A., Gualtieri, M., Brodolin, K., and Leonetti, J.-P. (2009). Myxopyronin: a punch in the jaws of bacterial RNA polymerase. *Future Microbiol.* *4*, 145–149.
- Upshur, R. (2008). *B. World Health Organ.* *86*, 654.
- Venugopal, A.A., and Johnson, S. (2012). Fidaxomicin: a novel macrocyclic antibiotic approved for treatment of *Clostridium difficile* infection. *Clin. Infect. Dis.* *54*, 568–574.
- Verma, J., Khedkar, V.M., and Coutinho, E.C. (2010). 3D-QSAR in drug design--a review. *Curr. Top. Med. Chem.* *10*, 95–115.
- Walsh, C. (2000). Molecular mechanisms that confer antibacterial drug resistance. *Nature* *406*, 775–781.
- Walsh, C.T., and Wenczewicz, T.A. (2014). Prospects for new antibiotics: a molecule-centered perspective. *J. Antibiot.* *67*, 7–22.
- Wermuth, C.G., Ganellin, C.R., Lindberg, P., and Mitscher, L.A. (1998). Glossary of terms used in medicinal chemistry (IUPAC Recommendations 1998). *Pure Appl. Chem.* *70*, 1129–1143.
- Whiteley, M., Bangera, M.G., Bumgarner, R.E., Parsek, M.R., Teitzel, G.M., Lory, S., and Greenberg, E.P. (2001). Gene expression in *Pseudomonas aeruginosa* biofilms. *Nature* *413*, 860–864.
- Whiteley, M., Lee, K.M., and Greenberg, E.P. (1999). Identification of genes controlled by quorum sensing in *Pseudomonas aeruginosa*. *P. Natl. Acad. Sci. USA.* *96*, 13904–13909.
- WHO: Global Tuberculosis Report **2014**: WHO/HTM/TB/2014.08.

- Williams, P., Bainton, N.J., Swift, S., Chhabra, S.R., Winson, M.K., Stewart, G.S.A.B., Salmond, G.P.C., and Bycroft, B.W. (1992). Small molecule-mediated density-dependent control of gene expression in prokaryotes: Bioluminescence and the biosynthesis of carbapenem antibiotics. *FEMS Microbiol. Lett.* *100*, 161–167.
- Wright, G.D. (2010). Q&A: Antibiotic resistance: where does it come from and what can we do about it? *BMC Biol.* *8*, 123–128.
- Xiao, G., Déziel, E., He, J., Lépine, F., Lesic, B., Castonguay, M.-H., Milot, S., Tampakaki, A.P., Stachel, S.E., and Rahme, L.G. (2006). MvfR, a key *Pseudomonas aeruginosa* pathogenicity LTTR-class regulatory protein, has dual ligands. *Mol. Microbiol.* *62*, 1689–1699.
- Yang, S.-Y. (2010). Pharmacophore modeling and applications in drug discovery: challenges and recent advances. *Drug Discov. Today* *15*, 444–450.
- Yu, S., Jensen, V., Seeliger, J., Feldmann, I., Weber, S., Schleicher, E., Häussler, S., and Blankenfeldt, W. (2009). Structure elucidation and preliminary assessment of hydrolase activity of PqsE, the *Pseudomonas* quinolone signal (PQS) response protein. *Biochemistry* *48*, 10298–10307.
- Zender, M., Klein, T., Henn, C., Kirsch, B., Maurer, C.K., Kail, D., Ritter, C., Dolezal, O., Steinbach, A., and Hartmann, R.W. (2013). Discovery and biophysical characterization of 2-amino-oxadiazoles as novel antagonists of PqsR, an important regulator of *Pseudomonas aeruginosa* virulence. *J. Med. Chem.* *56*, 6761–6774.
- Zhang, G., Campbell, E.A., Minakhin, L., Richter, C., Severinov, K., and Darst, S.A. (1999). Crystal structure of *Thermus aquaticus* core RNA polymerase at 3.3 Å resolution. *Cell* *98*, 811–824.
- Zhang, Y.-M., Frank, M.W., Zhu, K., Mayasundari, A., and Rock, C.O. (2008). PqsD is responsible for the synthesis of 2,4-dihydroxyquinoline, an extracellular metabolite produced by *Pseudomonas aeruginosa*. *J. Biol. Chem.* *283*, 28788–28794.
- Zignol, M., van Gemert, W., Falzon, D., Sismanidis, C., Glaziou, P., Floyd, K., and Raviglione, M. (2012). Surveillance of anti-tuberculosis drug resistance in the world: an updated analysis, 2007-2010. *Bull. World Health Organ.* *90*, 111–119D.
- Zlatopolskiy, B.D., Radzom, M., Zeeck, A., and de Meijere, A. (2006). Synthesis and precursor-directed biosynthesis of new hormaomycin analogues. *Eur. J. Org. Chem.* *2006*, 1525–1534.

## 6 Supporting Information

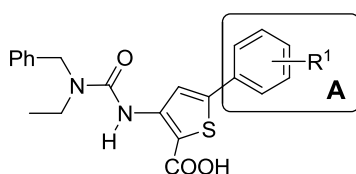
This section contains the relevant supporting information of the studies presented in section 3. It includes additional details on experimental procedures, as well as further figures and results.

### 6.1 Supporting Information for Publication A

Full supporting information is available online:

<http://www.sciencedirect.com/science/article/pii/S0223523413002924>

#### 6.1.1 Hansch Analysis of Ring A (compounds 3, 8–22)



For the investigation of the quantitative relationship between the biological activity and the substituents on the phenyl ring A,  $\pi$  (lipophilicity constant) [1] and  $\sigma$  (Hammett substituent constant) [1] were used in a multiple regression correlation methodology.

**Table S1.** Set of compounds and substituent parameters used for the multiple regression analysis.

Cpd	R <sup>1</sup>	IC <sub>50</sub> <i>E. coli</i> RNAP	pIC <sub>50</sub> <sup>a</sup>	$\sigma$	$\pi$
3	4-Cl	75 $\mu$ M	4.12	0.23	0.71
8	H	292 $\mu$ M	3.52	0	0
9	4-OCH <sub>3</sub>	240 $\mu$ M	3.62	-0.27	-0.02
10	4-CH <sub>3</sub>	137 $\mu$ M	3.86	-0.17	0.56
11	4-CF <sub>3</sub>	51 $\mu$ M	4.29	0.54	0.88
12	4-NO <sub>2</sub>	73 $\mu$ M	4.14	0.78	-0.28
13	4-CN	133 $\mu$ M	3.88	0.66	-0.57
14	4-OCF <sub>3</sub>	45 $\mu$ M	4.35	0.30	1.30
15	3-Cl	72 $\mu$ M	4.14	0.37	0.71
16	3-CF <sub>3</sub>	53 $\mu$ M	4.28	0.43	0.88
17	3-NO <sub>2</sub>	80 $\mu$ M	4.10	0.71	-0.28
18	3,4-di-Cl	22 $\mu$ M	4.66	0.60	1.42
19	2,4-di-Cl	32 $\mu$ M	4.49	0.46	1.42
20	2,5-di-Cl	35 $\mu$ M	4.46	0.60	1.42
21	3,5-di-Cl	25 $\mu$ M	4.60	0.74	1.42
22	3-CF <sub>3</sub> , 4-Cl	21 $\mu$ M	4.68	0.66	1.59

<sup>a</sup> pIC<sub>50</sub> = -log(IC<sub>50</sub>);

## 6.1.2 Biology

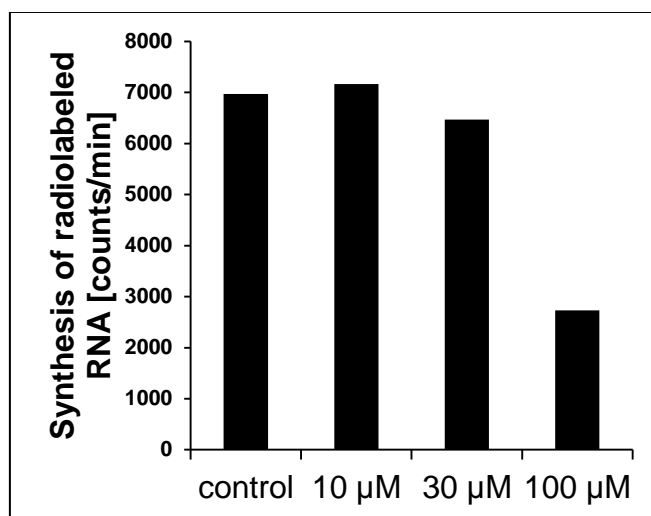


**Figure S1.** Effect of **18** on RNA synthesis in *E. coli TolC*.

**Table S2.** RNA inhibition and antibacterial activity of **4** and the references **5**, **6** and **7**.

Cpd	structure	Inhibition of RNAP <sup>a</sup>	MIC (μg/mL) <sup>b,c</sup>
<b>4</b>		<b>2% @ 25 μM</b>	<b>&gt;25</b>
<b>5</b>	 <b>4:</b> R = H <b>4a:</b> R = Et <b>4b:</b> R = tBu	<b>3% @ 25 μM</b>	<b>&gt;25</b>
<b>6</b>		<b>2% @ 50 μM</b>	<b>&gt;25</b>
<b>7</b>		<b>4% @ 100 μM</b>	<b>33</b>

<sup>a</sup> Inhibition of *E. coli* RNA polymerase; <sup>b</sup> Minimal inhibitory concentration in *E. coli TolC*; <sup>c</sup> >: MIC-determination was limited due to insufficient solubility of the tested compounds.

### 6.1.3 Docking pose and interaction map of compound 23

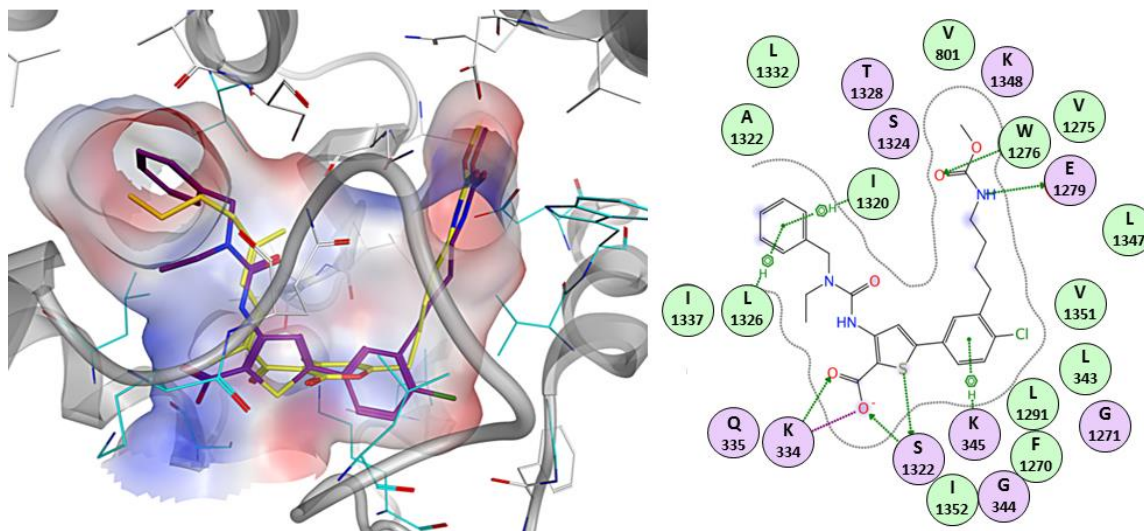
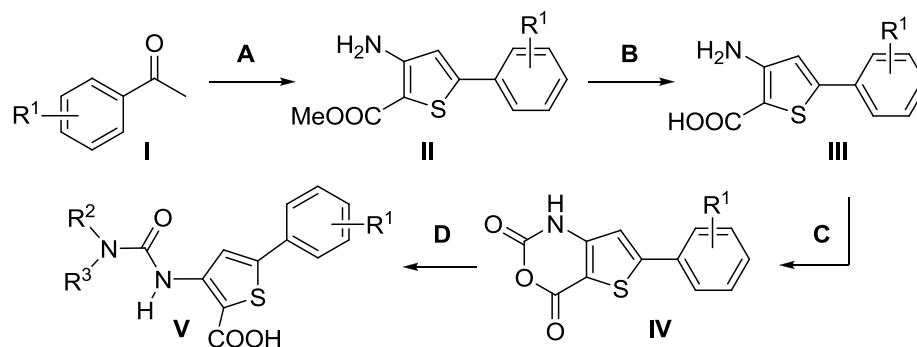


**Figure S2:** Docking simulation of compound **23** and two dimensional illustration of the interaction between **23** and RNAP. The main interacting amino acids and the key interactions are highlighted. Polar amino acids are illustrated in purple and hydrophobic amino acids in green circles

### 6.1.4 Chemistry

**Scheme S1:** Synthesis of 5-aryl-3-ureidothiophene-2-carboxylic acids.



Method A, general procedure for the synthesis of 5-Aryl-3-amino-2-carboxylic acid methylester (**II**) [2]:  $\text{POCl}_3$  (26.1 g, 0.17 mol) was added dropwise to DMF (24.9 g, 0.34 mol) maintaining the temperature beyond  $25\text{ }^\circ\text{C}$  (cooling in ice bath) and stirred for additional 15 min. The acetophenone **I** (85.0 mmol) was added slowly and the temperature was kept between  $40$  and  $60\text{ }^\circ\text{C}$ . After complete addition, the mixture was stirred for 30 minutes at room temperature. Hydroxylamine hydrochloride (23.6 g, 0.34 mol) was carefully added portionwise (exothermic reaction!) and the reaction was stirred for additional 30 min without heating. After cooling to room temperature, the mixture was poured into ice water (300 mL). The precipitated  $\beta$ -chloro-cinnamionitrile was collected by filtration, washed with  $\text{H}_2\text{O}$  (2 x 50 mL) and dried under reduced pressure over  $\text{CaCl}_2$ . In the next step sodium (1.93 g, 84.0 mmol.) was dissolved in MeOH (85 mL) and

methylthioglycolate (6.97 g, 65.6 mmol) was added to the stirred solution. The  $\beta$ -chloro-cinnamionitrile (61.1 mmol) was added and the mixture was heated to reflux for 30 min. After cooling to room temperature, the mixture was poured in ice water (300 mL). The precipitated solid was collected by filtration, washed with H<sub>2</sub>O (2 x 50 mL) and dried under reduced pressure over CaCl<sub>2</sub>. If necessary, recrystallisation was performed from EtOH.

Method B, general procedure for the synthesis of 5-Aryl-3-amino-2-carboxylic acid (**III**): The 5-Aryl-3-amino-2-carboxylic acid methyl ester (16.6 mmol) was added to a solution of KOH (60 mL, 0.6M in H<sub>2</sub>O) and MeOH (60 mL). The mixture was heated to reflux for 3 h, concentrated, and washed with EtOAc (2 x 50 mL). The aqueous layer was cooled with ice and acidified with a saturated aqueous solution of KHSO<sub>4</sub>. The precipitated solid was collected by filtration, washed with H<sub>2</sub>O (2 x 30 mL) and dried under reduced pressure over CaCl<sub>2</sub>.

Method C, general procedure for the synthesis of 5-Aryl-2-thiaisatoic-anhydrid (**IV**) [3,4]: To a solution of the 5-Aryl-3-amino-2-carboxylic acid (**III**) (5.28 mmol) in THF (50 mL) a solution of phosgene (6.10 mL, 20 wt% in toluene, 11.6 mmol) was added dropwise over a period of 30 min. The reaction mixture was stirred for 2 h at room temperature, followed by the addition of saturated aqueous solution of NaHCO<sub>3</sub> (30 mL) and H<sub>2</sub>O (50 mL). The resulting mixture was extracted with EtOAc/THF (1:1, 3 x 100 mL). The organic layer was washed with saturated aqueous NaCl (100 mL), dried (MgSO<sub>4</sub>) and concentrated. The crude material was suspended in a mixture of *n*-hexane/EtOAc (2:1, 50 mL) heated to 50 °C and after cooling to room temperature separated via filtration.

Method D, general procedure for the synthesis of 5-Aryl-3-ureidothiophene-2-carboxylic acid (**V**) [5]: The 5-Aryl-2-thiaisatoic-anhydrid (**IV**) (0.46 mmol) was suspended in water (7.5 mL) and the appropriate amine (4.60 mmol) was added. The reaction mixture was stirred, heated to 100 °C and then cooled to room temperature. The reaction mixture was poured into a mixture of concentrated HCl and ice (1:1) and extracted with EtOAc/THF (1:1, 60 mL). The organic layer was washed with aqueous HCl (2M), followed by saturated aqueous NaCl (2 x 50 mL), dried (MgSO<sub>4</sub>) and concentrated. The crude material was suspended in a mixture of *n*-hexane/EtOAc (2:1, 20 mL) heated to 50 °C and after cooling to room temperature separated via filtration.

**5-(4'-Chlorophenyl)-3-[(*N*-ethylbenzylamino)carbonylamino]-thiophen-2-carboxylic acid (**3**)**. The title compound was prepared from 4'-chloroacetophenone according to methods A–D. Yellow powder, m.p. 173–174 °C. <sup>1</sup>H NMR (300 MHz, DMSO-*d*<sub>6</sub>):  $\delta$  = 1.16 (t, *J* = 7.1 Hz, 3 H), 3.39 (q, *J* = 7.1 Hz, 2 H), 4.58 (s, 2 H), 7.24–7.38 (m, 5 H), 7.50 (d, *J* = 8.5 Hz, 2 H), 7.71 (d, *J* = 8.5 Hz, 2 H), 8.29 (s, 1 H), 10.06 (s, 1 H), 13.40 (br. s, 1 H, COOH) ppm. <sup>13</sup>C NMR (75 MHz, DMSO-*d*<sub>6</sub>):  $\delta$  = 13.1, 41.8, 49.3, 107.2, 117.8, 127.1, 127.1, 127.4, 128.5, 129.3, 131.5, 133.8, 138.1, 146.1, 146.7, 153.0, 165.6 ppm.

**Methyl-5-(4'-chlorophenyl)-3-[(*N*-ethylbenzylamino)carbonylamino]-thiophen-2-carboxylate (**4**)**. A mixture of **3** (150 mg, 0.36 mmol), K<sub>2</sub>CO<sub>3</sub> (58 mg, 0.42 mmol) and iodomethane (55.4 mg, 0.39 mmol) was stirred in DMF (15 mL)

at room temperature for 72 h. The reaction was stopped by addition of H<sub>2</sub>O (50 mL). The mixture was extracted with CH<sub>2</sub>Cl<sub>2</sub> (3 x 30 mL). The combined organic layers were washed with a saturated solution of K<sub>2</sub>CO<sub>3</sub> (3 x 50 mL) and with saturated NaCl (50 mL), dried (MgSO<sub>4</sub>) and evaporated *in vacuo* to yield the desired product as a light yellow powder. <sup>1</sup>H NMR (300 MHz, DMSO-*d*<sub>6</sub>) δ = 1.17 (t, *J* = 7.1 Hz, 3 H), 3.39 (d, *J* = 7.1 Hz, 2 H), 3.81 (s, 3 H, OCH<sub>3</sub>), 4.59 (s, 2 H), 7.23–7.40 (m, 5 H), 7.52 (d, *J* = 8.6 Hz, 2 H), 7.73 (d, *J* = 8.6 Hz, 2 H), 8.31 (s, 1 H), 9.78 (br. s, 1 H) ppm. <sup>13</sup>C NMR (75 MHz, DMSO-*d*<sub>6</sub>): δ = 13.1, 41.7, 49.3, 52.1, 105.9, 117.9, 127.2, 127.2, 127.5, 128.5, 129.3, 131.3, 134.0, 138.0, 146.9, 147.0, 152.9, 164.2 ppm.

**4,5,6,7,8,9-Hexahydro-2-(3-phenylureido)cycloocta[*b*]thiophene-3-carboxylic acid (5).** The title compound was prepared from **7** according to the procedure reported by Arhin et al. [9] <sup>1</sup>H NMR (300 MHz, DMSO-*d*<sub>6</sub>) δ = 1.15–1.30 (m, 2 H), 1.35–1.47 (m, 2 H), 1.50–1.66 (m, 4 H), 2.67 (t, *J* = 5.4 Hz, 2 H), 2.86 (t, *J* = 5.9 Hz, 2 H), 7.00 (t, *J* = 7.3 Hz, 1 H), 7.29 (dd, *J* = 7.8, 7.3 Hz, 2 H), 7.49 (d, *J* = 7.8 Hz, 2 H), 10.13 (s, 1 H), 10.72 (s, 1 H), 12.71 (br. s., 1 H, COOH) ppm. <sup>13</sup>C NMR (75 MHz, DMSO-*d*<sub>6</sub>): δ = 24.6, 25.2, 25.9, 29.7, 32.0, 110.0, 118.5, 122.4, 127.1, 128.8, 133.0, 139.2, 148.5, 151.1, 166.9 ppm.

**Ethyl 4,5,6,7,8,9-hexahydro-2-(3-phenylureido)cycloocta[*b*]thiophene-3-carboxylate (6).** The title compound was prepared according to the procedure reported by Arhin et al. [9] <sup>1</sup>H NMR (300 MHz, DMSO-*d*<sub>6</sub>): δ = 1.15–1.30 (m, 2 H), 1.32 (t, *J* = 7.1 Hz, 3 H), 1.35–1.49 (m, 2 H), 1.50–1.65 (m, 4 H), 2.63–2.74 (m, 2 H), 2.85 (t, *J* = 6.0 Hz, 2 H), 4.31 (q, *J* = 7.1 Hz, 2 H), 7.01 (t, *J* = 7.3 Hz, 1 H), 7.30 (dd, *J* = 7.6, 7.3 Hz, 2 H), 7.49 (d, *J* = 7.6 Hz, 2 H), 10.17 (br. s, 1 H), 10.66 (br. s, 1 H) ppm. <sup>13</sup>C NMR (75 MHz, DMSO-*d*<sub>6</sub>): δ = 14.0, 24.9, 25.2, 26.0, 29.5, 32.0, 60.0, 60.0, 109.2, 118.4, 122.4, 127.5, 128.8, 132.3, 139.1, 148.9, 151.1, 165.4 ppm.

***tert*-Butyl 4,5,6,7,8,9-hexahydro-2-(3-phenylureido)cycloocta[*b*]thiophene-3-carboxylate (7).** The title compound was prepared according to the procedure reported by Arhin et al. [9] <sup>1</sup>H NMR (300 MHz, CDCl<sub>3</sub>) δ = 1.26–1.31 (m, 2 H), 1.41–1.52 (m, 2 H), 1.57 (s, 9 H), 1.59–1.67 (m, 4 H), 2.67–2.77 (m, 2 H), 2.80–2.94 (m, 2 H), 6.83 (s, 1 H), 7.08–7.16 (tt, *J* = 7.4, 1.1 Hz, 1 H), 7.30–7.38 (m, 2 H), 7.46 (m, 2 H), 11.06 (s, 1 H) ppm. <sup>13</sup>C NMR (75 MHz, CDCl<sub>3</sub>) δ = 25.4, 25.6, 26.4, 26.7, 28.3, 30.1, 32.3, 81.6, 111.3, 120.3, 124.1, 128.3, 129.1, 133.1, 137.7, 149.3, 151.2, 166.6 ppm.

**5-(Phenyl)-3-[(*N*-ethylbenzylamino)carbonylamino]-thiophen-2-carboxylic acid (8).** The title compound was prepared from acetophenone according to methods A–D. Yellow powder, m.p. 169–171 °C. <sup>1</sup>H NMR (300 MHz, DMSO-*d*<sub>6</sub>): δ = 1.16 (t, *J* = 7.1 Hz, 3 H), 3.40 (q, *J* = 7.1 Hz, 2 H), 4.59 (s, 2 H), 7.24–7.50 (m, 8 H), 7.70 (m, 2 H), 8.29 (s, 1 H), 10.08 (s, 1 H), 13.33 (br. s, 1 H, COOH) ppm. <sup>13</sup>C NMR (75 MHz, DMSO-*d*<sub>6</sub>): δ = 13.1, 41.8, 49.3, 106.8, 117.3, 125.7, 127.1, 127.1, 128.5, 129.3, 129.4, 132.7, 138.1, 146.8, 147.7, 153.1, 165.7 ppm.

**5-(4'-Methoxyphenyl)-3-[(*N*-ethylbenzylamino)carbonylamino]-thiophen-2-carboxylic acid (9).** The title compound was prepared from 4'-methoxyacetophenone according to methods A–D. Beige powder, m.p. 169–170

°C.  $^1\text{H}$  NMR (300 MHz,  $\text{DMSO-}d_6$ ):  $\delta$  = 1.16 (t,  $J$  = 7.1, 3 H), 3.39 (q,  $J$  = 7.0 Hz, 2 H,  $\text{OCH}_3$ ), 3.80 (s, 3 H), 7.02 (d,  $J$  = 8.9 Hz, 2 H), 7.29–7.38 (m, 5 H), 7.63 (d,  $J$  = 8.9 Hz, 2 H), 8.17 (s, 1 H), 10.10 (s, 1 H), 13.21 (br.s, 1 H,  $\text{COOH}$ ) ppm.  $^{13}\text{C}$  NMR (75 MHz,  $\text{DMSO-}d_6$ ):  $\delta$  = 13.1, 41.8, 49.3, 55.3, 105.6, 114.7, 116.1, 125.3, 127.1, 127.1, 127.2, 128.5, 138.1, 147.0, 147.9, 153.1, 160.2, 165.8 ppm.

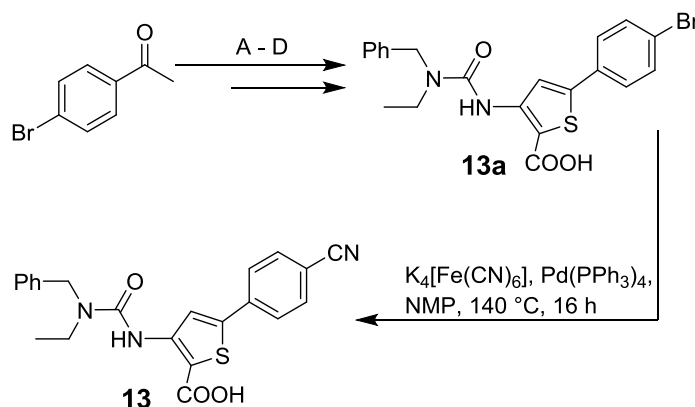
**5-(4'-Methylphenyl)-3-[(*N*-ethylbenzylamino)carbonylamino]-thiophen-2-carboxylic acid (10).** The title compound was prepared from 4'-methylacetophenone according to methods A–D. Orange powder, m.p. 174–178 °C.  $^1\text{H}$  NMR (300 MHz,  $\text{DMSO-}d_6$ ):  $\delta$  = 1.16 (t,  $J$  = 7.0 Hz, 3 H), 2.33 (s, 3 H,  $\text{CH}_3$ ), 3.39 (q,  $J$  = 7.0 Hz, 2 H), 4.58 (s, 2 H), 7.24–7.38 (m, 7 H), 7.58 (d,  $J$  = 8.2 Hz, 2 H), 8.24 (s, 1 H), 10.09 (s, 1 H), 13.31 (br. s, 1 H,  $\text{COOH}$ ) ppm.  $^{13}\text{C}$  NMR (75 MHz,  $\text{DMSO-}d_6$ ):  $\delta$  = 13.6, 21.3, 42.3, 49.8, 106.7, 117.2, 126.1, 127.6, 127.6, 129.0, 130.4, 138.6, 139.5, 147.3, 148.4, 153.5, 166.3 ppm.

**5-(4'-Trifluoromethylphenyl)-3-[(*N*-ethylbenzylamino)carbonylamino]-thiophen-2-carboxylic acid (11).** The title compound was prepared from 4'-trifluoromethylacetophenone according to methods A–D. Grey powder, m.p. 193–194 °C.  $^1\text{H}$  NMR (300 MHz,  $\text{DMSO-}d_6$ ):  $\delta$  = 1.16 (t,  $J$  = 7.1 Hz, 3 H), 3.40 (q,  $J$  = 7.1 Hz, 2 H), 4.59 (s, 2 H), 7.24–7.38 (m, 5 H), 7.79 (d,  $J$  = 8.4 Hz, 2 H), 7.91 (d,  $J$  = 8.4 Hz, 2 H), 8.41 (s, 1 H), 10.05 (s, 1 H), 13.47 (br. s, 1 H,  $\text{COOH}$ ) ppm.  $^{13}\text{C}$  NMR (75 MHz,  $\text{DMSO-}d_6$ ):  $\delta$  = 13.1, 41.8, 49.3, 108.2, 124.0 (q,  $J_{\text{CF}}$  = 272.0 Hz), 126.2 (q,  $J_{\text{CF}}$  = 3.7 Hz), 126.4, 127.2, 128.4, 128.5, 129.3 (q,  $J_{\text{CF}}$  = 32.0 Hz), 136.5, 138.1, 145.3, 146.7, 153.0, 165.6 ppm.

**5-(4'-Nitrophenyl)-3-[(*N*-ethylbenzylamino)carbonylamino]-thiophen-2-carboxylic acid (12).** The title compound was prepared from 4'-nitroacetophenone according to methods A–D. Yellow powder, m.p. 201–202 °C.  $^1\text{H}$  NMR (300 MHz,  $\text{DMSO-}d_6$ ):  $\delta$  = 1.16 (t,  $J$  = 7.1 Hz, 3 H), 3.40 (q,  $J$  = 7.1 Hz, 2 H), 4.59 (s, 2 H), 7.25–7.38 (m, 5 H), 7.96 (d,  $J$  = 8.9 Hz, 2 H), 8.25 (d,  $J$  = 8.9 Hz, 2 H), 8.45 (s, 1 H), 10.02 (s, 1 H), 13.53 (br. s, 1 H,  $\text{COOH}$ ) ppm.  $^{13}\text{C}$  NMR (75 MHz,  $\text{DMSO-}d_6$ ):  $\delta$  = 13.1, 41.8, 49.3, 109.2, 119.7, 124.5, 126.7, 127.2, 128.5, 138.0, 138.7, 144.3, 146.6, 147.2, 153.0, 165.5 ppm.

**5-(4'-Cyanophenyl)-3-[(*N*-ethylbenzylamino)carbonylamino]-thiophen-2-carboxylic acid (13).**

**Scheme 2.** Synthesis of compound **13**:



**5-(4'-Bromophenyl)-3-[(*N*-ethylbenzylamino)carbonylamino]-thiophen-2-carboxylic acid (13a)** was prepared from 4'-bromo-acetophenone according to methods A–D. <sup>1</sup>H NMR (300 MHz, DMSO-*d*<sub>6</sub>): δ ppm 1.16 (t, *J* = 7.0 Hz, 3 H), 3.39 (q, *J* = 7.0 Hz, 2 H), 4.58 (s, 2 H), 7.24–7.38 (m, 5 H), 7.65 (m, 4 H), 8.30 (s, 1 H), 10.06 (s, 1 H), 13.42 (br. s, 1 H, COOH) ppm.

The title compound **13** was prepared from **13a** according to the following procedure:[6] A stirred solution of **13a** (410 mg, 0.85 mmol), K<sub>4</sub>[Fe(CN)<sub>6</sub>]·3H<sub>2</sub>O (71.8 mg, 0.17 mmol) and Na<sub>2</sub>CO<sub>3</sub> (94.5 mg, 0.85 mmol) in NMP (6 mL) was degassed and kept under a nitrogen atmosphere. Pd(PPh<sub>3</sub>)<sub>4</sub> (30.0 mg, 3 Mol%) was added and the resulting mixture was heated for 16 h at 140 °C. The reaction mixture was allowed to cool to room temperature. An additional amount of Pd(PPh<sub>3</sub>)<sub>4</sub> (10.0 mg, 1 Mol%) was added and the mixture was heated for 2 h at 140 °C. After cooling to room temperature the reaction mixture was poured into a mixture concentrated HCl and ice (1:1, 50 mL) followed by extraction with EtOAc/THF (1:1, 60 mL). The organic layer was washed with aqueous HCl (2M), followed by saturated aqueous NaCl (2 x 50 mL), dried (MgSO<sub>4</sub>) and concentrated. The crude material was suspended in a mixture of *n*-hexane/EtOAc (2:1, 20 mL) heated to 50 °C and after cooling to room temperature separated via filtration. Yellow powder, m.p. 183–185 °C. <sup>1</sup>H NMR (300 MHz, DMSO-*d*<sub>6</sub>): δ = 1.16 (t, *J* = 6.7 Hz, 3 H), 3.40 (q, *J* = 6.7 Hz, 2 H), 4.59 (s, 2 H), 7.24–7.38 (m, 5 H), 7.86–7.93 (m, 4 H), 8.41 (s, 1 H), 10.06 (s, 1 H), 13.58 (br. s, 1 H, COOH) ppm. <sup>13</sup>C NMR (75 MHz, DMSO-*d*<sub>6</sub>): δ = 13.1, 41.8, 49.3, 108.9, 111.3, 118.5, 119.3, 126.4, 127.2, 128.5, 133.2, 136.9, 138.1, 144.9, 146.6, 153.0, 165.5 ppm.

**5-(4'-Trifluoromethoxyphenyl)-3-[(*N*-ethylbenzylamino)carbonylamino]-thiophen-2-carboxylic acid (14)**. The title compound was prepared from 4'-trifluoromethoxyacetophenone according to methods A–D. White powder, m.p. 187–190 °C. <sup>1</sup>H NMR (300 MHz, DMSO-*d*<sub>6</sub>): δ = 1.16 (t, *J* = 6.7 Hz, 3 H), 3.39 (q, *J* = 6.7 Hz, 2 H), 4.59 (s, 2 H), 7.24–7.38 (m, 5 H), 7.45 (d, *J* = 8.1 Hz, 2 H), 7.83 (d, *J* = 8.1 Hz, 2 H), 8.31 (s, 1 H), 10.07 (s, 1 H), 13.44 (br. s, 1 H, COOH) ppm. <sup>13</sup>C NMR (75 MHz, DMSO-*d*<sub>6</sub>): δ = 13.1, 41.8, 49.3, 107.5, 118.1, 120.0 ((q, *J*<sub>CF</sub> = 257.0 Hz), 121.8, 127.1, 127.8, 128.5, 132.0, 138.1, 145.7, 146.7, 148.7, 153.0, 165.6 ppm.

**5-(3'-Chlorophenyl)-3-[(*N*-ethylbenzylamino)carbonylamino]-thiophen-2-carboxylic acid (15)**. The title compound was prepared from 3'-chloroacetophenone according to methods A–D. Beige powder, m.p. 199–201 °C. <sup>1</sup>H NMR (300 MHz, DMSO-*d*<sub>6</sub>): δ = 1.16 (t, *J* = 7.1 Hz, 3 H), 3.40 (q, *J* = 7.1 Hz, 2 H), 4.58 (s, 2 H), 7.24–7.37 (m, 5 H), 7.45–7.50 (m, 2 H), 7.62–7.66 (m, 1 H), 7.70–7.73 (m, 1 H) 8.31 (s, 1 H), 10.05 (s, 1 H), 13.44 (br. s, 1 H, COOH) ppm. <sup>13</sup>C NMR (75 MHz, DMSO-*d*<sub>6</sub>): δ = 13.1, 41.8, 49.3, 107.6, 118.3, 124.5, 125.2, 127.1, 127.2, 128.5, 128.9, 131.2, 134.1, 134.7, 138.1, 145.6, 146.6, 153.0, 165.6 ppm.

**5-(3'-Trifluoromethylphenyl)-3-[(*N*-ethylbenzylamino)carbonylamino]-thiophen-2-carboxylic acid (16)**. The title compound was prepared from 3'-trifluoroacetophenone according to methods A–D. White powder, m.p. 207–209 °C. <sup>1</sup>H NMR (300 MHz, DMSO-*d*<sub>6</sub>): δ = 1.16 (t, *J* = 7.1 Hz, 3 H), 3.40 (q, *J* = 7.1 Hz, 3 H), 4.59 (s, 2 H), 7.24–7.38 (m, 5 H), 7.70 (dd, *J* = 7.8, 7.7 Hz, 1 H), 7.78

(d,  $J = 7.8$  Hz, 1 H), 7.94–7.97 (m, 1 H), 8.01 (d,  $J = 7.7$  Hz, 1 H), 8.39 (s, 1 H), 10.06 (s, 1 H), 13.50 (br. s, 1 H, COOH) ppm.  $^{13}\text{C}$  NMR (75 MHz, DMSO- $d_6$ ):  $\delta = 13.1, 41.8, 49.3, 108.9, 118.6, 121.9$  (q,  $J_{\text{CF}} = 3.7$  Hz), 123.8 (q,  $J_{\text{CF}} = 272.7$  Hz), 125.65 (q,  $J_{\text{CF}} = 3.7$  Hz), 127.1, 128.5, 129.8, 130.1 (q,  $J_{\text{CF}} = 32.8$  Hz), 130.6, 133.7, 138.1, 14.4, 146.6, 153.0, 165.6 ppm.

**5-(3'-Nitrophenyl)-3-[(*N*-ethylbenzylamino)carbonylamino]-thiophen-2-carboxylic acid (17).** The title compound was prepared from 3'-nitroacetophenone according to methods A–D. Beige powder, m.p. 184–185 °C.  $^1\text{H}$  NMR (300 MHz, DMSO- $d_6$ ):  $\delta = 1.17$  (t,  $J = 7.1$  Hz, 3 H), 3.40 (q,  $J = 7.1$  Hz, 2 H), 4.59 (s, 2 H), 7.24–7.38 (m, 5 H), 7.74 (dd,  $J = 8.1, 8.0$  Hz, 1 H), 8.14 (dd,  $J = 8.1, 1.7$  Hz, 1 H), 8.23 (dd,  $J = 8.1, 1.7$  Hz, 1 H), 8.38 (dd,  $J = 1.7$  Hz, 1 H), 8.41 (s, 1 H), 10.04 (s, 1 H), 13.53 (br. s, 1 H, COOH) ppm.  $^{13}\text{C}$  NMR (75 MHz, DMSO- $d_6$ ):  $\delta = 13.1, 41.8, 49.3, 108.2, 119.0, 119.1, 119.9, 123.6, 127.2, 128.5, 131.0, 132.0, 134.1, 138.0, 144.5, 146.6, 148.4, 153.0, 165.5$  ppm.

**5-(3',4'-dichlorophenyl)-3-[(*N*-ethylbenzylamino)carbonylamino]-thiophen-2-carboxylic acid (18).** The title compound was prepared from 3',4'-dichloroacetophenone according to methods A–D. Beige powder, m.p. 198–200 °C.  $^1\text{H}$  NMR (300 MHz, DMSO- $d_6$ ):  $\delta = 1.15$  (t,  $J = 7.1$  Hz, 3 H), 3.39 (q,  $J = 7.1$  Hz, 2 H), 4.58 (s, 2 H), 7.23–7.38 (m, 5 H), 7.63 (dd,  $J = 8.5, 1.7$  Hz, 1 H), 7.66 (d,  $J = 8.5$  Hz, 1 H), 7.89 (d,  $J = 1.7$  Hz, 2 H), 8.30 (s, 1 H), 10.03 (s, 1 H), 13.46 (br. s, 1 H, COOH) ppm.  $^{13}\text{C}$  NMR (75 MHz, DMSO- $d_6$ ):  $\delta = 13.1, 42.8, 49.3, 107.9, 118.7, 125.8, 127.1, 127.2, 128.5, 131.3, 131.6, 132.1, 133.2, 138.1, 144.3, 146.6, 153.0, 165.6$  ppm.

**5-(2',4'-dichlorophenyl)-3-[(*N*-ethylbenzylamino)carbonylamino]-thiophen-2-carboxylic acid (19).** The title compound was prepared from 2',4'-dichloroacetophenone according to methods A–D. Off-white powder, m.p. 212–214 °C.  $^1\text{H}$  NMR (300 MHz, DMSO- $d_6$ ):  $\delta = 1.15$  (t,  $J = 7.1$  Hz, 3 H), 3.39 (q,  $J = 7.1$  Hz, 2 H), 4.58 (s, 2 H), 7.23–7.37 (m, 5 H), 7.53 (dd,  $J = 8.5, 2.1$  Hz, 1 H), 7.68 (d,  $J = 8.5$  Hz, 1 H), 7.79 (d,  $J = 2.1$  Hz, 1 H), 8.27 (s, 1 H), 10.04 (s, 1 H), 13.51 (br. s, 1 H, COOH) ppm.  $^{13}\text{C}$  NMR (75 MHz, DMSO- $d_6$ ):  $\delta = 13.1, 41.8, 49.3, 108.8, 122.1, 127.1, 128.1, 128.5, 130.1, 130.5, 132.1, 132.4, 134.3, 138.0, 142.3, 145.6, 153.0, 165.6$  ppm.

**5-(2',5'-dichlorophenyl)-3-[(*N*-ethylbenzylamino)carbonylamino]-thiophen-2-carboxylic acid (20).** The title compound was prepared from 2',5'-dichloroacetophenone according to methods A–D. Brown powder, m.p. 172–174 °C.  $^1\text{H}$  NMR (300 MHz, DMSO- $d_6$ ):  $\delta = 1.16$  (t,  $J = 7.1$  Hz, 3 H), 3.40 (q,  $J = 7.1$  Hz, 2 H), 4.58 (s, 2 H), 7.24–7.37 (m, 5 H), 7.53 (dd,  $J = 8.6, 2.5$  Hz, 1 H), 7.65 (d,  $J = 8.6$  Hz, 1 H), 7.70 (d,  $J = 2.5$  Hz, 1 H), 8.26 (s, 1 H), 10.04 (s, 1 H), 13.53 (br. s, 1 H, COOH) ppm.  $^{13}\text{C}$  NMR (75 MHz, DMSO- $d_6$ ):  $\delta = 13.1, 41.8, 49.3, 109.1, 122.5, 127.1, 128.5, 130.0, 130.2, 130.5, 132.2, 132.3, 133.2, 138.0, 138.0, 141.8, 145.5, 153.0, 165.5$  ppm.

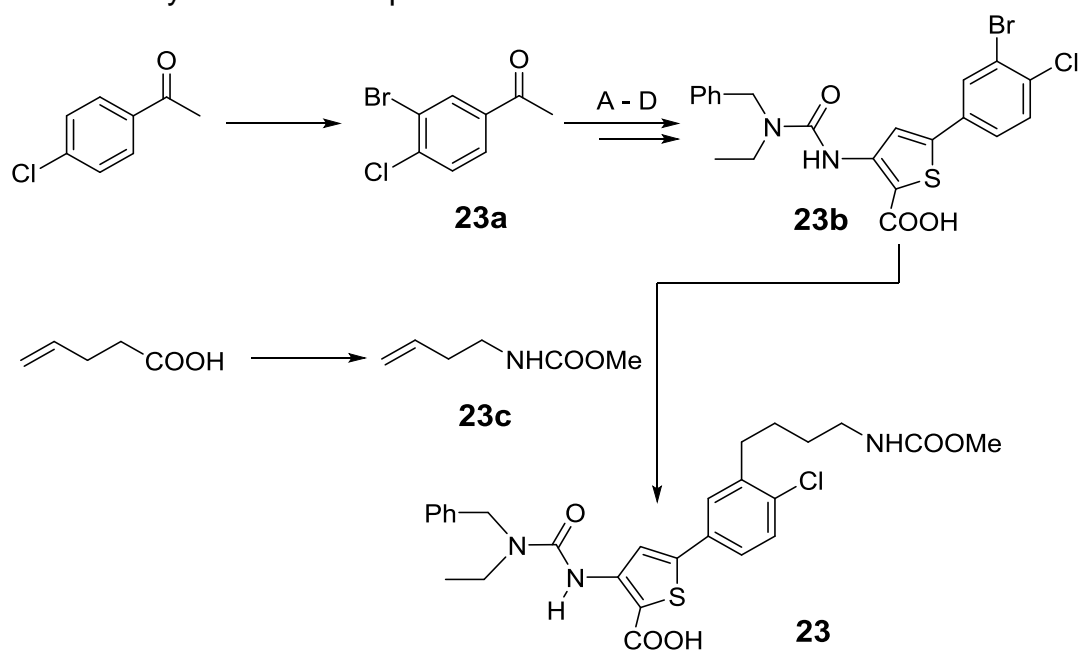
**5-(3',5'-dichlorophenyl)-3-[(*N*-ethylbenzylamino)carbonylamino]-thiophen-2-carboxylic acid (21).** The title compound was prepared from 2',4'-dichloroacetophenone according to methods A–D. Grey powder.  $^1\text{H}$  NMR (300 MHz, DMSO- $d_6$ ):  $\delta = 1.16$  (t,  $J = 6.9$  Hz, 3 H), 3.39 (q,  $J = 6.9$  Hz, 2 H), 4.58 (s, 1

H), 7.22–7.41 (m, 5 H), 7.64 (dd,  $J = 1.7$  Hz, 1 H), 7.71 (dd,  $J = 1.7$  Hz, 2 H), 8.34 (s, 1 H), 10.11 (s, 1 H) ppm.  $^{13}\text{C}$  NMR (75 MHz, DMSO- $d_6$ ):  $\delta = 13.1, 41.8, 49.3, 109.1, 119.4, 123.4, 124.3, 127.1, 127.2, 128.3, 128.5, 134.8, 135.0, 136.1, 138.1, 143.5, 146.2, 153.0, 165.6$  ppm.

**5-(3'-Trifluoromethyl,4'-Chlorophenyl)-3-[(*N*-ethylbenzylamino)carbonylamino]-thiophen-2-carboxylic acid (22).** The title compound was prepared from 3'-trifluoromethyl,4'-chloroacetophenone according to methods A–D. White powder, m.p. 202–203 °C.  $^1\text{H}$  NMR (300 MHz, DMSO- $d_6$ ):  $\delta = 0.86$  (t,  $J = 7.1$  Hz, 3 H), 3.40 (q,  $J = 7.1$  Hz, 2 H), 4.59 (s, 2 H), 7.24–7.38 (m, 5 H), 7.78 (d,  $J = 8.9$  Hz, 1 H), 7.96–8.02 (m,  $J = 6.3, 2.2$  Hz, 2 H), 8.37 (s, 1 H), 10.05 (s, 1 H), 13.54 (br. s, 1 H, COOH) ppm.  $^{13}\text{C}$  NMR (75 MHz, DMSO- $d_6$ ):  $\delta = 13.1, 41.8, 49.3, 108.3, 119.1, 122.5$  (q,  $J_{\text{CF}} = 272.7$  Hz), 124.6 (q,  $J_{\text{CF}} = 5.2$  Hz), 127.1, 127.4 (q,  $J_{\text{CF}} = 30.6$  Hz), 128.5, 131.0 (q,  $J_{\text{CF}} = 1.5$  Hz), 131.1, 132.3, 132.6, 138.0, 144.1, 146.6, 153.0, 165.5 ppm.

**5-(4'-Chloro-3'-(4''-((methoxycarbonyl)amino)butyl)-phenyl)-3-[(*N*-ethylbenzylamino) carbonylamino]-thiophen-2-carboxylic acid (23).**

**Scheme S3:** Synthesis of compound **23**:



**3'-Bromo-4'-chloro-acetophenone (23a)** was prepared from 4'-chloro-acetophenone [7]:  $\text{AlCl}_3$  (38.9 g, 0.29 mol) was slowly added to a solution of 4'-chloro-acetophenone (15.0 g, 97.7 mmol) in  $\text{CHCl}_2\text{CH}_3$  (250 mL) at 0 °C. Bromine (5.55 g, 0.11 mol) was added dropwise over 30 min. The resulting mixture was stirred for 72 h at room temperature. The reaction mixture was diluted with  $\text{CH}_2\text{Cl}_2$  (100 mL) and cautiously washed with aqueous NaOH (2M, 2 x 100 mL) and saturated aqueous NaCl (100 mL). The organic layer was dried ( $\text{MgSO}_4$ ) and the solvents were removed *in vacuo*. The crude product was crystallized from *n*-heptane affording 14.0 g of a crystalline solid. Orange crystals.

$^1\text{H}$  NMR (DMSO- $d_6$ , 300 MHz):  $\delta$  = 2.59 (s, 3 H), 7.78 (d,  $J$  = 8.4 Hz, 1 H), 7.93 (dd,  $J$  = 8.4, 2.0 Hz, 1 H), 8.24 (d,  $J$  = 2.0 Hz, 1 H) ppm.

**5-(3'-Bromo-4'-chlorophenyl)-3-[(*N*-ethylbenzylamino)carbonylamino]-thiophen-2-carboxylic acid (23b)** was prepared from 3'-bromo,4'-chloroacetophenone according to methods A–D. Yellow powder, m.p. 173–174 °C.  $^1\text{H}$  NMR (DMSO- $d_6$ , 300 MHz):  $\delta$  = 1.16 (t,  $J$  = 7.0 Hz, 3 H), 3.40 (q,  $J$  = 6.9 Hz, 2 H), 4.58 (s, 2 H), 7.07–7.45 (m, 5 H), 7.54–7.81 (m, 2 H), 8.04 (d,  $J$  = 1.8 Hz, 1 H), 8.31 (s, 1 H), 10.04 (s, 1 H), 13.49 (br. s, 1 H) ppm.  $^{13}\text{C}$  NMR (DMSO- $d_6$ , 75 MHz):  $\delta$  = 13.1, 41.8, 49.3, 107.9, 118.7, 122.5, 126.5, 127.1, 128.5, 130.4, 131.2, 133.3, 133.7, 138.0, 144.2, 146.6, 153.0, 165.6 ppm.

***N*-(Methoxycarbonyl)-3-butenylamine (23c)** was prepared from 4-pentenoic acid [8]: 4-Pentenoic acid (5.00 g, 50.0 mmol) and triethylamine (5.40 g, 53.0 mmol) were dissolved in toluene (75 mL). Diphenylphosphoryl azide (13.8 g, 50.2 mmol) was added via a syringe over 5 min and the resulting solution was heated for 2 h at 80 °C. The reaction was allowed to cool to 50 °C, MeOH (22 mL, 0.54 mol) was added and the resulting mixture was stirred at 50 °C for 14 h. The reaction mixture was cooled to room temperature and the solvents were removed under reduced pressure. The resulting yellow oil was diluted with Et<sub>2</sub>O (100 mL), water (50 mL) and a saturated aqueous solution of Na<sub>2</sub>CO<sub>3</sub> (10 mL). The aqueous layer was separated and extracted with Et<sub>2</sub>O (5 x 50 mL). The combined organic layers were washed with saturated NaCl (2 x 100 mL), dried (MgSO<sub>4</sub>) and concentrated to afford 5.00 g of a light brown oil. NMR purity ca. 90%. The compound was used in the next step without further purification.  $^1\text{H}$  NMR (300 MHz, CDCl<sub>3</sub>):  $\delta$  = 2.25 (m, 2 H), 3.25 (m, 2 H), 3.66 (s, 3 H, OCH<sub>3</sub>), 4.74 (br. s, 1 H, NH), 4.97–5.23 (m, 2 H), 5.75 (ddt,  $J$  = 17.1, 10.3, 6.8 Hz, 1 H) ppm.

The title compound **23** was prepared according to the following procedure: To a solution of **23c** (142 mg, 1.10 mmol) in anhydrous THF (1 mL) at 0 °C under nitrogen was added a solution of 9-BBN (0.5M in THF, 1.98 mL, 0.99 mmol). The mixture was allowed to warm to room temperature and stirred for 16 h. A solution of **23a** (300 mg, 0.61 mmol) in THF (3 mL), PdCl<sub>2</sub>(dppf) (17.4 mg, 3 Mol%) and aqueous NaOH (3M, 0.73 mL) were added and the reaction mixture was heated to reflux for 16 h. After cooling to room temperature the solvent was removed *in vacuo*. The crude material was purified via preparative HPLC (RP18, acetonitrile/H<sub>2</sub>O 50% → 95%). White powder, m.p. 62–65 °C.  $^1\text{H}$  NMR (300 MHz, acetone- $d_6$ ):  $\delta$  = 1.22 ppm (t,  $J$  = 7.1 Hz, 3 H), 1.55–1.82 (m, 4 H), 2.80–2.96 (m, 2 H), 3.11–3.27 (m, 2 H), 3.47 (q,  $J$  = 7.1 Hz, 2 H), 3.55 (s, 3 H, OCH<sub>3</sub>), 4.67 (s, 2 H), 6.20 (br. s, 1 H), 7.21–7.31 (m, 1 H), 7.31–7.43 (m, 4 H), 7.48 (d,  $J$  = 8.3 Hz, 1 H), 7.59 (dd,  $J$  = 8.3, 2.1 Hz, 1 H), 7.75 (d,  $J$  = 2.1 Hz, 1 H), 8.42 (s, 1 H), 10.17 (s, 1 H).  $^{13}\text{C}$  NMR (75 MHz, acetone- $d_6$ ):  $\delta$  = 13.6, 27.9, 33.8, 41.2, 41.3, 42.7, 50.5, 51.8, 107.4, 119.0, 126.0, 128.1, 128.5, 129.0, 129.5, 131.1, 133.4, 135.2, 139.5, 142.1, 148.4, 149.0, 154.3, 154.4, 157.8, 166.4 ppm.

**5-(3',4'-dichlorophenyl)-3-ureido-thiophen-2-carboxylic acid (24)**. The title compound was prepared from 3',4'-dichloroacetophenone according to methods A–D. Yellow powder, m.p. 217–218 °C.  $^1\text{H}$  NMR (300 MHz, DMSO- $d_6$ ):  $\delta$  = 6.76 (br. s, 2 H, NH<sub>2</sub>), 7.64 (dd,  $J$  = 8.4, 2.1 Hz, 2 H), 7.7 (d,  $J$  = 8.4 Hz, 1 H), 7.85 (s,  $J$  = 2.1 Hz, 1 H), 8.31 (s, 1 H), 9.29 (s, 1 H), 13.20 (br. s, 1 H, COOH) ppm.  $^{13}\text{C}$

NMR (75 MHz, DMSO- $d_6$ ):  $\delta$  = 107.8, 119.4, 125.9, 127.2, 131.4, 131.5, 132.1, 133.4, 143.6, 146.2, 154.6, 164.6 ppm.

**5-(3',4'-dichlorophenyl)-3-[(*N*-*i*-propylamino)carbonylamino]-thiophen-2-carboxylic acid (25).** The title compound was prepared from 3',4'-dichloroacetophenone according to methods A–D. Yellow powder, m.p. 212–214 °C.  $^1\text{H}$  NMR (300 MHz, DMSO- $d_6$ ):  $\delta$  = 1.11 (d,  $J$  = 6.5 Hz, 6 H), 3.77 (q,  $J$  = 6.5 Hz, 1 H), 7.58–7.65 (m, 2 H), 7.69 (d,  $J$  = 8.4 Hz, 1 H), 7.89 (d,  $J$  = 1.8 Hz, 1 H), 8.33 (s, 1 H), 9.24 (s, 1 H), 13.24 (br. s, 1 H, COOH) ppm.  $^{13}\text{C}$  NMR (75 MHz, DMSO- $d_6$ ):  $\delta$  = 22.7, 41.3, 107.3, 119.4, 125.8, 127.2, 131.4, 131.5, 132.1, 133.5, 143.6, 146.3, 153.0, 164.6 ppm.

**5-(3',4'-dichlorophenyl)-3-[(*N*-*n*-butylamino)carbonylamino]-thiophen-2-carboxylic acid (26).** The title compound was prepared from 3',4'-dichloroacetophenone according to methods A–D. Yellow powder, m.p. 216–217 °C.  $^1\text{H}$  NMR (300 MHz, DMSO- $d_6$ ):  $\delta$  = 0.89 (t,  $J$  = 7.3 Hz, 3 H), 1.26–1.48 (m, 4 H), 3.06–3.12 (m, 2 H), 7.64 (dd,  $J$  = 8.4, 2.1 Hz, 2 H), 7.70 (d,  $J$  = 8.4 Hz, 1 H), 7.89 (d,  $J$  = 2.1 Hz, 1 H), 8.32 (s, 1 H), 9.29 (s, 1 H), 13.18 (br. s, 1 H, COOH) ppm.  $^{13}\text{C}$  NMR (75 MHz, DMSO- $d_6$ ):  $\delta$  = 13.6, 19.5, 25.1, 31.5, 107.3, 119.4, 125.8, 127.2, 131.4, 131.5, 132.1, 133.4, 143.6, 146.3, 153.7, 164.6 ppm.

**5-(3',4'-dichlorophenyl)-3-[(*N*-*n*-pentylamino)carbonylamino]-thiophen-2-carboxylic acid (27).** The title compound was prepared from 3',4'-dichloroacetophenone according to methods A–D. Yellow powder, m.p. 213–215 °C.

$^1\text{H}$  NMR (300 MHz, DMSO- $d_6$ ):  $\delta$  = 0.87 (t,  $J$  = 6.8 Hz, 3 H), 1.26–1.31 (m, 4 H), .40–1.49 (m, 2 H), 3.05–3.11 (m, 2 H), 7.64 (dd,  $J$  = 8.4, 2.0 Hz, 1 H), 7.66 (br. s, 1 H), .69 (d,  $J$  = 2.0 Hz, 1 H), 7.89 (d,  $J$  = 8.4 Hz, 1 H), 8.32 (s, 1 H), 9.29 (s, 1 H), 13.19 (br. s, 1 H, COOH) ppm.  $^{13}\text{C}$  NMR (75 MHz, DMSO- $d_6$ ):  $\delta$  = 13.9, 21.8, 28.6, 29.1, 39.3, 107.3, 119.4, 125.8, 127.2, 131.4, 131.5, 132.1, 133.4, 143.6, 146.3, 153.7, 164.6 ppm.

**5-(3',4'-dichlorophenyl)-3-[(*N*-*n*-hexylamino)carbonylamino]-thiophen-2-carboxylic acid (28).** The title compound was prepared from 3',4'-dichloroacetophenone according to methods A–D. Beige powder, m.p. 198–200 °C.  $^1\text{H}$  NMR (300 MHz, DMSO- $d_6$ ):  $\delta$  = 0.86 (t,  $J$  = 6.9 Hz, 3 H), 1.27–1.45 (m, 8 H), 3.08 (m, 2 H), 7.64 (dd,  $J$  = 8.4, 2.1 Hz, 3 H), 7.68 (d,  $J$  = 8.4 Hz, 1 H), 7.89 (d,  $J$  = 2.1 Hz, 1 H), 8.32 (s, 1 H), 9.29 (s, 1 H), 13.18 (br. s, 1 H, COOH) ppm.  $^{13}\text{C}$  NMR (75 MHz, DMSO- $d_6$ ):  $\delta$  = 13.9, 22.1, 26.1, 29.4, 31.0, 39.3, 107.3, 119.4, 125.8, 127.2, 131.3, 131.4, 132.1, 133.4, 143.6, 146.3, 153.7, 164.6 ppm.

**5-(3',4'-dichlorophenyl)-3-[(*N*-phenylamino)carbonylamino]-thiophen-2-carboxylic acid (29).** The title compound was prepared from 3',4'-dichloroacetophenone according to methods A–D. Yellow powder, m.p. 219–220 °C.

$^1\text{H}$  NMR (300 MHz, DMSO- $d_6$ ):  $\delta$  = 7.01 (t,  $J$  = 7.4 Hz, 1 H), 7.30 (dd,  $J$  = 8.0, 7.4 Hz, 2 H), 7.53 (d,  $J$  = 8.0 Hz, 2 H), 7.64–7.68 (dd,  $J$  = 8.5, 1.5 Hz, 1 H), 7.72 (d,  $J$  = 8.5 Hz, 1 H), 7.95 (d,  $J$  = 1.5 Hz, 1 H), 8.37 (s, 1 H), 9.64 (s, 1 H), 10.02 (s, 1 H), 13.37 (br. s, 1 H, COOH) ppm.  $^{13}\text{C}$  NMR (75 MHz, DMSO- $d_6$ ):  $\delta$  = 108.8,

118.6, 119.5, 122.3, 125.9, 127.3, 128.8, 131.4, 131.6, 132.1, 133.3, 139.4, 143.9, 145.2, 151.3, 164.5 ppm.

**5-(3',4'-dichlorophenyl)-3-[(*N*-benzylamino)carbonylamino]-thiophen-2-carboxylic acid (30).** The title compound was prepared from 3',4'-dichloroacetophenone according to methods A–D. Yellow powder, m.p. 214–216 °C. <sup>1</sup>H NMR (300 MHz, DMSO-*d*<sub>6</sub>): δ = 4.32 (d, *J* = 5.7 Hz, 2 H), 7.23–7.37 (m, 5 H), 7.65 (dd, *J* = 8.4, 2.1 Hz, 1 H), 7.70 (d, *J* = 8.4 Hz, 1 H), 7.91 (d, *J* = 2.1 Hz, 1 H), 8.22 (t, *J* = 5.7 Hz, 1 H), 8.34 (s, 1 H), 9.43 (s, 1 H), 13.24 (br. s, 1 H, COOH) ppm. <sup>13</sup>C NMR (75 MHz, DMSO-*d*<sub>6</sub>): δ = 43.0, 107.7, 119.4, 125.9, 126.8, 127.2, 127.3, 128.3, 131.4, 131.5, 132.1, 133.4, 139.8, 143.7, 146.0, 153.8, 164.6 ppm.

**5-(3',4'-dichlorophenyl)-3-[(*N*-phenethylamino)carbonylamino]-thiophen-2-carboxylic acid (31).** The title compound was prepared from 3',4'-dichloroacetophenone according to methods A–D. Yellow powder, m.p. 205–207 °C. <sup>1</sup>H NMR (300 MHz, DMSO-*d*<sub>6</sub>): δ = 2.77 (t, *J* = 7.5 Hz, 2 H), 3.30–3.38 (m, 2 H), 7.17–7.34 (m, 5 H), 7.65 (dd, *J* = 8.5, 2.1 Hz, 1 H), 7.70 (d, *J* = 8.5 Hz, 1 H), 7.79 (t, *J* = 4.7 Hz, 1 H), 7.90 (d, *J* = 2.1 Hz, 1 H), 8.34 (s, 1 H), 9.32 (s, 1 H), 13.21 (br. s, 1 H, COOH) ppm. <sup>13</sup>C NMR (75 MHz, DMSO-*d*<sub>6</sub>): δ = 35.5, 40.9, 107.5, 119.4, 125.9, 126.1, 127.2, 128.3, 128.6, 131.4, 131.5, 132.1, 133.4, 139.5, 143.7, 146.1, 153.8, 164.6 ppm.

**5-(3',4'-dichlorophenyl)-3-[(*N*-methylphenylamino)carbonylamino]-thiophen-2-carboxylic acid (32).** The title compound was prepared from 3',4'-dichloroacetophenone according to methods A–D. Yellow powder, m.p. 215–216 °C. <sup>1</sup>H NMR (300 MHz, DMSO-*d*<sub>6</sub>): δ = 3.27 (s, 3 H, CH<sub>3</sub>), 7.38–7.54 (m, 5 H), 7.65 (d, *J* = 8.5 Hz, 1 H), 7.70 (d, *J* = 8.5 Hz, 1 H), 7.91 (s, 1 H), 8.34 (s, 1 H), 9.60 (s, 1 H), 13.25 (br. s, 1 H, COOH) ppm. <sup>13</sup>C NMR (75 MHz, DMSO-*d*<sub>6</sub>): δ = 37.0, 107.9, 118.3, 125.9, 127.3, 127.5, 127.9, 130.1, 131.4, 131.6, 132.1, 133.3, 141.9, 144.2, 146.0, 152.5, 165.0 ppm.

**5-(3',4'-dichlorophenyl)-3-[(*N*-methylbenzylamino)carbonylamino]-thiophen-2-carboxylic acid (33).** The title compound was prepared from 3',4'-dichloroacetophenone according to methods A–D. Yellow powder, m.p. 212–214 °C. <sup>1</sup>H NMR (300 MHz, DMSO-*d*<sub>6</sub>): δ = 3.02 (s, 3 H, CH<sub>3</sub>), 4.59 (s, 2 H), 7.25–7.39 (m, 5 H), 7.67 (dd, *J* = 8.5, 1.5 Hz, 1 H), 7.70 (d, *J* = 8.5 Hz, 1 H), 7.94 (d, *J* = 1.5 Hz, 1 H), 8.33 (s, 1 H), 10.03 (s, 1 H), 13.50 (br. s, 1 H, COOH) ppm. <sup>13</sup>C NMR (75 MHz, DMSO-*d*<sub>6</sub>): δ = 34.2, 51.3, 108.1, 118.7, 125.9, 127.2, 127.3, 128.6, 131.4, 131.6, 132.1, 133.3, 137.7, 144.3, 146.5, 153.4, 165.5 ppm.

**5-(3',4'-dichlorophenyl)-3-[(*N*-ethylphenylamino)carbonylamino]-thiophen-2-carboxylic acid (34).** The title compound was prepared from 3',4'-dichloroacetophenone according to methods A–D. Green powder, m.p. 210–212 °C. <sup>1</sup>H NMR (300 MHz, DMSO-*d*<sub>6</sub>): δ = 1.10 (t, *J* = 7.1 Hz, 3 H), 3.72 (q, *J* = 7.1 Hz, 2 H), 7.38–7.55 (m, 5 H), 7.65 (dd, *J* = 8.5, 2.1 Hz, 1 H), 7.70 (d, *J* = 8.5 Hz, 1 H), 7.92 (d, *J* = 2.1 Hz, 1 H), 8.35 (s, 1 H), 9.47 (s, 1 H), 13.21 (br. s, 1 H, COOH) ppm. <sup>13</sup>C NMR (75 MHz, DMSO-*d*<sub>6</sub>): δ = 13.4, 43.7, 107.8, 118.4, 125.9, 127.3, 128.3, 128.7, 130.2, 131.4, 131.6, 132.1, 133.3, 139.9, 144.2, 146.0, 152.1, 165.0 ppm.

**5-(3',4'-dichlorophenyl)-3-[(*N*-*n*-propylbenzylamino)carbonylamino]-thiophen-2-carboxylic acid (35).** The title compound was prepared from 3',4'-dichloroacetophenone according to methods A–D. Yellow powder, m.p. 195–197 °C. <sup>1</sup>H NMR (300 MHz, DMSO-*d*<sub>6</sub>): δ = 0.88 (t, *J* = 7.5 Hz, 3 H), 1.55–1.67 (m, 2 H), 3.29 (t, *J* = 7.5 Hz, 2 H), 4.59 (s, 2 H), 7.24–7.37 (m, 5 H), 7.65–7.71 (m, 2 H), 7.93–7.95 (m, 1 H), 8.33 (s, 1 H), 10.07 (s, 1 H), 13.53 (br. s, 1 H, COOH) ppm. <sup>13</sup>C NMR (75 MHz, DMSO-*d*<sub>6</sub>): δ = 11.0, 21.0, 48.9, 49.8, 107.9, 118.7, 125.9, 127.1, 127.3, 128.5, 131.4, 131.6, 132.1, 133.3, 138.1, 144.4, 146.6, 153.1, 165.7 ppm.

**5-(3',4'-dichlorophenyl)-3-[(*N*-*n*-propylphenethylamino)carbonylamino]-thiophen-2-carboxylic acid (36).** The title compound was prepared from 3',4'-dichloroacetophenone according to methods A–D. White powder, m.p. 178–179 °C. <sup>1</sup>H NMR (300 MHz, DMSO-*d*<sub>6</sub>): δ = 0.88 (t, *J* = 7.4 Hz, 3 H), 1.60 (m, 2 H), 2.89 (t, *J* = 7.4 Hz, 2 H), 3.25 (t, *J* = 7.4 Hz, 2 H), 3.50 (t, *J* = 7.4 Hz, 2 H), 7.19–7.32 (m, 5 H), 7.65–7.71 (m, 2 H), 7.93 (m, 1 H), 8.33 (s, 1 H), 10.03 (s, 1 H), 13.56 (br. s, 1 H, COOH) ppm. <sup>13</sup>C NMR (75 MHz, DMSO-*d*<sub>6</sub>): δ = 11.0, 21.2, 34.1, 49.0, 49.1, 197.7, 118.7, 125.9, 126.2, 127.3, 128.4, 128.8, 131.4, 131.6, 132.1, 133.3, 138.7, 144.4, 146.7, 152.6, 165.8 ppm.

**5-(3',4'-dichlorophenyl)-3-[(*N*-*n*-butylphenylamino)carbonylamino]-thiophen-2-carboxylic acid (37).** The title compound was prepared from 3',4'-dichloroacetophenone according to methods A–D. Green powder, m.p. 187–188 °C. <sup>1</sup>H NMR (300 MHz, DMSO-*d*<sub>6</sub>): δ = 0.87 (t, *J* = 7.1 Hz, 3 H), 1.17–1.51 (m, 4 H), 3.69 (t, *J* = 7.3 Hz, 2 H), 7.37–7.70 (m, 7 H), 7.87–7.95 (m, 1 H), 8.35 (s, 1 H), 9.48 (s, 1 H), 13.21 (br. s, 1 H, COOH) ppm. <sup>13</sup>C NMR (75 MHz, DMSO-*d*<sub>6</sub>): δ = 13.7, 19.3, 29.8, 48.4, 107.7, 118.4, 125.9, 127.3, 128.2, 128.6, 130.2, 131.4, 131.6, 132.1, 133.3, 140.2, 144.2, 146.1, 152.4, 165.0 ppm.

**5-(3',4'-dichlorophenyl)-3-[(*N*-*n*-butylbenzylamino)carbonylamino]-thiophen-2-carboxylic acid (38).** The title compound was prepared from 3',4'-dichloroacetophenone according to methods A–D. Yellow powder, m.p. 193–194 °C. <sup>1</sup>H NMR (300 MHz, DMSO-*d*<sub>6</sub>): δ = 0.88 (t, *J* = 7.4 Hz, 3 H), 1.24–1.36 (m, 2 H), 1.50–1.65 (m, 2 H), 3.26–3.38 (m, 2 H), 4.59 (s, 2 H), 7.26–7.35 (m, 5 H), 7.60–7.70 (m, 2 H), 7.90–7.96 (m, 1 H), 8.33 (s, 1 H), 10.06 (s, 1 H), 13.52 (br. s, 1 H, COOH) ppm. <sup>13</sup>C NMR (75 MHz, DMSO-*d*<sub>6</sub>): δ = 13.6, 19.5, 29.8, 47.0, 49.8, 107.9, 118.7, 125.9, 127.1, 127.3, 128.5, 131.4, 131.6, 132.1, 133.3, 138.1, 144.4, 146.6, 153.1, 165.7 ppm.

**5-(3',4'-dichlorophenyl)-3-[(*N*-*n*-butylphenethylamino)carbonylamino]-thiophen-2-carboxylic acid (39).** The title compound was prepared from 3',4'-dichloroacetophenone according to methods A–D. White powder, m.p. 178–179 °C. <sup>1</sup>H NMR (300 MHz, DMSO-*d*<sub>6</sub>): δ = 0.88 (t, *J* = 7.3 Hz, 3 H), 1.24–1.37 (m, 2 H), 1.50–1.60 (m, 2 H), 2.89 (t, *J* = 7.8 Hz, 2 H), 3.28 (t, *J* = 7.3 Hz, 2 H), 3.50 (t, *J* = 7.8 Hz, 2 H), 7.19–7.32 (m, 5 H), 7.65–7.72 (m, 2 H), 7.94 (d, *J* = 1.5 Hz, 1 H), 8.33 (s, 1 H), 10.03 (s, 1 H), 13.54 (br. s, 1 H, COOH) ppm. <sup>13</sup>C NMR (75 MHz, DMSO-*d*<sub>6</sub>): δ = 13.7, 19.6, 30.1, 34.1, 47.1, 49.1, 107.7, 118.7, 125.9, 126.2, 127.3, 128.4, 128.8, 131.4, 131.6, 132.1, 133.3, 138.7, 144.3, 146.7, 152.6, 165.8 ppm.

**5-(3',4'-dichlorophenyl)-3-[(*N*-dibenzylamino)carbonylamino]-thiophen-2-carboxylic acid (40).** The title compound was prepared from 3',4'-dichloroacetophenone according to methods A–D. White powder, m.p. 190–191 °C.

<sup>1</sup>H NMR (300 MHz, DMSO-*d*<sub>6</sub>): δ = 4.64 (s, 4 H), 7.26–7.38 (m, 10 H), 7.65–7.71 (m, 2 H), 7.92–7.94 (m, 1 H), 8.35 (s, 1 H), 10.08 (s, 1 H), 12.66 (br. s, 1 H, COOH) ppm. <sup>13</sup>C NMR (75 MHz, DMSO-*d*<sub>6</sub>): δ = 49.9, 50.1, 118.8, 125.9, 127.1, 127.3, 127.3, 128.6, 128.6, 128.9, 130.0, 131.4, 131.6, 131.8, 132.1, 133.3, 137.2, 137.2, 144.2, 146.2, 153.5, 165.4 ppm.

**6.1.5 HPLC purity****Table S3.** Purity and retention times of compounds **3–40**.

Compound	Purity [%]	Retention time [min] <sup>a</sup>
3	100	14.52
4	99	18.61
5	95	14.80
6	100	16.33
7	96	18.84
8	99	13.38
9	98	13.51
10	96	14.09
11	98	14.59
12	98	13.47
13	97	12.61
14	99	14.69
15	99	14.57
16	97	14.44
17	98	13.40
18	100	15.45
19	99	15.14
20	99	14.80
21	95	15.64
22	97	15.29
23	95	14.49
24	100	11.24
25	98	13.45
26	99	14.09
27	100	15.05
28	100	15.63
29	98	15.00
30	96	14.25
31	97	14.64
32	98	14.56
33	96	14.85
34	99	15.36
35	98	15.91
36	99	16.58
37	95	16.30
38	99	16.44
39	98	16.93
40	96	16.36

<sup>a</sup> In a gradient run the percentage of acetonitrile (containing 0.1% trifluoroacetic acid) was

### 6.1.6 References

- [1] C. Hansch and A. Leo, *Substituent Constants for Correlation Analysis in Chemistry and Biology*. Wiley-Interscience, New York, 1979.
- [2] H. Hartmann, J. Liebscher, A simple method for the synthesis of 5-aryl-3-amino-2-alkoxycarbonylthiophenes, *Synthesis* (1984) 275–276.
- [3] F. Fabis, S. Jolivet-Fouchet, M. Robba, H. Landelle, S. Rault, Thiaisatoic anhydrides: Efficient synthesis under microwave heating conditions and study of their reactivity, *Tetrahedron* 54 (1998) 10789–10800.
- [4] L. Foulon, E. Braud, F. Fabis, J.C. Lancelot, S. Rault, Synthesis and combinatorial approach of the reactivity of 6-and 7-arylthieno [3,2-d][1,3] oxazine-2,4-diones. *Tetrahedron* 59 (2003) 10051–10057.
- [5] F.X. Le Foulon, E. Braud, F. Fabis, J.C. Lancelot, S. Rault, Solution-phase parallel synthesis of a 1140-member ureidothiophene carboxylic acid library. *J. Comb. Chem.* 7 (2005) 253–257.
- [6] T. Schareina, A. Zapf, M. Beller, Improving palladium-catalyzed cyanation of aryl halides: development of a state-of-the-art methodology using potassium hexacyanoferrate(II) as cyanating agent. *J. Organomet. Chem.* 689 (2004) 4576–4583.
- [7] M.K. Ameriks, S.D. Bembenek, M.T. Burdett, I.C. Choong, J.P. Edwards, D. Gebauer, Y. Gu, L. Karlsson, H.E. Purkey, B.L. Staker, S. Sun, R.L. Thurmond, J. Zhu, Diazinones as P2 replacements for pyrazole-based cathepsin S inhibitors. *Bioorg. Med. Chem. Lett.* 20 (2010) 4060–4064.
- [8] J.R. Dunetz, R.L. Danheiser, Synthesis of Highly Substituted Indolines and Indoles via Intramolecular [4+2] Cycloaddition of Ynamides and Conjugated Enynes. *J. Am. Chem. Soc.* 127 (2005) 5776–5777.
- [9] F. Arhin, O. Bélanger, S. Ciblat, M. Dehbi, D. Delorme, E. Dietrich, D. Dixit, Y. Lafontaine, D. Lehoux, J. Liu, G.A. McKay, G. Moeck, R. Reddy, Y. Rose, R. Srikumar, K.S.E. Tanaka, D.M. Williams, P. Gros, J. Pelletier, T.R. Parr, A.R. Far, A new class of small molecule RNA polymerase inhibitors with activity against rifampicin-resistant *Staphylococcus aureus*. *Bioorgan. Med. Chem.* 14 (2006) 5812–5832.

## 6.2 Supporting Information for Publication B

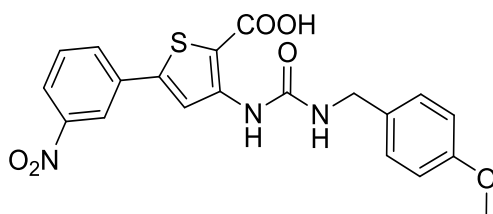
Full supporting information is available online:

[http://pubs.acs.org/doi/suppl/10.1021/cb5005433/suppl\\_file/cb5005433\\_si\\_001.pdf](http://pubs.acs.org/doi/suppl/10.1021/cb5005433/suppl_file/cb5005433_si_001.pdf)

### 6.2.1 Supplemental experimental procedures

**Intrinsic fluorescence quenching assay.** Intrinsic fluorescence quenching assay was performed as described by *Mukhopadhyay et al.* (1) with slight modifications. Fluorescence emission intensities of RNAP core enzyme in TB [100  $\mu$ l; 50 mM Tris-HCl (pH 8.0), 100 mM KCl, 10 mM MgCl<sub>2</sub>, 1 mM dithiothreitol, 0.01 % Tween 20, 5% glycerol] were measured before and 10 min after addition of the inhibitors [10  $\mu$ l; TB, 50% DMSO]. Employing a Polarstar Omega (BMG Labtech, Ortenberg, Germany) 280 nm and 350 nm were chosen as excitation and emission wavelengths, respectively. The observed reductions of intrinsic fluorescence at each inhibitor concentration were corrected for dimethyl sulfoxide/ buffer dilution and the inner-filter effect using N-acetyltryptophanamide. Data were plotted as percent quenching of the intrinsic fluorescence in dependence of inhibitor concentration. The highest observed quenching was set at 100%. Data are means of three independent determinations. For non-linear regression analysis GraphPad Prism 5 (GraphPad Software, La Jolla, CA, USA) was used. Experimental data of rifampicin was fitted to a one-site binding model, whereas data of compound 6, which showed a biphasic quenching, was fitted to a two-affinity model (2) as demonstrated by *Döppenschmitt et al.* (3) earlier.

#### 3-(3-(4-Methoxybenzyl)ureido)-5-(3-nitrophenyl)thiophene-2-carboxylic acid



The title compound was prepared from 3'-nitroacetophenone according to the general procedures A-D. <sup>1</sup>H NMR (DMSO-d<sub>6</sub>, 300 MHz):  $\delta$  = 13.22 (br. s, 1H), 9.41 (s, 1H), 8.44 (s, 1H), 8.37 (t,  $J$  = 1.7 Hz, 1H), 8.23 (dd,  $J$  = 1.7, 8.1 Hz, 1H), 8.09–8.20 (m 2H), 7.75 (t,  $J$  = 8.1 Hz, 1H), 7.24 (d,  $J$  = 8.6 Hz, 2H), 6.90 (d,  $J$  = 8.6 Hz, 2H), 4.24 (d,  $J$  = 5.6 Hz, 2H), 3.73 (s, 3H) ppm. <sup>13</sup>C NMR (DMSO-d<sub>6</sub>, 75 MHz):  $\delta$  = 164.5, 158.3, 153.8, 148.4, 146.1, 143.8, 134.2, 131.9, 131.6, 131.0, 128.7, 123.5, 119.8, 119.6, 113.7, 107.9, 55.0, 42.5 ppm. HPLC-Purity: 96.3 %

## 6.2.2 Supplemental figures

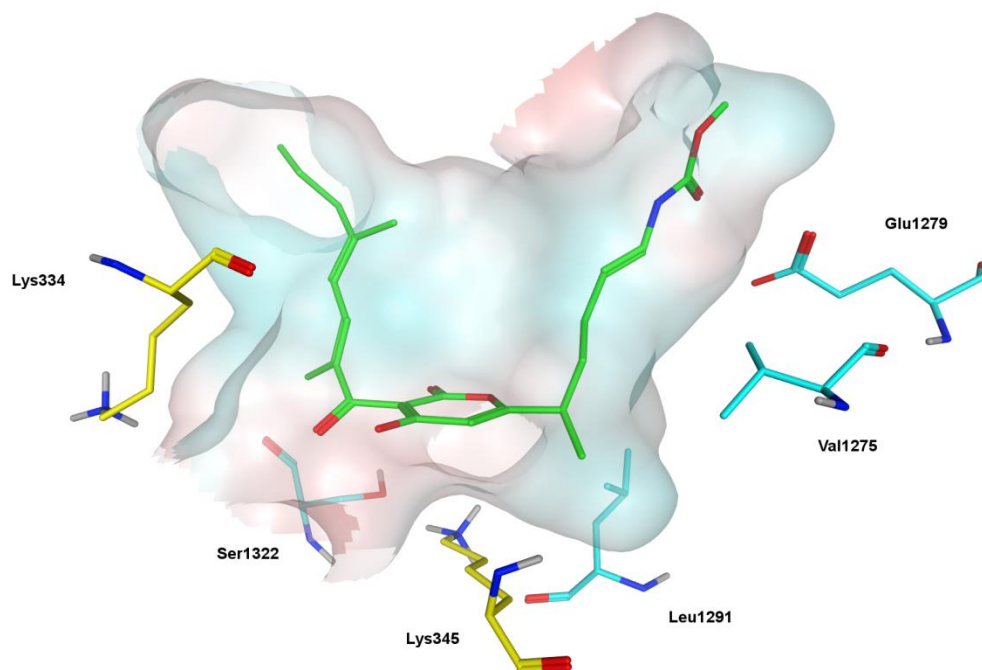


**Figure S1.** Myx binding pocket including mutated amino acids. Myxopyronin A is colored in green.  $\beta$  subunit amino acids are colored in turquoise,  $\beta'$  subunit amino acids are colored in yellow.

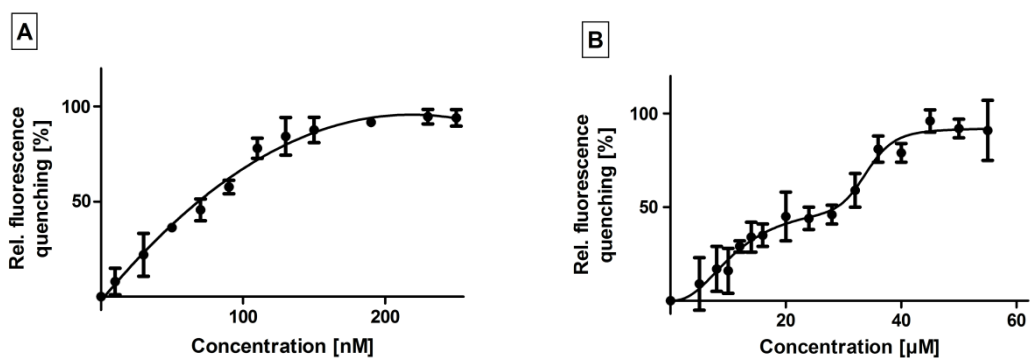


**Figure S2.** Effect of increasing inhibitor concentrations on the intrinsic fluorescence of RNAP. (A) rifampicin (B) **6**

For rifampicin, as expected and as already shown for myxopyronin (1), a monophasic curve progression was obtained, meaning that the compound is binding to a single binding site.

In contrast, **6** exhibits a biphasic character of the curve indicating that the compounds bind to more than one single binding site

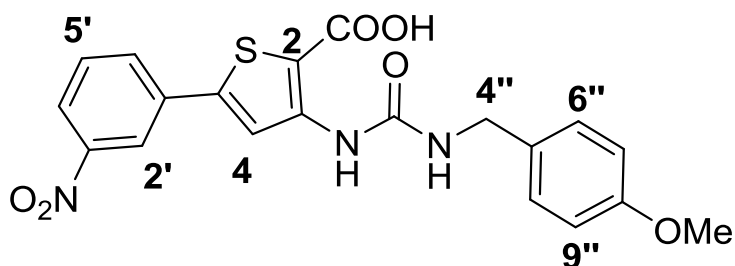


**Figure S3.** Numbering of atoms of compound 13.

### 6.2.3 Supplemental tables

**Table S1.** Antibigram of the MRSA strains

Antibiotic MRSA	/	COL	USA300 Lac	5191	R44
ampicillin		R	R	R	R
oxacillin		R	R	R	R
gentamicin		S	S	S	S
ciprofloxacin		S	R	R	S
moxifloxacin		S	I	R	S
erythromycin		S	R	R	R
clindamycin		S	S	R	R
linezolid		S	S	S	S
daptomycin		S	S	S	S
vancomycin		S	S	S	S
tetracyclin		R	S	S	R
tigecycline		S	S	S	S
fosfomicin		S	S	R	S
fusidinsäure		S	S	S	S
rifampicin		S	S	S	S
trimethoprim/sulfamethoxazol		S	S	S	R

R, resistant; I, intermediary resistant; S, susceptible

**Table S2.** MIC value determination in *Ec* TolC “switch region” mutants

Compd	<i>Ec</i> TolC wild type MIC [ $\mu\text{g/ml}$ ]	<i>Ec</i> TolC $\beta'$ K334G MIC [ $\mu\text{g/ml}$ ]	<i>Ec</i> TolC $\beta'$ K334E MIC [ $\mu\text{g/ml}$ ]	<i>Ec</i> TolC $\beta'$ K345T MIC [ $\mu\text{g/ml}$ ]	<i>Ec</i> TolC $\beta'$ K345N MIC [ $\mu\text{g/ml}$ ]	<i>Ec</i> TolC $\beta$ V1275M MIC [ $\mu\text{g/ml}$ ]	<i>Ec</i> TolC $\beta$ E1279K MIC [ $\mu\text{g/ml}$ ]	<i>Ec</i> TolC $\beta$ L1291F MIC [ $\mu\text{g/ml}$ ]
<b>A1</b>	12.5–25	25	> 25	>25	25	25	25	25
<b>A2</b>	25	12.5	> 25	12.5–25	25	25	25	12.5–25
<b>A4</b>	25	50	> 50	25–50	50	25	25	25
<b>A5</b>	12.5	25	> 25	12.5–25	12.5	25	12.5	12.5
<b>A7</b>	25	25	> 50	25–50	25	25	25	25
<b>Myx</b>	1.25	10	> 10	> 25	> 25	> 25	> 25	2.5
<b>Rif</b>	6.25	6.25	6.25	12.5	12.5	12.5	6.25–12.5	6.25–12.5

**Table S3.** *In vitro* transcription assay with wild type/ mutant RNAPs

Compd	RNAP wild type IC <sub>50</sub> [μM]	RNAP β S1322E IC <sub>50</sub> [μM]	RNAP β' Δ334–5 IC <sub>50</sub> [μM]	RNAP β' K334A IC <sub>50</sub> [μM]	RNAP β' K334E IC <sub>50</sub> [μM]	RNAP β' K345A IC <sub>50</sub> [μM]
<b>A1</b>	21.3 ± 0.1	18.7 ± 0.9	22.1 ± 1.8	23 ± 0.1	21.6 ± 1.3	16.6 ± 2
<b>A5</b>	18.8 ± 1.9	17.9 ± 1.3	21.7 ± 3.9	20.5 ± 2.9	nd <sup>a</sup>	12.2 ± 0.5
<b>A7</b>	35.4 ± 0.8	34.8 ± 2.5	35.3 ± 2.3	32.8 ± 5.2	33.6 ± 0.3	27.5 ± 4.9
<b>A8</b>	11.6 ± 0.7	9.4 ± 1.9	10.3 ± 0.5	9.9 ± 0.5	7.7 ± 0.1	7.3 ± 1.2
<b>A10</b>	22.6 ± 0.1	20.7 ± 0.8	22.1 ± 0.8	21.5 ± 1.8	24 ± 4.7	19.6 ± 1.6
<b>A11</b>	16.5 ± 2.9	12.5 ± 0.1	15.7 ± 0.6	15.6 ± 0.8	nd <sup>a</sup>	12.8 ± 0.3
<b>B2</b>	16.5 ± 1.3	13.9 ± 0.7	15.5 ± 1.5	14.8 ± 2.4	13.3 ± 1.5	12.6 ± 0.5
<b>Myx</b>	0.28 ± 0.02	5.4 ± 0.1	0.63 ± 0.09	0.13 ± 0.02	0.49 ± 0.10	> 4
<b>Rif</b>	33.6 ± 2.3 <sup>b</sup>	> 500 <sup>b</sup>	12.5 ± 1.6 <sup>b</sup>	21 ± 0.6 <sup>b</sup>	nd <sup>a</sup>	19 ± 1 <sup>b</sup>

<sup>a</sup> nd: not determined, <sup>b</sup>: IC<sub>50</sub> [nM]

**Table S4.** Plasmid details. Plasmid pVS10, the pIA-derivatives and MF10 encode the *E. coli* rpoA-rpoB -rpoC [His6] and rpoZ ORFs under control of a T7 promoter (4). Plasmid pRL663 encodes C-terminally hexahistidine-tagged *E. coli* RNAP  $\beta'$  subunit under control of a  $\beta$  tac promoter (5). Plasmid pRL706 encodes C-terminally hexahistidine-tagged *E. coli* RNAP  $\beta$  subunit under control of a trc promoter (6).

Plasmid	Amino Acid Substitution	RNAP subunit
pVS10	-	-
pIA878	S1322E	$\beta$
pIA879	K334A	$\beta'$
pIA882	K345A	$\beta'$
pIA883	$\Delta$ 334-5	$\beta'$
MF10	K334E	$\beta'$
pRL663 derivative	K345N	$\beta'$
pRL663 derivative	K345T	$\beta'$
pRL706 derivative	V1275M	$\beta$
pRL706 derivative	L1291F	$\beta$

#### 6.2.4 Supplemental references

- Mukhopadhyay, J., Das, K., Ismail, S., Koppstein, D., Jang, M., Hudson, B., Sarafianos, S., Tuske, S., Patel, J., Jansen, R., Irschik, H., Arnold, E., and Ebright, R.-H. (2008) *Cell* 135, 295–307.
- J. W. Wells. Analysis and interpretation of binding at equilibrium. In: E. C. Hulme (ed.) *Receptor-Ligand Interactions*, IRL Press, Oxford (1992), 288–349.
- Döppenschmitt, S., Spahn-Langguth, H., Regårdh C.-G., Langguth, P. (1998) *Pharm. Res.* 15 (7), 1001–6.
- Belogurov, G.-A., Vassilyeva, M.-N., Svetlov, V., Klyuyev, S., Grishin, N.-V., Vassilyev, D.-G., and Artsimovitch, I. (2007) *Mol. Cell* 26, 117–129.
- Wang, D., Meier, T., Chan, C., Feng, G., Lee, D., and Landick, R. (1995) *Cell* 81 (3), 341–350.
- Severinov, K., Mooney, R., Darst, S.-A., and Landick, R. (1997) *J. Biol. Chem.* 272 (39), 24137–24140.
- Hartmann, H., Liebscher, J. (1984) *Synthesis* 3, 275–276.
- Fabis, F., Jolivet-Fouchet, S., Robba, M., Landelle, H., Rault, S. (1998) *Tetrahedron* 54, 10789–10800.
- Foulon, L., Braud, E., Fabis, F., Lancelot, J.-C., and Rault, S. (2003), *Tetrahedron* 59, 10051–10057.
- Le Foulon, F.-X., Braud, E., Fabis, F., Lancelot, J.-C., and Rault, S. (2005) *J. Comb. Chem.* 7, 253–257.

## 6.3 Supporting Information for Publication C

Full supporting information is available online:

[http://onlinelibrary.wiley.com/store/10.1002/cbic.201402666/asset/supinfo/cbic\\_201402666\\_sm\\_miscellaneous\\_information.pdf?v=1&s=74c688f0c2861498377e6c59b4952a528743ef18](http://onlinelibrary.wiley.com/store/10.1002/cbic.201402666/asset/supinfo/cbic_201402666_sm_miscellaneous_information.pdf?v=1&s=74c688f0c2861498377e6c59b4952a528743ef18)

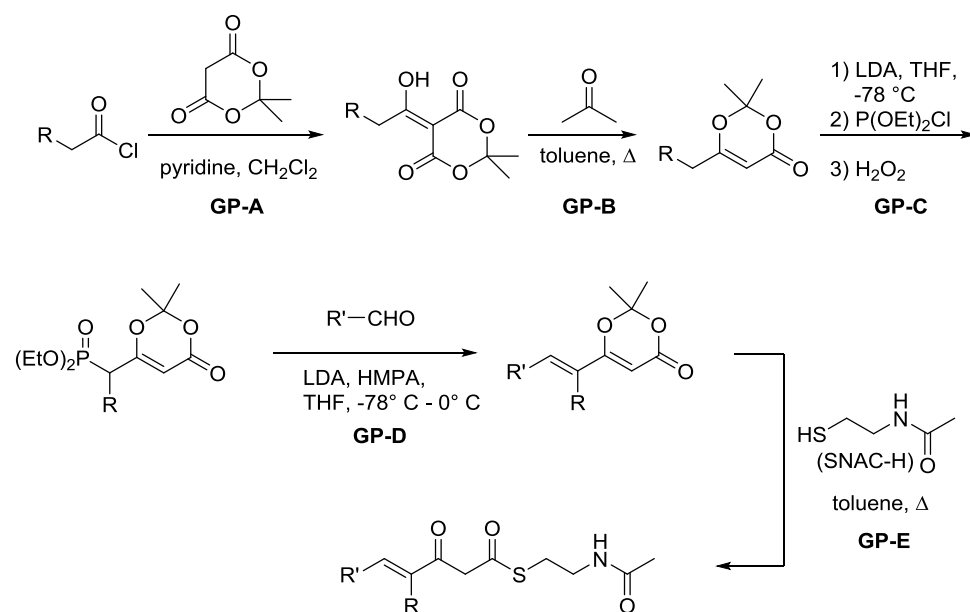
### 6.3.1 Experimental procedures

#### 6.3.1.1 Chemistry

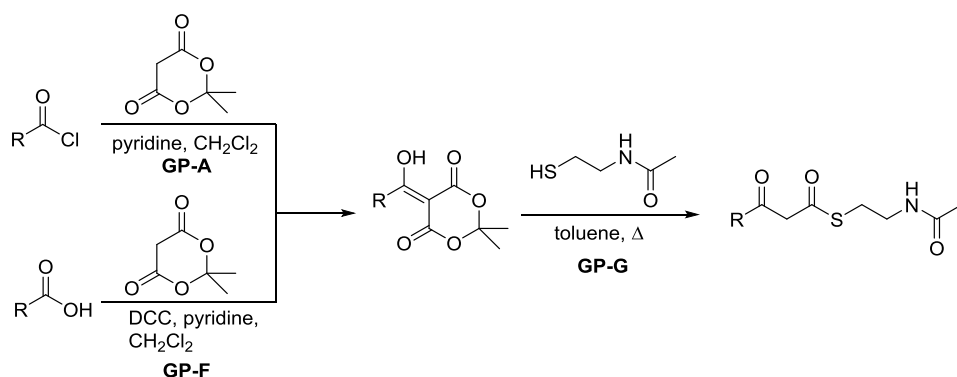
##### Materials and methods

Starting materials were purchased from commercial suppliers and used without further purification. Column flash chromatography was performed on silica gel (40–63  $\mu\text{M}$ ), and reaction progress was monitored by TLC on TLC Silica Gel 60 F<sub>254</sub> (Merck). All moisture-sensitive reactions were performed under nitrogen atmosphere using oven-dried glassware and anhydrous solvents.  $^1\text{H}$  and  $^{13}\text{C}$  NMR spectra were recorded on Bruker Fourier spectrometers (500/300 or 126/75 MHz) at ambient temperature with the chemical shifts recorded as  $\delta$  values in ppm units by reference to the hydrogenated residues of deuterated solvent as internal standard. Coupling constants ( $J$ ) are given in Hz and signal patterns are indicated as follows: s, singlet; d, doublet; dd, doublet of doublets; t, triplet; q, quartet; quin, quintet; sxt, sextet; m, multiplet, br., broad signal.

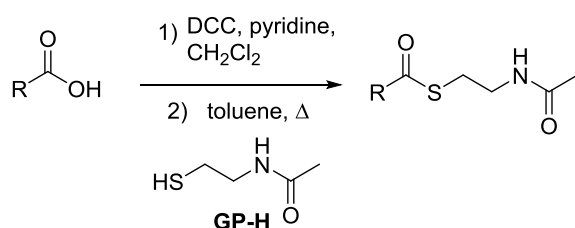
##### Synthesis and spectroscopic data of compounds 1–18



**Scheme 1: General Synthesis of unsaturated  $\beta$ -keto-*N*-acetylcysteine (SNAC)-esters**



**Scheme 2: General synthesis of  $\beta$ -keto-*N*-acetylcysteine (SNAC)-esters.**



**Scheme 3: Synthesis of *N*-acetylcysteine (SNAC)-esters**

### Precursor compounds could be synthesized by the following methods:

General Procedure **A** for synthesis of acylmeldrums acids from acyl chlorides:<sup>[1]</sup> To a solution of meldrums acid (10.8 g, 75.0 mmol) and pyridine (12.0 g, 0.15 mol) in anhydrous  $\text{CH}_2\text{Cl}_2$  (50 mL) at 0 °C was added dropwise a solution of the appropriate acyl chloride (80.0 mmol) in anhydrous  $\text{CH}_2\text{Cl}_2$  (20 mL). The resulting orange mixture was stirred for 1 h at 0 °C and then for 1 h at room temperature. The reaction mixture was diluted with  $\text{CH}_2\text{Cl}_2$  (50 mL) and washed with aqueous 2M HCl (3 x 50 mL), brine (2 x 50 mL), dried ( $\text{MgSO}_4$ ) and concentrated under reduced pressure. The crude material was filtered over a short pad of  $\text{SiO}_2$  eluting with *n*-hexane/ EtOAc 2:1.

General Procedure **B** for synthesis of oxinones from acylmeldrums acids:<sup>[2]</sup> The appropriate acylmeldrums acid (20.0 mmol) was dissolved in toluene (25 mL) and acetone (2.0 mL). The solution was heated under reflux for 2 h. The solvents were removed under reduced pressure and the crude material was purified by flash chromatography ( $\text{SiO}_2$ , *n*-hexane/EtOAc) or vacuum distillation.

General Procedure **C** for synthesis of dioxinon phosphonates:<sup>[3]</sup> To a solution of diisopropylamine (7.18 mL, 51.1 mmol) in THF (30 mL) was added dropwise a solution of *n*-BuLi (2.5M in *n*-hexane, 20.5 mL, 51.1 mmol) at 0 °C. After stirring for 30 minutes, the reaction mixture was cooled to -78 °C and the appropriate 2,2-dimethyl-4*H*-1,3-dioxin-4-one (36.5 mmol) was added over 5 min. After 40 min chlorodiethylphosphite (7.62 mL, 53.0 mmol) was added and the cooling bath was removed. When the mixture reached room temperature, it was diluted with

Et<sub>2</sub>O (200 mL), washed with half-saturated brine (100 mL), dried (MgSO<sub>4</sub>) and concentrated *in vacuo*. The resulting yellow oil was dissolved in CH<sub>2</sub>Cl<sub>2</sub> (60 mL) and aqueous H<sub>2</sub>O<sub>2</sub> (30%, 13 mL) was carefully added at 0 °C. The solution was stirred for 1 h and diluted with EtOAc (200 mL). After separation, the organic layer was washed with brine (2 x 100 mL), dried (MgSO<sub>4</sub>) and concentrated *in vacuo*. The crude material was purified by flash chromatography (SiO<sub>2</sub>, EtOAc).

General Procedure **D** for the Horner-Wadsworth-Emmons olefination for the preparation of unsaturated dioxinones:<sup>[4]</sup> To a solution of diisopropylamine (1.04 mL, 7.13 mmol) in THF (20 mL) was added a solution of *n*-BuLi (2.5M in *n*-hexane, 2.85 mL, 7.13 mmol) at 0 °C. After stirring for 30 min, the reaction mixture was cooled to -78 °C. A solution of the appropriate phosphonate (6.84 mmol) in THF (10 mL) was added to the reaction mixture, and the resulting mixture was warmed to 0 °C and stirred for 15 min. After cooling to -78 °C, HMPA (2.10 mL, 12.1 mmol) was added and stirring was continued for 30 min. A solution of the appropriate aldehyde (6.84 mmol) in THF (10 mL) was added slowly. The reaction mixture was allowed to warm slowly to 0 °C and stirred for 1 h. After diluting with EtOAc (80 mL), the mixture was washed with saturated aqueous NH<sub>4</sub>Cl (3 x 40 mL) and brine (50 mL). The organic layer was dried (MgSO<sub>4</sub>) and concentrated. The crude material was purified by flash chromatography (SiO<sub>2</sub>, *n*-hexane/EtOAc).

General procedure **E** for synthesis of β-keto-*N*-acetylcysteamine (SNAC)-esters from dioxinones:<sup>[5]</sup> A degassed solution of the appropriate dioxinone (0.95 mmol), *N*-acetylcysteamine (SNAC-H, 0.15 g, 1.25 mmol) in toluene (6 mL) was refluxed for 16 h under a nitrogen atmosphere. After cooling to room temperature the solvent was evaporated under reduced pressure and the crude product was purified by flash column chromatography (SiO<sub>2</sub>, *n*-hexane/EtOAc = 1:1 → EtOAc) to afford the desired SNAC ester.

General procedure **F** for synthesis of acylmeldrums acids from carboxylic acids via DCC coupling:<sup>[6]</sup> A solution of the appropriate acid (10.6 mmol) and DCC (2.19 g, 10.6 mmol) in anhydrous CH<sub>2</sub>Cl<sub>2</sub> (20 mL) was stirred for 30 min at 0°C. A white solid precipitated. DMAP (1.94 g, 15.9 mmol) and meldrums acid (1.52 g, 10.6 mmol) were subsequently added. The cooling bath was removed and the reaction mixture was stirred for 2 h at room temperature. The insoluble urea was filtered off and the filter-cake was washed with ice-cold CH<sub>2</sub>Cl<sub>2</sub> (10 mL). The combined filtrates were washed with 1M HCl (2 x 50 mL), H<sub>2</sub>O (2 x 50 mL) and brine (75 mL), dried (MgSO<sub>4</sub>) and concentrated. To remove last residues of urea, the crude material was filtered over cotton.

General procedure **G** for synthesis of β-keto-*N*-acetylcysteamine (SNAC)-esters from acylmeldrums acids:<sup>[5]</sup> A degassed solution of the appropriate acylmeldrums acid (0.80 mmol), *N*-acetylcysteamine (SNAC-H, 0.12 g, 1.00 mmol) in toluene (6 mL) was refluxed for 16 h under a nitrogen atmosphere. After cooling to room temperature the solvent was evaporated under reduced pressure and the crude product was purified by flash column chromatography (SiO<sub>2</sub>, *n*-hexane/EtOAc = 1:1 → EtOAc) to afford the desired β-keto-SNAC ester.

General procedure **H** for synthesis of *N*-acetylcysteamine (SNAC)-esters from carboxylic acids via DCC coupling: A solution of the appropriate acid (1.06 mmol)

and DCC (0.41 g, 1.06 mmol) in anhydrous CH<sub>2</sub>Cl<sub>2</sub> (5 mL) was stirred for 30 min at 0°C. A white solid precipitated. DMAP (0.37 g, 1.59 mmol) and SNAC-H (0.24 g, 1.06 mmol) were subsequently added. The cooling bath was removed and the reaction mixture was stirred for 2 h at room temperature. The insoluble urea was filtered off and the filter-cake was washed with ice-cold CH<sub>2</sub>Cl<sub>2</sub> (10 mL). The combined filtrates were evaporated *in vacuo* and the crude product was purified by flash column chromatography (SiO<sub>2</sub>, *n*-hexane/EtOAc = 1:1 → EtOAc) to afford the desired SNAC ester.

### Synthesis and spectroscopic data of intermediates.

**(E)-3-(3-Hydroxyphenyl)acrylaldehyde (IM-1).** The title compound was prepared from 3-hydroxybenzaldehyde according to the following procedure: A mixture of 3-hydroxybenzaldehyde (5.00 g, 41.0 mmol) and vinyl acetate (4.15 mL, 45.1 mmol) in acetonitrile (15 mL) was added at room temperature to a suspension of potassium carbonate (6.80 g, 49.2 mmol) in acetonitrile (50 mL) and water (0.2 mL). The reaction mixture was refluxed for 40 h and cooled to room temperature. The reaction mixture was diluted with water (50 mL) and EtOAc (50 mL). The aqueous layer was separated and extracted with EtOAc (2 x 50 mL). The combined organic layers were dried (MgSO<sub>4</sub>) and concentrated *in vacuo*. The residue was purified by flash column chromatography (SiO<sub>2</sub>, *n*-hexane/EtOAc = 8:1 → 2:1) to afford the title compound. Yield: 25%, orange solid. <sup>1</sup>H NMR (DMSO-d<sub>6</sub>): δ = 9.68 (br. s, 1H), 9.65 (d, *J* = 7.7 Hz, 1H), 7.65 (d, *J* = 15.8 Hz, 1H), 7.27 (t, *J* = 8.0 Hz, 1H), 7.17 (d, *J* = 8.0 Hz, 1H), 7.08 (t, *J* = 2.4 Hz, 1H), 6.89 (ddd, *J* = 8.0, 2.4, 1.0 Hz, 1H), 6.73 (dd, *J* = 15.8, 7.7 Hz, 1H) ppm. <sup>13</sup>C NMR (DMSO-d<sub>6</sub>): δ = 194.4, 157.8, 153.5, 135.3, 130.1, 128.3, 119.6, 118.4, 115.0 ppm.

**(E)-3-(3-((*tert*-Butyldimethylsilyl)oxy)phenyl)acrylaldehyde (IM-2).** The title compound was prepared from **IM-1** according to the following procedure: Imidazole (0.86 g, 12.7 mmol) was added to a solution of **IM-1** (0.76 g, 5.13 mmol) and *tert*-butyldimethylchlorosilane (0.92 g, 6.10 mmol) in anhydrous *N,N*-dimethylformamide (10 mL). The mixture was stirred for 3 h, diluted with 5% aqueous NaHCO<sub>3</sub> (50 mL), and extracted with EtOAc (4 x 50 mL). The combined organic layers were washed with brine (100 mL), dried (MgSO<sub>4</sub>), and evaporated *in vacuo* to yield the title compound. Yield: 82%, yellow oil. <sup>1</sup>H NMR (DMSO-d<sub>6</sub>): δ = 9.66 (d, *J* = 7.7 Hz, 1H), 7.71 (d, *J* = 15.9 Hz, 1H), 7.34–7.38 (m, 2H), 7.19–7.22 (m, 1H), 6.94–6.99 (m, 1H), 6.84 (dd, *J* = 15.9, 7.7 Hz, 1H), 0.96 (s, 9H), 0.21 (s, 6H) ppm. <sup>13</sup>C NMR (DMSO-d<sub>6</sub>): δ = 194.3, 155.5, 152.9, 135.6, 130.2, 128.7, 122.7, 121.9, 119.8, 25.5, 17.9, -4.6 ppm.

**(E)-3-(3-Bromophenyl)acrylaldehyde (IM-3).** The title compound was prepared from 3-bromobenzaldehyde according to the following procedure: A solution of 3-bromobenzaldehyde (5.00 g, 27.0 mmol) in H<sub>2</sub>O (6 mL) was filled into a 100 mL three-necked round bottom flask equipped with a thermometer. NaOH (54.0 mg, 1.35 mmol) was added and dissolved. A solution of vinylacetate (0.41 g, 10.4 mmol) in H<sub>2</sub>O (1 mL) was added dropwise. The temperature was kept at 25 °C and NaOH (270 mg, 0.68 mmol) in H<sub>2</sub>O (1 mL) was added *via* a syringe. Afterwards another portion of vinylacetate (0.41 g, 10.4 mmol) in H<sub>2</sub>O (1 mL) was added and the reaction mixture was stirred over night at room temperature. The

reaction was neutralized with acetic acid, diluted with 50 mL H<sub>2</sub>O and extracted with Et<sub>2</sub>O (2 x 100 mL). The organic layers were combined, washed with brine (100 mL), dried (MgSO<sub>4</sub>), and evaporated *in vacuo*. The residue was purified by flash chromatography (SiO<sub>2</sub>, *n*-hexane/EtOAc = 20:1 → 15:1). Yield: 12%, yellow oil. <sup>1</sup>H NMR (CDCl<sub>3</sub>): δ = 9.72 (d, *J* = 7.5 Hz, 1H), 7.71 (s, 1H), 7.57 (d, *J* = 7.7 Hz, 1H), 7.50 (d, *J* = 7.7 Hz, 1H), 7.40 (d, *J* = 15.9 Hz, 1H), 7.32 (t, *J* = 7.7 Hz, 1H), 6.70 (dd, *J* = 15.9, 7.5 Hz, 1H) ppm. <sup>13</sup>C NMR (CDCl<sub>3</sub>): δ = 193.2, 150.6, 136.1, 134.0, 131.2, 130.6, 129.7, 126.9, 123.2 ppm.

**Pent-4-yn-1-ol (IM-4).** The title compound was prepared according to the following procedure: 4-Pentynoic acid (3.00 g, 30.6 mmol) was dissolved in anhydrous THF (90 mL) and cooled to 0 °C. Triethylamine (4.69 mL, 33.6 mmol) and methylchloroformate (2.60 mL, 33.6 mmol) were subsequently added and the reaction was stirred at 0 °C for 20 min. The occurring white precipitate was filtered off, afterwards under a nitrogen atmosphere and the filtrate was added to a solution of NaBH<sub>4</sub> (1.85 g, 49.9 mmol) in water (60 mL) at 0 °C. The resulting mixture was stirred for 1 h at 0 °C and for additional 2 h at room temperature. The reaction was carefully quenched with 1M HCl (20 mL) until bubbling ceased. The mixture was extracted with EtOAc (3 x 100 mL). The combined organic layers were washed with a saturated solution of NaHCO<sub>3</sub> (100 mL) and brine (100 mL), dried (MgSO<sub>4</sub>) and concentrated *in vacuo* to yield the title compound. Yield: 39%, colorless liquid. <sup>1</sup>H NMR (CDCl<sub>3</sub>): δ = 3.75 (t, *J* = 6.4 Hz, 2H), 2.31 (dt, *J* = 7.0, 2.7 Hz, 2H), 1.97 (t, *J* = 2.7 Hz, 1H), 1.85 (s, 1H), 1.77 (quin, *J* = 6.4 Hz, 2H) ppm. <sup>13</sup>C NMR (CDCl<sub>3</sub>): δ = 83.8, 68.7, 61.4, 31.0, 14.9 ppm.

**Pent-4-ynal (IM-5).** The title compound was prepared from **IM-4** according to the general procedure shown for **IM-7** and used in the next step without further purification.

**4-(*tert*-Butyldimethylsilyloxy)butan-1-ol (IM-6).** The title compound was prepared according to the following procedure: To a suspension of potassium hydride (1.32 g, 33.0 mmol) in THF (40 mL) 1,4-butanediol (3.00 g, 33.3 mmol) was added at room temperature and stirred for 45 min. A voluminous white precipitate formed. To the reaction mixture was added *tert*-butyldimethylsilyl chloride (4.97 g, 33.0 mmol) and stirring was continued for 45 min. The mixture was diluted with Et<sub>2</sub>O (200 mL), washed with aqueous K<sub>2</sub>CO<sub>3</sub> (10%, 50 mL) and brine (2 x 100 mL), dried (MgSO<sub>4</sub>) and concentrated *in vacuo*. Yield: 99%, colorless oil. <sup>1</sup>H NMR (CDCl<sub>3</sub>): δ = 3.63–3.69 (m, 4H), 2.51 (t, *J* = 5.6 Hz, 1H), 1.62–1.69 (m, 4H), 0.91 (s, 9H), 0.08 (s, 6H) ppm. <sup>13</sup>C NMR (CDCl<sub>3</sub>): δ = 63.3, 62.7, 30.2, 29.8, 25.9, 18.3, –5.4 ppm.

**4-(*tert*-Butyldimethylsilyloxy)butanal (IM-7).** The title compound was prepared from **IM-6** according to the following procedure: To a stirred suspension of PCC (10.6 g, 49.2 mmol) and NaOAc (0.49 g, 9.84 mmol) in CH<sub>2</sub>Cl<sub>2</sub> (100 mL) a solution of the alcohol **IM-6** (6.70 g, 32.8 mmol) in CH<sub>2</sub>Cl<sub>2</sub> (100 mL) was added. After 7 h the reaction mixture was diluted with Et<sub>2</sub>O (100 mL) and the mixture was filtered over short pad of celite. The solvents were evaporated *in vacuo* and the residue was purified by flash chromatography (SiO<sub>2</sub>, *n*-hexane/EtOAc = 20:1 → 10:1). Yield: 30%, colorless oil. <sup>1</sup>H NMR (CDCl<sub>3</sub>): δ = 9.79 (t, *J* = 1.7 Hz, 1H), 3.65 (t, *J* = 6.0 Hz, 2H), 2.51 (dt, *J* = 7.1, 1.7 Hz, 2H), 1.86 (quin, *J* = 6.5 Hz, 2H),

0.89 (s, 9H), 0.05 (s, 6H) ppm.  $^{13}\text{C}$  NMR ( $\text{CDCl}_3$ ):  $\delta$  = 202.6, 62.1, 40.8, 25.9, 25.5, 18.3, -5.4 ppm.

**(E)-6-(tert-Butyldimethylsilyloxy)hex-2-enal (IM-8).** The title compound was prepared from **IM-7** according to the following procedure: To a solution formylmethylenetriphenylphosphorane (3.01 g, 9.90 mmol) in benzene (80 mL), a solution of the aldehyde **IM-7** (2.00 g, 9.90 mmol) in benzene (15 mL) was added and the mixture was heated under reflux for 24 h. After removal of the solvent, the crude material was purified by flash chromatography ( $\text{SiO}_2$ , *n*-hexane/EtOAc = 12:1  $\rightarrow$  10:1). Yield: 58%, light yellow oil.  $^1\text{H}$  NMR ( $\text{CDCl}_3$ ):  $\delta$  = 9.46 (d,  $J$  = 7.9 Hz, 1H), 6.84 (dd,  $J$  = 15.7, 6.8 Hz, 1H), 6.08 (ddt,  $J$  = 15.7, 7.9, 1.5 Hz, 1H), 3.61 (t,  $J$  = 6.1 Hz, 2H), 2.34–2.41 (m, 2H), 1.63–1.72 (m, 2H), 0.84 (s, 9H), 0.00 (s, 6H) ppm.  $^{13}\text{C}$  NMR ( $\text{CDCl}_3$ ):  $\delta$  = 194.0, 158.6, 133.0, 62.0, 30.9, 29.3, 25.9, 18.3, 15.4 ppm.

**3-((tert-Butyldimethylsilyl)oxy)benzoic acid (IM-9).** The title compound was prepared from 3-hydroxybenzoic acid according to the following procedure: Imidazole (1.36 g, 20.0 mmol) was added to a solution of 3-hydroxybenzoic acid (1.00 g, 7.24 mmol) and *tert*-butyldimethylchlorosilane (1.31 g, 8.69 mmol) in anhydrous *N,N*-dimethylformamide (15 mL). The mixture was stirred for 3 h at room temperature and then diluted with acetone (50 mL). The solvents were evaporated *in vacuo* and the residue was dissolved in EtOAc (50 mL). The organic layer was washed with  $\text{H}_2\text{O}$  (2 x 40 mL) and brine (30 mL), dried ( $\text{MgSO}_4$ ), and evaporated *in vacuo* to yield the title compound. Yield: 38%, colorless crystals.  $^1\text{H}$  NMR ( $\text{CDCl}_3$ )  $\delta$  = 7.73 (td,  $J$  = 8.0, 1.1 Hz, 1H), 7.58 (t,  $J$  = 2.5 Hz, 1H), 7.34 (t,  $J$  = 8.0 Hz, 1H), 7.10 (ddd,  $J$  = 8.0, 2.5, 1.1 Hz, 1H), 1.01 (s, 9H), 0.24 (s, 6H) ppm.  $^{13}\text{C}$  NMR ( $\text{CDCl}_3$ )  $\delta$  = 171.7, 155.8, 130.7, 129.5, 125.7, 123.2, 121.5, 25.6, 18.2, -4.5 ppm.

**(S)-(2-Acetamidoethyl) 3-((tert-butyl dimethylsilyl)oxy)benzothioate (IM-10).** The title compound was prepared from **IM-9** according to the general procedure **H**: Yield 51%, white solid.  $^1\text{H}$  NMR ( $\text{CDCl}_3$ )  $\delta$  = 7.57 (d,  $J$  = 7.7 Hz, 1H), 7.39–7.44 (m, 1H), 7.32 (t,  $J$  = 7.7 Hz, 1H), 7.03–7.12 (m, 1H), 5.92 (br. s., 1H), 3.50–3.60 (m, 1H), 3.23 (t,  $J$  = 6.4 Hz, 1H), 1.98 (s, 3H), 1.01 (s, 9H), 0.23 (s, 6H) ppm.  $^{13}\text{C}$  NMR ( $\text{CDCl}_3$ )  $\delta$  = 191.6, 169.9, 155.6, 137.6, 129.3, 125.1, 119.9, 118.1, 76.8, 76.6, 76.2, 39.3, 28.2, 25.2, 22.8, -4.9 ppm

**5-(1-Hydroxyethylidene)-2,2-dimethyl-1,3-dioxane-4,6-dione (IM-11).** The title compound was prepared from acetyl chloride according to the general procedure **A**: Yield: 83%, yellow solid.  $^1\text{H}$  NMR ( $\text{CDCl}_3$ ):  $\delta$  = 15.12 (s, 1H), 2.68 (s, 3H), 1.74 (s, 6H) ppm.  $^{13}\text{C}$  NMR ( $\text{CDCl}_3$ ):  $\delta$  = 194.6, 170.2, 160.4, 104.9, 91.8, 26.8, 23.5 ppm.

**6-Methyl-2,2-dimethyl-4H-1,3-dioxin-4-one (IM-12).** The title compound was prepared from **IM-11** according to the general procedure **B**: Yield: 85%, yellow oil.  $^1\text{H}$  NMR ( $\text{CDCl}_3$ ):  $\delta$  = 5.19 (s, 1H), 1.94 (s, 3H), 1.64 (s, 6H) ppm.  $^{13}\text{C}$  NMR ( $\text{CDCl}_3$ ):  $\delta$  = 168.6, 161.1, 106.2, 93.7, 24.9, 19.8 ppm.

**Diethyl 1-(2,2-dimethyl-4-oxo-4H-1,3-dioxin-6-yl)methylphosphonate (IM-13).** The title compound was prepared from **IM-12** according to the general procedure **C**: Yield: 62%, yellow resin.  $^1\text{H}$  NMR ( $\text{CDCl}_3$ )  $\delta$  = 5.39 (d,  $J$  = 3.6 Hz, 1H), 4.08–4.24 (m, 4H), 2.80 (d,  $J$  = 22.1 Hz, 2H), 1.71 (s, 6H), 1.35 (t,  $J$  = 7.1 Hz, 6H)

ppm.  $^{13}\text{C}$  NMR (75 MHz,  $\text{CDCl}_3$ ):  $\delta$  = 163.0 (d,  $J$  = 9.7 Hz), 160.5, 107.1, 96.2 (d,  $J$  = 8.2 Hz), 62.6 (d,  $J$  = 6.7 Hz), 32.4 (d,  $J$  = 137.1 Hz), 24.9, 16.3 (d,  $J$  = 6.0 Hz) ppm.

**6-((1E,3E)-Hepta-1,3-dien-1-yl)-2,2-dimethyl-4H-1,3-dioxin-4-one (IM-14).** The title compound was prepared from **IM-13** according to the general procedure **D** using *trans*-2-hexen-1-al as aldehyde: Yield: 42%.  $^1\text{H}$  NMR ( $\text{CDCl}_3$ ):  $\delta$  = 6.92 (dd,  $J$  = 15.2, 9.9 Hz, 1H), 5.98–6.14 (m, 2H), 5.90 (d,  $J$  = 15.2 Hz, 1H), 5.21 (s, 1H), 2.16 (q,  $J$  = 7.2 Hz, 2H), 1.72 (s, 6H), 1.46 (sxt,  $J$  = 7.4 Hz, 2H), 0.95 (t,  $J$  = 7.4 Hz, 3H) ppm.  $^{13}\text{C}$  NMR ( $\text{CDCl}_3$ ):  $\delta$  = 163.5, 161.7, 143.4, 138.5, 128.9, 120.6, 105.9, 93.6, 34.8, 24.8, 21.8, 13.4 ppm.

**5-(1-Hydroxypropylidene)-2,2-dimethyl-1,3-dioxane-4,6-dione (IM-15).** The title compound was prepared from propionyl chloride according to the general procedure **A**: Yield: 93%, orange crystals.  $^1\text{H}$  NMR ( $\text{CDCl}_3$ ):  $\delta$  = 15.35 (br. s, 1H), 3.10 (q,  $J$  = 7.4 Hz, 2H), 1.72 (s, 6H), 1.25 (t,  $J$  = 7.4 Hz, 3H) ppm.  $^{13}\text{C}$  NMR ( $\text{CDCl}_3$ ):  $\delta$  = 198.9, 170.2, 160.2, 104.8, 90.9, 29.4, 26.7, 9.6 ppm.

**6-Ethyl-2,2-dimethyl-4H-1,3-dioxin-4-one (IM-16).** The title compound was prepared from **IM-15** according to the general procedure **B**: Yield: 80%, yellow oil.  $^1\text{H}$  NMR ( $\text{CDCl}_3$ ):  $\delta$  = 5.22 (t,  $J$  = 1.0 Hz, 1H), 2.24 (dq,  $J$  = 7.6, 1.0 Hz, 2H), 1.67 (s, 6H), 1.12 (t,  $J$  = 7.6 Hz, 3H) ppm.  $^{13}\text{C}$  NMR ( $\text{CDCl}_3$ ):  $\delta$  = 173.1, 161.5, 106.2, 92.2, 26.7, 24.9, 9.9 ppm.

**Diethyl 1-(2,2-dimethyl-4-oxo-4H-1,3-dioxin-6-yl)ethylphosphonate (IM-17).** The title compound was prepared from **IM-16** according to the general procedure **C**: Yield: 75%. Light yellow oil.  $^1\text{H}$  NMR ( $\text{CDCl}_3$ ):  $\delta$  = 5.37 (d,  $J$  = 3.5 Hz, 1H), 4.08–4.18 (m, 4H), 2.77 (dq,  $J$  = 23.9, 7.3 Hz, 1H), 1.69 (s, 6H), 1.30–1.45 (m, 9H) ppm.  $^{13}\text{C}$  NMR ( $\text{CDCl}_3$ ):  $\delta$  = 168.1 (d,  $J$  = 8.2 Hz), 160.8 (d,  $J$  = 2.2 Hz), 106.8, 94.9 (d,  $J$  = 6.7 Hz), 62.1 (dd,  $J$  = 6.7, 4.5 Hz), 36.9 (d,  $J$  = 137.1 Hz), 24.8 (d,  $J$  = 70.8 Hz), 16.4 (d,  $J$  = 6.0 Hz), 12.1 (d,  $J$  = 6.0 Hz) ppm.

**5-((2E,4E)-1-Hydroxy-2,5-dimethylocta-2,4-dien-1-ylidene)-2,2-dimethyl-1,3-dioxane-4,6-dione (IM-18).** The title compound was prepared from **IM-17** according to the general procedure **D** using **IM-41** as aldehyde: Yield: 60 %, yellow oil.  $^1\text{H}$  NMR ( $\text{CDCl}_3$ )  $\delta$  = 7.09 (d,  $J$  = 11.8 Hz, 1H), 6.14 (dd,  $J$  = 11.8, 1.2 Hz, 1H), 5.41 (s, 1H), 2.12 (t,  $J$  = 7.5 Hz, 2H), 1.85 (s, 3H), 1.83 (s, 3H), 1.68 (s, 6H), 1.47 (sxt,  $J$  = 7.4 Hz, 2H), 0.87 (t,  $J$  = 7.4 Hz, 3H) ppm.  $^{13}\text{C}$  NMR ( $\text{CDCl}_3$ )  $\delta$  = 166.0, 162.3, 148.5, 130.0, 124.0, 120.6, 105.7, 91.2, 42.7, 24.8, 20.9, 17.0, 13.6, 11.9 ppm.

**2,2-Dimethyl-6-((2E,4E)-octa-2,4-dien-2-yl)-4H-1,3-dioxin-4-one (IM-19).** The title compound was prepared from **IM-17** according to the general procedure **D** using *trans*-2-hexen-1-al as aldehyde: Yield: 42%.  $^1\text{H}$  NMR ( $\text{CDCl}_3$ ):  $\delta$  = 6.85 (d,  $J$  = 11.3 Hz, 1H), 6.36 (dd,  $J$  = 14.8, 11.3 Hz, 1H), 6.07 (dt,  $J$  = 14.8, 7.5 Hz, 1H), 5.42 (s, 1H), 2.15–2.20 (m, 2H), 1.86 (s, 3H) 1.68 (s, 6H) 1.39–1.48 (m, 2H), 0.90 (t,  $J$  = 7.4 Hz, 1H) ppm.  $^{13}\text{C}$  NMR ( $\text{CDCl}_3$ ):  $\delta$  = 165.7, 162.2, 143.3, 134.3, 125.9, 124.4, 105.8, 91.6, 35.3, 24.9, 22.1, 13.6, 12.1 ppm.

**(E)-2,2-Dimethyl-6-(oct-2-en-2-yl)-4H-1,3-dioxin-4-one (IM-20).** The title compound was prepared from **IM-17** according to the general procedure **D** using hexanal as aldehyde: Yield: 37%, colorless oil.  $^1\text{H}$  NMR ( $\text{CDCl}_3$ ):  $\delta$  = 6.41 (t,  $J$  =

7.4 Hz, 1H), 5.40 (s, 1H), 2.20 (q,  $J = 7.4$  Hz, 2H), 1.79 (s, 3H), 1.70 (s, 6H), 1.40–1.49 (m, 2H), 1.27–1.36 (m, 4H), 0.90 (t,  $J = 6.9$  Hz, 3H) ppm.  $^{13}\text{C}$  NMR ( $\text{CDCl}_3$ ):  $\delta = 165.8, 162.5, 138.1, 126.9, 105.9, 91.2, 31.6, 28.7, 28.5, 24.9, 22.4, 13.9, 12.1$  ppm.

**2,2-Dimethyl-6-((2E,4E)-5-phenylpenta-2,4-dien-2-yl)-4H-1,3-dioxin-4-one (IM-21).** The title compound was prepared from **IM-17** according to the general procedure **D** using *trans*-cinnamaldehyde: Yield: 50%, yellow oil.  $^1\text{H}$  NMR ( $\text{CDCl}_3$ ):  $\delta = 7.48\text{--}7.51$  (m, 2H), 7.30–7.40 (m, 4H), 7.14 (dd,  $J = 14.1, 11.3$  Hz, 1H), 7.06 (d,  $J = 11.3$  Hz, 1H), 6.90 (d,  $J = 14.1$  Hz, 1H), 5.54 (s, 1H), 2.02 (s, 3H), 1.75 (s, 6H) ppm.  $^{13}\text{C}$  NMR ( $\text{CDCl}_3$ ):  $\delta = 165.3, 162.2, 139.2, 136.6, 134.0, 128.8, 127.0, 127.0, 123.7, 106.0, 92.3, 25.0, 12.5$  ppm.

**(E)-2,2-Dimethyl-6-(5-phenylpent-2-en-2-yl)-4H-1,3-dioxin-4-one (IM-22).** The title compound was prepared from **IM-17** according to the general procedure **D** using hydrocinnamaldehyde as aldehyde: Yield: 13%, colorless resin. *E*-isomer only.  $^1\text{H}$  NMR ( $\text{CDCl}_3$ ):  $\delta = 7.12\text{--}7.32$  (m, 5H), 6.44 (t,  $J = 7.5$  Hz, 1H), 5.40 (s, 1H), 2.76 (t,  $J = 7.6$  Hz, 2H), 2.48–2.56 (m, 2H), 1.73 (s, 3H), 1.70 (s, 6H) ppm.  $^{13}\text{C}$  NMR ( $\text{CDCl}_3$ ):  $\delta = 165.6, 162.4, 141.0, 136.5, 128.4, 128.3, 127.8, 126.2, 106.0, 91.5, 35.0, 30.6, 24.9, 12.1$  ppm.

**6-((2E,4E)-5-(3-((tert-Butyldimethylsilyl)oxy)phenyl)penta-2,4-dien-2-yl)-2,2-dimethyl-4H-1,3-dioxin-4-one (IM-23).** The title compound was prepared from **IM-17** according to the general procedure **D** using **IM-2** as aldehyde: Yield: 16%, yellow oil.  $^1\text{H}$  NMR ( $\text{CDCl}_3$ ):  $\delta = 7.22$  (dd,  $J = 7.8, 7.8$  Hz, 1H), 7.02–7.12 (m, 3H), 6.93 (dd,  $J = 1.9, 1.8$  Hz, 1H), 6.75–6.88 (m, 2H), 5.53 (s, 1H), 2.02 (s, 3H), 1.75 (s, 6H), 1.01 (s, 9H), 0.23 (s, 6H) ppm.  $^{13}\text{C}$  NMR ( $\text{CDCl}_3$ ):  $\delta = 165.3, 162.3, 156.1, 139.2, 138.1, 134.0, 129.7, 127.0, 123.9, 120.6, 120.2, 118.6, 106.0, 92.3, 25.7, 25.1, 18.2, 12.6, 4.4$  ppm.

**6-((2E,4E)-5-(3-Bromophenyl)penta-2,4-dien-2-yl)-2,2-dimethyl-4H-1,3-dioxin-4-one (IM-24)** The title compound was prepared from **IM-17** according to the general procedure **D** using **IM-3** as aldehyde: Yield: 50%, yellow solid.  $^1\text{H}$  NMR ( $\text{CDCl}_3$ )  $\delta = 7.61$  (t,  $J = 1.6$  Hz, 1H), 7.34–7.44 (m, 2H), 7.22 (t,  $J = 7.8$  Hz, 1H), 7.10 (dd,  $J = 14.3, 11.4$  Hz, 1H), 7.02 (d,  $J = 11.4$  Hz, 1H), 6.78 (d,  $J = 14.3$  Hz, 1H), 5.54 (s, 1H), 2.02 (s, 3H), 1.74 (s, 6H) ppm.  $^{13}\text{C}$  NMR ( $\text{CDCl}_3$ ):  $\delta = 165.0, 162.0, 138.7, 137.2, 133.3, 131.4, 130.2, 129.5, 128.0, 125.7, 125.0, 122.9, 106.0, 92.6, 25.0, 12.5$  ppm.

**(4E,6E)-(S)-2-Acetamidoethyl-7-(3-((tert-butyldimethylsilyl)oxy)phenyl)-4-methyl-3-oxohepta-4,6-dienethioate (IM-25).** The title compound was prepared from **IM-23** according to the general procedure **E**: Yield: 53%, yellow oil.  $^1\text{H}$  NMR ( $\text{CDCl}_3$ ):  $\delta = 7.11\text{--}7.30$  (m, 2H), 6.96–7.11 (m, 2H), 6.70–6.96 (m, 3H), 6.11 (br. s, 1H), 4.01 (s, 2H), 3.35–3.51 (m, 2H), 3.08 (q,  $J = 6.1$  Hz, 2H), 1.97 (s, 3H), 1.93 (s, 3H), 0.96 (s, 9H), 0.18 (s, 6H) ppm.  $^{13}\text{C}$  NMR ( $\text{CDCl}_3$ ):  $\delta = 193.1, 193.0, 170.3, 156.0, 141.3, 137.5, 135.5, 129.8, 128.1, 124.0, 121.1, 120.5, 118.8, 52.8, 39.2, 29.2, 25.6, 23.1, 18.2, 11.8, -4.4$  ppm.

**(E)-5-(1-Hydroxy-2-methylhept-2-en-6-yn-1-ylidene)-2,2-dimethyl-1,3-dioxane-4,6-dione (IM-26).** The title compound was prepared from **IM-17** according to the general procedure **D** using **IM-5** as aldehyde: Yield: 53 %, colorless oil.  $^1\text{H}$  NMR ( $\text{CDCl}_3$ )  $\delta = 6.40$  (dt,  $J = 7.2, 1.1$  Hz, 1H), 5.43 (s, 1H),

2.39–2.50 (m, 2H), 2.29–2.37 (m, 2H), 1.95–2.00 (m, 1H), 1.81 (s, 3H), 1.70 (s, 6H) ppm.  $^{13}\text{C}$  NMR ( $\text{CDCl}_3$ ):  $\delta$  = 165.3, 162.2, 134.9, 128.5, 106.0, 91.8, 83.0, 69.1, 27.6, 24.9, 17.9, 12.3 ppm.

**6-((2E,4E)-8-((tert-Butyldimethylsilyloxy)octa-2,4-dien-2-yl)-2,2-dimethyl-4H-1,3-dioxin-4-one (IM-27).** The title compound was prepared from **IM-17** according to the general procedure **D** using **IM-8** as aldehyde: Yield: 29%, yellow oil.  $^1\text{H}$  NMR ( $\text{CDCl}_3$ ):  $\delta$  = 6.83 (d,  $J$  = 11.2 Hz, 1H), 6.39 (ddd,  $J$  = 14.9, 11.2, 1.0 Hz, 1H), 6.09 (td,  $J$  = 14.9, 7.2 Hz, 1H), 5.44 (s, 1H), 3.61 (t,  $J$  = 6.2 Hz, 2H), 2.26 (q,  $J$  = 7.2 Hz, 2H), 1.87 (s, 3H), 1.71 (s, 6H), 1.58–1.67 (m, 2H), 0.89 (s, 9H), 0.04 (s, 6H) ppm.  $^{13}\text{C}$  NMR ( $\text{CDCl}_3$ ):  $\delta$  = 165.4, 162.3, 143.0, 137.8, 134.2, 126.1, 124.7, 105.9, 91.8, 62.4, 32.0, 29.3, 25.9, 25.0, 18.3, 12.2, –5.3 ppm.

**5-(1-Hydroxybutylidene)-2,2-dimethyl-1,3-dioxane-4,6-dione (IM-28).** The title compound was prepared from butyryl chloride according to the general procedure **A**:

Yield: 92%, yellow oil.  $^1\text{H}$  NMR ( $\text{CDCl}_3$ ):  $\delta$  = 15.30 (s, 1H), 3.05 (t,  $J$  = 7.5 Hz, 2H), 1.73 (s, 6H), 1.72 (sxt,  $J$  = 7.5 Hz, 2H), 1.03 (t,  $J$  = 7.5 Hz, 3H) ppm.  $^{13}\text{C}$  NMR ( $\text{CDCl}_3$ ):  $\delta$  = 198.0, 170.5, 160.2, 104.7, 91.3, 37.4, 26.8, 19.6, 13.8 ppm.

**6-Propyl-2,2-dimethyl-4H-1,3-dioxin-4-one (IM-29).** The title compound was prepared from **IM-28** according to the general procedure **B**: Yield: 82%, yellow oil.  $^1\text{H}$  NMR ( $\text{CDCl}_3$ ):  $\delta$  = 5.22 (s, 1H), 2.18 (t,  $J$  = 7.5 Hz, 2H), 1.66 (s, 6H), 1.57 (sxt,  $J$  = 7.5 Hz, 2H), 0.95 (t,  $J$  = 7.5 Hz, 3H) ppm.  $^{13}\text{C}$  NMR ( $\text{CDCl}_3$ ):  $\delta$  = 171.9, 161.4, 106.2, 93.1, 35.4, 24.9, 19.1, 13.4 ppm.

**Diethyl 1-(2,2-dimethyl-4-oxo-4H-1,3-dioxin-6-yl)propylphosphonate (IM-30).** The title compound was prepared from **IM-29** according to the general procedure **C**: Yield: 45%, light yellow oil.  $^1\text{H}$  NMR (acetone- $d_6$ ):  $\delta$  = 5.46 (d,  $J$  = 3.4 Hz, 1H), 4.08–4.23 (m, 4H), 2.83 (ddd,  $J$  = 22.9, 10.8, 4.3 Hz, 1H), 1.77–2.01 (m, 2H), 1.69 (s, 6H), 1.26–1.34 (m, 6H), 1.00 (t,  $J$  = 7.4 Hz, 3H) ppm.  $^{13}\text{C}$  NMR (acetone- $d_6$ ):  $\delta$  = 167.5 (d,  $J$  = 8.2 Hz), 160.6 (d,  $J$  = 2.2 Hz), 107.6, 97.1 (d,  $J$  = 8.2 Hz), 63.7 (d,  $J$  = 6.7 Hz), 45.7 (d,  $J$  = 136.4 Hz), 25.3 (d,  $J$  = 7.5 Hz), 21.0 (d,  $J$  = 3.7 Hz), 16.8 (d,  $J$  = 6.0 Hz), 12.7 (d,  $J$  = 15.7 Hz) ppm.

**2,2-Dimethyl-6-((3E,5E)-6-phenylhexa-3,5-dien-3-yl)-4H-1,3-dioxin-4-one (IM-31).** The title compound was prepared from **IM-30** according to the general procedure **D** using *trans*-cinnamaldehyde: Yield: 25%, yellow solid.  $^1\text{H}$  NMR ( $\text{CDCl}_3$ ) 3E,5E-isomer only:  $\delta$  = 7.41 (m, 2H), 7.19–7.32 (m, 3H), 7.03 (dd,  $J$  = 14.8, 11.3 Hz, 1H), 6.92 (d,  $J$  = 11.3 Hz, 1H), 6.82 (d,  $J$  = 14.8 Hz, 1H), 5.50 (s, 1H), 2.41 (q,  $J$  = 7.6 Hz, 2H), 1.67 (s, 6H), 1.06 (t,  $J$  = 7.6 Hz, 3H) ppm.  $^{13}\text{C}$  NMR ( $\text{CDCl}_3$ ):  $\delta$  = 164.6, 162.4, 139.5, 136.6, 133.7, 133.5, 128.8, 127.0, 123.4, 106.0, 92.0, 25.0, 20.1, 14.4 ppm.

**Ethyl 2-methyloctanoate (IM-32).** The title compound was prepared from **IM-35** according to the following procedure: The unsaturated ester **IM-35** (1.20 g, 6.60 mmol) was dissolved in EtOH (50 mL). After addition of Pd/C (5%, 6 mg) the mixture was hydrogenated in a Parr apparatus at 3 bar  $\text{H}_2$  for 24 h. The catalyst was filtered off and the filter cake was washed with EtOAc (30 mL). The combined filtrates were concentrated *in vacuo*. The residue was dissolved in  $\text{CH}_2\text{Cl}_2$  (50 mL) and filtered over a short pad of  $\text{SiO}_2$  eluting with  $\text{CH}_2\text{Cl}_2$ . The

solvent was removed *in vacuo*. Yield: 73%, colorless liquid.  $^1\text{H}$  NMR ( $\text{CDCl}_3$ ):  $\delta$  = 4.13 (q,  $J$  = 7.1 Hz, 2H), 2.42 (tq,  $J$  = 6.9, 6.5 Hz, 1H), 1.59–1.71 (m, 1H), 1.33–1.46 (m, 1H), 1.22–1.33 (m, 8H), 1.26 (t,  $J$  = 7.1 Hz, 3H), 1.14 (d,  $J$  = 6.9 Hz, 3H), 0.88 (t,  $J$  = 6.7 Hz, 3H) ppm.  $^{13}\text{C}$  NMR ( $\text{CDCl}_3$ ):  $\delta$  = 177.0, 60.0, 39.6, 33.8, 31.7, 29.2, 27.2, 22.6, 17.1, 14.3, 14.0 ppm.

**2-Methyloctanoic acid (IM-33).** The title compound was prepared from **IM-32** according to the following procedure: To a solution of the ester **IM-32** (0.90 g, 4.80 mmol) in MeOH (25 mL) was added a solution of NaOH (0.97 g, 24.2 mmol) in  $\text{H}_2\text{O}$  (8 mL). The resulting mixture was heated under reflux for 16 h. After cooling to room temperature the MeOH was evaporated *in vacuo*. The aqueous layer was cooled to 0 °C and acidified to pH 2 by addition of HCl (2M). The mixture was extracted with EtOAc (3 x 40 mL). The combined organic layers were dried ( $\text{MgSO}_4$ ) and concentrated under reduced pressure. Yield: 92%, white solid.  $^1\text{H}$  NMR ( $\text{CDCl}_3$ ):  $\delta$  = 10.97 (br. s, 1H), 2.45 (tq,  $J$  = 7.1, 6.9 Hz, 1H), 1.64–1.75 (m, 1H), 1.69 (quin,  $J$  = 7.1, 1H), 1.25–1.37 (m, 8H), 1.18 (d,  $J$  = 6.9 Hz, 3H), 0.89 (t,  $J$  = 6.7 Hz, 3H) ppm.  $^{13}\text{C}$  NMR ( $\text{CDCl}_3$ ):  $\delta$  = 183.5, 39.4, 33.5, 31.7, 29.2, 27.1, 22.6, 16.8, 14.0 ppm.

**5-(1-Hydroxy-2-methyloctylidene)-2,2-dimethyl-1,3-dioxane-4,6-dione (IM-34).** The title compound was prepared from **IM-33** according to the general procedure **F**:

Yield: 64 %, orange oil. Keto/enol = 1:3.  $^1\text{H}$  NMR ( $\text{CDCl}_3$ ):  $\delta$  = 15.46 (br. s, 1H), 4.03 (sxt,  $J$  = 6.8 Hz, 1H), 1.72 (s, 6H), 1.17–1.50 (m, 10H), 1.20 (d,  $J$  = 6.8 Hz, 3H), 0.85 (t,  $J$  = 6.8 Hz, 3H) ppm.  $^{13}\text{C}$  NMR ( $\text{CDCl}_3$ ):  $\delta$  = 202.1, 170.8, 160.1, 104.6, 91.0, 37.9, 34.0, 31.6, 29.2, 27.2, 26.8, 22.5, 17.4, 14.0 ppm.

**(2E,4E)-Ethyl 2-methylocta-2,4-dienoate (IM-35).** The title compound was prepared according to the following procedure: (1-Ethoxycarbonylmethyl)triphenylphosphonium bromide (8.86 g, 20.0 mmol) and  $\text{K}_2\text{CO}_3$  (4.00 g, 28.9 mmol) were dissolved in a mixture of  $\text{CH}_2\text{Cl}_2$  (60 mL) and  $\text{H}_2\text{O}$  (50 mL). After the dropwise addition of *trans*-2-hexen-1-al (1.50 g, 15.0 mmol) the reaction mixture was heated under reflux overnight. The organic layer was washed with  $\text{H}_2\text{O}$  (2 x 50 mL), dried ( $\text{MgSO}_4$ ) and concentrated *in vacuo*. The residue was purified by flash chromatography ( $\text{SiO}_2$ , *n*-hexane/EtOAc = 10:1). Yield: 87%, light yellow oil. 2E,4E/2Z,4E = 20:1.  $^1\text{H}$  NMR ( $\text{CDCl}_3$ ) 2E,4E-isomer only:  $\delta$  = 7.17 (d,  $J$  = 11.2 Hz, 1H), 6.35 (tq,  $J$  = 15.0, 11.2, 1.4 Hz, 1H), 6.07 (dt,  $J$  = 15.0, 7.5 Hz, 1H), 4.21 (q,  $J$  = 7.1 Hz, 2H), 2.17 (q,  $J$  = 7.3 Hz, 2H), 1.93 (s, 3H), 1.47 (sxt,  $J$  = 7.3 Hz, 2H), 1.31 (t,  $J$  = 7.1 Hz, 3H), 0.93 (t,  $J$  = 7.3 Hz, 3H) ppm.  $^{13}\text{C}$  NMR ( $\text{CDCl}_3$ ):  $\delta$  = 168.7, 142.9, 138.6, 126.1, 125.1, 60.4, 35.3, 22.2, 14.3, 13.7, 12.5 ppm.

**(2E,4E)-2-Methylocta-2,4-dienoic acid (IM-36).** The title compound was prepared from **IM-35** according to the following procedure: To a solution of the ester **IM-35** (1.30 g, 7.10 mmol) in MeOH (30 mL) was added a solution of NaOH (1.32 g, 33.1 mmol) in  $\text{H}_2\text{O}$  (10 mL). The resulting mixture was heated under reflux for 16 h. After cooling to room temperature the MeOH was evaporated *in vacuo*. The aqueous layer was cooled to 0 °C and acidified to pH 2 by addition of HCl (2M). The mixture was extracted with EtOAc (3 x 50 mL). The combined organic layers were dried ( $\text{MgSO}_4$ ) and concentrated under reduced pressure.

Yield. 91%; yellow solid.  $2E,4E/2Z,4E = 20:1$ .  $^1\text{H}$  NMR ( $\text{CDCl}_3$ )  $2E,4E$ -isomer only:  $\delta = 11.36$  (br. s, 1H), 7.30 (d,  $J = 11.3$  Hz, 1H), 6.38 (dd,  $J = 15.1, 11.3$  Hz, 1H), 6.15 (dt,  $J = 15.1, 7.5$  Hz, 1H), 2.12–2.28 (m, 2H), 1.94 (s, 3H), 1.41–1.52 (m, 2H), 0.94 (t,  $J = 7.4$  Hz, 3H) ppm.  $^{13}\text{C}$  NMR ( $\text{CDCl}_3$ ):  $\delta = 174.3, 144.5, 141.1, 126.1, 124.1, 35.4, 22.1, 13.7, 12.1$  ppm.

**(2E,4E)-Ethyl 2-methyl-5-phenylpenta-2,4-dienoate (IM-37).** The title compound was prepared according to the following procedure: (1-Ethoxycarbonylmethyl)triphenylphosphonium bromide (8.86 g, 20.0 mmol) and  $\text{K}_2\text{CO}_3$  (4.00 g, 28.9 mmol) were dissolved in a mixture of  $\text{CH}_2\text{Cl}_2$  (60 mL) and  $\text{H}_2\text{O}$  (50 mL). After the dropwise addition of *E*-cinnamaldehyde (1.98 g, 15.0 mmol) the reaction mixture was heated under reflux overnight. The organic layer was washed with  $\text{H}_2\text{O}$  (2 x 50 mL), dried ( $\text{MgSO}_4$ ) and concentrated *in vacuo*. The residue was purified by flash chromatography ( $\text{SiO}_2$ , *n*-hexane/EtOAc = 10:1). Yield: 93%, light yellow oil.  $2E,4E/2Z,4E = 11:1$ .  $^1\text{H}$  NMR ( $\text{CDCl}_3$ )  $2E,4E$ -isomer only:  $\delta = 7.41$  (m, 2H), 7.20–7.32 (m, 3H), 7.20 (d,  $J = 11.3$  Hz, 1H), 6.99 (dd,  $J = 15.5, 11.3$  Hz, 1H), 6.80 (d,  $J = 15.5$  Hz, 1H), 4.15 (q,  $J = 7.1$  Hz, 2H), 1.98 (s, 3H), 1.26 (t,  $J = 7.1$  Hz, 3H) ppm.  $^{13}\text{C}$  NMR ( $\text{CDCl}_3$ ):  $\delta = 168.4, 138.9, 138.1, 136.6, 128.7, 128.6, 127.5, 127.0, 124.0, 60.6, 14.3, 12.9$  ppm.

**(2E,4E)-2-Methyl-5-phenylpenta-2,4-dienoic acid (IM-38).** The title compound was prepared from **IM-37** according to the following procedure: To a solution of the ester **IM-37** (3.00 g, 14.8 mmol) in MeOH (80 mL) was added a solution of NaOH (2.77 g, 69.3 mmol) in  $\text{H}_2\text{O}$  (20 mL). The resulting mixture was heated under reflux for 16 h. After cooling to room temperature the MeOH was evaporated *in vacuo*. The aqueous layer was cooled to 0 °C and acidified to pH 2 by addition of HCl (2M). The mixture was extracted with EtOAc (3 x 100 mL). The combined organic layers were dried ( $\text{MgSO}_4$ ) and concentrated under reduced pressure. Yield: 97%, white solid.  $2E,4E/2Z,4E = 11:1$ .  $^1\text{H}$  NMR ( $\text{CDCl}_3$ )  $2E,4E$ -isomer only:  $\delta = 11.27$  (br. s, 1H), 7.40–7.44 (m, 3H), 7.23–7.32 (m, 2H), 7.22 (d,  $J = 11.2$  Hz, 1H), 7.00 (dd,  $J = 15.4, 11.2$  Hz, 1H), 6.85 (d,  $J = 15.4$  Hz, 1H), 1.99 (s, 3H) ppm.  $^{13}\text{C}$  NMR ( $\text{CDCl}_3$ ):  $\delta = 173.9, 140.6, 140.2, 136.4, 128.9, 128.8, 127.2, 126.4, 123.7, 12.5$  ppm.

**Ethyl (E)-3-methylhex-2-enoate (IM-39).** The title compound was prepared according to the following procedure: To a solution of NaH (1.46 g, 60.9 mmol) in THF (250 mL) was added dropwise a solution of triethyl phosphonoacetate (13.0 g, 58.1 mmol) in THF (50 mL) at 0 °C. The resulting mixture was allowed to warm to room temperature and stirred for 30 minutes. A solution of 2-pentanone (5.00 g, 58.1 mmol) in THF (50 mL) was slowly added and the reaction was heated to 80 °C overnight. The reaction was quenched by addition of a saturated  $\text{NH}_4\text{Cl}$  solution (200 mL). The resulting mixture was extracted with  $\text{Et}_2\text{O}$  (3 x 100 mL). The combined organic layers were washed with  $\text{H}_2\text{O}$  (100 mL) and brine (100 mL) and dried over  $\text{MgSO}_4$ . The solvents were evaporated *in vacuo* to afford a yellow liquid. The crude material was purified by flash column chromatography ( $\text{SiO}_2$ , *n*-hexane/EtOAc = 20:1) to afford the title compound as a colorless liquid. Yield: 88%, colorless liquid.  $E/Z = 3.2:1$ ,  $^1\text{H}$  NMR ( $\text{CDCl}_3$ ) *E*-isomer only:  $\delta = 5.66$  (q,  $J = 1.2$  Hz, 1H), 4.14 (q,  $J = 7.1$  Hz, 2H), 2.15 (d,  $J = 1.3$  Hz, 3H), 2.08–2.14 (m, 2H), 1.51 (sxt,  $J = 7.4$ , 2H), 1.28 (t,  $J = 7.1$  Hz, 3H), 0.91 (t,  $J = 7.4$  Hz, 3H) ppm.  $^{13}\text{C}$  NMR ( $\text{CDCl}_3$ ):  $\delta = 166.9, 159.9, 115.6, 59.4, 42.9, 20.5, 18.6, 14.3, 13.6$  ppm.

**(E)-3-Methylhex-2-en-1-ol (IM-40).** The title compound was prepared from **IM-39** according to the following procedure: A suspension of  $\text{LiAlH}_4$  in anhydrous  $\text{Et}_2\text{O}$  (60 mL) was cooled to 0 °C.  $\text{AlCl}_3$  was added and the resulting mixture was stirred for 15 minutes. A solution of **IM-43** (5.00 g, 32.0 mmol) in  $\text{Et}_2\text{O}$  (15 mL) was added and stirring was continued for 1.5 h at 0 °C. Addition of an aqueous solution of NaOH (5% m/m, 20 mL) lead to precipitation of aluminium hydroxides. The reaction mixture was filtered over a short bed of  $\text{MgSO}_4$  which was rinsed with  $\text{Et}_2\text{O}$  (50 mL). Removal of the solvent *in vacuo* afforded the title compound as a colorless liquid. Yield: 44%, colorless oil. *E/Z* = 4:1,  $^1\text{H}$  NMR ( $\text{CDCl}_3$ ) *E*-isomer only:  $\delta$  = 5.41 (tq,  $J$  = 6.9, 1.3 Hz, 1H), 4.07–4.20 (m, 2H), 2.00 (t,  $J$  = 7.5 Hz, 2H), 1.66 (d,  $J$  = 1.3 Hz, 3H), 1.39–1.51 (m, 2H), 0.89 (t,  $J$  = 7.4 Hz, 3H) ppm.  $^{13}\text{C}$  NMR ( $\text{CDCl}_3$ ):  $\delta$  = 139.9, 123.3, 59.4, 41.6, 20.7, 16.1, 13.7 ppm.

**(E)-3-Methylhex-2-enal (IM-41).** The title compound was prepared from **IM-40** according to the following procedure: To a stirred suspension of PCC (4.28 g, 19.9 mmol) and NaOAc (200 mg, 3.98 mmol) in  $\text{CH}_2\text{Cl}_2$  (100 mL) a solution of the alcohol **IM-40** (1.60 g, 14.0 mmol) in  $\text{CH}_2\text{Cl}_2$  (100 mL) was added. After 7 h the reaction mixture was diluted with  $\text{Et}_2\text{O}$  (100 mL) and the mixture was filtered over short pad of celite. The solvents were evaporated *in vacuo* and the residue was purified by flash chromatography ( $\text{SiO}_2$ , *n*-hexane/ $\text{EtOAc}$  = 20:1 → 10:1). Yield: 46%, colorless oil. *E/Z* = 2:1,  $^1\text{H}$  NMR ( $\text{CDCl}_3$ ) *E*-isomer only:  $\delta$  = 9.99 (d,  $J$  = 8.0 Hz, 1H), 5.87 (dq,  $J$  = 8.0, 1.2 Hz, 1H), 2.19 (t,  $J$  = 7.4 Hz, 2H), 2.15 (d,  $J$  = 1.2 Hz, 3H), 1.54 (q,  $J$  = 7.4 Hz, 2H), 0.93 (t,  $J$  = 7.4 Hz, 3H) ppm.  $^{13}\text{C}$  NMR ( $\text{CDCl}_3$ ):  $\delta$  = 191.3, 164.1, 127.4, 42.6, 20.3, 17.4, 13.6 ppm.

**Ethyl (2E,4E)-2,5-dimethylocta-2,4-dienoate (IM-42).** The title compound was prepared from **IM-41** according to the following procedure: To a suspension of NaH (0.16 g, 6.55 mmol) in THF (30 mL) was added dropwise a solution of triethyl phosphonoacetate (1.49 g, 6.24 mmol) in THF (5 mL) at 0 °C. The resulting mixture was allowed to warm to room temperature and stirred for 30 minutes. **IM-41** (0.70 g, 6.24 mmol), dissolved in THF (5 mL) was slowly added and the reaction was stirred at room temperature over night. The reaction was quenched by addition of a saturated  $\text{NH}_4\text{Cl}$  solution (50 mL). The resulting mixture was extracted with  $\text{Et}_2\text{O}$  (3 x 30 mL). The combined organic layers were washed with  $\text{H}_2\text{O}$  (30 mL) and brine (30 mL) and dried over  $\text{MgSO}_4$ . The solvents were evaporated *in vacuo* to afford a yellow liquid. The residue was purified by flash column chromatography ( $\text{SiO}_2$ , *n*-hexane/ $\text{EtOAc}$  = 20:1) to afford the title compound as a colorless oil. Yield: 57%, colorless oil. Mixture of regioisomers, approx: 2*E*,4*E* = 53%, 2*E*,4*Z* = 26%, 2*Z*,4*E* = 13%, 2*Z*,4*Z* = 7%;  $^1\text{H}$  NMR ( $\text{CDCl}_3$ ): 2*E*,4*E* and 2*E*,4*Z* isomers only:  $\delta$  = 7.58–7.67 (m, 1H), 6.17–6.21 (m, 0.35H), 6.16 (dq,  $J$  = 11.8, 1.3 Hz, 0.65H), 4.22 (q,  $J$  = 7.1 Hz, 2H), 2.28 (t,  $J$  = 7.5 Hz, 0.70H), 2.14 (t,  $J$  = 7.5 Hz, 1.30H), 1.85–1.95 (m, 6H), 1.43–1.57 (m, 2H), 1.31 (t,  $J$  = 7.1 Hz, 3H), 0.86–0.98 (m, 3H) ppm.  $^{13}\text{C}$  NMR ( $\text{CDCl}_3$ ) mixture of regioisomers:  $\delta$  = 169.1, 169.0, 148.5, 148.3, 148.1, 134.4, 134.1, 124.6, 124.4, 121.5, 120.7, 60.4, 42.8, 39.6, 34.6, 33.1, 31.9, 30.3, 29.7, 24.7, 21.5, 21.0, 20.8, 20.6, 20.5, 17.1, 14.3, 14.2, 14.1, 14.1, 13.9, 13.7, 12.4, 12.3 ppm.

**(2E,4E)-2,5-Dimethylocta-2,4-dienoic acid (IM-43).** The title compound was prepared from **IM-42** according to the following procedure: To a solution of the ester **IM-42** (0.70 g, 3.57 mmol) in MeOH (15 mL) was added a solution of NaOH (0.70 g, 17.5 mmol) in  $\text{H}_2\text{O}$  (5 mL). The resulting mixture was heated under reflux

for 2 h. After cooling to room temperature the MeOH was evaporated *in vacuo*. The aqueous layer was cooled to 0 °C and acidified to pH 2 by addition of HCl (2M). The mixture was extracted with EtOAc (3 x 100 mL). The combined organic layers were dried (MgSO<sub>4</sub>) and concentrated under reduced pressure. Yield: 83 %, yellow oil. Mixture of regioisomers, approx: 2*E*,4*E* = 53%, 2*E*,4*Z* = 26%, 2*Z*,4*E* = 13%, 2*Z*,4*Z* = 7%; <sup>1</sup>H NMR (CDCl<sub>3</sub>) 2*E*,4*E* and 2*E*,4*Z* isomers only: δ = 7.44–7.51 (m, 1H), 6.12–6.18 (m, 0.35H), 6.12 (dq, *J* = 11.9, 1.2 Hz, 0.65H), 4.22 (q, *J* = 7.1 Hz, 2H), 2.30 (t, *J* = 7.5 Hz, 0.70H), 2.17 (t, *J* = 7.5 Hz, 1.30H), 1.85–1.95 (m, 6H), 1.44–1.59 (m, 2H), 0.86–1.03 (m, 3H) ppm. <sup>13</sup>C NMR (CDCl<sub>3</sub>) mixture of regioisomers: δ = 174.6, 174.5, 173.8, 152.3, 150.2, 149.9, 136.8, 136.5, 124.7, 123.5, 123.4, 121.6, 120.8, 42.8, 39.6, 34.7, 33.2, 24.8, 21.6, 21.0, 20.6, 20.5, 20.5, 17.2, 13.9, 13.7, 12.0, 11.9 ppm.

**(4*E*,6*E*)-(S)-2-Acetamidoethyl-10-((*tert*-butyldimethylsilyl)oxy)-4-methyl-3-oxodeca-4,6-dienethioate (IM-44).** The title compound was prepared from **IM-27** according to the general procedure **E**: Yield 99 %. Keto/enol = 3:1 <sup>1</sup>H NMR (acetone-d<sub>6</sub>): δ = 12.86 (s, 0.25H, enol C=COH), 7.40–7.60 (m, 1H, NH), 7.22 (d, *J* = 10.7 Hz, 0.75H, keto CH=CMe), 7.11 (d, *J* = 11.3 Hz, 0.25H, enol CH=CMe), 6.84 (m, 0.25H), 6.48–6.61 (m, 0.75H, CH=CH), 6.32 (dt, *J* = 15.0, 7.3 Hz, 0.75H, keto CHCH<sub>2</sub>), 6.13 (dt, *J* = 14.8, 7.2 Hz, 0.25H, enol CHCH<sub>2</sub>), 5.81 (s, 0.25H, enol CO=CH), 4.09 (s, 1.50H, keto COCH<sub>2</sub>), 3.66–3.71 (m, 2H, CH<sub>2</sub>O), 3.32–3.43 (m, 2H, CH<sub>2</sub>N), 3.00–3.12 (m, 2H, CH<sub>2</sub>S), 1.91–1.60 (m, 8H), 0.90 (s, 9H), 0.06 (s, 6H) ppm. <sup>13</sup>C NMR (acetone-d<sub>6</sub>): δ = 194.2, 193.6, 171.3, 171.0, 146.0, 142.5, 134.4, 127.7, 62.9, 60.6, 53.4, 39.7, 32.9, 32.8, 32.4, 26.4, 22.8, 20.9, 18.9, 14.6, 11.6, –5.1 ppm.

### Synthesis and spectroscopic data of precursor compounds

**(S)-2-Acetamidoethyl-(4*E*,6*E*)-4,7-dimethyl-3-oxodeca-4,6-dienethioate (1).** The title compound was from **IM-18** prepared according to the general procedure **E**: Yield 65 %. Keto/enol = 4:1, 4*E*,6*E*/4*Z*,6*E* = 2:1. <sup>1</sup>H NMR (acetone-d<sub>6</sub>) 4*E*,6*E*-isomer keto only: δ = 7.49 (dd, *J* = 11.5, 1.2 Hz, 1H), 7.29 (br. s, 1H), 6.27–6.37 (m, 1H), 4.12 (s, 2H), 3.32 (q, *J* = 6.8 Hz, 2H), 3.02 (t, *J* = 6.8 Hz, 2H), 2.15–2.25 (m, 2H), 1.95 (s, 3H), 1.85 (s, 3H), 1.84 (s, 3H), 1.53 (sxt, *J* = 7.4 Hz, 2H), 0.91 (t, *J* = 7.4 Hz, 3H) ppm. <sup>13</sup>C NMR (acetone-d<sub>6</sub>) 4*E*,6*E*-isomer keto only: δ = 194.0, 193.5, 170.2, 151.7, 138.2, 133.9, 122.1, 53.9, 43.5, 39.6, 29.8, 22.9, 21.7, 17.5, 14.1, 11.4 ppm. MS (ESI) *m/z*: 312.0 [M+H]<sup>+</sup>

**(4*E*,6*E*)-(S)-2-Acetamidoethyl-4-methyl-3-oxodeca-4,6-dienethioate (2).** The title compound was from **IM-19** prepared according to the general procedure **E**: Yield 25 %. Keto/enol = 4:1 4*E*,6*E*/4*Z*,6*E* = 8:1. <sup>1</sup>H NMR (DMSO-d<sub>6</sub>) 4*E*,6*E*-isomer keto only: δ = 8.03 (br. s, 1H), 7.21 (d, *J* = 11.0 Hz, 1H), 6.48–6.54 (m, 1H), 6.30 (dt, *J* = 15.1, 7.5 Hz, 1H), 4.15 (s, 2H), 3.17 (m, 2H), 2.92 (t, *J* = 6.9 Hz, 2H), 2.14–2.22 (m, 2H), 1.77–1.79 (m, 6H), 1.40–1.48 (m, 2H), 0.90 (t, *J* = 7.5 Hz, 3H) ppm. <sup>13</sup>C NMR (DMSO-d<sub>6</sub>) 4*E*,6*E*-isomer keto only: δ = 193.8, 193.0, 169.4, 145.6, 141.9, 132.9, 126.8, 52.4, 38.1, 34.8, 28.5, 22.5, 21.6, 13.6, 11.3 ppm. MS (ESI) *m/z*: 298.1 [M+H]<sup>+</sup>

**(4*E*,6*E*)-(S)-2-Acetamidoethyl-3-oxodeca-4,6-dienethioate (3).** The title compound was prepared from **IM-14** according to the general procedure **E**: Yield 50 %. Orange powder. Keto/enol = 1:2 <sup>1</sup>H NMR (acetone-d<sub>6</sub>) 4*E*,6*E*-isomer enol

only:  $\delta$  = 12.46 (s, 1H), 7.36 (br. s, 1H), 7.13 (dd,  $J$  = 15.2, 10.7, 1H), 6.27–6.35 (m, 1H), 6.11–6.20 (m, 1H), 5.94 (d,  $J$  = 15.2 Hz, 1H), 5.65 (s, 1H), 3.37 (q,  $J$  = 6.6 Hz, 2H), 3.08 (t,  $J$  = 6.6 Hz, 2H), 2.12–2.22 (m, 2H), 1.87 (s, 3H), 1.41–1.51 (m, 2H), 0.92 (t,  $J$  = 7.5 Hz, 3H) ppm.  $^{13}\text{C}$  NMR (acetone- $d_6$ ) 4*E*,6*E*-isomer enol only:  $\delta$  = 195.1, 192.3, 168.5, 143.8, 140.5, 130.5, 123.6, 101.3, 39.9, 35.8, 28.8, 22.9, 22.8, 14.0 ppm. MS (ESI)  $m/z$ : 284.1  $[\text{M}+\text{H}]^+$

**(*E*)-(S)-2-Acetamidoethyl-4-methyl-3-oxodec-4-enethioate (4).** The title compound was prepared from **IM-20** according to the general procedure **E**: Yield 66%, yellow oil. Keto/enol = 3:1  $^1\text{H}$  NMR (acetone- $d_6$ ) 4*E*,6*E*-isomer keto only:  $\delta$  = 7.35 (br. s, 1H, NH), 6.81 (t,  $J$  = 7.3 Hz, 1H), 4.06 (s, 2H), 3.33 (q,  $J$  = 6.7 Hz, 2H), 3.01 (t,  $J$  = 6.7 Hz, 2H), 2.53–2.65 (m, 2H), 2.21–2.34 (m, 2H), 1.87 (s, 3H), 1.75 (s, 3H), 1.42–1.55 (m, 2H), 1.30–1.37 (m, 4H), 0.89 (t,  $J$  = 7.0 Hz, 3H) ppm.  $^1\text{H}$  NMR (acetone- $d_6$ ) 4*E*,6*E*-isomer keto only:  $\delta$  = 194.1, 193.4, 170.6, 146.9, 137.5, 53.5, 39.6, 32.3, 29.8, 29.6, 28.9, 23.2, 22.9, 14.3, 11.4 ppm. MS (ESI)  $m/z$ : 300.2  $[\text{M}+\text{H}]^+$

**(S)-2-Acetamidoethyl-4-methyl-3-oxodecanethioate (5).** The title compound was prepared from **IM-34** according to the general procedure **G**: Yield 75%, yellow resin. Keto/enol = 3:1  $^1\text{H}$  NMR (acetone- $d_6$ ) keto only:  $\delta$  = 7.74 (br. s, 1H), 3.86 (s, 2H), 3.38 (quin,  $J$  = 6.8 Hz, 2H), 3.04 (q,  $J$  = 6.8 Hz, 2H), 2.69 (quin,  $J$  = 6.8 Hz, 1H), 1.95 (s, 3H), 1.25–1.39 (m, 10H), 1.07 (d,  $J$  = 6.8 Hz, 3H), 0.87 (t,  $J$  = 6.8 Hz, 3H) ppm.  $^{13}\text{C}$  NMR (acetone- $d_6$ ) keto only:  $\delta$  = 206.0 (HMBC), 193.0, 172.3, 56.2, 47.3, 39.8, 33.2, 32.4, 30.0, 29.3, 27.7, 23.3, 22.8, 16.1, 14.4 ppm. MS (ESI)  $m/z$ : 302.8  $[\text{M}+\text{H}]^+$

**(4*E*,6*E*)-(S)-2-Acetamidoethyl-4-methyl-3-oxo-7-phenylhepta-4,6-dienethioate (6).** The title compound was prepared from **IM-21** according to the general procedure **E**: Yield 60 %, yellow solid. Keto/enol = 2:1,  $^1\text{H}$  NMR (acetone- $d_6$ ):  $\delta$  = 12.82 (s, 0.35H, enol C=COH), 7.99 (br. s, 1H, NH), 7.60–7.66 (m, 2H), 7.26–7.52 (m, 5H), 7.13 (d,  $J$  = 14.7 Hz, 0.65H, keto CMe=CH), 6.99 (d,  $J$  = 13.9 Hz, 0.35H, enol CMe=CH), 5.88 (s, 0.35H, enol CO=CH), 4.19 (s, 1.30H, keto COCH<sub>2</sub>), 3.37–3.47 (m, 2H, CH<sub>2</sub>N), 3.13 (t,  $J$  = 6.8 Hz, 0.70H, keto CH<sub>2</sub>S), 3.06 (t,  $J$  = 6.7 Hz, 1.30H, enol CH<sub>2</sub>S), 1.98–1.99 (m, 6H, COCH<sub>3</sub>, C=CCH<sub>3</sub>) ppm.  $^{13}\text{C}$  NMR (acetone- $d_6$ ):  $\delta$  = 194.4, 194.2, 173.3, 173.2, 142.6, 142.1, 139.8, 137.9, 137.5, 136.3, 135.8, 130.0, 129.8, 129.7, 129.5, 128.4, 128.1, 125.3, 125.3, 98.4, 53.3, 40.4, 39.9, 29.3, 28.3, 22.7, 20.9, 12.6, 11.9 ppm. MS (ESI)  $m/z$ : 332.1  $[\text{M}+\text{H}]^+$

**(4*E*,6*E*)-(S)-2-Acetamidoethyl-4-ethyl-3-oxo-7-phenylhepta-4,6-dienethioate (7).** The title compound was prepared from **IM-31** according to the general procedure **E**: Yield 88 %, yellow resin. Keto/enol = 2:1, 4*E*,6*E*/4*Z*,6*E* = 10:1.  $^1\text{H}$  NMR (acetone- $d_6$ ) 4*E*,6*E*-isomer only:  $\delta$  = 12.99 (br. s, 0.35H, enol C=COH), 7.58–7.69 (m, 2H), 7.24–7.57 (m, 6H), 7.08–7.18 (m, 0.65H), 7.00 (d,  $J$  = 14.5 Hz, 0.35H), 5.95 (s, 0.35H, enol CO=CH), 4.19 (s, 1.30H, keto COCH<sub>2</sub>), 3.33–3.45 (m, 2H, CH<sub>2</sub>N), 3.12 (t,  $J$  = 6.8 Hz, 0.70H, enol CH<sub>2</sub>S), 3.05 (t,  $J$  = 6.7 Hz, 1.30H, keto CH<sub>2</sub>S), 2.56 (q,  $J$  = 7.5 Hz, 0.70H, enol CH<sub>2</sub>CH<sub>3</sub>), 2.55 (q,  $J$  = 7.5 Hz, 1.30H, keto CH<sub>2</sub>CH<sub>3</sub>), 1.92 (s, 1.05H, enol COCH<sub>3</sub>), 1.90 (s, 1.95H, keto COCH<sub>3</sub>), 1.11 (s, 1.05H, enol CH<sub>2</sub>CH<sub>3</sub>), 1.00 (s, 1.95H, keto CH<sub>2</sub>CH<sub>3</sub>) ppm.  $^{13}\text{C}$  NMR (acetone- $d_6$ ):  $\delta$  = 193.6, 193.5, 171.0, 142.7, 142.1, 142.0, 140.1, 137.9,

135.4, 130.0, 129.8, 129.7, 129.6, 128.4, 128.1, 125.0, 124.9, 98.2, 53.6, 40.0, 39.7, 29.6, 28.8, 22.9, 20.3, 19.8, 15.2, 14.7 ppm. MS (ESI) *m/z*: 346.0 [M+H]<sup>+</sup>

**(E)-(S)-2-Acetamidoethyl-4-methyl-3-oxo-7-phenylhept-4-enethioate (8).** The title compound was prepared from **IM-22** according to the general procedure **E**: Yield 62 %. Keto/enol = 3:1, <sup>1</sup>H NMR (acetone-d<sub>6</sub>): δ = 12.83 (s, 0.25H, enol C=COH), 7.47 (br. s, 1H, NH), 7.21–7.32 (m, 4H, Ar-H), 7.16–7.21 (m, 1H, Ar-H), 6.85 (t, *J* = 7.2 Hz, 0.75H, keto CMe=CH), 6.67 (t, *J* = 7.4 Hz, 0.25H, enol CMe=CH), 5.73 (s, 0.25H, CO=CH), 4.04 (s, 1.50H, keto COCH<sub>2</sub>), 3.31–3.42 (m, 2H, CH<sub>2</sub>N), 3.08 (t, *J* = 6.8 Hz, 0.50H, keto CH<sub>2</sub>S), 3.02 (t, *J* = 6.9 Hz, 1.50H, enol CH<sub>2</sub>S), 2.75–2.84 (m, 2 H, CH<sub>2</sub>Ph), 2.53–2.65 (m, 2H, CH<sub>2</sub>CH=C), 1.90 (s, 0.75H, enol COCH<sub>3</sub>), 1.90 (s, 2.25H, keto COCH<sub>3</sub>), 1.73 (s, 0.75H, enol C=CCH<sub>3</sub>), 1.67 (s, 2.25H, keto C=CCH<sub>3</sub>) ppm. <sup>13</sup>C NMR (acetone-d<sub>6</sub>): keto only: δ = 194.1, 193.4, 171.2, 145.7, 145.6, 142.2, 138.0, 129.4, 129.3, 127.0, 53.4, 39.7, 35.1, 32.0, 22.9, 11.3 ppm. MS (ESI) *m/z*: 334.1 [M+H]<sup>+</sup>

**(4E,6E)-(S)-2-Acetamidoethyl-7-(3-hydroxyphenyl)-4-methyl-3-oxohepta-4,6-dienethioate (9).** The title compound was prepared from **IM-25** according to the following procedure: To a solution of **IM-25** (0.08 g, 0.17 mmol) in THF (1.50 mL) was added a solution of *n*Bu<sub>4</sub>NF (1.0 M THF solution, 0.21 mL, 0.21 mmol) at 0 °C. After stirring for 6 h at room temperature, the reaction was stopped by adding saturated aqueous NH<sub>4</sub>Cl (10 mL). The crude products were extracted with EtOAc (3 x 10 mL), and the combined organic layers were washed with brine, dried (MgSO<sub>4</sub>), and concentrated *in vacuo*. The residue was purified by flash column chromatography (SiO<sub>2</sub>, *n*-hexane/EtOAc = 1:1 → EtOAc) to afford the title compound. Yield 92%, yellow solid. Keto/enol = 5:1, 4E,6E/4Z,6E = 3:1. <sup>1</sup>H NMR (DMSO-d<sub>6</sub>) keto only: δ = 9.51 (s, 1H), 8.03 (t, *J* = 5.30 Hz, 1H), 7.13–7.44 (m, 3H), 6.86–7.13 (m, 3H), 6.68–6.80 (m, 1H), 4.20 (s, 2H), 3.18 (q, *J* = 6.7 Hz, 2H), 2.94 (t, *J* = 6.7 Hz, 2H), 1.92 (s, 3H), 1.79 (s, 3H) ppm. <sup>13</sup>C NMR (DMSO-d<sub>6</sub>): δ = 193.5, 192.9, 169.3, 157.7, 141.6, 141.2, 137.4, 134.8, 129.8, 124.4, 118.5, 116.4, 113.9, 52.5, 38.1, 28.5, 22.5, 11.5 ppm. MS (ESI) *m/z*: 347.9 [M+H]<sup>+</sup>

**(S)-2-Acetamidoethyl-(4E,6E)-7-(3-bromophenyl)-4-methyl-3-oxohepta-4,6-dienethioate (10).** The title compound was prepared from **IM-24** according to the general procedure **E**: Yield 40 %, yellow solid. Keto/enol = 1:1, <sup>1</sup>H NMR (CDCl<sub>3</sub>) keto only: δ = 7.65 (t, *J* = 1.9 Hz, 1H), 7.39–7.42 (m, 1H), 7.36–7.38 (m, 1H), 7.23 (t, *J* = 7.9 Hz, 1H), 7.16 (dd, *J* = 11.0, 1.3 Hz, 1H), 7.12 (dd, *J* = 14.8, 11.0 Hz, 1H), 6.88 (d, *J* = 14.8 Hz, 1H), 6.07 (br. s, 1H), 4.05 (s, 2H), 3.48 (m, 2H), 3.11 (t, *J* = 6.6 Hz, 2H), 2.02 (d, *J* = 1.3 Hz, 3H), 1.97 (s, 3H) ppm. <sup>13</sup>C NMR (CDCl<sub>3</sub>): δ = 193.1, 193.0, 170.4, 140.5, 139.4, 138.9, 136.4, 130.2, 129.9, 126.0, 125.7, 125.2, 123.0, 52.9, 39.2, 29.2, 23.1, 11.9 ppm. MS (ESI) *m/z*: 411.7 [M+H]<sup>+</sup>

**(S)-2-Acetamidoethyl-(E)-4-methyl-3-oxonon-4-en-8-ynethioate (11).** The title compound was prepared from **IM-26** according to the general procedure **G**: Yield 50 %. Keto/enol = 3:1. <sup>1</sup>H NMR (CDCl<sub>3</sub>) keto only: δ = 6.62–6.72 (m, 1H), 6.08 (br. s, 1H), 3.98 (s, 2H), 3.47 (m, 2H), 3.10 (t, *J* = 6.2 Hz, 2H), 2.28–2.57 (m, 4H), 2.01 (t, *J* = 2.6 Hz, 1H), 1.97 (s, 3H), 1.82 (s, 3H) ppm. <sup>13</sup>C NMR (CDCl<sub>3</sub>): δ = 193.3, 193.1, 170.5, 143.0, 138.1, 82.6, 69.5, 52.6, 39.2, 29.2, 28.1, 23.2, 17.6, 11.5 ppm. MS (ESI) *m/z*: 281.9 [M+H]<sup>+</sup>

**(4E,6E)-(S)-2-Acetamidoethyl-10-hydroxy-4-methyl-3-oxodeca-4,6-dienethioate (12).** The title compound was prepared from **IM-44** according to the following procedure: To a solution of **IM-44** (0.17 g, 0.40 mmol) in THF (4.0 mL) was added a solution of *n*Bu<sub>4</sub>NF (1.0 M in THF, 1.0 mL, 1.00 mmol) at 0 °C. After stirring for 6 h at room temperature, the reaction was stopped by adding saturated aqueous NH<sub>4</sub>Cl (30 mL). The mixture was extracted with EtOAc (3 x 30 mL), and the combined organic layers were washed with brine, dried (MgSO<sub>4</sub>), and concentrated *in vacuo*. The residue was purified by flash column chromatography (SiO<sub>2</sub>, *n*-hexane/EtOAc = 1:1 → EtOAc) to afford the title compound. Yield 96 %, yellow oil. Keto/enol = 3:1. <sup>1</sup>H NMR (acetone-d<sub>6</sub>): δ = 12.78 (s, 0.25H, enol C=COH), 7.95–8.04 (m, 1H, NH), 7.25 (d, *J* = 10.7 Hz, 0.75H, keto CH=CMe), 7.08 (d, *J* = 11.3 Hz, 0.25H, enol CH=CMe), 6.49–6.63 (m, 1H, CH=CH), 6.35 (dt, *J* = 15.0, 7.3 Hz, 0.75H, keto CHCH<sub>2</sub>), 6.16 (dt, *J* = 14.8, 7.2 Hz, 0.25H, enol CHCH<sub>2</sub>), 5.80 (s, 0.25H, enol CO=CH), 4.12 (s, 1.50H, keto COCH<sub>2</sub>), 3.60 (t, *J* = 6.5 Hz, 2H, CH<sub>2</sub>OH), 3.33–3.45 (m, 2H, CH<sub>2</sub>N), 3.11 (t, *J* = 6.8 Hz, 0.50H, enol CH<sub>2</sub>S), 3.04 (t, *J* = 6.7 Hz, 1.50H, ketoCH<sub>2</sub>S), 2.24–2.34 (m, 2H, C=CCH<sub>2</sub>), 1.98 (s, 0.75H, enol COCH<sub>3</sub>), 1.97 (s, 2.25H, keto COCH<sub>3</sub>), 1.87 (s, 0.75H, enol C=CCH<sub>3</sub>), 1.82 (s, 2.25H, keto C=CCH<sub>3</sub>), 1.63–1.71 (m, 2H, CH<sub>2</sub>CH<sub>2</sub>OH) ppm. <sup>13</sup>C NMR (acetone-d<sub>6</sub>) keto only: δ = 194.7, 194.4, 173.5, 146.6, 143.1, 134.2, 127.5, 62.1, 53.1, 39.9, 32.5, 30.7, 29.2 (HSQC), 22.7, 11.6 ppm. MS (ESI) *m/z*: 314.2 [M+H]<sup>+</sup>

**(S)-2-Acetamidoethyl butanethioate (13).** The title compound was prepared from butyryl chloride according to the general procedure **H**: Yield 81%, yellow oil. <sup>1</sup>H NMR (acetone-d<sub>6</sub>) δ = 7.36 (br. s, 1H), 3.28–3.34 (m, 2H), 2.98 (t, *J* = 6.9 Hz, 2H), 2.55 (t, *J* = 7.4 Hz, 2H), 1.87 (s, 3H), 1.65 (app. sxt., *J* = 7.4 Hz, 2 H), 0.92 (t, *J* = 7.4 Hz, 3H) ppm. <sup>13</sup>C NMR (acetone-d<sub>6</sub>) δ = 199.1, 170.6, 46.4, 39.8, 29.0, 22.9, 19.8, 13.7 ppm. MS (ESI) *m/z*: 190.1 [M+H]<sup>+</sup>

**(S)-2-Acetamidoethyl benzothioate (14).** The title compound was prepared from benzoic acid according to the general procedure **H**: Yield 75%, white resin. <sup>1</sup>H NMR (acetone-d<sub>6</sub>): δ = 7.92–8.00 (m, 2H), 7.67 (tt, *J* = 7.4, 1.3 Hz, 1H), 7.54 (tt, *J* = 7.4, 1.3, 2H), 7.38 (br. s, 1H), 3.36–3.50 (m, 2H), 3.20 (t, *J* = 6.9 Hz, 2H), 1.88 (s, 3H) ppm. <sup>13</sup>C NMR (acetone-d<sub>6</sub>): δ = 191.8, 170.3, 138.0, 134.6, 129.8, 127.9, 39.7, 22.9 ppm. MS (ESI) *m/z*: 224.0 [M+H]<sup>+</sup>

**(S)-2-Acetamidoethyl-3-hydroxybenzothioate (15).** The title compound was prepared from 3-hydroxybenzoic acid according to the general procedure **H**: Yield 62%, white solid. <sup>1</sup>H NMR (acetone-d<sub>6</sub>): δ = 9.15 (br. s, 1H), 7.54 (br. s, 1H), 7.40–7.46 (m, 2H), 7.35 (t, *J* = 8.1 Hz, 1H), 7.10–7.15 (m, 1H), 3.40–3.49 (m, 2H), 3.19 (t, *J* = 6.7 Hz, 2H), 1.92 (s, 3H) ppm. <sup>13</sup>C NMR (acetone-d<sub>6</sub>) δ = 191.6, 171.0, 158.9, 139.3, 130.9, 121.7, 119.1, 114.4, 39.8, 29.3, 22.9 ppm. MS (ESI) *m/z*: 239.9 [M+H]<sup>+</sup>

**(S)-2-Acetamidoethyl-(2E,4E)-2,5-dimethylocta-2,4-dienethioate (16).** The title compound was prepared from **IM-43** according to the general procedure **H**: Yield 43%, yellow oil. Mixture of regioisomers, approx: 2E,4E = 53%, 2E,4Z = 26%, 2Z,4E = 13%, 2Z,4Z = 7%; <sup>1</sup>H NMR (acetone-d<sub>6</sub>) 2E,4E isomer only: δ = 7.58–7.67 (m, 2H), 6.23 (dq, *J* = 11.5, 1.3 Hz, 1H), 3.30–3.36 (m, 2H), 3.03 (t, *J* = 6.6 Hz, 2H), 2.18 (t, *J* = 7.4 Hz, 2H), 1.93 (s, 3H), 1.88 (s, 3H), 1.87 (s, 3H), 1.51 (app. sxt., *J* = 7.4 Hz, 2H), 0.89 (t, *J* = 7.4 Hz, 3H) ppm. <sup>13</sup>C NMR (acetone-d<sub>6</sub>)

2*E*,4*E* isomer only:  $\delta$  = 192.9, 170.4, 150.9, 134.0, 133.2, 121.3, 43.3, 39.9, 29.1, 22.9, 21.7, 17.4, 14.1, 12.6 ppm. MS (ESI) *m/z*: 270.1 [M+H]<sup>+</sup>

**(2*E*,4*E*)-(S)-2-Acetamidoethyl-2-methylocta-2,4-dienethioate (17).** The title compound was prepared from **IM-36** according to the general procedure **H**: Yield 30%, yellow oil. <sup>1</sup>H NMR (acetone-*d*<sub>6</sub>):  $\delta$  = 7.69 (br. t, 1H), 7.16 (d, *J* = 10.9 Hz, 1H), 6.46 (d, *J* = 15.1, 10.9 Hz, 1H), 6.24 (d, *J* = 15.1, 7.3 Hz, 1H), 3.31–3.39 (m, 2H), 3.05 (t, *J* = 6.8 Hz, 2H), 2.18–2.24 (m, 2H), 1.94 (s, 3H), 1.93 (s, 3H), 1.44–1.52 (m, 2H), 0.92 (t, *J* = 7.3 Hz, 3H) ppm. <sup>13</sup>C NMR (acetone-*d*<sub>6</sub>):  $\delta$  = 193.0, 171.3, 145.6, 138.4, 133.5, 126.7, 40.0, 36.0, 28.9, 22.9, 22.8, 14.0, 12.7 ppm. MS (ESI) *m/z*: 256.1 [M+H]<sup>+</sup>

**(2*E*,4*E*)-(S)-2-Acetamidoethyl-2-methyl-5-phenylpenta-2,4-dienethioate (18).** The title compound was prepared from **IM-38** according to the general procedure **H**: Yield 43%, yellow oil. 2*E*,4*E*/2*Z*,4*E* = 14:1, <sup>1</sup>H NMR (acetone-*d*<sub>6</sub>) 4*E*,6*E*-isomer only:  $\delta$  = 7.74 (t, *J* = 5.2 Hz, 1H), 7.59–7.63 (m, 2H), 7.28–7.40 (m, 4H), 7.28 (dd, *J* = 14.6, 11.0 Hz, 1H), 7.05 (d, *J* = 14.6 Hz, 1H), 3.35–3.44 (m, 2H), 3.11 (t, *J* = 6.7 Hz, 2H), 2.08 (s, 3H), 2.02 (s, 3H) ppm. <sup>13</sup>C NMR (acetone-*d*<sub>6</sub>):  $\delta$  = 192.9, 170.9, 141.5, 138.2, 137.6, 135.7, 129.9, 129.7, 128.3, 124.6, 39.9, 29.2 (HSQC), 22.9, 13.0 ppm. MS (ESI) *m/z*: 290.1 [M+H]<sup>+</sup>

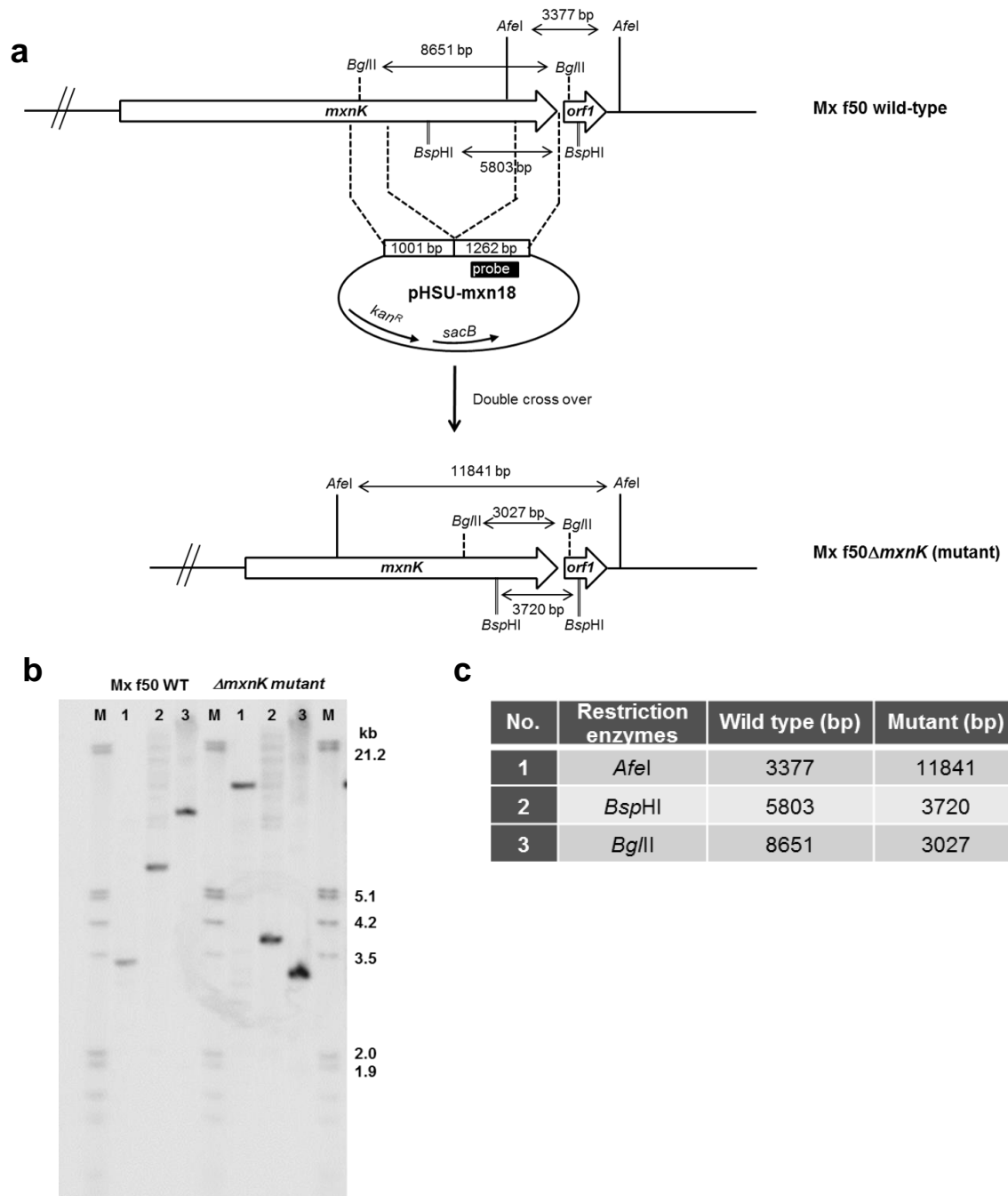
### 6.3.1.2 Construction of in-frame deletion mutant and point mutation mutants in *Myxococcus fulvus* Mx f50

**Table S1.** List of Strains and Plasmids used in this study

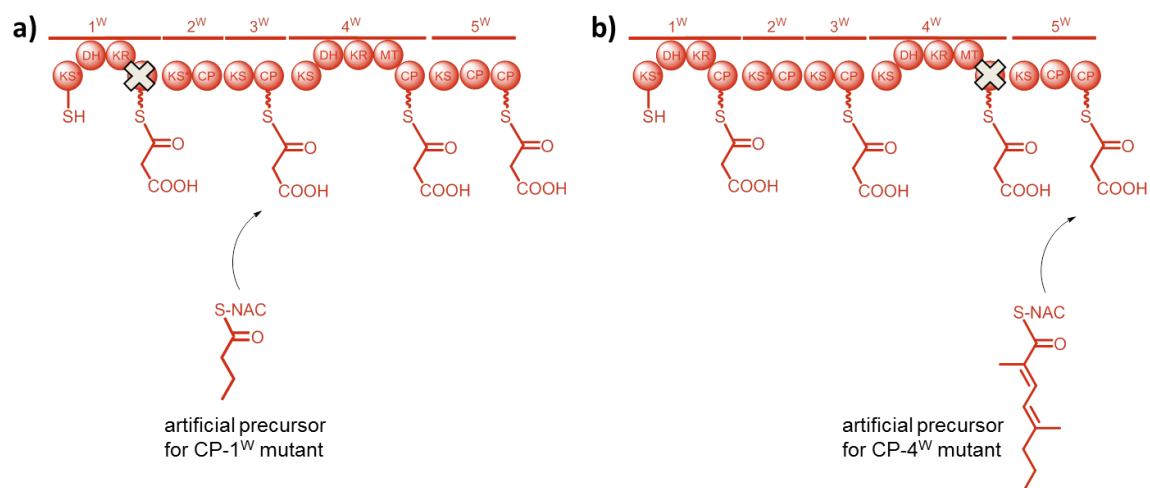
Strain/Plasmid	Description	Reference
<b><i>E. coli</i> strains</b>		
HS996	Host for general cloning experiments	Invitrogen
SCS110	Host for cloning experiments to prepare plasmid DNA free of Dam or Dcm methylation	Stratagene
<b><i>Myxococcus fulvus</i> strains</b>		
Mx f50	Myxopyronin producing wild-type strain	Irschik et al. <sup>[7]</sup>
Mx f50ΔpHSU-mxn18 (Δ <i>mxnK</i> )	<i>mxnK</i> in-frame deletion mutant; no myxopyronin production	this study
Mx f50ΔpHSU-mxn48 (ΔCP-1 <sup>W</sup> , point mutation at CP-1 <sup>W</sup> , S1686A)	CP-1 <sup>W</sup> point mutation; myxopyronin production (trace amount)	this study
Mx f50ΔpHSU-mxn49 (ΔCP-4 <sup>W</sup> , point mutation at CP-4 <sup>W</sup> , S5168A)	CP-3 <sup>W</sup> point mutation; myxopyronin production (trace amount)	this study
<b>Plasmids</b>		
pSWU41	Vector contains a neomycin phosphotransferase ( <i>nptII</i> ) gene for selection and a levansucrose ( <i>sacB</i> ) gene for counter selection	Wu et al. <sup>[8]</sup>
pHSU-mxn18	<i>mxnK</i> gene deletion construct, in which a 5624 bp fragment of <i>mxnC-mxnH</i> was deleted in-frame	
pHSU-mxn48	CP-1 <sup>W</sup> point mutation construct in which the active site serine residue is exchanged with alanine residue (S1668A)	this study
pHSU-mxn49	CP-3 <sup>W</sup> point mutation construct in which the active site serine residue is exchanged with alanine residue (S5168A)	this study

Table S2. List of primers used in this study

Primer name	Sequence (5'→3')	Restriction sites (in bold)
mxn54	GCGTTGAT <b>GGATCC</b> ACAGCA	<i>Bam</i> HI
mxn55	TGTATC <b>GCGGCCGCT</b> CAGTGCCGCTGAACCCGAAC	<i>Not</i> I
mxn56	GATACAG <b>GCGGCCGCT</b> TTCCGAGTCCAGCAGC	<i>Not</i> I
mxn57	GTATC <b>GAGCTC</b> ATCTGCTGTCCTCTGCCT	<i>Sac</i> I
mxn70	CTTGCGCCCTGAGTGCTT	
mxn71	AACACCTCACGGTCCGAC	
mxn72	CCCATCGTCCACAGCTTC	
mxn73	GCACTACAAGCGGCTCTG	
mxn169	GATACAC <b>CGATCG</b> CACGAGTTCCGAGTCCTC	<i>Pvu</i> II
mxn170	CTGCAGGATGAGGGCGTC	
mxn171	TCGACGCCCTCATCCTGCAGGAGTTGATGGCGGAGCTG	
mxn172	TCTATG <b>GCGGCCGCG</b> AGCGCGACCTTGATGAC	<i>Not</i> I
mxn174	GATACAC <b>CGATCGG</b> ACACACACCCGGAAGCTG	<i>Pvu</i> II
mxn175	ATCACCAGCGCGTCGAC	
mxn176	CGGCGTCGACGCGCTGGTGAATCTGAGAATCGTCC	
mxn177	TCTATG <b>GAGCTC</b> TTGAGCTGCAGGATGACC	<i>Not</i> I
mxn185	TCGCTCATCCTGCAGGA	
mxn187	CGAGTCGAGTCCCATGG	
mxn189	CAACAGCTTCCTCGACG	
mxn191	TCCCTGGTGAATCTGAGA	
mxn193	GGAGTCGACGCCGAAC	
mxn195	TCGGA CTGATGAAGGGGT	
mxn205	CCTTCGGGGAGATGTTGA	
mxn206	GAAGGCCTCCACGTTCTC	
pJET1.2For	CGACTCACTATAGGGAGAGCGGC	
pJET1.2Rev	AAGAACATCGATTTTCCATGGCAG	
pSWU41-F	GTGCAAAAAAGCGGTTAG	



**Figure S1.** Schematic representation of in-frame deletion of 5.6 kb *mxnK* by construct pHSU-*mxn18*, (a), confirmation by Southern blot (b) and the expected fragment size after hydrolysis of wild type and mutant genomic DNA with a set of three restriction enzymes and a DIG-labelled 602 bp probe amplified from Mx f50 genomic DNA using the primers *mxn79* and *mxn80*. M: Marker III (Roche), 1: hydrolysis with *AfeI*, 2: hydrolysis with *Bsp*HI, 3: hydrolysis with *Bgl*II.



**Figure S2.** Schematic illustration of mutasynthesis using *M. fulvus* Mx X50 mutants with partially functional western chain assembly line. a) A culture of a CP-1<sup>W</sup> mutant was supplemented with the appropriate precursor which is incorporated in the subsequent biosynthesis pathway. b) A culture of a CP-4<sup>W</sup> mutant was supplemented with the appropriate precursor which is incorporated in the subsequent biosynthesis pathway.

### 6.3.2 Characterization of the myxopyronin derivatives W1-W18

#### Calculated and expected masses

**Table S3.** Characterization of novel myxopyronin A analogues with representative fragmentation patterns observed

	Chemical formula	Calculated mass $m/z$ $[M+H]^+$	Observed $m/z$ $[M+H]^+$	Fragmentation due to losses of			
				H <sub>2</sub> O ( $m/z$ = 18)	CH <sub>3</sub> OH ( $m/z$ = 32)	H <sub>2</sub> N-CO <sub>2</sub> CH <sub>3</sub> ( $m/z$ = 75)	H <sub>2</sub> N-CO <sub>2</sub> CH <sub>3</sub> , CO <sub>2</sub> ( $m/z$ = 119)
Myx A	C <sub>23</sub> H <sub>32</sub> NO <sub>6</sub>	418.22241	418.22217	400.2112	386.1957	343.18988	299.20017
W1	C <sub>23</sub> H <sub>32</sub> NO <sub>6</sub>	418.22241	418.22227	400.2111	386.1956	343.18981	299.20007
W2	C <sub>22</sub> H <sub>30</sub> NO <sub>6</sub>	404.20676	404.20666	386.1958	372.1802	329.17446	285.18464
W4	C <sub>22</sub> H <sub>32</sub> NO <sub>6</sub>	406.22241	406.22250	388.2107	374.1955	331.18951	287.19987
W6	C <sub>25</sub> H <sub>28</sub> NO <sub>6</sub>	438.19111	438.19103	420.1793	406.1639	363.15828	319.16866
W7	C <sub>26</sub> H <sub>30</sub> NO <sub>6</sub>	452.20676	452.20686	434.1954	420.1814	377.17400	333.18430
W8	C <sub>25</sub> H <sub>30</sub> NO <sub>6</sub>	440.20676	440.20659	422.1952	408.1795	365.17410	321.18438
W9	C <sub>25</sub> H <sub>28</sub> NO <sub>7</sub>	454.18602	454.18643	436.1746	n.o	379.15314	335.16345
W10	C <sub>25</sub> H <sub>26</sub> NO <sub>6</sub>	516.10163	516.10175	498.0907	484.0753	441.06942	397.07952
W11	C <sub>21</sub> H <sub>26</sub> NO <sub>6</sub>	388.17546	388.17557	n.o	n.o	313.14233	269.15311
W12	C <sub>22</sub> H <sub>30</sub> NO <sub>7</sub>	420.20167	420.20148	402.1905	n.o	345.16920	301.17982
W13	C <sub>23</sub> H <sub>32</sub> NO <sub>6</sub>	418.22241	418.22232	400.2116	386.1959	343.18984	299.19999
W14	C <sub>26</sub> H <sub>30</sub> NO <sub>6</sub>	452.20676	452.20670	434.1973	420.1802	377.17516	333.18508
W16	C <sub>23</sub> H <sub>32</sub> NO <sub>6</sub>	418.22241	418.22235	400.2113	386.1959	343.18972	299.20000
W17	C <sub>22</sub> H <sub>30</sub> NO <sub>6</sub>	404.20676	404.20675	386.1963	372.1820	329.17496	285.18512
W18	C <sub>25</sub> H <sub>28</sub> NO <sub>6</sub>	438.19111	438.19118	420.1804	406.1649	363.15886	319.16910

**n.o. = not observed**

### 6.3.3 References

- [1] Y. Oikawa, K. Sugano, O. Yonemitsu, *J. Org. Chem.* **1978**, *43*(10), 2087-2088.
- [2] B. M. Trost, J. P. N. Papillon, T. Nussbaumer, *J. Am. Chem. Soc.* **2005**, *127*, 17921-17937.
- [3] R. K. Boeckman Jr., T. M. Kamenecka, S.G. Nelson, J. R. Pruitt, T.E. Barta, *Tetrahedron Lett.* **1991**, *32*, 2581-2584.
- [4] T. Yoshinari, K. Ohmori, M. G. Schrems, A. Pfaltz, K. Suzuki, *Angew. Chem. Int. Ed.* **2010**, *49*, 881-885.
- [5] I. H. Gilbert, M. Ginty, J. A. O'Neill, T. J. Simpson, J. Staunton, C. L. Willis, *Bioorg. Med. Chem. Lett.* **1995**, *5*, 1587-1590.
- [6] S. P. Raillard, C. Weiwei, E. Sullivan, W. Bajjalieh, A. Bhandari, T. A. Baer, *J. Comb. Chem.* **2002**, *4*, 470-474.
- [7] H. Irschik, K. Gerth, G. Höfle, W. Kohl, H. Reichenbach, *J. Antibiot.* **1983**, *36*, 1651-1684.
- [8] S. S. Wu, D. Kaiser, *J. Bacteriol.* **1996**, *178*, 5817-5821.

## 6.4 Supporting Information for Publication D

Full supporting information is available online:

[http://pubs.acs.org/doi/suppl/10.1021/jm401102e/suppl\\_file/jm401102e\\_si\\_001.pdf](http://pubs.acs.org/doi/suppl/10.1021/jm401102e/suppl_file/jm401102e_si_001.pdf)

### 6.4.1 Experimental procedures

#### 6.4.1.1 Chemistry

##### 6.4.1.1.1 Synthesis and spectroscopic data of compounds 1–12

**Methyl 3-amino-5-(4'-methoxyphenyl)thiophene-2-carboxylate (IIa).** The title compound was prepared from 4'-methoxyacetophenone according to general procedure **A** and used directly in the next step without further purification.  $^1\text{H}$  NMR (DMSO- $d_6$ , 500 MHz):  $\delta$  = 7.56 (d,  $J$  = 8.8 Hz, 2 H), 7.00 (d,  $J$  = 8.8 Hz, 2 H), 6.86 (s, 1 H), 6.56 (br. s, 2 H), 3.79 (s, 3 H, OCH<sub>3</sub>), 3.72 (s, 3 H, OCH<sub>3</sub>) ppm.  $^{13}\text{C}$  NMR (DMSO- $d_6$ , 126 MHz):  $\delta$  = 163.9, 160.0, 155.7, 147.7, 127.0, 125.3, 114.9, 114.6, 95.7, 55.3, 50.8 ppm.

**Methyl 3-amino-5-(4'-phenoxyphenyl)thiophene-2-carboxylate (IIb).** The title compound was prepared from 4'-phenoxyacetophenone according to general procedure **A** and used directly in the next step without further purification.  $^1\text{H}$  NMR (DMSO- $d_6$ , 500 MHz):  $\delta$  = 7.64 (d,  $J$  = 8.8 Hz, 2 H), 7.46–7.40 (m, 2 H), 7.22–7.17 (m, 1 H), 7.11–7.06 (m, 2 H), 7.04 (d,  $J$  = 8.8 Hz, 2 H), 6.91 (s, 1 H), 6.59 (br. s, 2 H), 3.72 (s, 3 H, OCH<sub>3</sub>) ppm.  $^{13}\text{C}$  NMR (DMSO- $d_6$ , 126 MHz):  $\delta$  = 163.9, 157.7, 155.9, 147.0, 130.2, 127.8, 127.4, 124.1, 119.3, 118.7, 115.7, 96.2, 50.9 ppm.

**Methyl 3-amino-5-(4'-bromophenyl)thiophene-2-carboxylate (IIc).** The title compound was prepared from 4'-bromoacetophenone according to general procedure **A**.  $^1\text{H}$  NMR (CDCl<sub>3</sub>, 300 MHz):  $\delta$  = 7.51 (d,  $J$  = 8.0 Hz, 2 H), 7.43 (d,  $J$  = 8.0 Hz, 2 H), 6.75 (s, 1 H), 5.49 (br. s., 2 H), 3.85 (s, 3 H, OCH<sub>3</sub>) ppm.  $^{13}\text{C}$  NMR (CDCl<sub>3</sub>, 75 MHz):  $\delta$  = 164.8, 154.2, 147.6, 132.3, 132.1, 127.3, 123.0, 115.8, 100.7, 51.3 ppm.

**3-Amino-5-(4'-methoxyphenyl)thiophene-2-carboxylic acid (IIIa).** The title compound was prepared from **IIa** according to general procedure **B**.  $^1\text{H}$  NMR (DMSO- $d_6$ , 300 MHz):  $\delta$  = 7.55 (d,  $J$  = 8.8 Hz, 2 H), 6.99 (d,  $J$  = 8.8 Hz, 2 H), 6.84 (s, 1 H), 3.79 (s, 3 H, OCH<sub>3</sub>) ppm.  $^{13}\text{C}$  NMR (DMSO- $d_6$ , 75 MHz):  $\delta$  = 165.3, 159.9, 155.3, 147.0, 127.0, 125.6, 115.0, 114.6, 97.1, 55.3 ppm.

**3-Amino-5-(4'-phenoxyphenyl)thiophene-2-carboxylate (IIIb).** The title compound was prepared from **IIb** according to general procedure **B**.  $^1\text{H}$  NMR (DMSO- $d_6$ , 500 MHz):  $\delta$  = 7.63 (d,  $J$  = 8.8 Hz, 2 H), 7.47–7.38 (m, 2 H), 7.23–7.16 (m, 1 H), 7.08 (d,  $J$  = 8.8 Hz, 2 H), 7.06–6.99 (m, 2 H), 6.90 (s, 1 H) ppm.  $^{13}\text{C}$  NMR (DMSO- $d_6$ , 126 MHz):  $\delta$  = 165.2, 157.5, 155.9, 146.3, 130.2, 128.1, 127.3, 124.0, 119.2, 118.7, 115.8, 97.7 ppm.

**3-Amino-5-(4'-bromophenyl)thiophene-2-carboxylic acid (IIIc).** The title compound was prepared from **IIc** according to general procedure **B**.  $^1\text{H}$  NMR (DMSO- $d_6$ , 500 MHz):  $\delta$  = 7.63 (d,  $J$  = 8.8 Hz, 2 H), 7.57 (d,  $J$  = 8.8 Hz, 2 H), 6.98 (s, 1 H) ppm.  $^{13}\text{C}$  NMR (DMSO- $d_6$ , 126 MHz):  $\delta$  = 165.2, 155.1, 145.3, 132.2,

132.1, 127.5, 122.0, 116.8, 98.5 ppm.

**6-(4'-Methoxyphenyl)-2,4-dihydro-1*H*-thieno[3,2-*d*][1,3]oxazine-2,4-dione**

**(IVa).** The title compound was prepared from **IIIa** according to general procedure **C**. <sup>1</sup>H NMR (DMSO-*d*<sub>6</sub>, 300 MHz): δ = 12.28 (s, 1 H), 7.74 (d, *J* = 8.9 Hz, 2 H), 7.12 (s, 1 H), 7.04 (d, *J* = 8.9 Hz, 2 H), 3.82 (s, 3 H, OCH<sub>3</sub>) ppm. <sup>13</sup>C NMR (DMSO-*d*<sub>6</sub>, 75 MHz): δ = 161.1, 155.5, 155.0, 149.6, 148.6, 127.9, 124.1, 114.8, 111.2, 103.1, 55.4 ppm.

**6-(4'-Phenoxyphenyl)-2,4-dihydro-1*H*-thieno[3,2-*d*][1,3]oxazine-2,4-dione**

**(IVb).** The title compound was prepared from **IIIb** according to general procedure **C**. <sup>1</sup>H NMR (DMSO-*d*<sub>6</sub>, 500 MHz): δ = 12.33 (br. s., 1 H), 7.83 (d, *J* = 8.8 Hz, 2 H), 7.48–7.43 (m, 2 H), 7.23 (t, *J* = 7.4 Hz, 1 H), 7.18 (s, 1 H), 7.13–7.10 (m, 2 H), 7.08 (d, *J* = 8.8 Hz, 2 H) ppm. <sup>13</sup>C NMR (DMSO-*d*<sub>6</sub>, 126 MHz): δ = 158.9, 155.4, 155.0, 154.8, 149.6, 148.5, 130.3, 128.4, 126.4, 124.4, 119.6, 118.6, 112.1, 103.8 ppm.

**6-(4'-Bromophenyl)-2,4-dihydro-1*H*-thieno[3,2-*d*][1,3]oxazine-2,4-dione (IVc).**

The title compound was prepared from **IIIc** according to general procedure **C**. <sup>1</sup>H NMR (DMSO-*d*<sub>6</sub>, 500 MHz): δ = 12.39 (br. s., 1 H), 7.77 (d, *J* = 8.8 Hz, 2 H), 7.70 (d, *J* = 8.8 Hz, 2 H), 7.29 (s, 1 H) ppm. <sup>13</sup>C NMR (DMSO-*d*<sub>6</sub>, 126 MHz): δ = 155.1, 153.5, 149.7, 148.6, 132.4, 130.8, 128.3, 123.8, 113.4, 104.7 ppm.

**3-(3''-Benzyl-3''-ethylureido)-5-(4'-methoxyphenyl)thiophene-2-carboxylic acid (1).**

The title compound was prepared from **IVa** according to general procedure **D**. <sup>1</sup>H NMR (DMSO-*d*<sub>6</sub>, 300 MHz): δ = 13.21 (br. s, 1 H, COOH), 10.10 (s, 1 H), 8.17 (s, 1 H), 7.63 (d, *J* = 8.9 Hz, 2 H), 7.38–7.29 (m, 5 H), 7.02 (d, *J* = 8.9 Hz, 2 H), 3.80 (s, 3 H, OCH<sub>3</sub>), 3.39 (q, *J* = 7.1 Hz, 2 H), 1.16 (t, *J* = 7.1, 3 H) ppm. <sup>13</sup>C NMR (DMSO-*d*<sub>6</sub>, 75 MHz): δ = 165.8, 160.2, 153.1, 147.9, 147.0, 138.1, 128.5, 127.2, 127.1, 127.1, 125.3, 116.1, 114.7, 105.6, 55.3, 49.3, 41.8, 13.1 ppm.

**5-(4'-Methoxyphenyl)-3-ureidothiophene-2-carboxylic acid (2).**

The title compound was prepared from **IVa** according to general procedure **D**. <sup>1</sup>H NMR (DMSO-*d*<sub>6</sub>, 300 MHz): δ = 12.92 (br. s., 1 H, COOH), 9.30 (s, 1 H), 8.15 (s, 1 H), 7.60 (d, *J* = 8.8 Hz, 2 H), 7.01 (d, *J* = 8.8 Hz, 2 H), 6.81 (br. s, 2 H), 3.76 (s, 3 H, OCH<sub>3</sub>) ppm. <sup>13</sup>C NMR (DMSO-*d*<sub>6</sub>, 75 MHz): δ = 164.8, 160.0, 154.7, 147.1, 146.6, 127.1, 125.4, 116.7, 114.7, 105.4, 55.3 ppm.

**5-(4'-Phenoxyphenyl)-3-ureidothiophene-2-carboxylic acid (3).**

The title compound was prepared from **IVb** according to general procedure **D**. <sup>1</sup>H NMR (DMSO-*d*<sub>6</sub>, 300 MHz): δ = 12.99 (br. s., 1 H, COOH), 9.30 (s, 1 H), 8.21 (s, 1 H), 7.68 (d, *J* = 8.8 Hz, 2 H), 7.49–7.38 (m, 2 H), 7.25–7.14 (m, 1 H), 7.13–7.02 (m, 4 H), 6.90–6.60 (m, 2 H) ppm. <sup>13</sup>C NMR (DMSO-*d*<sub>6</sub>, 75 MHz): δ = 164.7, 157.7, 155.9, 154.6, 146.5, 146.4, 130.2, 127.9, 127.5, 124.1, 119.3, 118.8, 117.5, 106.1 ppm.

**3-(3''-(Carboxymethyl)ureido)-5-(4'-methoxyphenyl)thiophene-2-carboxylic acid (4).**

The title compound was prepared from **IVa** according to general procedure **D**. <sup>1</sup>H NMR (DMSO-*d*<sub>6</sub>, 300 MHz): δ = 12.79 (br. s., 2 H, COOH), 9.47

(s, 1 H), 8.13 (s, 1 H), 8.08 (t,  $J = 5.6$  Hz, 1 H), 7.61 (d,  $J = 8.8$  Hz, 2 H), 7.01 (d,  $J = 8.8$  Hz, 2 H), 3.83–3.77 (m, 2 H) 3.80 (s, 3 H, OCH<sub>3</sub>) ppm. <sup>13</sup>C NMR (DMSO-*d*<sub>6</sub>, 75 MHz):  $\delta = 171.9, 164.7, 160.1, 154.1, 147.2, 146.1, 127.1, 125.4, 116.7, 114.7, 105.7, 55.3, 41.3$  ppm.

**3-(3''-(2-Carboxyethyl)ureido)-5-(4'-methoxyphenyl)thiophene-2-carboxylic acid (5).** The title compound was prepared from **IVa** according to general procedure **D**. <sup>1</sup>H NMR (DMSO-*d*<sub>6</sub>, 300 MHz):  $\delta = 12.58$  (br. s., 2 H, COOH), 9.34 (s, 1 H), 8.16 (s, 1 H), 7.90–7.72 (m, 1 H), 7.60 (d,  $J = 8.4$  Hz, 2 H), 7.01 (d,  $J = 8.4$  Hz, 2 H), 3.80 (s, 3 H, OCH<sub>3</sub>), 3.33–3.24 (m, 2 H), 2.44 (t,  $J = 6.2$  Hz, 2 H) ppm. <sup>13</sup>C NMR (DMSO-*d*<sub>6</sub>, 75 MHz)  $\delta = 173.0, 164.7, 160.1, 153.8, 147.1, 146.3, 127.1, 125.4, 116.7, 114.7, 105.4, 55.3, 35.6, 34.3$  ppm.

**(S)-3-(3''-(1-Carboxyethyl)ureido)-5-(4'-methoxyphenyl)thiophene-2-carboxylic acid (6).** The title compound was prepared from **IVa** according to general procedure **D**. <sup>1</sup>H NMR (DMSO-*d*<sub>6</sub>, 300 MHz):  $\delta = 12.76$  (br. s., 2 H, COOH), 9.43 (s, 1 H), 8.14 (s, 1 H), 8.09 (d,  $J = 7.1$  Hz, 1 H), 7.61 (d,  $J = 8.8$  Hz, 2 H), 7.03 (d,  $J = 8.8$  Hz, 2 H), 4.22–4.08 (m, 1 H), 3.81 (s, 3 H, OCH<sub>3</sub>), 1.32 (d,  $J = 7.30$  Hz, 3 H, CH<sub>3</sub>) ppm. <sup>13</sup>C NMR (DMSO-*d*<sub>6</sub>, 75 MHz):  $\delta = 174.7, 164.7, 160.1, 153.5, 147.2, 146.1, 127.1, 125.4, 116.6, 114.7, 105.6, 55.3, 48.3, 17.4$  ppm.

**(S)-3-(3''-(1-Carboxy-2-phenylethyl)ureido)-5-(4'-methoxyphenyl)thiophene-2-carboxylic acid (7).** The title compound was prepared from **IVa** according to general procedure **D**. <sup>1</sup>H NMR (DMSO-*d*<sub>6</sub>, 300 MHz):  $\delta = 12.84$  (br. s., 2 H, COOH), 9.42 (s, 1 H), 8.15 (d,  $J = 7.9$  Hz, 1 H), 8.09 (s, 1 H), 7.69–7.51 (m,  $J = 8.8$  Hz, 2 H), 7.37–7.25 (m, 4 H), 7.25–7.17 (m, 1 H), 7.03–6.97 (m,  $J = 8.8$  Hz, 2 H), 4.56–4.28 (m, 1 H), 3.79 (s, 3 H, OCH<sub>3</sub>), 3.11 (dd,  $J = 13.9, 4.6$  Hz, 1 H), 2.88 (dd,  $J = 13.9, 9.8$  Hz, 1 H) ppm. <sup>13</sup>C NMR (DMSO-*d*<sub>6</sub>, 75 MHz):  $\delta = 173.6, 164.6, 160.1, 153.7, 147.1, 145.9, 137.7, 129.0, 128.2, 127.1, 126.4, 125.4, 116.7, 114.7, 105.8, 55.3, 54.4, 36.9$  ppm.

**5-(4'-Methoxyphenyl)-3-(3''-phenethylureido)thiophene-2-carboxylic acid (8).** The title compound was prepared from **IVa** according to general procedure **D**. <sup>1</sup>H NMR (DMSO-*d*<sub>6</sub>, 300 MHz):  $\delta = 12.96$  (br. s., 1 H, CCOH), 9.33 (s, 1 H), 8.18 (s, 1 H), 7.84–7.70 (m, 1 H), 7.61 (d,  $J = 8.3$  Hz, 2 H), 7.39–7.13 (m, 5 H), 7.02 (d,  $J = 8.3$  Hz, 2 H), 3.80 (s, 3 H, OCH<sub>3</sub>), 3.42–3.26 (m, 2 H), 2.90–2.67 (m, 2 H) ppm. <sup>13</sup>C NMR (DMSO-*d*<sub>6</sub>, 75 MHz):  $\delta = 164.8, 160.0, 153.8, 147.2, 146.5, 139.5, 128.6, 128.3, 127.1, 126.1, 125.4, 116.7, 114.7, 105.2, 55.3, 41.0, 35.5$  ppm.

**(R)-3-(3''-(1-Carboxyethyl)ureido)-5-(4'-methoxyphenyl)thiophene-2-carboxylic acid (9).** The title compound was prepared from **IVa** according to general procedure **D**. <sup>1</sup>H NMR (DMSO-*d*<sub>6</sub>, 300 MHz):  $\delta = 12.76$  (br. s., 2 H, CCO), 9.43 (s, 1 H), 8.14 (s, 1 H), 8.09 (d,  $J = 7.1$  Hz, 1 H), 7.61 (d,  $J = 8.9$  Hz, 2 H), 7.01 (d,  $J = 8.9$  Hz, 2 H), 4.22–4.08 (m, 1 H), 3.80 (s, 3 H, OCH<sub>3</sub>), 1.31 (d,  $J = 7.4$  Hz, 3 H, CH<sub>3</sub>) ppm. <sup>13</sup>C NMR (DMSO-*d*<sub>6</sub>, 75 MHz):  $\delta = 174.7, 164.7, 160.1, 153.5, 147.2, 146.1, 127.1, 125.4, 116.6, 114.7, 105.6, 55.3, 48.3, 17.4$  ppm.

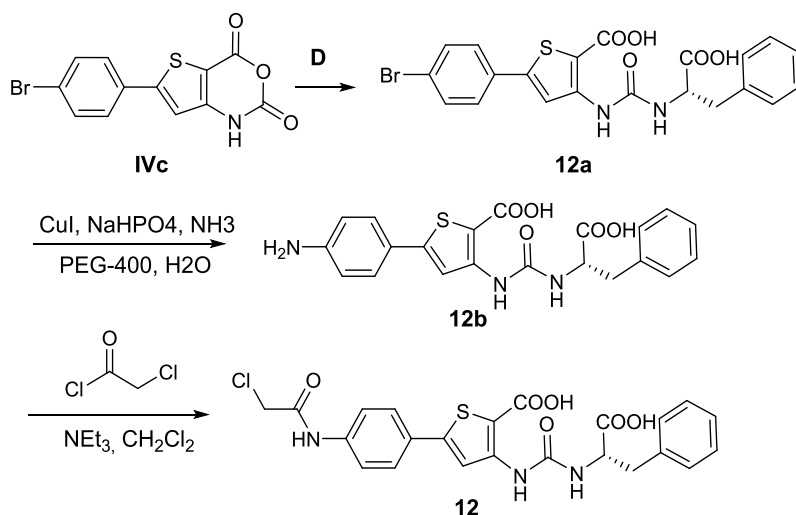
**(R)-3-(3''-(1-Carboxy-2-phenylethyl)ureido)-5-(4'-methoxyphenyl)thiophene-2-carboxylic acid (10).** The title compound was prepared from **IVa** according to

general procedure **D**.  $^1\text{H}$  NMR (DMSO- $d_6$ , 300 MHz):  $\delta$  = 12.84 (br. s., 2 H, CCOH), 9.42 (s, 1 H), 8.15 (d,  $J$  = 7.9 Hz, 1 H), 8.09 (s, 1 H), 7.59 (d,  $J$  = 8.8 Hz, 2 H), 7.37–7.25 (m, 4 H), 7.25–7.17 (m, 1 H), 7.00 (d,  $J$  = 8.8 Hz, 2 H), 4.56–4.28 (m, 1 H), 3.79 (s, 3 H, OCH<sub>3</sub>), 3.11 (dd,  $J$  = 13.9, 4.6 Hz, 1H), 2.88 (dd,  $J$  = 13.9, 9.8 Hz, 1 H) ppm.  $^{13}\text{C}$  NMR (DMSO- $d_6$ , 75 MHz):  $\delta$  = 173.6, 164.6, 160.1, 153.7, 147.1, 145.9, 137.7, 129.0, 128.2, 127.1, 126.4, 125.4, 116.7, 114.7, 105.8, 55.3, 54.4, 36.9 ppm.

**3-(3''-(2-Carboxypropan-2-yl)ureido)-5-(4'-methoxyphenyl)thiophene-2-carboxylic acid (11)**. The title compound was prepared from **IVa** according to general procedure **D**.  $^1\text{H}$  NMR (DMSO- $d_6$ , 300 MHz):  $\delta$  = 12.59 (br. s., 2 H, CCOH), 9.37 (s, 1 H), 8.13 (s, 1 H), 8.01 (s, 1 H), 7.61 (d,  $J$  = 8.8 Hz, 2 H), 7.00 (d,  $J$  = 8.8 Hz, 2 H), 3.80 (s, 3 H, OCH<sub>3</sub>), 1.40 (s, 6 H, (CH<sub>3</sub>)<sub>2</sub>) ppm.  $^{13}\text{C}$  NMR (DMSO- $d_6$ , 75 MHz):  $\delta$  = 176.0, 164.7, 160.0, 153.0, 147.2, 146.1, 127.1, 125.4, 116.5, 114.7, 105.4, 55.3, 54.9, 25.3 ppm.

**(S)-3-(3''-(1-Carboxy-2-phenylethyl)ureido)-5-(4'-(2-chloroacetamido)phenyl)thiophene-2-carboxylic acid (12)**.

#### Scheme S2: Synthesis of compound 12.



**(S)-3-(3''-(1-Carboxy-2-phenylethyl)ureido)-5-(4'-bromophenyl)thiophene-2-carboxylic acid (12a)** was prepared from **IVc** according to general procedure **D**.  $^1\text{H}$  NMR (DMSO- $d_6$ , 300 MHz):  $\delta$  = 12.93 (br. s., 2 H, CCOH), 9.42 (s, 1 H), 8.23 (s, 1 H), 8.17 (d,  $J$  = 7.9 Hz, 1 H), 7.70–7.54 (m, 4 H), 7.38–7.14 (m, 5 H), 4.47–4.30 (m, 1 H), 3.11 (dd,  $J$  = 13.9, 4.8 Hz, 1 H), 2.88 (dd,  $J$  = 13.9, 9.7 Hz, 1 H) ppm.  $^{13}\text{C}$  NMR (DMSO- $d_6$ , 75 MHz):  $\delta$  = 173.5, 164.5, 153.7, 145.7, 145.4, 137.7, 132.2, 132.0, 129.0, 128.2, 127.6, 126.4, 122.3, 118.5, 107.3, 54.4, 37.0 ppm.

**(S)-3-(3''-(1-Carboxy-2-phenylethyl)ureido)-5-(4'-aminophenyl)thiophene-2-carboxylic acid (12b)** was prepared from **12a** according to the following procedure: CuI (10 mg, 5.30  $\mu\text{mol}$ ), **12a** (127 mg, 0.26 mmol), Na<sub>3</sub>PO<sub>4</sub>·12 H<sub>2</sub>O (100 mg, 0.26 mmol), 25–28% aqueous ammonia (0.5 mL) and PEG-400 (1 mL) were added to a sealed tube. The reaction was stirred at 100 °C for 24 h, cooled

to 0 °C and cautiously acidified with 1 M HCl to pH 4–5. The resulting mixture was extracted with EtOAc (3 x 50 mL). The combined organic layers were washed with water (50 mL) and brine (50 mL), dried over MgSO<sub>4</sub> and concentrated to afford the title compound. The crude product was used in the next step without further purification.

**(S)-3-(3''-(1-Carboxy-2-phenylethyl)ureido)-5-(4'-(2-chloroacetamido)phenyl)thiophene -2-carboxylic acid (12)** was prepared from **12b** according to the following procedure: A solution of **12b** (142 mg, 1.10 mmol) and triethylamine (142 mg, 1.10 mmol) in CH<sub>2</sub>Cl<sub>2</sub> (6 mL) was stirred at -78 °C under stream of nitrogen. 2-Chloroacetyl chloride in CH<sub>2</sub>Cl<sub>2</sub> (4 mL) was added slowly and stirring was continued for 1 h at -78 °C, 1 h at 0 °C and 1 h at room temperature. The solution was diluted with ice water (30 mL) and acidified with a saturated solution of KHSO<sub>4</sub>. The resulting mixture was extracted with EtOAc (3 x 50 mL). The combined organic layers were then washed with water (50 mL) and brine (50 mL), dried over MgSO<sub>4</sub> and concentrated *in vacuo*. The crude material was purified via preparative HPLC (RP18, acetonitrile/H<sub>2</sub>O 50% → 95%) to yield the title compound as a light green solid. (Purity: 90%) <sup>1</sup>H NMR (DMSO-*d*<sub>6</sub>, 300 MHz): δ = 12.89 (br. s., 2 H, CCOH), 10.48 (s, 1 H), 9.41 (s, 1 H), 8.16 (d, *J* = 7.8 Hz, 1 H), 8.15 (s, 1 H), 7.73–7.62 (m, 4 H), 7.33–7.20 (m, 5 H), 4.43–4.34 (m, 1 H), 4.27 (s, 2 H, CH<sub>2</sub>Cl), 3.14–3.07 (m, 1 H), 2.92–2.84 (m, 1 H) ppm. <sup>13</sup>C NMR (DMSO-*d*<sub>6</sub>, 176 MHz): δ = 173.7, 164.9, 164.7, 153.8, 146.8, 145.9, 139.4, 137.8, 129.1, 128.3, 128.2, 126.5, 126.4, 119.8, 117.3, 106.3, 54.5, 43.6, 36.9 ppm.

#### 6.4.1.2 Biology and biophysics

##### 6.4.1.2.1 SPR - mutagenesis studies

###### *Preparation of PqsD mutant*

R223A PqsD mutant was generated using the QuikChange Site-Directed Mutagenesis Kit (Stratagene, La Jolla, CA) according to the manufacturer's instructions using the pET28b(+)/pqsD plasmid as a template. Briefly, pqsD gene was amplified through 16 cycles of PCR. After treatment with DpnI, the PCR product was transformed into *E. coli* strain XL1-Blue. Plasmid DNA was purified using the GenElute™ HP Plasmid Miniprep Kit (Sigma-Aldrich, St. Louis, MO) and sequenced to confirm the site-directed mutations. The primer sequence of the mutations:

Primer-design:

Arg223Ala-Mutante:

Wild: 5' GCGAGTTCCTCATGCGCGGCCGCGCCGATGTTTCGAGC 3'

Mut: 5' GCGAGTTCCTCATGCGCGGCGCGCCGATGTTTCGAGC 3'

Sequence of the Primer:

R223A\_PqsD\_Forward:

5' GCGAGTTCCTCATGCGCGGCCGCGCCGATGTTTCGAGC 3'

R223A\_PqsD\_Reverse:

5' GCTCGAACATCGGCGCGCCGCGCATGAGGAACTCGC 3'

### 6.4.2 Selectivity data for hit compounds: PqsD vs. RNAP inhibition

**Table S1.** Inhibitory activities of several virtual hit compounds against PqsD and RNAP and the derived selectivity factors.

R	IC <sub>50</sub> PqsD [μM]	IC <sub>50</sub> RNAP [μM]	Selectivity factor <sup>[a]</sup>
4-OCH <sub>3</sub>	6	241	40
3,4-di-Cl	4	22	5.5
3-CF <sub>3</sub> , 4-Cl	3	21	7.0
2,5-di-Cl	9	35	4.0
4-NO <sub>2</sub>	10	73	7.3
4-CF <sub>3</sub>	8	51	6.4
4-OCF <sub>3</sub>	9	45	5.0
H	50	292	6.0

<sup>[a]</sup> Selectivity factor was calculated as IC<sub>50</sub>(RNAP) IC<sub>50</sub>(PqsD)<sup>-1</sup>

### 6.4.3 Results from SPR experiments

#### 6.4.3.1 Competition experiments for identification of the binding mode

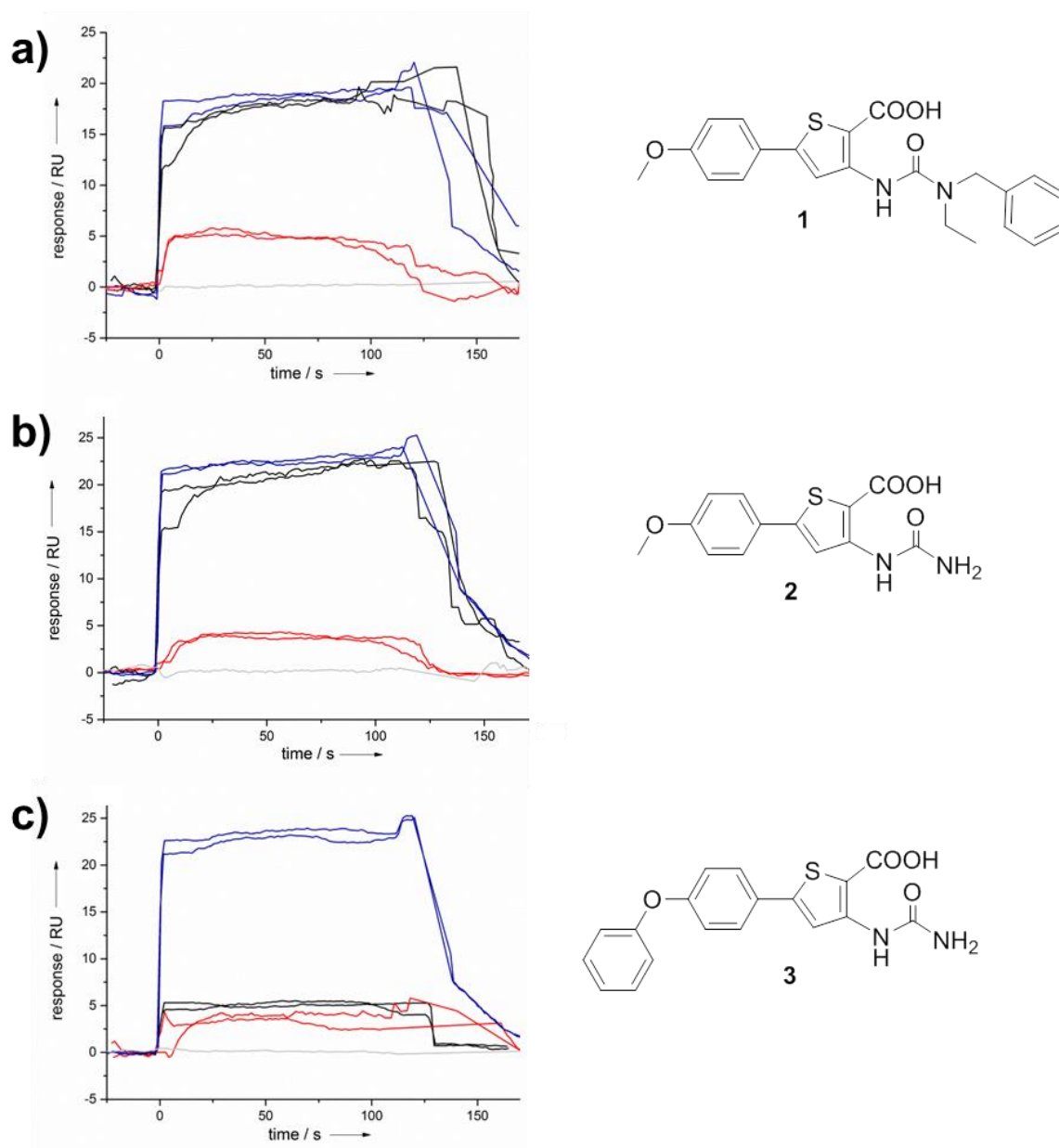


**Figure S1.** SPR-competition experiments with model compounds **1–3** competitor compounds **A** (black) and **B** (red) from the 2-nitrophenyl methanol class. Reference without competition is shown in blue. A reduced response in competition with **A** can be observed exclusively for compound **3**. The reference signal is shown in grey.

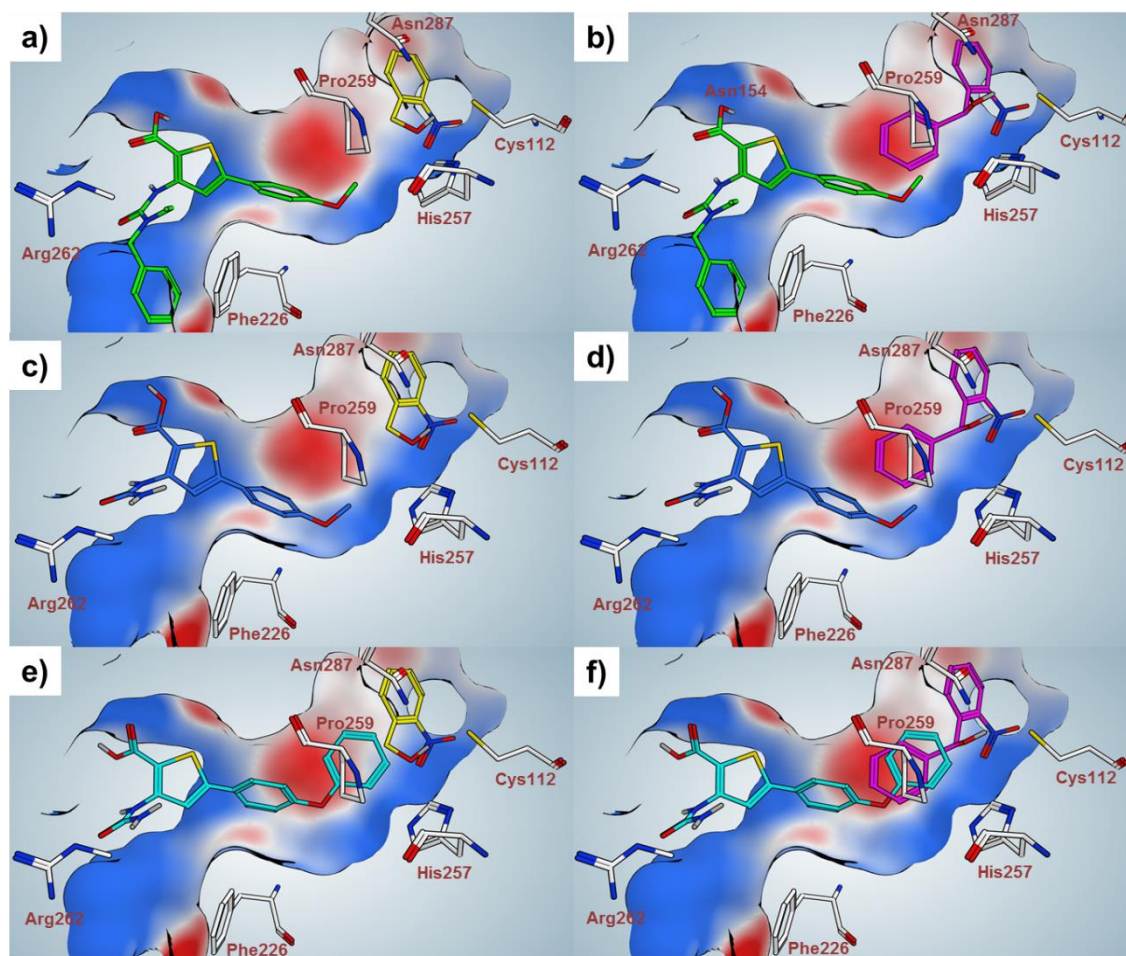


**Figure S2.** Visualization of the SPR-competition results shown in Figure S1. Competitor **A** (yellow), competitor **B** (magenta) a) **A** does not affect the binding of **1** (green). b) **B** leads to sterical clash with methoxy group of **1** (green). c) **A** does not affect the binding of **2** (blue). d) **B** leads to sterical clash with methoxy group of **2** (blue). e) **A** leads to sterical clash with phenoxy group of **3** (turquoise). f) **B** leads to sterical clash with phenoxy group of **3** (turquoise).

#### 6.4.3.2 Experiment with R223A mutant and compound 2

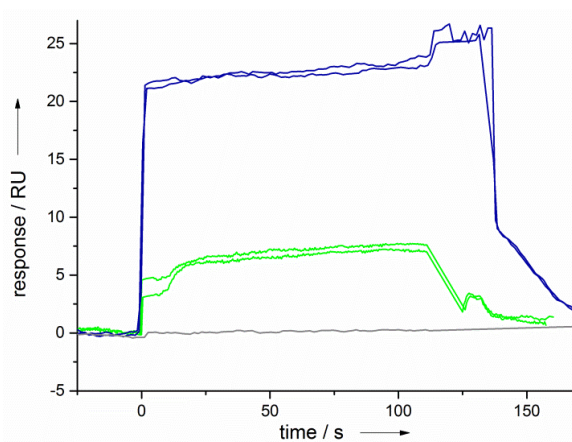


**Figure S3.** SPR-experiment with compound 2 revealed different responses with PqsD wildtype (blue) and the R223A mutant (green)

## 6.4.4. STD-NMR spectrum of 7

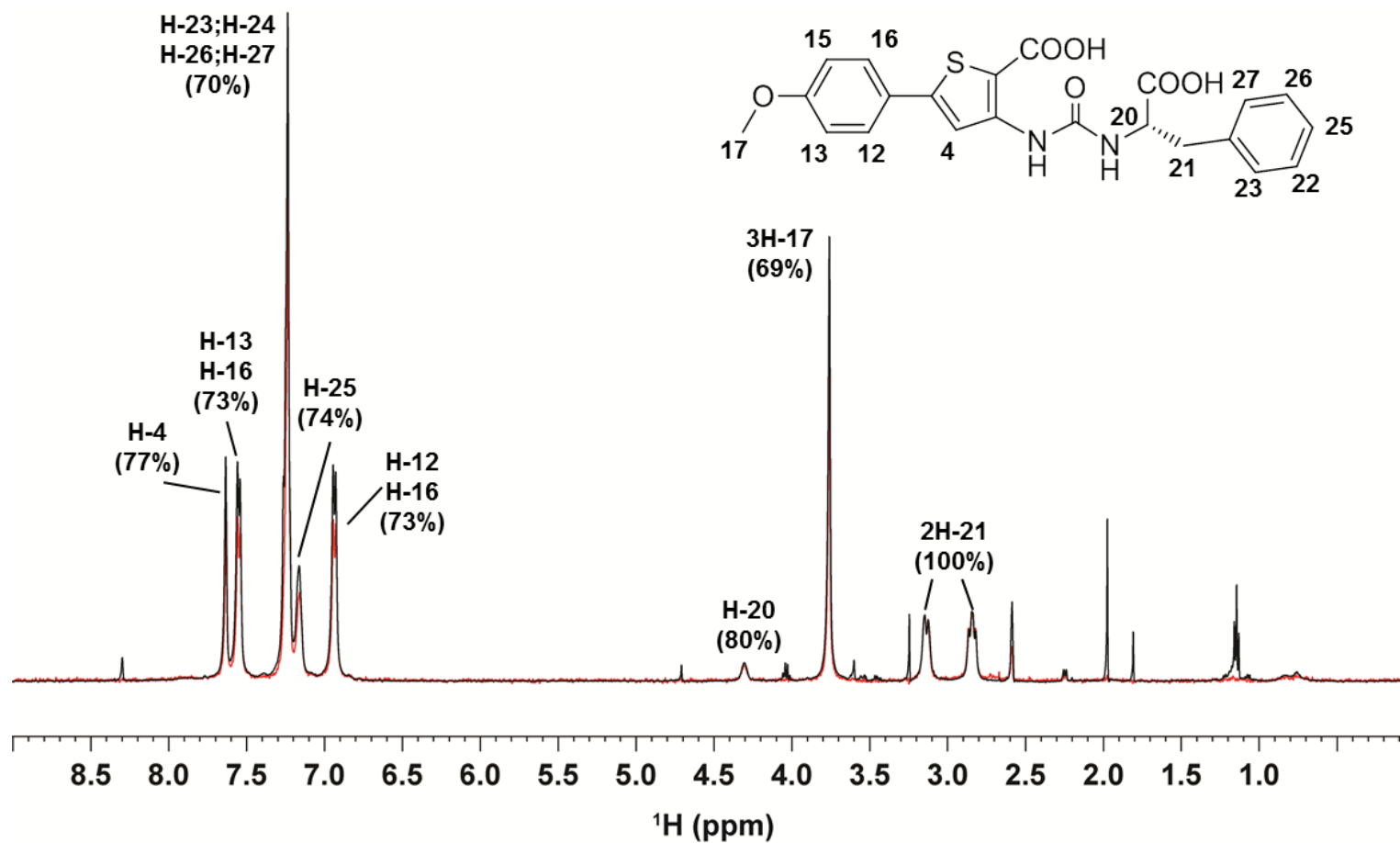


**Figure S4.** Reference (black) and STD NMR difference (red) spectra of compound 7 in complex with PqsD. Samples comprising 100:1 7/PqsD were prepared in 20 mM  $\text{Na}_3\text{PO}_4$ , 50 mM NaCl, and 5 mM  $\text{MgCl}_2$ , pH 7.0, and spectra were recorded at 298 K. Overlaid spectra were normalized to the signals for 2H-21, which gave the strongest enhancement

6.4.5. MALDI-ToF-MS spectra  
6.4.5.1 PqsD

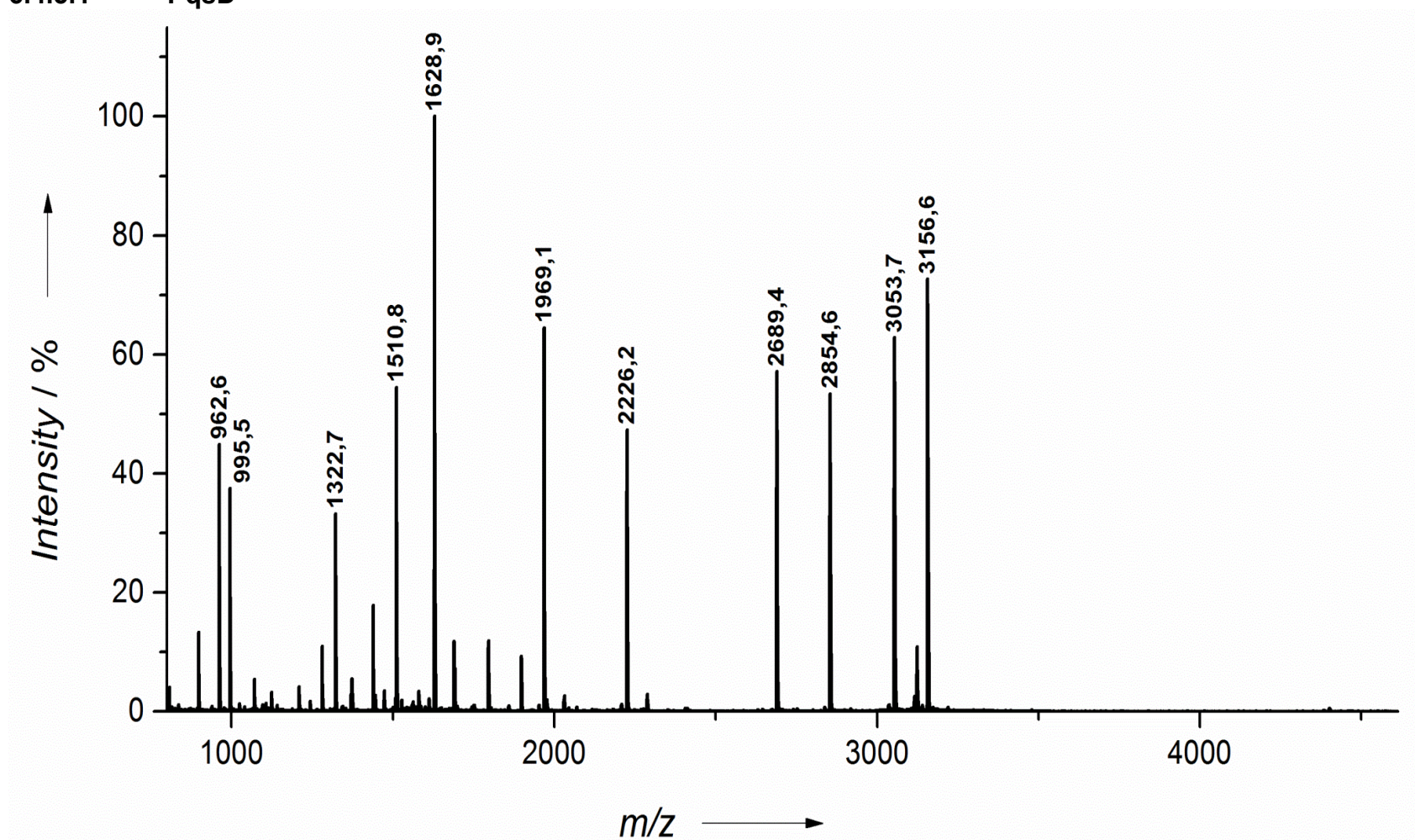


**Figure S5.** MALDI-ToF-MS analysis of tryptic digested PqsD. For the sake of clarity, only signals >15% intensity are labeled.

## 6.4.5.2 PqsD + 12

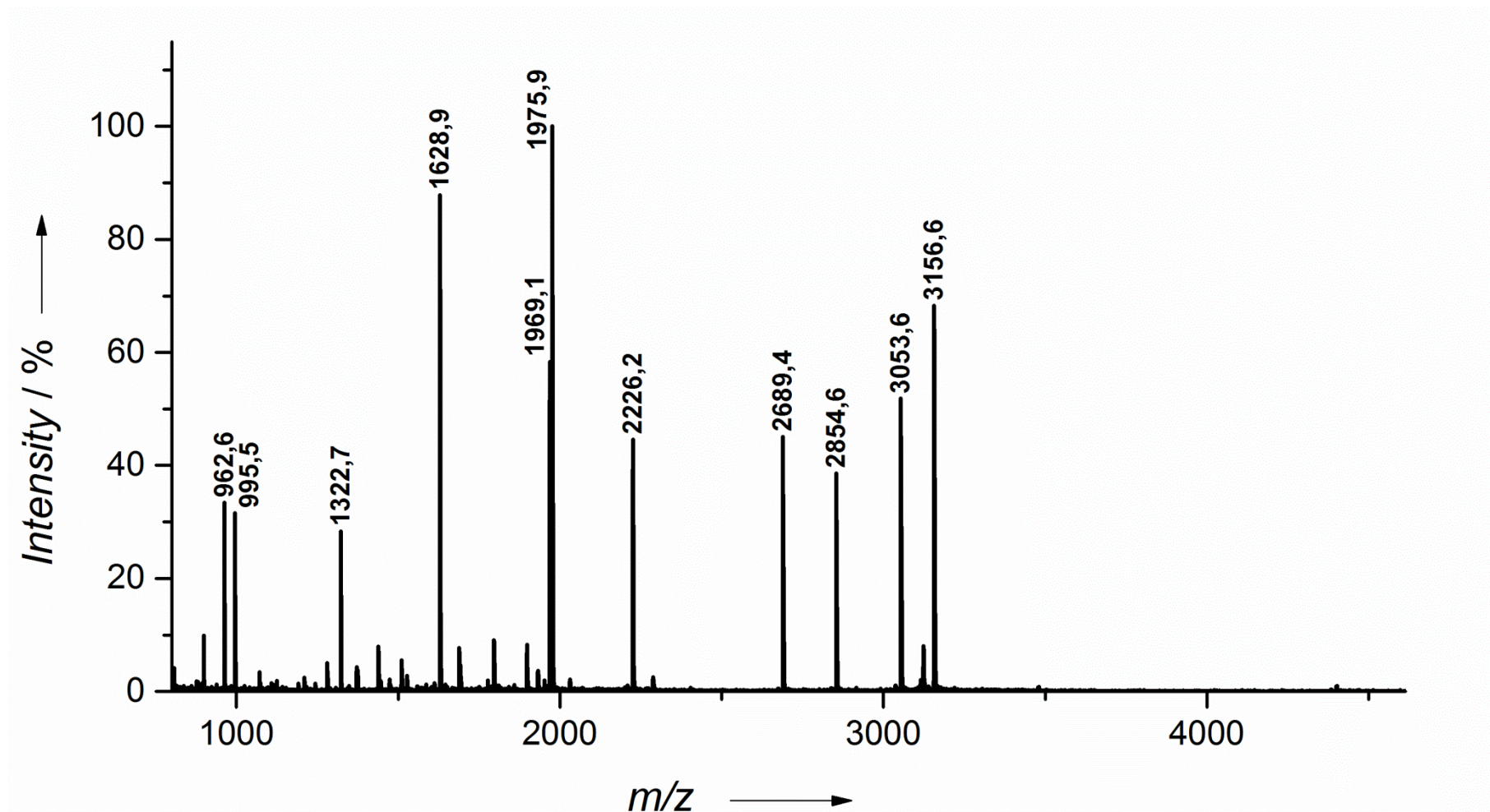


**Figure S6.** MALDI-ToF-MS analysis of tryptic digested PqsD after preincubation with **12**. For the sake of clarity, only signals >15% intensity are labeled.

## 6.4.6 LC-ESI-MS data

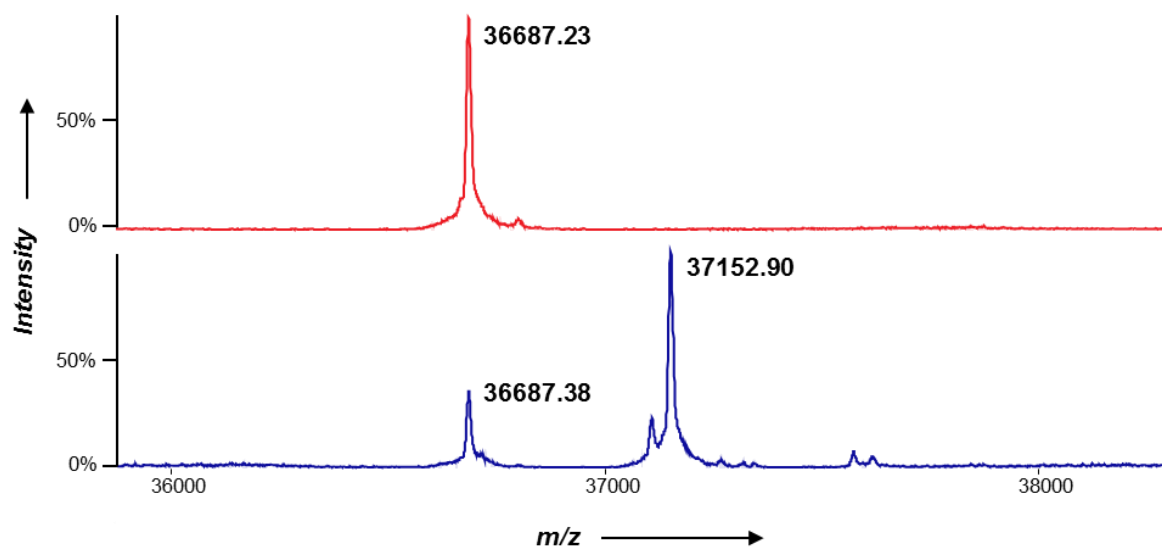


**Figure S7.** LC-ESI-MS data. Top panel (red): Reference sample containing only PqsD. Bottom panel (blue): PqsD after 30 minutes preincubation with compound **12**. Mass shift of 465 Da indicates covalent binding of **12**.

## 6.4.7 HPLC purities

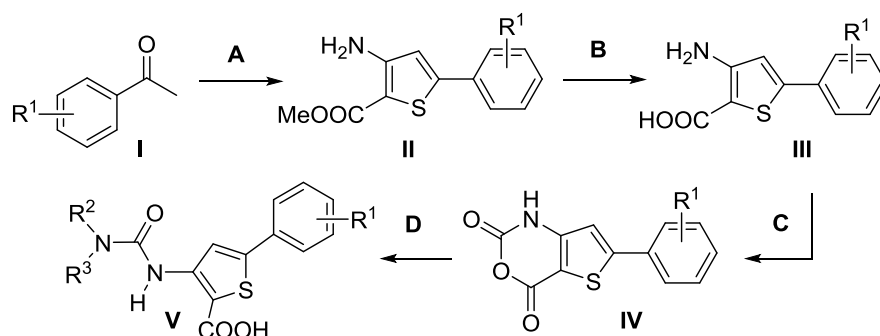
**Table S2.** Purities and retention times of compounds **1–12**.

Compound	Purity [%]	Retention time [min] <sup>a</sup>
<b>1</b>	<b>98</b>	<b>13.51</b>
<b>2</b>	<b>97</b>	<b>9.74</b>
<b>3</b>	<b>95</b>	<b>12.32</b>
<b>4</b>	<b>97</b>	<b>9.65</b>
<b>5</b>	<b>95</b>	<b>9.82</b>
<b>6</b>	<b>95</b>	<b>10.06</b>
<b>7</b>	<b>100</b>	<b>10.86</b>
<b>8</b>	<b>96</b>	<b>13.60</b>
<b>9</b>	<b>98</b>	<b>10.01</b>
<b>10</b>	<b>97</b>	<b>11.97</b>
<b>11</b>	<b>99</b>	<b>10.44</b>
<b>12</b>	<b>90</b>	<b>10.76</b>

<sup>a</sup> In a gradient run the percentage of acetonitrile (containing 0.1% trifluoroacetic acid) was increased from a initial concentration of 0% at 0 min to 100% at 15 min and kept at 100% for 5 min.

## 6.5 Supporting Information for Publication E

### 6.5.1 Synthesis and spectroscopic data of compounds 1–24



**Scheme S1:** General synthesis of 5-aryl-3-ureidothiophene-2-carboxylic acids.

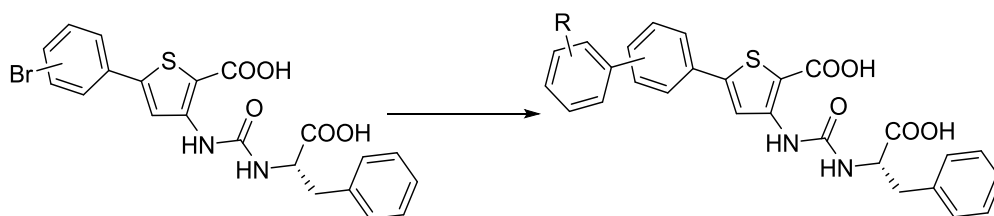
Method A, general procedure for the synthesis of 5-Aryl-3-amino-2-carboxylic acid methylester (**II**) [1]:  $\text{POCl}_3$  (26.1 g, 0.17 mol) was added dropwise to DMF (24.9 g, 0.34 mol) maintaining the temperature beyond 25 °C (cooling in ice bath) and stirred for additional 15 min. The acetophenone **I** (85.0 mmol) was added slowly and the temperature was kept between 40 and 60 °C. After complete addition, the mixture was stirred for 30 minutes at room temperature. Hydroxylamine hydrochloride (23.6 g, 0.34 mol) was carefully added portionwise (exothermic reaction!) and the reaction was stirred for additional 30 min without heating. After cooling to room temperature, the mixture was poured into ice water (300 mL). The precipitated  $\beta$ -chloro-cinnamionitrile was collected by filtration, washed with  $\text{H}_2\text{O}$  (2 x 50 mL) and dried under reduced pressure over  $\text{CaCl}_2$ . In the next step sodium (1.93 g, 84.0 mmol) was dissolved in MeOH (85 mL) and methylthioglycolate (6.97 g, 65.6 mmol) was added to the stirred solution. The  $\beta$ -chloro-cinnamionitrile (61.1 mmol) was added and the mixture was heated to reflux for 30 min. After cooling to room temperature, the mixture was poured in ice water (300 mL). The precipitated solid was collected by filtration, washed with  $\text{H}_2\text{O}$  (2 x 50 mL) and dried under reduced pressure over  $\text{CaCl}_2$ . If necessary, recrystallisation was performed from EtOH.

Method B, general procedure for the synthesis of 5-Aryl-3-amino-2-carboxylic acid (**III**): The 5-Aryl-3-amino-2-carboxylic acid methyl ester (16.6 mmol) was added to a solution of KOH (60 mL, 0.6M in  $\text{H}_2\text{O}$ ) and MeOH (60 mL). The mixture was heated to reflux for 3 h, concentrated, and washed with EtOAc (2 x 50 mL). The aqueous layer was cooled with ice and acidified with a saturated aqueous solution of  $\text{KHSO}_4$ . The precipitated solid was collected by filtration, washed with  $\text{H}_2\text{O}$  (2 x 30 mL) and dried under reduced pressure over  $\text{CaCl}_2$ .

Method C, general procedure for the synthesis of 5-Aryl-2-thioisatoic-anhydrid (**IV**) [2,3]: To a solution of the 5-Aryl-3-amino-2-carboxylic acid (**III**) (5.28 mmol) in THF (50 mL) a solution of phosgene (6.10 mL, 20 wt% in toluene, 11.6 mmol) was added dropwise over a period of 30 min. The reaction mixture was stirred for 2 h at room temperature, followed by the addition of saturated aqueous solution of  $\text{NaHCO}_3$  (30 mL) and  $\text{H}_2\text{O}$  (50 mL). The resulting mixture was extracted with EtOAc/THF (1:1, 3 x 100 mL). The organic layer was washed with saturated aqueous NaCl (100 mL), dried ( $\text{MgSO}_4$ ) and concentrated. The crude material was suspended in a mixture of

*n*-hexane/EtOAc (2:1, 50 mL) heated to 50 °C and after cooling to room temperature separated via filtration.

Method D, general procedure for the synthesis of 5-Aryl-3-ureidothiophene-2-carboxylic acid (**V**) [4]: The 5-Aryl-2-thiaisatoic-anhydrid (**IV**) (0.46 mmol) was suspended in water (7.5 mL) and the appropriate amine (0.92 mmol) was added. After addition of triethylamine (1.84 mmol), the reaction mixture was stirred, heated to 100 °C and then cooled to room temperature. The reaction mixture was poured into a mixture of concentrated HCl and ice (1:1) and extracted with EtOAc/THF (1:1, 60 mL). The organic layer was washed with aqueous HCl (2M), followed by saturated aqueous NaCl (2 x 50 mL), dried (MgSO<sub>4</sub>) and concentrated. The crude material was suspended in a mixture of *n*-hexane/EtOAc (2:1, 20 mL) heated to 50 °C and after cooling to room temperature separated *via* filtration.



**Scheme S2:** General procedure for Suzuki coupling.

Method E, general procedure for the synthesis of (**VI**):[5] A mixture of the bromo-aryl compound (1 eq, 0.20 mmol), the boronic acid (2 eq, 0.40 mmol), Pd(PPh<sub>3</sub>)<sub>4</sub> (0.1 eq, 0.02 mmol) and Na<sub>2</sub>CO<sub>3</sub> (6 eq, 1.20 mmol) in H<sub>2</sub>O (2 mL), THF (6mL) and Toluol (6 mL) were heated at 80°C under N<sub>2</sub> flow overnight. The reaction mixture was poured into a mixture of concentrated HCl and ice (1:1, 50 mL) and extracted with EtOAc (2 x 50 mL). The organic layer was washed with H<sub>2</sub>O, dried (MgSO<sub>4</sub>) and evaporated. The crude product was purified using preparative HPLC.

**Methyl 3-amino-5-(4'-methoxyphenyl)thiophene-2-carboxylate (IIa).** The title compound was prepared from 4'-methoxyacetophenone according to general procedure **A** and used directly in the next step without further purification. <sup>1</sup>H NMR (DMSO-d<sub>6</sub>, 500 MHz): δ = 7.56 (d, *J* = 8.8 Hz, 2H), 7.00 (d, *J* = 8.8 Hz, 2H), 6.86 (s, 1H), 6.56 (br. s, 2H), 3.79 (s, 3H, OCH<sub>3</sub>), 3.72 (s, 3H, OCH<sub>3</sub>) ppm. <sup>13</sup>C NMR (DMSO-d<sub>6</sub>, 125 MHz): δ = 163.9, 160.0, 155.7, 147.7, 127.0, 125.3, 114.9, 114.6, 95.7, 55.3, 50.8 ppm.

**Methyl 3-amino-5-phenylthiophene-2-carboxylate (IIb)** The title compound was prepared from acetophenone according to general procedure **A** and used directly in the next step without further purification. <sup>1</sup>H NMR (DMSO-d<sub>6</sub>, 500 MHz): δ = 7.61–7.64 (m, 2H), 7.43–7.47 (m, 2H), 7.38–7.42 (m, 1H), 6.98 (s, 1H), 6.59 (br. s, 2H), 3.73 (s, 3H) ppm. <sup>13</sup>C NMR (DMSO-d<sub>6</sub>, 125 MHz): δ = 163.9, 155.5, 147.5, 132.7, 129.2, 129.1, 125.5, 116.2, 96.6, 50.9 ppm.

**Methyl 3-amino-7-methoxy-4,5-dihydronaphtho[1,2-*b*]thiophene-2-carboxylate (IIc).** The title compound was prepared from 6-methoxy tetralone according to the following procedure:[6] The conversion to the β-chloro-cinnamonitrile was performed like described in the general procedure A. For the next, sodium sulphite nonahydrate

(10.9 g, 45.5 mmol) was suspended in DMF (50 mL) and heated to 40 °C for 30 min. A solution of the  $\beta$ -chloro-cinnamionitrile (5.00 g, 22.8 mmol) in DMF (20 mL) was added dropwise and the resulting mixture was stirred at 50 °C for 2 h. Methyl bromoacetate (6.96 g, 45.5 mmol) was dissolved in DMF (20 mL), slowly added and stirring was continued overnight. A solution Na (1.05 g, 45.5) in dry ethanol (100 mL) was freshly prepared and added to the reaction mixture. After 1.5 h, the reaction was cooled to room temperature and diluted with cold H<sub>2</sub>O (200 mL). The product appeared as a yellow solid and was filtered off. The product turned grey after washing with 100 mL cold H<sub>2</sub>O and drying under vacuum. <sup>1</sup>H NMR (DMSO-d<sub>6</sub>, 300 MHz):  $\delta$  = 7.28 (d,  $J$  = 8.4 Hz, 1H), 6.89 (s, 1H), 6.82 (dd,  $J$  = 2.4, 8.4 Hz, 1H), 6.50 (br. s, 2H), 3.78 (s, 3H), 3.73 (s, 3H), 2.90 (tt,  $J$  = 7.5, 8.1 Hz, 2H), 2.61 (tt,  $J$  = 7.5, 8.1 Hz, 2H) ppm. <sup>13</sup>C NMR (DMSO-d<sub>6</sub>, 75 MHz):  $\delta$  = 164.2, 159.7, 153.3, 140.2, 137.6, 125.7, 124.6, 122.9, 113.9, 112.4, 94.7, 55.2, 50.8, 28.0, 20.3 ppm.

**Methyl 3-amino-5-(3-bromophenyl)thiophene-2-carboxylate (IIId).** The title compound was prepared from 3'-bromoacetophenone according to general procedure **A** and used directly in the next step without further purification. <sup>1</sup>H NMR (DMSO-d<sub>6</sub>, 500 MHz):  $\delta$  = 7.80 (t,  $J$  = 1.9 Hz, 1H), 7.63 (ddd,  $J$  = 0.9, 1.9, 7.9 Hz, 1H), 7.59 (ddd,  $J$  = 0.9, 1.9, 7.9 Hz, 1H), 7.40 (t,  $J$  = 7.9 Hz, 1H), 7.04 (s, 1H), 6.60 (br. s, 2H), 3.74 (s, 3H) ppm. <sup>13</sup>C NMR (DMSO-d<sub>6</sub>, 125 MHz):  $\delta$  = 163.8, 155.3, 145.4, 135.0, 131.8, 131.3, 127.9, 124.7, 122.5, 117.3, 97.3, 51.0 ppm.

**Methyl 3-amino-5-(4'-bromophenyl)thiophene-2-carboxylate (IIe).** The title compound was prepared from 4'-bromoacetophenone according to general procedure **A** and used directly in the next step without further purification. <sup>1</sup>H NMR (CDCl<sub>3</sub>, 300 MHz):  $\delta$  = 7.51 (d,  $J$  = 8.0 Hz, 2 H), 7.43 (d,  $J$  = 8.0 Hz, 2 H), 6.75 (s, 1 H), 5.49 (br. s., 2 H), 3.85 (s, 3 H, OCH<sub>3</sub>) ppm. <sup>13</sup>C NMR (CDCl<sub>3</sub>, 75 MHz):  $\delta$  = 164.8, 154.2, 147.6, 132.3, 132.1, 127.3, 123.0, 115.8, 100.7, 51.3 ppm.

**3-Amino-5-(4'-methoxyphenyl)thiophene-2-carboxylic acid (IIIa).** The title compound was prepared from **IIa** according to general procedure **B** and used directly in the next step without further purification. <sup>1</sup>H NMR (DMSO-d<sub>6</sub>, 300 MHz):  $\delta$  = 7.55 (d,  $J$  = 8.8 Hz, 2 H), 6.99 (d,  $J$  = 8.8 Hz, 2 H), 6.84 (s, 1 H), 3.79 (s, 3 H, OCH<sub>3</sub>) ppm. <sup>13</sup>C NMR (DMSO-d<sub>6</sub>, 75 MHz):  $\delta$  = 165.3, 159.9, 155.3, 147.0, 127.0, 125.6, 115.0, 114.6, 97.1, 55.3 ppm.

**3-Amino-5-phenylthiophene-2-carboxylic acid (IIIb).** The title compound was prepared from **IIb** according to general procedure **B** and used directly in the next step without further purification. <sup>1</sup>H NMR (DMSO-d<sub>6</sub>, 500 MHz):  $\delta$  = 7.56–7.69 (m, 2H), 7.33–7.50 (m, 3H), 6.96 (s, 1H) ppm. <sup>13</sup>C NMR (DMSO-d<sub>6</sub>, 125 MHz):  $\delta$  = 165.2, 155.1, 146.8, 133.0, 129.2, 129.0, 125.5, 116.3, 98.1 ppm.

**3-Amino-7-methoxy-4,5-dihydronaphtho[1,2-b]thiophene-2-carboxylic acid (IIIc).** The title compound was prepared from **IIc** according to general procedure **B** and used directly in the next step without further purification. <sup>1</sup>H NMR (DMSO-d<sub>6</sub>, 300 MHz):  $\delta$  = 7.27 (d,  $J$  = 8.2 Hz, 1H), 6.89 (br. s., 1H), 6.81 (d,  $J$  = 8.2 Hz, 1H), 3.77 (s, 3H), 2.89 (t,  $J$  = 7.0 Hz, 2H), 2.55–2.68 (m, 2H) ppm. <sup>13</sup>C NMR (DMSO-d<sub>6</sub>, 75 MHz):  $\delta$  = 165.6, 159.5, 152.7, 139.3, 137.5, 125.9, 124.4, 123.1, 113.9, 112.4, 96.5, 55.2, 28.1, 20.4 ppm.

**3-Amino-5-(3-bromophenyl)thiophene-2-carboxylic acid (IIIId).** The title compound was prepared from **IIId** according to general procedure **B** and used directly in the next

step without further purification.  $^1\text{H}$  NMR (DMSO- $d_6$ , 500 MHz):  $\delta$  = 7.79 (t,  $J$  = 1.9 Hz, 1H), 7.62 (ddd,  $J$  = 0.9, 1.9, 7.9 Hz, 1H), 7.58 (ddd,  $J$  = 0.9, 1.9, 7.9 Hz, 1H), 7.39 (t,  $J$  = 7.9 Hz, 1H), 7.03 (s, 1H) ppm.  $^{13}\text{C}$  NMR (DMSO- $d_6$ , 125 MHz):  $\delta$  = 165.2, 155.0, 144.7, 135.3, 131.6, 131.3, 127.8, 124.6, 122.4, 117.4, 98.8 ppm.

**3-Amino-5-(4'-bromophenyl)thiophene-2-carboxylic acid (IIIe).** The title compound was prepared from **Ile** according to general procedure **B** and used directly in the next step without further purification.  $^1\text{H}$  NMR (DMSO- $d_6$ , 500 MHz):  $\delta$  = 7.63 (d,  $J$  = 8.8 Hz, 2 H), 7.57 (d,  $J$  = 8.8 Hz, 2 H), 6.98 (s, 1 H) ppm.  $^{13}\text{C}$  NMR (DMSO- $d_6$ , 125 MHz):  $\delta$  = 165.2, 155.1, 145.3, 132.2, 132.1, 127.5, 122.0, 116.8, 98.5 ppm.

**3-Aminothiophene-2-carboxylic acid (III f).** The title compound was prepared from Methyl 3-amino-2-thiophenecarboxylate according to general procedure **B** and used directly in the next step without further purification.  $^1\text{H}$  NMR (DMSO- $d_6$ , 300 MHz):  $\delta$  = 7.47 (d,  $J$  = 5.4 Hz, 1 H), 6.59 (d,  $J$  = 5.4 Hz, 1 H) ppm.

**6-(4'-Methoxyphenyl)-2,4-dihydro-1H-thieno[3,2-d][1,3]oxazine-2,4-dione (IVa).** The title compound was prepared from **IIIa** according to general procedure **D** and used directly in the next step without further purification.  $^1\text{H}$  NMR (DMSO- $d_6$ , 300 MHz):  $\delta$  = 12.28 (s, 1 H), 7.74 (d,  $J$  = 8.9 Hz, 2 H), 7.12 (s, 1 H), 7.04 (d,  $J$  = 8.9 Hz, 2 H), 3.82 (s, 3 H, OCH<sub>3</sub>) ppm.  $^{13}\text{C}$  NMR (DMSO- $d_6$ , 75 MHz):  $\delta$  = 161.1, 155.5, 155.0, 149.6, 148.6, 127.9, 124.1, 114.8, 111.2, 103.1, 55.4 ppm.

**6-Phenyl-2H-thieno[3,2-d][1,3]oxazine-2,4(1H)-dione (IVb).** The title compound was prepared from **IIIb** according to general procedure **D** and used directly in the next step without further purification.  $^1\text{H}$  NMR (DMSO- $d_6$ , 500 MHz):  $\delta$  = 7.76–7.83 (m, 2H), 7.47–7.54 (m, 3H), 7.26 (s, 1H) ppm.  $^{13}\text{C}$  NMR (DMSO- $d_6$ , 125 MHz):  $\delta$  = 155.2, 155.1, 149.8, 148.6, 131.5, 130.5, 129.5, 126.3, 112.8, 104.4 ppm.

**3-Methoxy-5,6-dihydro-8H-naphtho[2',1':4,5]thieno[3,2-d][1,3]oxazine-8,10(7H)-dione (IVc).** The title compound was prepared from **IIIc** according to general procedure **D** and used directly in the next step without further purification.  $^1\text{H}$  NMR (DMSO- $d_6$ , 300 MHz):  $\delta$  = 12.19 (br. s., 1H), 7.46 (d,  $J$  = 8.5 Hz, 1H), 6.95 (d,  $J$  = 2.3 Hz, 1H), 6.87 (dd,  $J$  = 2.3, 8.5 Hz, 1H), 3.80 (s, 3H), 2.94 (tt,  $J$  = 7.1, 7.8 Hz, 2H), 2.80 (tt,  $J$  = 7.1, 7.8 Hz, 2H) ppm.  $^{13}\text{C}$  NMR (DMSO- $d_6$ , 75 MHz):  $\delta$  = 160.8, 155.1, 149.0, 147.7, 147.4, 138.3, 125.6, 123.6, 121.8, 114.0, 112.9, 101.8, 55.4, 27.6, 20.1 ppm.

**6-(3-bromophenyl)-2H-thieno[3,2-d][1,3]oxazine-2,4(1H)-dione (IVd).** The title compound was prepared from **III d** according to general procedure **D** and used directly in the next step without further purification.  $^1\text{H}$  NMR (DMSO- $d_6$ , 500 MHz):  $\delta$  = 12.41 (br. s., 1H), 8.05 (t,  $J$  = 1.7 Hz, 1H), 7.80 (ddd,  $J$  = 1.0, 1.9, 7.9 Hz, 1H), 7.69 (ddd,  $J$  = 1.0, 1.9, 7.9 Hz, 1H), 7.46 (t,  $J$  = 8.04 Hz, 1H), 7.36 (s, 1H) ppm.  $^{13}\text{C}$  NMR (DMSO- $d_6$ , 125 MHz):  $\delta$  = 155.1, 152.9, 149.3, 148.5, 133.8, 133.1, 131.5, 128.7, 125.5, 122.7, 113.9, 105.2 ppm.

**6-(4'-Bromophenyl)-2,4-dihydro-1H-thieno[3,2-d][1,3]oxazine-2,4-dione (IVe).** The title compound was prepared from **IIIe** according to general procedure **D** and used directly in the next step without further purification.  $^1\text{H}$  NMR (DMSO- $d_6$ , 500 MHz):  $\delta$  = 12.39 (br. s., 1H), 7.77 (d,  $J$  = 8.8 Hz, 2H), 7.70 (d,  $J$  = 8.8 Hz, 2H), 7.29 (s, 1H) ppm.  $^{13}\text{C}$  NMR (DMSO- $d_6$ , 125 MHz):  $\delta$  = 155.1, 153.5, 149.7, 148.6, 132.4, 130.8, 128.3, 123.8, 113.4, 104.7 ppm.

**2H-Thieno[3,2-*d*][1,3]oxazine-2,4(1H)-dione (IVf).** The title compound was prepared from **III**f according to general procedure **D** and used directly in the next step without further purification. <sup>1</sup>H NMR (DMSO-*d*<sub>6</sub>, 300 MHz): δ = 12.21 (br. s., 1H), 8.24 (d, *J* = 5.2 Hz, 1H), 6.94 (d, *J* = 5.2 Hz, 1H) ppm.

**6-(4-Methoxy-2-methylphenyl)-2H-thieno[3,2-*d*][1,3]oxazine-2,4(1H)-dione (IVg).** The title compound was prepared from **III**g according to general procedure **D** and used directly in the next step without further purification. <sup>1</sup>H NMR (DMSO-*d*<sub>6</sub>, 300 MHz): δ = 12.23 (br. s., 1H), 7.43 (d, *J* = 8.57 Hz, 1H), 6.84–7.01 (m, 3H), 3.80 (s, 3H), 2.41 (s, 3H) ppm. <sup>13</sup>C NMR (DMSO-*d*<sub>6</sub>, 75 MHz): δ = 160.3, 155.0, 154.9, 148.8, 148.5, 137.5, 131.2, 123.9, 116.6, 115.5, 112.1, 104.4, 55.3, 20.9 ppm.

**(S)-5-(3-Bromophenyl)-3-(3-(1-carboxy-2-phenylethyl)ureido)thiophene-2-carboxylic acid (Va).** The title compound was prepared from **IV**d according to general procedure **E** and used directly in the next step without further purification. <sup>1</sup>H NMR (DMSO-*d*<sub>6</sub>, 500 MHz): δ = 12.88 (br. s., 2H), 9.42 (s, 1H), 8.23 (s, 1H), 8.18 (d, *J* = 7.9 Hz, 1H), 7.81 (t, *J* = 1.7 Hz, 1H), 7.64–7.69 (ddd, *J* = 1.0, 1.9, 7.9 Hz, 1H, 1H), 7.57–7.62 (ddd, *J* = 1.0, 1.9, 7.9 Hz, 1H, 1H), 7.25–7.33 (m, 4H), 7.17–7.25 (m, 1H), 4.39 (ddd, *J* = 4.6, 8.0, 9.5 Hz, 1H), 3.11 (dd, *J* = 4.8, 13.9 Hz, 1H), 2.88 (dd, *J* = 9.8, 13.9 Hz, 1H) ppm. <sup>13</sup>C NMR (DMSO-*d*<sub>6</sub>, 125 MHz): δ = 173.6, 164.5, 153.7, 145.5, 144.7, 137.7, 135.0, 131.8, 131.4, 129.1, 128.2, 128.0, 126.4, 124.8, 122.5, 119.0, 107.8, 54.4, 37.0 ppm.

**(S)-5-(4-Bromophenyl)-3-(3-(1-carboxy-2-phenylethyl)ureido)thiophene-2-carboxylic acid (Vb).** The title compound was prepared from **IV**e according to general procedure **E** and used directly in the next step without further purification. <sup>1</sup>H NMR (DMSO-*d*<sub>6</sub>, 300 MHz): δ = 12.93 (br. s., 2H), 9.42 (s, 1H), 8.23 (s, 1H), 8.17 (d, *J* = 7.9 Hz, 1H), 7.54–7.70 (m, 4H), 7.14–7.38 (m, 5H), 4.30–4.47 (m, 1H), 3.04–3.17 (m, 1H), 2.80–2.95 (m, 1H) ppm. <sup>13</sup>C NMR (DMSO-*d*<sub>6</sub>, 75 MHz): δ = 173.5, 164.5, 153.7, 145.7, 145.4, 137.7, 132.2, 132.0, 129.0, 128.2, 127.6, 126.4, 122.3, 118.5, 107.3, 54.4, 37.0 ppm.

**5-(4-Methoxyphenyl)-3-(3-(phosphonomethyl)ureido)thiophene-2-carboxylic acid (1).** The title compound was prepared from **IV**a according to general procedure **D**. <sup>1</sup>H NMR (DMSO-*d*<sub>6</sub>, 300 MHz): δ = 9.43 (s, 1H), 8.15 (s, 1H), 7.89–8.09 (m, 1H), 7.60 (d, *J* = 8.6 Hz, 2H), 7.02 (d, *J* = 8.6 Hz, 2H), 3.80 (s, 3H), 3.25–3.50 (m, 2H) ppm. <sup>13</sup>C NMR (DMSO-*d*<sub>6</sub>, 75 MHz): δ = 164.5, 160.0, 153.9, 147.0, 146.1, 127.0, 125.4, 116.9, 114.7, 105.7, 55.3, 36.2–37.8 (d, HSQC, N-C-P) ppm. MS (ESI) *m/z*: 386.8 [M+H]<sup>+</sup>

**(S)-3-(3-(1-carboxy-2-(4-hydroxyphenyl)ethyl)ureido)-5-(4-methoxyphenyl) thiophene-2-carboxylic acid (2).** The title compound was prepared from **IV**a according to general procedure **D**. <sup>1</sup>H NMR (DMSO-*d*<sub>6</sub>, 300 MHz): δ = 12.81 (br. s., 2H), 9.41 (s, 1H), 9.20 (br. s., 1H), 8.07–8.12 (m, 1H), 8.09 (s, 1H), 7.59 (d, *J* = 8.7 Hz, 2H), 7.06 (d, *J* = 8.3 Hz, 2H), 7.00 (d, *J* = 8.7 Hz, 1H), 6.68 (d, *J* = 8.3 Hz, 2H), 4.20–4.38 (m, 1H), 3.79 (s, 3H), 2.97 (dd, *J* = 4.4, 13.7 Hz, 1H), 2.76 (dd, *J* = 9.7, 13.7 Hz, 1H) ppm. <sup>13</sup>C NMR (DMSO-*d*<sub>6</sub>, 75 MHz): δ = 173.8, 164.6, 160.1, 155.9, 153.7, 147.1, 145.9, 130.0, 127.7, 127.1, 125.4, 116.8, 115.0, 114.7, 105.7, 55.3, 54.8, 36.2 ppm. MS (ESI) *m/z*: 456.9 [M+H]<sup>+</sup>

**(S)-3-(3-(1-Carboxy-2-(4-methoxyphenyl)ethyl)ureido)-5-(4-methoxyphenyl)thiophene-2-carboxylic acid (3).** The title compound was prepared from **IV**a according to

general procedure **D**.  $^1\text{H}$  NMR (DMSO- $d_6$ , 300 MHz):  $\delta$  = 12.83 (br. s., 2H), 9.41 (s, 1H), 8.12 (d,  $J$  = 8.01 Hz, 1H), 8.09 (s, 1H), 7.59 (d,  $J$  = 8.75 Hz, 2H), 7.19 (d,  $J$  = 8.50 Hz, 2H), 7.00 (d,  $J$  = 8.80 Hz, 2H), 6.86 (d,  $J$  = 8.57 Hz, 2H), 4.25–4.42 (m, 1H), 3.79 (s, 3H), 3.71 (s, 3H), 2.96–3.11 (m, 1H), 2.71–2.87 (m, 1H) ppm.  $^{13}\text{C}$  NMR (DMSO- $d_6$ , 75 MHz):  $\delta$  = 173.7, 164.6, 160.1, 157.9, 153.7, 147.1, 145.9, 130.1, 129.5, 127.1, 125.4, 116.7, 114.7, 113.7, 105.7, 55.3, 54.9, 54.7, 36.1 ppm. MS (ESI)  $m/z$ : 471.0  $[\text{M}+\text{H}]^+$

**(S)-3-(3-(1-Carboxy-2-(4-chlorophenyl)ethyl)ureido)-5-(4-methoxyphenyl)thiophene-2-carboxylic acid (4)**. The title compound was prepared from **IVa** according to general procedure **D**.  $^1\text{H}$  NMR (DMSO- $d_6$ , 300 MHz):  $\delta$  = 12.88 (br. s., 2H), 9.42 (s, 1H), 8.14 (d,  $J$  = 8.0 Hz, 1H), 8.08 (s, 1H), 7.59 (d,  $J$  = 8.8 Hz, 2H), 7.36 (d,  $J$  = 8.5 Hz, 2H), 7.29 (d,  $J$  = 8.5 Hz, 2H), 7.00 (d,  $J$  = 8.8 Hz, 2H), 4.29–4.47 (m, 1H), 3.79 (s, 3H), 3.03–3.15 (m, 1H), 2.80–2.97 (m, 1H) ppm.  $^{13}\text{C}$  NMR (DMSO- $d_6$ , 75 MHz):  $\delta$  = 173.4, 164.6, 160.1, 153.7, 147.2, 145.8, 136.7, 131.2, 131.0, 128.2, 127.1, 125.4, 116.7, 114.7, 105.8, 55.3, 54.2, 36.3 ppm. MS (ESI)  $m/z$ : 475.1  $[\text{M}+\text{H}]^+$

**(S)-3-(3-(Carboxy(phenyl)methyl)ureido)-5-(4-methoxyphenyl)thiophene-2-carboxylic acid (5)**. The title compound was prepared from **IVa** according to general procedure **D**.  $^1\text{H}$  NMR (DMSO- $d_6$ , 300 MHz):  $\delta$  = 12.90 (br. s., 2H), 9.55 (s, 1H), 8.60 (d,  $J$  = 7.0 Hz, 1H), 8.15 (s, 1H), 7.61 (d,  $J$  = 8.1 Hz, 2H), 7.25–7.53 (m, 5H), 7.01 (d,  $J$  = 8.1 Hz, 2H), 5.28 (d,  $J$  = 7.0 Hz, 1H), 3.80 (s, 3H) ppm.  $^{13}\text{C}$  NMR (DMSO- $d_6$ , 75 MHz):  $\delta$  = 172.4, 164.5, 160.1, 153.5, 147.1, 145.8, 137.4, 128.6, 128.0, 127.6, 127.1, 125.4, 116.9, 114.7, 106.1, 57.2, 55.3 ppm. MS (ESI)  $m/z$ : 427.0  $[\text{M}+\text{H}]^+$

**(S)-3-(3-(1-Carboxy-3-phenylpropyl)ureido)-5-(4-methoxyphenyl)thiophene-2-carboxylic acid (6)**. The title compound was prepared from **IVa** according to general procedure **D**.  $^1\text{H}$  NMR (DMSO- $d_6$ , 300 MHz):  $\delta$  = 12.82 (br. s., 2H), 9.51 (s, 1H), 7.97–8.34 (m, 2H), 7.61 (d,  $J$  = 8.5 Hz, 2H), 7.12–7.39 (m, 5H), 7.01 (d,  $J$  = 8.5 Hz, 2H), 4.06–4.18 (m, 1H), 3.80 (s, 3H), 2.69 (t,  $J$  = 7.1 Hz, 2H), 1.76–2.16 (m, 2H) ppm.  $^{13}\text{C}$  NMR (DMSO- $d_6$ , 75 MHz):  $\delta$  = 174.2, 164.8, 160.1, 153.8, 147.3, 146.1, 141.0, 128.4, 128.3, 127.1, 126.0, 125.4, 116.7, 114.7, 105.6, 55.3, 52.3, 33.0, 31.5 ppm. MS (ESI)  $m/z$ : 455.0  $[\text{M}+\text{H}]^+$

**(S)-3-(3-(1-Carboxy-2-methylpropyl)ureido)-5-(4-methoxyphenyl)thiophene-2-carboxylic acid (7)**. The title compound was prepared from **IVa** according to general procedure **D**.  $^1\text{H}$  NMR (DMSO- $d_6$ , 300 MHz):  $\delta$  = 12.72 (br. s., 2H), 9.49 (s, 1H), 8.16 (s, 1H), 7.99 (d,  $J$  = 8.4 Hz, 1H), 7.60 (d,  $J$  = 8.8 Hz, 2H), 7.01 (d,  $J$  = 8.8 Hz, 2H), 4.07–4.15 (m, 1H), 3.80 (s, 3H), 2.04–2.17 (m, 1H), 0.85 - 1.01 (m, 6H) ppm.  $^{13}\text{C}$  NMR (DMSO- $d_6$ , 75 MHz):  $\delta$  = 173.6, 164.5, 160.0, 154.1, 147.0, 146.0, 127.1, 125.4, 117.0, 114.7, 105.8, 58.1, 55.3, 29.8, 19.2, 17.9 ppm. MS (ESI)  $m/z$ : 392.9  $[\text{M}+\text{H}]^+$

**(S)-3-(3-(1-Carboxy-2-hydroxyethyl)ureido)-5-(4-methoxyphenyl)thiophene-2-carboxylic acid (8)**. The title compound was prepared from **IVa** according to general procedure **D**.  $^1\text{H}$  NMR (DMSO- $d_6$ , 300 MHz):  $\delta$  = 12.77 (br. s., 2H), 9.50 (s, 1H), 8.01–8.23 (m, 2H), 7.60 (d,  $J$  = 8.8 Hz, 2H), 7.01 (d,  $J$  = 8.8 Hz, 2H), 5.00 (br. s., 1H), 4.17–4.29 (m, 1H), 3.80 (s, 3H), 3.62–3.77 (m, 2H) ppm.  $^{13}\text{C}$  NMR (DMSO- $d_6$ , 75 MHz):  $\delta$  = 172.5, 164.5, 160.0, 153.9, 147.0, 145.9, 127.0, 125.4, 116.9, 114.7, 105.9, 61.5, 55.5, 55.3 ppm. MS (ESI)  $m/z$ : 380.8  $[\text{M}+\text{H}]^+$

**(S)-3-(3-(3-Amino-1-carboxy-3-oxopropyl)ureido)-5-(4-methoxyphenyl)thiophene-2-carboxylic acid (9).** The title compound was prepared from **IVa** according to general procedure **D**.  $^1\text{H}$  NMR (DMSO- $d_6$ , 300 MHz):  $\delta$  = 12.76 (br. s., 2H), 9.44 (s, 1H), 8.13 (s, 1H), 8.08 (d,  $J$  = 7.7 Hz, 1H), 7.61 (d,  $J$  = 8.8 Hz, 2H), 7.38 (br. s., 1H), 7.02 (d,  $J$  = 8.8 Hz, 2H), 6.92 (br. s., 1H), 4.40–4.56 (m, 1H), 3.80 (s, 3H), 2.55–2.64 (m, 1H), 2.45–2.55 (m, 1H) ppm.  $^{13}\text{C}$  NMR (DMSO- $d_6$ , 75 MHz):  $\delta$  = 173.4, 171.0, 164.6, 160.1, 153.6, 147.1, 146.0, 127.1, 125.4, 116.8, 114.7, 105.8, 55.3, 49.6, 37.0 ppm. MS (ESI)  $m/z$ : 407.9  $[\text{M}+\text{H}]^+$

**(S)-3-(3-(1-Carboxy-2-(1H-indol-3-yl)ethyl)ureido)-5-(4-methoxyphenyl)thiophene-2-carboxylic acid (10).** The title compound was prepared from **IVa** according to general procedure **D**.  $^1\text{H}$  NMR (DMSO- $d_6$ , 300 MHz):  $\delta$  = 12.80 (br. s., 2H), 10.85 (br. s., 1H), 9.43 (s, 1H), 8.15 (d,  $J$  = 7.7 Hz, 1H), 8.10 (s, 1H), 7.53–7.65 (m, 3H), 7.34 (d,  $J$  = 7.9 Hz, 1H), 7.17 (d,  $J$  = 2.0 Hz, 1H), 6.95–7.12 (m, 4H), 4.40–4.51 (m, 1H), 3.79 (s, 3H), 3.21 (dd,  $J$  = 14.7, 4.7 Hz, 1H), 3.03 (dd,  $J$  = 14.7, 9.0 Hz, 1H) ppm.  $^{13}\text{C}$  NMR (DMSO- $d_6$ , 75 MHz):  $\delta$  = 174.0, 164.6, 160.0, 153.7, 147.1, 145.9, 136.1, 127.1, 127.1, 125.4, 123.6, 120.9, 118.4, 118.1, 116.8, 114.7, 111.4, 109.9, 105.7, 55.3, 53.7, 27.3 ppm. MS (ESI)  $m/z$ : 480.0  $[\text{M}+\text{H}]^+$

**((2-Carboxy-5-(4-methoxyphenyl)thiophen-3-yl)carbamoyl)-L-glutamic acid (11).** The title compound was prepared from **IVa** according to general procedure **D**.  $^1\text{H}$  NMR (DMSO- $d_6$ , 300 MHz):  $\delta$  = 12.59 (br. s., 3H), 9.48 (s, 1H), 8.14 (s, 1H), 8.06 (d,  $J$  = 7.64 Hz, 1H), 7.61 (d,  $J$  = 8.80 Hz, 2H), 7.01 (d,  $J$  = 8.85 Hz, 2H), 4.10–4.23 (m, 1H), 3.80 (s, 3H), 2.23–2.44 (m, 2H), 1.93–2.07 (m, 1H), 1.72–1.89 (m, 1H) ppm.  $^{13}\text{C}$  NMR (DMSO- $d_6$ , 75 MHz):  $\delta$  = 173.9, 173.7, 164.8, 160.1, 153.8, 147.2, 146.0, 127.1, 125.4, 116.6, 114.7, 105.8, 55.4, 52.0, 30.1, 26.6 ppm. MS (ESI)  $m/z$ : 423.0  $[\text{M}+\text{H}]^+$

**(S)-3-(3-(1-Carboxy-2-phenylethyl)ureido)-5-(4-hydroxyphenyl)thiophene-2-carboxylic acid (12).** The title compound was prepared from **B** according to the following procedure: **B** (1 eq, 0.25 mmol) was filled in a crimp vial which was sealed afterwards. The vessel was evacuated and subsequently flushed with  $\text{N}_2$ . This cycle was repeated three times. Dry DCM (5 mL) were added and the resulting solution was cooled to  $-78^\circ\text{C}$ .  $\text{BBr}_3$  (12 eq, 3.00 mmol) were added and the reaction was stirred for 48 h and allowed to warm to room temperature. Afterwards the reaction was cooled to  $-78^\circ\text{C}$  again and quenched by the addition of MeOH (5 mL). After warming up to room temperature, 2M HCl (5 mL) were added and the resulting mixture was extracted with EtOAc (3 x 20 mL). The organic layer was washed with brine (50 mL), dried ( $\text{MgSO}_4$ ) and evaporated. The crude product was purified using preparative HPLC.  $^1\text{H}$  NMR (DMSO- $d_6$ , 300 MHz):  $\delta$  = 12.82 (br. s., 2H), 9.87 (br. s., 1H), 9.41 (s, 1H), 8.14 (d,  $J$  = 7.9 Hz, 1H), 8.03 (s, 1H), 7.47 (d,  $J$  = 8.5 Hz, 2H), 7.14–7.35 (m, 5H), 6.82 (d,  $J$  = 8.5 Hz, 2H), 4.35–4.41 (m, 1H), 3.10 (dd,  $J$  = 4.7, 13.9 Hz, 1H), 2.87 (dd,  $J$  = 9.7, 13.9 Hz, 1H) ppm.  $^{13}\text{C}$  NMR (DMSO- $d_6$ , 75 MHz):  $\delta$  = 173.6, 164.6, 158.6, 153.7, 147.8, 145.9, 137.7, 129.0, 128.2, 127.1, 126.4, 123.8, 116.1, 116.0, 105.2, 54.4, 36.9 ppm. MS (ESI)  $m/z$ : 426.8  $[\text{M}+\text{H}]^+$

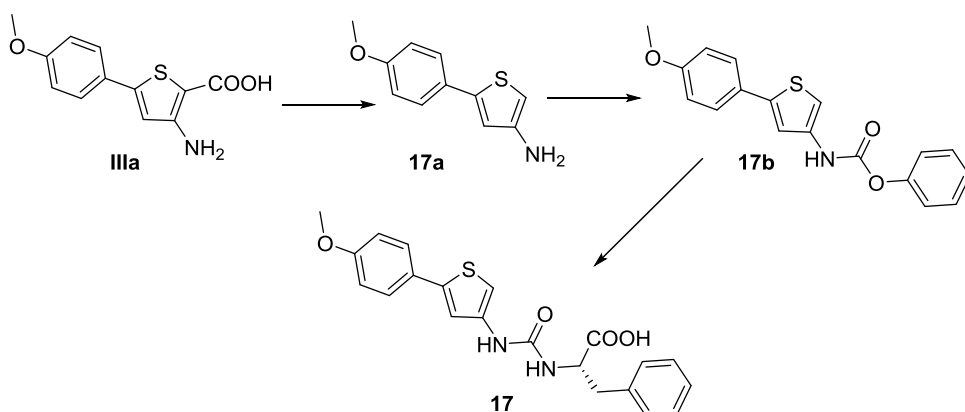
**(S)-3-(3-(1-Carboxy-2-phenylethyl)ureido)-5-phenylthiophene-2-carboxylic acid (13).** The title compound was prepared from **IVb** according to general procedure **D**.  $^1\text{H}$  NMR (DMSO- $d_6$ , 300 MHz):  $\delta$  = 12.89 (br. s., 2H), 9.42 (s, 1H), 8.21 (s, 1H), 8.17 (d,  $J$  = 7.9 Hz, 1H), 7.65 (d,  $J$  = 6.9 Hz, 2H), 7.36–7.54 (m, 3H), 7.16–7.35 (m, 5H), 4.33–4.47 (m, 1H), 3.10 (dd,  $J$  = 4.8, 13.9 Hz, 1H), 2.88 (dd,  $J$  = 9.7, 13.9 Hz, 1H) ppm.  $^{13}\text{C}$  NMR (DMSO- $d_6$ , 75 MHz):  $\delta$  = 173.6, 164.6, 153.7, 146.9, 145.7, 137.7,

132.7, 129.3, 129.2, 129.1, 128.2, 126.4, 125.6, 117.9, 106.9, 54.4, 37.0 ppm. MS (ESI)  $m/z$ : 411.0  $[M+H]^+$

**(S)-3-(3-(1-Carboxy-2-phenylethyl)ureido)thiophene-2-carboxylic acid (14).** The title compound was prepared from **IVf** according to general procedure **D**.  $^1\text{H}$  NMR (DMSO- $d_6$ , 300 MHz):  $\delta$  = 12.84 (br. s., 2H), 9.38 (s, 1H), 8.10 (d,  $J$  = 8.0 Hz, 1H), 7.83 (d,  $J$  = 5.5 Hz, 1H), 7.69 (d,  $J$  = 5.5 Hz, 1H), 7.14–7.37 (m, 5H), 4.37 (dt,  $J$  = 3.4, 4.8 Hz, 1H), 3.09 (dd,  $J$  = 4.7, 13.9 Hz, 1H), 2.86 (dd,  $J$  = 9.7, 13.2 Hz, 1H) ppm.  $^{13}\text{C}$  NMR (DMSO- $d_6$ , 75 MHz):  $\delta$  = 173.6, 164.7, 153.7, 145.4, 137.7, 131.5, 129.0, 128.2, 126.4, 121.8, 107.8, 54.3, 37.0 ppm. MS (ESI)  $m/z$ : 335.0  $[M+H]^+$

**(S)-3-(3-(1-Carboxy-2-phenylethyl)ureido)-5-(4-methoxy-2-methylphenyl)thiophene-2-carboxylic acid (15).** The title compound was prepared from **IVg** according to general procedure **D**.  $^1\text{H}$  NMR (DMSO- $d_6$ , 300 MHz):  $\delta$  = 12.86 (br. s., 2H), 9.41 (s, 1H), 8.14 (d,  $J$  = 8.0 Hz, 1H), 7.86 (s, 1H), 7.33 (d,  $J$  = 8.6 Hz, 1H), 7.18–7.33 (m, 5H), 6.91 (d,  $J$  = 2.5 Hz, 1H), 6.84 (dd,  $J$  = 8.6, 2.6 Hz, 1H), 3.08 (dd,  $J$  = 14.1, 4.8 Hz, 1H), 2.86 (dd,  $J$  = 14.1, 9.7 Hz, 1H), 2.36 (s, 3 H) ppm.  $^{13}\text{C}$  NMR (DMSO- $d_6$ , 75 MHz):  $\delta$  = 173.6, 164.6, 159.5, 153.7, 146.7, 145.0, 137.7, 137.0, 130.8, 129.0, 128.2, 126.4, 125.1, 120.9, 116.4, 111.9, 106.7, 55.2, 54.4, 36.9, 20.9 ppm. MS (ESI)  $m/z$ : 454.7  $[M+H]^+$

**(S)-3-(3-(1-Carboxy-2-phenylethyl)ureido)-7-methoxy-4,5-dihydronaphtho[1,2-*b*]thiophene-2-carboxylic acid (16).** The title compound was prepared from **IVc** according to general procedure **D**.  $^1\text{H}$  NMR (DMSO- $d_6$ , 300 MHz):  $\delta$  = 12.83 (br. s., 2H), 8.70 (s, 1H), 7.47 (d,  $J$  = 8.3 Hz, 1H), 7.34 (d,  $J$  = 8.3 Hz, 1H), 7.19–7.32 (m, 4H), 6.89 (d,  $J$  = 2.3 Hz, 1H), 6.83 (dd,  $J$  = 2.4, 8.3 Hz, 1H), 4.35–4.49 (m, 1H), 3.78 (s, 3H), 3.10 (dd,  $J$  = 4.7, 13.7 Hz, 1H), 2.88 (dd,  $J$  = 8.7, 13.7 Hz, 1H), 2.76 (app t,  $J$  = 7.6 Hz, 2H), 2.25–2.45 (m, 2H) ppm.  $^{13}\text{C}$  NMR (DMSO- $d_6$ , 75 MHz):  $\delta$  = 173.4, 164.0, 159.7, 154.0, 143.0, 139.3, 137.9, 137.4, 132.8, 129.3, 128.2, 126.4, 124.4, 123.1, 113.8, 112.5, 111.8, 55.2, 54.1, 37.6, 28.5, 23.3 ppm. MS (ESI)  $m/z$ : 466.8  $[M+H]^+$



**Scheme S3:** Synthesis of compound **17**.

**5-(4-Methoxyphenyl)thiophen-3-amine (17a)** was prepared from **IIIa** according to the following procedure: To a solution of **IIIa** (4.4 mmol) in DCM, was added HCl (2 M aq, 10 mL). The resulting mixture was heated to 80 °C for 18 h. The reaction was cooled to room temperature and alkalized with 2M KOH. The aqueous layer was extracted with DCM (3 x 50 mL). The organic phase was washed with brine (1 x 100

mL), dried (MgSO<sub>4</sub>) and evaporated to yield the title compound which was used in the next step without further purification.

**Phenyl (5-(4-methoxyphenyl)thiophen-3-yl)carbamate (17b)** was prepared from **17a** according to the following procedure: To a solution of **17a** (3.4 mmol) in dry DCM (30 mL), pyridine (3.4 mmol) was added and the resulting mixture was cooled to 0 °C. Phenyl chloroformate (3.4 mmol) was added dropwise at 0 °C. The reaction was allowed to warm to room temperature and stirred until the reaction was completed (checked by TLC). The solvent was evaporated and the residue was suspended in ice water. After acidification with a saturated KHSO<sub>4</sub> solution, the aqueous layer was extracted with DCM (3 x 50 mL). The organic phase was washed with an ice cold half saturated KHSO<sub>4</sub> solution (2 x 50 mL) and brine (1 x 50 mL), dried (MgSO<sub>4</sub>) and evaporated to yield the title compound which was sufficiently pure to be used in the next step without further purification.

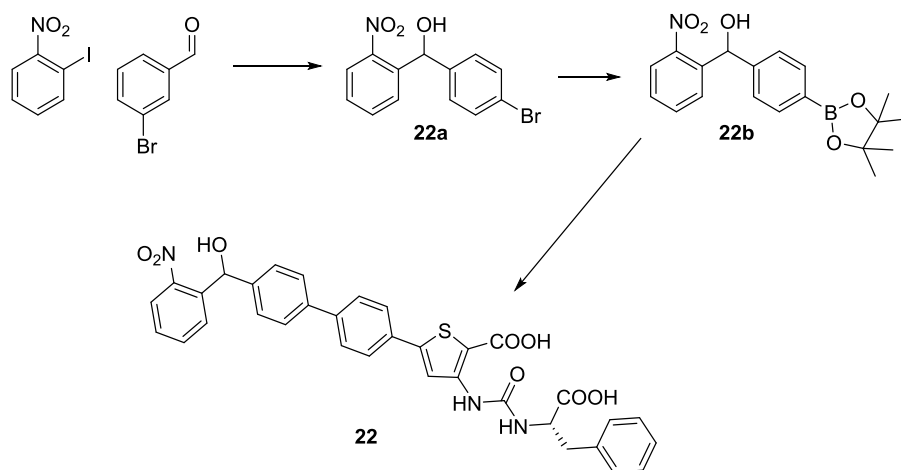
**((5-(4-Methoxyphenyl)thiophen-3-yl)carbamoyl)-L-phenylalanine (17)**: The title compound was prepared from **17b** according to the following procedure: **17b** (1eq), triethylamine and L-phenylalanine were dissolved in dry DMSO (7 mL) and stirred at 50°C for 50 h until the reaction was completed. The reaction mixture was poured into a mixture of concentrated HCl and ice (1:1) and extracted with EtOAc/THF (1:1, 60 mL). The organic layer was washed with aqueous HCl (2M), followed by saturated aqueous NaCl (2 x 50 mL), dried (MgSO<sub>4</sub>) and concentrated. The crude material was suspended in a mixture of *n*-hexane/EtOAc (2:1, 20 mL) heated to 50 °C and after cooling to room temperature separated *via* filtration. <sup>1</sup>H NMR (DMSO-d<sub>6</sub>, 300 MHz): δ = 12.78 (br. s., 1H), 8.90 (s, 1H), 7.51 (d, *J* = 8.8 Hz, 2H), 7.18–7.35 (m, 5H), 7.14 (d, *J* = 1.3 Hz, 1H), 7.03 (d, *J* = 1.3 Hz, 1H), 6.97 (d, *J* = 8.8 Hz, 2H), 6.35 (d, *J* = 8.0 Hz, 1H), 4.45 (dt, *J* = 5.2, 7.7 Hz, 1H), 3.78 (s, 3H), 3.03–3.16 (m, 1H), 2.87–3.03 (m, 1H) ppm. <sup>13</sup>C NMR (DMSO-d<sub>6</sub>, 75 MHz): δ = 173.5, 158.9, 154.5, 141.1, 138.2, 137.3, 129.2, 128.2, 126.5, 126.4, 126.3, 116.1, 114.5, 103.4, 55.2, 53.7, 37.3 ppm. MS (ESI) *m/z*: 397.0 [M+H]<sup>+</sup>

**(S)-5-([1,1'-Biphenyl]-3-yl)-3-(3-(1-carboxy-2-phenylethyl)ureido)thiophene-2-carboxylic acid (18)**. The title compound was prepared from **Va** according to general procedure **E**. <sup>1</sup>H NMR (DMSO-d<sub>6</sub>, 500 MHz): δ = 12.90 (br. s., 2H), 9.44 (s, 1H), 8.28 (s, 1H), 8.19 (d, *J* = 7.9 Hz, 1H), 7.84 (t, *J* = 1.7 Hz, 1H), 7.71 - 7.75 (m, 2H), 7.69 (td, *J* = 1.7, 7.8 Hz, 1H), 7.65 (td, *J* = 1.7, 7.8 Hz, 1H), 7.53–7.57 (m, 1H), 7.47–7.52 (m, 2H), 7.39–7.43 (m, 1H), 7.26–7.33 (m, 4H), 7.20–7.24 (m, 1H), 4.40 (ddd, *J* = 4.7, 7.9, 9.7 Hz, 1H), 3.11 (dd, *J* = 4.7, 14.0 Hz, 1H), 2.88 (dd, *J* = 9.7, 14.0 Hz, 1H) ppm. <sup>13</sup>C NMR (DMSO-d<sub>6</sub>, 125 MHz): δ = 173.6, 164.6, 153.7, 146.7, 145.7, 141.3, 139.4, 137.7, 133.4, 130.0, 129.1, 129.0, 128.2, 127.9, 127.6, 126.9, 126.4, 124.8, 123.7, 118.3, 107.1, 54.4, 37.0 ppm. MS (ESI) *m/z*: 487.0 [M+H]<sup>+</sup>

**(S)-3-(3-(1-Carboxy-2-phenylethyl)ureido)-5-(4'-(hydroxymethyl)-[1,1'-biphenyl]-3-yl)thiophene-2-carboxylic acid (19)**. The title compound was prepared from **Va** according to general procedure **E**. <sup>1</sup>H NMR (DMSO-d<sub>6</sub>, 500 MHz): δ = 12.99 (br. s., 2H), 9.44 (s, 1H), 8.28 (s, 1H), 8.19 (d, *J* = 7.9 Hz, 1H), 7.84 (t, *J* = 1.7 Hz, 1H), 7.67–7.71 (m, 3H), 7.62–7.65 (m, 1H), 7.51–7.56 (m, 1H), 7.43 (d, *J* = 8.5 Hz, 2H), 7.26–7.33 (m, 4H), 7.19–7.24 (m, 1H), 4.56 (s, 2H), 4.40 (ddd, *J* = 4.7, 8.1, 9.8 Hz, 1H), 3.11 (dd, *J* = 4.7, 13.9 Hz, 1H), 2.88 (dd, *J* = 9.8, 13.9 Hz, 1H) ppm. <sup>13</sup>C NMR (DMSO-d<sub>6</sub>, 125 MHz): δ = 173.6, 164.6, 153.7, 146.8, 145.7, 142.3, 141.2, 137.7, 137.7, 133.4, 130.0, 129.1, 128.2, 127.5, 127.1, 126.6, 126.4, 124.6, 123.6, 118.3, 107.1, 62.6, 54.4, 37.0 ppm. MS (ESI) *m/z*: 517.0 [M+H]<sup>+</sup>

**(S)-5-([1,1'-Biphenyl]-4-yl)-3-(3-(1-carboxy-2-phenylethyl)ureido)thiophene-2-carboxylic acid (20)**. The title compound was prepared from **Vb** according to general procedure E.  $^1\text{H}$  NMR (DMSO- $d_6$ , 500 MHz):  $\delta$  = 12.90 (br. s, 2H), 9.45 (s, 1H), 8.26 (s, 1H), 8.19 (d,  $J$  = 8.0 Hz, 1H), 7.73–7.78 (m, 4H), 7.69–7.73 (m, 2H), 7.46–7.51 (m, 2H), 7.37–7.41 (m, 1H), 7.27–7.33 (m, 4H), 7.19–7.24 (m, 1H), 4.41 (ddd,  $J$  = 4.8, 8.0, 9.7 Hz, 1H), 3.11 (dd,  $J$  = 4.8, 13.9 Hz, 1H), 2.89 (dd,  $J$  = 9.7, 13.9 Hz, 1H) ppm.  $^{13}\text{C}$  NMR (DMSO- $d_6$ , 125 MHz):  $\delta$  = 173.6, 164.6, 153.7, 146.4, 145.8, 140.7, 139.1, 137.7, 131.8, 129.0, 129.0, 128.2, 127.8, 127.4, 126.5, 126.4, 126.1, 117.9, 107.0, 54.4, 36.9 ppm. MS (ESI)  $m/z$ : 486.4  $[\text{M}+\text{H}]^+$

**(S)-3-(3-(1-Carboxy-2-phenylethyl)ureido)-5-(4'-(hydroxymethyl)-[1,1'-biphenyl]-4-yl)thiophene-2-carboxylic acid (21)**. The title compound was prepared from **Vb** according to general procedure E.  $^1\text{H}$  NMR (DMSO- $d_6$ , 500 MHz):  $\delta$  = 12.97 (br. s, 2H), 9.44 (s, 1H), 8.25 (s, 1H), 8.19 (d,  $J$  = 7.9 Hz, 1H), 7.76 (d,  $J$  = 8.7 Hz, 2H), 7.73 (d,  $J$  = 8.7 Hz, 2H), 7.68 (d,  $J$  = 8.2 Hz, 2H), 7.42 (d,  $J$  = 8.2 Hz, 2H), 7.26–7.33 (m, 4H), 7.19–7.24 (m, 1H), 4.55 (s, 2H), 4.35–4.45 (m, 1H), 3.11 (dd,  $J$  = 4.7, 14.0 Hz, 1H), 2.88 (dd,  $J$  = 9.8, 14.0 Hz, 3H) ppm.  $^{13}\text{C}$  NMR (DMSO- $d_6$ , 125 MHz):  $\delta$  = 173.6, 164.6, 153.7, 146.5, 145.8, 142.3, 140.6, 137.7, 137.4, 131.6, 129.1, 128.2, 127.3, 127.1, 126.4, 126.2, 126.1, 117.8, 106.8, 62.6, 54.4, 37.0 ppm. MS (ESI)  $m/z$ : 516.9  $[\text{M}+\text{H}]^+$



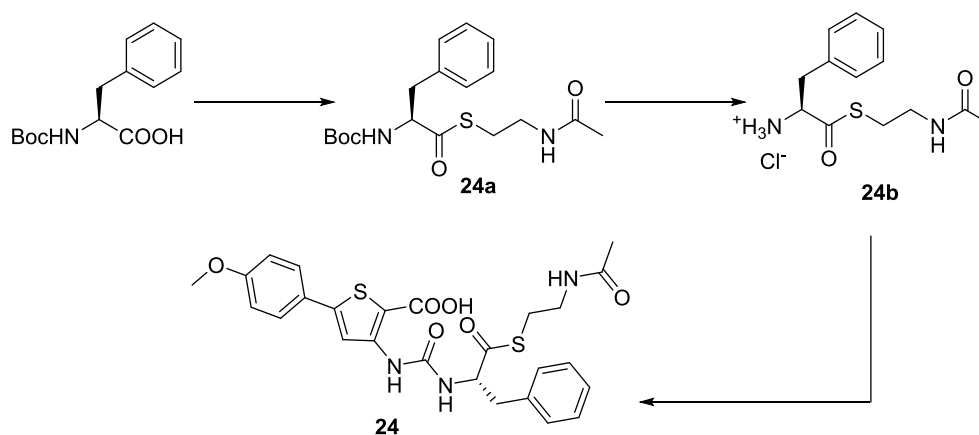
**Scheme S3:** Synthesis of compound **22**.

**(4-Bromophenyl)(2-nitrophenyl)methanol (22a)** was prepared according to the following procedure: A solution of 2-iodo-nitrobenzene (1.0 eq) in THF (10mL/g reagent) was cooled to  $-40\text{ }^\circ\text{C}$  and a solution of phenylmagnesium chloride (2M in THF, 1.1 eq) was added dropwise. The solution was stirred for 30 min at  $-40\text{ }^\circ\text{C}$ , 3-bromobenzaldehyde was added and the reaction was completed at  $-40\text{ }^\circ\text{C}$  (checked by TLC). The mixture was quenched with a saturated solution of  $\text{NH}_4\text{Cl}$  (5 mL) and diluted with water (5 mL). The aqueous phase was extracted with ethyl acetate (three times) and the combined organic layers were washed with brine, dried, and concentrated under reduced pressure. The residue was purified by column chromatography over silica gel to yield the desired product.  $^1\text{H}$  NMR ( $\text{CDCl}_3$ , 300 MHz):  $\delta$  = 7.81 (dd,  $J$  = 1.3, 7.8 Hz, 1H), 7.57 (dd,  $J$  = 1.3, 7.8 Hz, 1H), 7.52 (td,  $J$  = 1.3, 7.8 Hz, 1H), 7.32 (d,  $J$  = 8.6 Hz, 2H), 7.37 (td,  $J$  = 1.3, 7.8 Hz, 1H), 7.07 (d,  $J$  = 8.6 Hz, 2H), 6.23 (d,  $J$  = 4.4 Hz, 1H), 3.14 (d,  $J$  = 4.4 Hz, 1H) ppm.  $^{13}\text{C}$  NMR ( $\text{CDCl}_3$ , 75 MHz):  $\delta$  = 148.0, 140.4, 137.9, 133.5, 131.5, 129.2, 128.7, 128.6, 124.7, 121.9, 70.7 ppm.

**(2-Nitrophenyl)(4-(4,4,5,5-tetramethyl-1,3,2-dioxaborolan-2-yl)phenyl)methanol (22b)** was prepared from **22a** according to the following procedure: **22a** (1 eq), bis(pinakolato)diboron (1.2 eq) and potassium acetate (3 eq) were dissolved in dry 1,4-Dioxane (20 mL). The system was evacuated and subsequently flushed with nitrogen three times. [1,1'-Bis(diphenylphosphino)ferrocene]dichloro palladium (0.05 eq) was added and the resulting mixture was heated to 85 °C for 24 h. The reaction was cooled to room temperature and the solvent was evaporated. The residue was dissolved in EtOAc (150 mL), the organic layer was washed with H<sub>2</sub>O (1 x 100 mL) and brine (1 x 100 mL) and dried (MgSO<sub>4</sub>). The solvent was evaporated and the crude product was purified by flash column chromatography (EtOAc/ hexane 1:6) to yield the title compound. <sup>1</sup>H NMR (CDCl<sub>3</sub>, 300 MHz): δ = 7.90 (dd, *J* = 1.3, 8.2 Hz, 1H), 7.77 (d, *J* = 8.0 Hz, 2H), 7.68 (dd, *J* = 1.3, 7.6 Hz, 1H), 7.59 (dt, *J* = 1.3, 7.6 Hz, 1H), 7.42 (ddd, *J* = 1.3, 7.6, 8.2 Hz, 1H), 7.32 (d, *J* = 8.0 Hz, 2H), 6.41 (d, *J* = 4.4 Hz, 1H), 3.26 (d, *J* = 4.4 Hz, 1H), 1.33 (s, 12H) ppm. <sup>13</sup>C NMR (CDCl<sub>3</sub>, 75 MHz): δ = 148.3, 144.5, 138.3, 134.9, 133.3, 129.5, 128.4, 126.1, 124.6, 83.8, 71.2, 24.8 ppm.

**3-(3-((S)-1-Carboxy-2-phenylethyl)ureido)-5-(4'-(hydroxy(2-nitrophenyl)methyl)-[1,1'-biphenyl]-4-yl)thiophene-2-carboxylic acid (22)** The title compound was prepared from **Va** and **22b** according to general procedure **E**. <sup>1</sup>H NMR (300 MHz, acetone-*d*<sub>6</sub>): δ = 9.53 (s, 1H), 8.40 (s, 1H), 7.98 (dd, *J* = 1.2, 7.9 Hz, 1H), 7.93 (dd, *J* = 1.2, 8.2 Hz, 1H), 7.74–7.84 (m, 5H), 7.70 (d, *J* = 8.2 Hz, 2H), 7.53–7.60 (m, 1H), 7.47 (d, *J* = 8.2 Hz, 2H), 7.40 (d, *J* = 7.9 Hz, 1H), 7.26–7.37 (m, 4H), 7.18–7.25 (m, 1H), 6.51 (s, 1H), 4.69–4.80 (m, 1H), 3.29 (dd, *J* = 5.0, 14.0 Hz, 1H), 3.07 (dd, *J* = 8.85, 14.0 Hz, 1H) ppm. <sup>13</sup>C NMR (75 MHz, acetone-*d*<sub>6</sub>): δ = 173.8, 165.6, 154.7, 149.5, 148.8, 148.1, 143.9, 142.1, 140.1, 140.0, 138.6, 134.1, 133.4, 130.3, 130.0, 129.3, 129.3, 128.7, 128.5, 127.6, 127.5, 127.3, 125.0, 118.9, 107.1, 70.8, 55.5, 38.6 ppm. MS (ESI) *m/z*: 637.9 [M+H]<sup>+</sup>

**(S)-3-(3-(1-Carboxy-2-(1*H*-imidazol-4-yl)ethyl)ureido)-5-(4-methoxyphenyl)thiophene-2-carboxylic acid (23)**. The title compound was prepared from **IVa** according to general procedure **D**. <sup>1</sup>H NMR (DMSO-*d*<sub>6</sub>, 300 MHz): δ = 9.59 (br. s., 1H), 8.10 (d, *J* = 7.73 Hz, 1H), 8.00 (s, 1H), 7.82 (d, *J* = 0.7 Hz, 1H), 7.50 (d, *J* = 8.9 Hz, 2H), 6.88–6.95 (m, 3H), 4.27–4.41 (m, 1H), 3.71 (s, 3H), 2.98 (dd, *J* = 4.7, 15.0 Hz, 1H), 2.83 (dd, *J* = 9.3, 15.0 Hz, 1H) ppm. <sup>13</sup>C NMR (DMSO-*d*<sub>6</sub>, 75 MHz): δ = 173.5, 165.5, 159.9, 153.8, 146.0, 144.9, 134.3, 132.6, 126.9, 125.7, 116.9, 116.7, 114.7, 108.2, 55.3, 53.2, 28.5 ppm. MS (ESI) *m/z*: 430.9 [M+H]<sup>+</sup>



**Scheme S4:** Synthesis of compound **24**.

**S-(2-Acetamidoethyl)(S)-2-((tert-butoxycarbonyl)amino)-3-phenylpropane thioate (24a)** was prepared according to the following procedure:[7] A solution of boc-*L*-phenylalanine (400 mg, 1.50 mmol), N-acetylcysteamine (215 mg, 1.80 mmol) and DMAP (18.3 mg, 0.15 mmol) in dry DCM (10 mL) was cooled to 0°C. DCC (371 mg, 1.80 mmol), dissolved in DCM (10 mL) was added dropwise and the ice bath was removed afterwards. Stirring was continued for 48 h until the reaction was completed. The solids were filtered off and rinsed with cold DCM (10 mL). The filtrate was washed with 1M HCl (30 mL), a saturated NaHCO<sub>3</sub> solution (30 mL), H<sub>2</sub>O (30 mL) and brine (30 mL). After drying (MgSO<sub>4</sub>), the solvent was evaporated and the residue was purified via column flash chromatography (100% EtOAc) to yield the desired product. <sup>1</sup>H NMR (Acetone-*d*<sub>6</sub>, 300 MHz): δ = 7.18–7.35 (m, 5H), 6.63 (d, *J* = 8.5 Hz, 1H), 4.46 (ddd, *J* = 4.5, 8.5, 10.2 Hz, 1H), 3.33 (q, *J* = 6.9 Hz, 2H), 3.21 (dd, *J* = 4.5, 14.1 Hz, 1H), 2.98 (t, *J* = 6.9 Hz, 2H), 2.87–2.95 (m, 1H), 1.88 (s, 3H), 1.34 (s, 9H) ppm.

**(S)-1-((2-Acetamidoethyl)thio)-1-oxo-3-phenylpropan-2-aminium chloride (24b)** was prepared from **24a** according to the following procedure:[8] A solution of **24a** (475 mg, 1.30 mmol) in dry DCM (5 mL) was cooled to 0 °C. TFA (1.30 mL) was added very slowly and the resulting mixture was stirred at 0 °C for 2 h. The mixture was concentrated to about 2 mL, then diluted with 2 mL DCM and again concentrated. This cycle was repeated three times and afterwards, the entire solvent was evaporated. The residue was dissolved in EtOAc (30 mL) and the resulting organic layer was washed with 1M NaOH (10 mL). The solvent was evaporated again and the residue was treated with H<sub>2</sub>O (2 mL) and 2M HCl (2 mL). After washing the aqueous phase with EtOAc (2 x 2 mL), it was lyophilized to yield the title compound. <sup>1</sup>H NMR (DMSO-*d*<sub>6</sub>, 300 MHz): δ = 7.23–7.37 (m, 5H), 7.13 (br. s., 3H), 4.34–4.49 (m, 1H), 3.04–3.28 (m, 4H), 2.90–3.00 (m, 2H), 1.79 (s, 3H) ppm. <sup>13</sup>C NMR (DMSO-*d*<sub>6</sub>, 75 MHz): δ = 196.0, 169.4, 134.4, 129.6, 128.6, 127.3, 59.5, 37.7, 36.8, 28.3, 22.5 ppm.

**(S)-3-(3-(1-((2-Acetamidoethyl)thio)-1-oxo-3-phenylpropan-2-yl)ureido)-5-(4-methoxyphenyl)thiophene-2-carboxylic acid (24)** The title compound was prepared from **24b** according to the following procedure: **24b** (52.0 mg, 0.19 mmol) and **Via** (63.0 mg, 0.21 mmol) were mixed in a reaction vial and capped. The system was evacuated and subsequently flushed with N<sub>2</sub>. This cycle was repeated five times. Dry DMSO (2 mL) was added and the reactants were dissolved under stirring. Dry triethylamine (42.5 mg, 0.42 mmol) was added dropwise with a Hamilton syringe and the resulting mixture was stirred at room temperature for 2 h. The reaction mixture was poured into a mixture of concentrated HCl and ice (1:1, 50 mL) and extracted with EtOAc/THF (1:1, 3 x 60 mL). The organic layer was washed with 2M HCl (2 x 50 mL), followed by brine (1 x 50 mL), dried (MgSO<sub>4</sub>) and concentrated. The crude material was purified using preparative HPLC. <sup>1</sup>H NMR (500 MHz, DMSO-*d*<sub>6</sub>): δ = 13.09 (br. s., 1H), 9.51 (s, 1H), 8.54 (d, *J* = 7.6 Hz, 1H), 8.07 (s, 1H), 8.03 (t, *J* = 5.5 Hz, 1H), 7.59 (d, *J* = 8.8 Hz, 2H), 7.26–7.33 (m, 4H), 7.18–7.25 (m, 1H), 7.00 (d, *J* = 8.8 Hz, 2H), 4.53 (ddd, *J* = 4.6, 7.7, 10.4 Hz, 1H), 3.79 (s, 3H), 3.07–3.21 (m, 3H), 2.80–2.95 (m, 3H), 1.78 (s, 3H) ppm. <sup>13</sup>C NMR (125 MHz, DMSO-*d*<sub>6</sub>): δ = 201.4, 169.2, 164.7, 160.1, 153.4, 147.4, 145.6, 137.2, 129.0, 128.3, 127.1, 126.6, 125.2, 116.5, 114.7, 106.0, 61.4, 55.3, 38.1, 37.0, 27.9, 22.ppm. MS (ESI) *m/z*: 541.8 [M+H]<sup>+</sup>

## 6.5.2 Surface plasmon resonance (SPR)

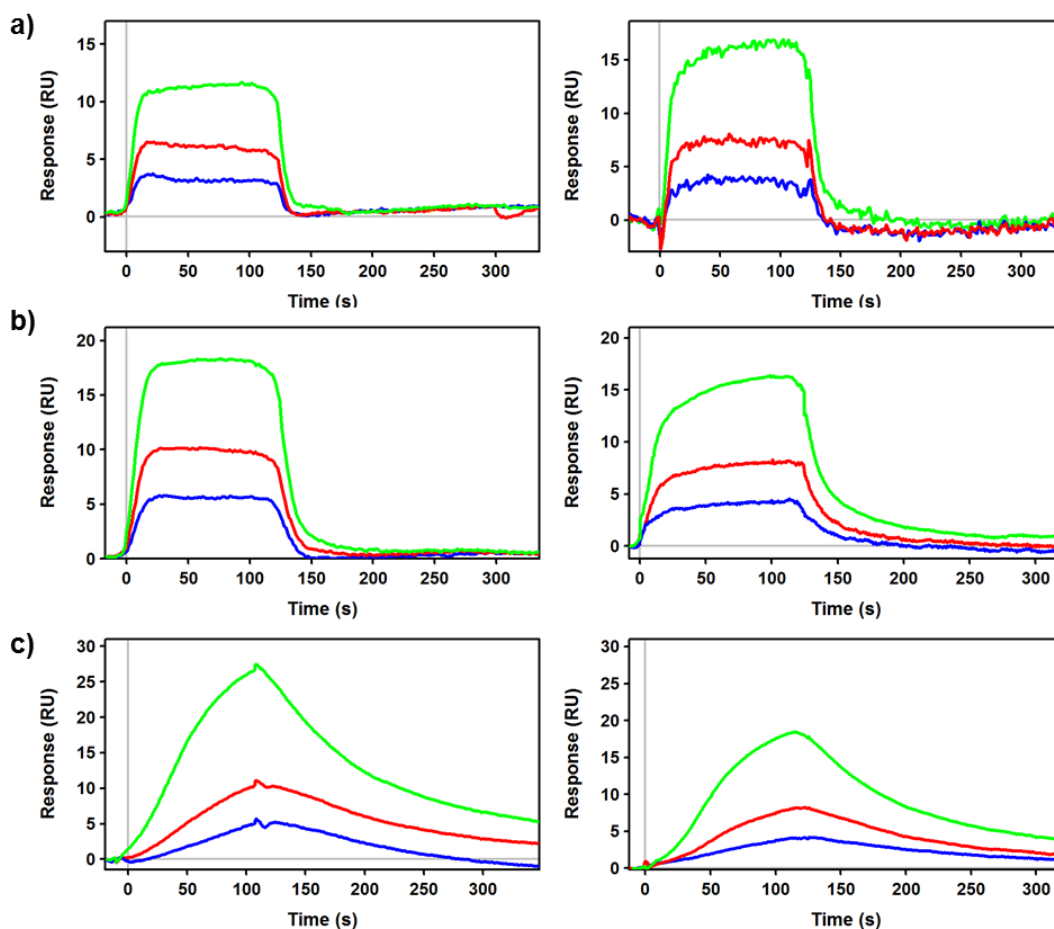


**Figure S1:** SPR sensorgrams of **B** (Figure S1a), **21** (Figure S1b) and **22** (Figure S1c) at increasing concentrations (blue  $\rightarrow$  red  $\rightarrow$  green). Left panel: Before treatment with ACoA; Right panel: After treatment with ACoA.

## 6.5.3 References

- [1] H. Hartmann, J. Liebscher, A simple method for the synthesis of 5-aryl-3-amino-2-alkoxycarbonylthiophenes, *Synthesis* (1984) 275–276.
- [2] F. Fabis, S. Jolivet-Fouchet, M. Robba, H. Landelle, S. Rault, Thiaisatoic anhydrides: Efficient synthesis under microwave heating conditions and study of their reactivity, *Tetrahedron* 54 (1998) 10789–10800.
- [3] L. Foulon, E. Braud, F. Fabis, J.C. Lancelot, S. Rault, Synthesis and combinatorial approach of the reactivity of 6-and 7-arylthieno [3,2-d][1,3] oxazine-2,4-diones. *Tetrahedron* 59 (2003) 10051–10057.
- [4] F.X. Le Foulon, E. Braud, F. Fabis, J.C. Lancelot, S. Rault, Solution-phase parallel synthesis of a 1140-member ureidothiophene carboxylic acid library. *J. Comb. Chem.* 7 (2005) 253–257.
- [5] K. Sambasivarao, K. G. Arun, D. D. Kodrand, Synthesis of 9,10-Diarylanthracene Derivatives. *Synthesis* (2004) 549–557.
- [6] E. Perspice, V. Jouan-Hureau, R. Ragno, F. Ballante, S. Sartini, C. La Motta, F. Da Settimo, B. Chen, G. Kirsch, S. Schneider, B. Faivre, S. Hesse, Design synthesis and biological evaluation of new classes of thieno[3,2-d]pyrimidine and thieno[1,2,3]triazine as inhibitor of vascular endothelial growth factor receptor-2 (VEGFR-2). *Eur. J. Med. Chem* (2013) 765–781.
- [7] S. Flohr, V. Jungmann, H. Waldmann, Chemoenzymatic synthesis of nucleopeptides. *Chem. Eur. J.* (1999) 669–681.
- [8] R. Muchiri, K. D. Walker, Taxol biosynthesis: Tyrocidine Synthetase A catalyzes the production of phenylisoserinyl CoA and other amino phenylpropanoyl thioesters. (2012) 679–685.

## 7 Appendix

### 7.1 Curriculum Vitae

#### PERSÖNLICHE DATEN

Name	Jan Henning Sahner
Geburtsdaten	25. November 1985 in Saarbrücken
Familienstand	ledig
Nationalität	deutsch

#### WISSENSCHAFTLICHER WERDEGANG

ab 01/2012	<b>Promotion</b> unter Anleitung von Prof. Rolf Hartmann am Helmholtz-Institut für Pharmazeutische Forschung Saarland (HIPS), Saarbrücken Titel der Dissertation: <i>“Rational development of anti-infectives with novel target-sites and new mechanisms of action to overcome bacterial resistances;.”</i>
04/2014 – 06/2014	<b>Forschungsaufenthalt</b> bei Prof. Dr. Celerino Abad-Zapatero und Prof. Dr. Michael Johnson, Department of Pharmaceutical Biotechnology, University of Illinois at Chicago, USA.
05/2011 – 10/2011	Diplomarbeit unter Anleitung von Prof. Dr. Claus-Michael Lehr an der Universität des Saarlandes. Experimentelle Arbeiten unter Anleitung von Dr. Claudius Weiler bei Boehringer Ingelheim Pharma GmbH & Co. KG. Titel der Arbeit: <i>„Beeinflussung der Oberflächenmorphologie sprühgetrockneter Partikel.“</i>
10/2006 – 09/2010	<b>Studium der Pharmazie</b> , Universität des Saarlandes Abschluss: 2. Staatsexamen (Note 1,0)

#### SCHULBILDUNG

08/1996 – 06/2005	Allgemeine Hochschulreife, Marienschule Saarbrücken, Abschluss: Abitur
08/1992 – 06/1996	Grundschule Lindenschule, Riegelsberg

#### MITGLIEDSCHAFTEN

Alumni und Freunde der Fachrichtung Pharmazie an der Universität des Saarlandes e.V.  
Deutsche Pharmazeutische Gesellschaft (DPhG)

## 7.2 Publications

J. H. Sahner, M. Empting, A. Kamal, E. Weidel, C. Börger, and R. W. Hartmann. Exploring the chemical space of ureidothiophene-2-carboxylic acids as inhibitors of the quorum sensing enzyme PqsD from *Pseudomonas aeruginosa*. *Eur. J. Med. Chem.* **2014**, submitted.

J. H. Sahner, H. Sucipto, S. C. Wenzel, M. Groh, R. W. Hartmann, R. Müller. Advanced Mutasynthesis Studies on Natural  $\alpha$ -Pyrone-Antibiotics from *Myxococcus fulvus*. *ChemBioChem* **2015**, DOI: 10.1002/cbic.201402666.

M. Fruth, A. Plaza, S. Hinsberger, J. H. Sahner, J. Haupenthal, M. Bischoff, R. Jansen, R. Müller, R. W. Hartmann. Binding mode characterization of novel RNA polymerase inhibitors using a combined biochemical and NMR approach. *ACS Chem. Biol.* **2014**, *9*, 2656-2663.

J. H. Sahner, C. Brengel, M. P. Storz, M. Groh, A. Plaza, R. Müller, R. W. Hartmann. Combining in Silico and Biophysical Methods for the Development of *Pseudomonas aeruginosa* Quorum Sensing Inhibitors: An Alternative Approach for Structure-Based Drug Design. *J. Med. Chem.* **2013**, *56*, 8656-8664.

J. H. Sahner, M. Groh, M. Negri, J. Haupenthal, R. W. Hartmann. Novel small molecule inhibitors targeting the “switch region” of bacterial RNAP: Structure-based optimization of a virtual screening hit. *Eur. J. Med. Chem.* **2013**, *65*, 223-231.

C. Weiler, J. H. Sahner, M. Munz, C. M. Lehr. Effect of Molecular Weight and Process Parameters on the Morphology of Spray-Dried Dextran Particles. *Respiratory Drug Delivery* **2012**, 421-426.

## 7.3 Conference Contributions

### 7.3.1 Oral Presentations

J. H. Sahner, C. Brengel, M. Groh, M. P. Storz, A. Plaza, M. Negri, R. W. Hartmann. Combining virtual screening and biophysical methods as an efficient alternative to HTS, exemplified for the discovery of PqsD *P. aeruginosa* quorum sensing inhibitors. *Antimicrobial Drug Discovery Conference*, June **2013**, Madrid, Spain.

J. H. Sahner, C. Brengel, M. Groh, M. P. Storz, A. Plaza, M. Negri, R. W. Hartmann. Combining virtual screening and biophysical methods as an efficient alternative to HTS, exemplified for the discovery of PqsD *P. aeruginosa* quorum sensing inhibitors. *Summer symposium – Graduate School of Natural Product Research*, July **2013**, Saarbrücken, Germany.

### 7.3.2 Poster Presentations

J. H. Sahner, C. Brengel, M. Groh, M. P. Storz, A. Plaza, M. Negri, R. Müller, R. W. Hartmann. Combining *in Silico* and Biophysical Methods for the Development of *Pseudomonas aeruginosa* Quorum Sensing Inhibitors: An Alternative Approach for Structure-Based Drug Design. *Frontiers in Medicinal Chemistry*, March **2014**, Tübingen, Germany.

J. H. Sahner, M. Negri, M. Groh, J. Hauptenthal, R. W. Hartmann. Is RNAP a suitable target for CADD? RNAP-myxopyronin complexes as starting points for MD simulations, homology modeling and 3D-pharmacophore virtual screening. 22<sup>nd</sup> International Symposium on Medicinal Chemistry, September **2012**, Berlin, Germany.

J. H. Sahner, M. Negri, M. Groh, J. Hauptenthal, R. W. Hartmann. Novel Small Molecule Inhibitors Targeting Bacterial RNAP. Structure-Based Optimization of a Virtual Screening Hit. VAAM International Workshop – Biology and Chemistry of Antibiotic-Producing Bacteria and Fungi, September **2012**, Braunschweig, Germany.

## 8 Acknowledgements

Zu aller erst möchte ich mich bei Herrn Prof. Dr. Rolf W. Hartmann dafür bedanken, dass ich meine Arbeit unter seiner Leitung anfertigen durfte. Herzlichen Dank dafür, dass Sie mich mit interessanten Themen betraut, mich immer unterstützt, mir Freiräume gegeben und mir vertraut haben.

Weiterhin gilt mein aufrichtiger Dank den folgenden Personen:

Herrn Prof. Dr. Müller für die Übernahme des Korreferats und seine Rolle als mein wissenschaftlicher Begleiter während meiner Promotion.

Frau Prof. Dr. Holzgrabe für die Begutachtung meiner Arbeit.

Herrn Prof. Kazmaier für sein Engagement als Leiter der Graduiertenschule Naturstoffforschung.

Dr. Matthias Groh für die Einweisung und Unterstützung in die Synthesechemie, sowie für zahllose unvergessene wissenschaftliche und darüber hinaus gehende Diskussionen.

Hilda Sucipto, Dr. Silke Wenzel und Prof. Dr. Rolf Müller für die interessante Kooperation im Myxopyronin Projekt durch die mir auch Einblicke in die Welt der pharmazeutischen Biotechnologie ermöglicht wurden.

Dr. Jörg Haupenthal, für die Leitung des RNAP Projekts

Drs. Anke Steinbach und Martin Empting für die Leitung des PQS-Projekts.

Dr. Matthias Groh, Christian Brengel, Michael Storz, Hilda Sucipto, Dr. Alberto Plaza, Dr. Matthias Negri, Dr. Jörg Haupenthal Dr. Silke Wenzel, Dr. Martin Empting, Martina Fruth, Ahmed Kamal, Lilli Weidel und Dr. Carsten Börger für die gute Zusammenarbeit.

Jeaninne Jung, Jannine Ludwig, Simone Amann und Carina Scheid für ihre Hilfe bei der Durchführung biologischer Experimente.

Katrin Schmitt für ihre Hilfsbereitschaft und die Organisation im Sekretariat

Dr. Stefan Böttcher für seine Unterstützung in allen Fragen zu HPLC/MS Experimenten.

Dr. Matthias Negri für die Einarbeitung und Hilfestellungen im Bezug auf Docking und Modeling Software.

Dr. Josef Zapp für die Messung zahlloser NMR Spektren.

Christian Brengel, Andreas Thomann und Michael Zender für die Auflockerung des Arbeitsalltags im Labor und Büro, die nicht selten in Zwerchfell-Krämpfen und sinnfreiem Gelaber gipfelte.

Prof. Dr. Cele Abad-Zapatero, für seine aufopferungsvolle Betreuung während meines Aufenthaltes an der University of Illinois at Chicago. Ich hatte eine super Zeit!

Lothar Jager für die Lösung nahezu aller technischer Probleme für die sich sonst niemand zuständig fühlte.

Michael Hoffmann für die Hilfe bei besonders diffizilen HPLC/MS Messungen.

Allen aktuellen und ehemaligen Mitarbeitern der Arbeitskreise Hartmann und Müller (HIPS bzw. UdS) sowie Johnson und Mankin (University of Illinois at Chicago) die hier nicht namentlich erwähnt sind für die kollegiale Atmosphäre die ich in den letzten knapp drei Jahren genießen durfte.

Der Stiftung der Deutschen Wirtschaft (SDW) für ein Promotionsstipendium das mir neben materieller Förderung vor allem auf ideeller Ebene viel gegeben hat.

Meinen Freunden, die mich auch mal daran erinnern haben, dass es neben der Arbeit auch andere Dinge im Leben gibt.

Meinen Eltern Friedel und Manfred, die mir meine Ausbildung ermöglicht und mich immer unterstützt haben sowie meiner Schwester Kathy die mir immer ein Vorbild war.

Meiner Katrin dafür, dass sie mich mit all meinen Macken erträgt und mir den Rücken stärkt. Danke dass du immer für mich da bist und an mich glaubst!